LC-NMR and Other Hyphenated NMR Techniques

LC-NMR and Other Hyphenated NMR Techniques

Overview and Applications

Maria Victoria Silva Elipe
Amgen, Inc.

WILEY
A JOHN WILEY & SONS, INC., PUBLICATION

Published by John Wiley & Sons, Inc., Hoboken, New Jersey.
Published simultaneously in Canada.

Library of Congress Cataloging-in-Publication Data:

Silva Elipe, Maria Victoria, 1963-
LC-NMR and other hyphenated NMR techniques : overview and applications / Maria Victoria Silva Elipe.
p. cm.
Includes bibliographical references and index.
ISBN 978-0-470-54834-9 (hardback)
1. Nuclear magnetic resonance spectroscopy–Industrial applications. 2. Organic compounds–Analysis. 3. Drug development. I. Title.
QD96.N8S54 2012
543'.66–dc23

2011018343

Printed in the United States of America

10 9 8 7 6 5 4 3 2 1

To my parents, Joaquin Silva Garcia and Maria Elipe Ruiz,
for their love, dedication, and memories that will last a lifetime.

To my husband, Regnar Llego Madarang, and my children,
Eva Silva Madarang and Regnar Silva Madarang, for their love.

Contents

Preface

Since the subject of nuclear magnetic resonance (NMR) was awarded its first Nobel Prize in 1952 due to its successful detection by Bloch and Purcell in 1945, the technology and its applications have developed tremendously. The first two decades were focused on technical developments of instrumentation and methodologies to apply to the structure determination of compounds. During the late 1970s, several research groups developed modifications of NMR probes to convert them to an online mode for the analysis of sample mixtures. However, with the hardware and software technology available at that time, it was difficult to hyphenate high-performance liquid chromatography (HPLC) and NMR to perform those analyses. During the past two decades, interest in sample mixture analysis and screening methods has been the driver for the latest developments and applications of hyphenated analytical techniques with NMR. Improvements in solvent suppression NMR techniques have facilitated the coupling to NMR of HPLC with reversed-phase columns, for what is known today as LC-NMR. Further technological developments have also supported the hyphenation of mass spectrometry (MS) to LC-NMR as LC-MS-NMR. In addition, other analytical separation techniques have been hyphenated to NMR. However, the only ones commercially available and commonly used are capillary HPLC (capLC) as capLC-NMR and solid-phase extraction (SPE) as SPE-NMR, including SPE hyphenated to MS-NMR as SPE-MS-NMR. Many laboratories in industry and academia have NMR as a hyphenated technique as part of their instrumentation to solve structural problems. This technology has become an important option for complex analysis.

The aim of this book is to provide an overview of the applications of hyphenated NMR techniques in industry and academia. The book is focused on understanding the pros and cons of NMR as a hyphenated and a non-hyphenated technique for the structural determination analysis of samples as organic materials. The purpose of the basic overview of the main concepts for structural elucidation by NMR and technical issues for online NMR is to facilitate an understanding of the pros and cons of the technique. A major emphasis of the book is on the application of hyphenated NMR in industry and academia. For completeness, the book has a chapter dedicated to the historical development of hyphenated NMR techniques, and another chapter focused on a comparison of other methodologies used to analyze sample mixtures.

The book begins with a description of basic NMR concepts for the structural elucidation of organic compounds, the historical development of NMR and hyphenated NMR in the structural elucidation world, followed by applications of hyphenated NMR as LC-NMR and LC-MS-NMR in industry and academia, such as to natural products, degradation products, impurity characterization, drug metabolism, food analysis, drug discovery, polymers, and others. Another chapter is dedicated to other analytical separation techniques hyphenated with NMR and MS-NMR, with special emphasis on capillary capLC and SPE due to be available commercially, and their applications compared to the other hyphenated NMR techniques. A special chapter is directed at understanding the applications of NMR online and off-line for structure elucidation, chiral analysis, in situ reaction monitoring, and analysis of sample mixtures by other NMR methodologies.

The audience for this book includes scientists in industry and academia who work and analyze complex sample mixtures in the areas of organic chemistry, medicinal chemistry, process chemistry, analytical chemistry, drug metabolism, separation science, natural products, chemical engineering, and others. In addition, the book contains the fundamentals of NMR and applications of hyphenated NMR techniques for college instructors to use as a complementary textbook for undergraduate and, especially, for graduate courses. The book is an excellent source of information and references for NMR basics, especially for applications of hyphenated NMR in industry and academia. The book also contains updated information on the latest advancements and applications of LC-NMR and other analytical techniques hyphenated with NMR focused on structural elucidation as of early 2011. The approach is based on explaining the basic pros and cons of the technique in a practical way, to make it easier for nonexperts in the field to understand the technology. Examples are provided, illustrated with figures and detailed explanations. Other books targeting those concepts have been used as reference material.

Previous to this book, I wrote some review articles and a book chapter. I gratefully acknowledge Elsevier for permitting me to use materials from one

of the review articles [M.V. Silva Elipe, Advantages and Disadvantages of Nuclear Magnetic Resonance Spectroscopy as Hyphenated Technique, *Anal. Chim. Acta* **497** (2003), 1–25]. My sincere gratitude to Dr. Ray Bakhtiar (Drug Metabolism of MRL at Rahway) and Dr. Byron H. Arison (currently retired but previously at Drug Metabolism of MRL at Rahway) for their interest, support, and encouragement through constructive discussions, and to D. Knapp and U. Parikh (Medicinal Chemistry of MRL at Rahway) for technical help in online connection of radioactivity and MS detectors to an LC-NMR system. I am especially thankful to my father, Joaquin Silva Garcia, and my mother, Maria Elipe Ruiz, for their encouragement, love, and dedication to their children (the author and her siblings, Pedro Luis Silva Elipe and Maria Eva Silva Elipe). Last but not least, I thank my husband, Regnar Llego Madarang, for his support, and my children, Eva Silva Madarang and Regnar Silva Madarang, for their patience and support. There are not enough words to express my appreciation.

MARIA VICTORIA SILVA ELIPE

Thousand Oaks, California

Abbreviations, Symbols, and Units

ACN	acetonitrile
ACN-*d3*	deuterated acetonitrile
API	atmospheric pressure ionization, active principal ingredient
APCI	atmospheric pressure chemical ionization
B	applied magnetic field along x or y axis
B_{eff}	effective magnetic field
bd	broad doublet
B_0	applied magnetic field along z axis
bs	broad singlet
bt	broad triplet
°C	degree Celsius or centigrade
capLC	capillary liquid chromatography
CAT	computer of averaging transients
CD	circular dichroism
CD_3CN	deuterated acetonitrile
CD_3OD	deuterated methanol
CE	capillary electrophoresis
CEC	capillary electrochromatography
CHPLC	capillary high-performace liquid chromatography
CI	chemical ionization
cIPT	capillary isotachophoresis
cm	centimeter
COSY	correlation spectroscopy
CW	continuous wave

CYP	cytochrome P450 enzyme
CZE	capillary zone electrophoresis
d	doublet
D	deuterium
1D	one dimension
2D	two dimensions
Da	dalton
dd	doublet of doublets
ddd	doublet of doublet of doublets
DEPT	distortionless enhancement by polarization transfer
DEPT-135	distortionless enhancement by polarization transfer at 135° angle
DEPTQ	distortionless enhancement by polarization transfer, including the detection of quaternary nuclei
DI	direct injection
DMSO-*d6*	dimethyl-*d6* sulfoxide
DNP	dynamic nuclear polarization
D_2O	deuterated water or deuterium oxide
DOSY	diffusion-ordered spectroscopy
DQF	double quantum filter
dt	doublet of triples
E	energy
EOF	electroosmotic flow
EPR	electron paramagnetic resonance
ERETIC	electronic reference to access in vivo concentrations
ESI	electrospray ionization
FIA	flow injection analysis
FID	free induction decay
FT	Fourier transform
GC	gas chromatography
GHz	gigahertz
GPC	gel permeation chromatography
GSH	glutathione
h	Planck's constant
HETCOR	heteronuclear correlation spectroscopy
HMBC	heteronuclear multiple bond correlation
HMQC	heteronuclear multiple quantum correlation
HOD	residual water from deuterated solvents
HPLC	high-performance liquid chromatography
HSQC	heteronuclear single quantum coherence
Hz	hertz
I	nuclear spin

ICH	International Conference of Harmonisation of Technical Requirements
INADEQUATE	incredible natural abundance double quantum transfer experiment
INEPT	intensive nuclei enhanced by polarization transfer
IR	infrared
J	coupling constant
k	Boltzmann constant
K	kelvin
LC	liquid chromatography
LOD	limit of detection
μL	microliter
mL	milliliter
m	meter; multiplet
mm	millimeter
M	molar; molecular ion
mM	millimolar
μM	micromolar
ms	millisecond
MEK	methyl ethyl ketone
MHz	megahertz
MS	mass spectrometry
MSPD	matrix solid-phase dispersion
MW	molecular weight
m/z	mass over charge
NMR	nuclear magnetic resonance
NOE	nuclear Overhauser effect
NOESY	nuclear Overhauser effect spectroscopy
oct	octet
PAT	process analytical technology
PCA	principal components analysis
pCEC	pressured capillary electrochromatography
PEEK	poly(ether ether ketone)
PKDM	pharmacokinetics drug metabolism
ppm	part per million
q	quartet
qNMR	quantitation NMR
qui	quintet
RDC	residual dipolar coupling
RF	radio frequency
ROE	rotating frame Overhauser effect
ROESY	rotating frame Overhauser effect spectroscopy

RT	room temperature
s	seconds; singlet
SEC	size-exclusion chromatography
SFE	supercritical fluid extraction
SFC	supercritical fluid chromatography
S/N	signal-to-noise ratio
SPE	solid-phase extraction
spt	septet
sxt	sextet
t	triplet
T	temperature, tesla
T_1	spin-lattice or longitudinal relaxation time
T_2	spin-spin or transverse relaxation time
td	triplet of doublets
TIC	total ion chromatogram
TMS	tetramethylsilane
TOCSY	total correlation spectroscopy
UF	ultrafast
UV	ultraviolet
WET	water suppression enhanced through T_1 effects

γ	gyromagnetic ratio
δ	chemical shift
ν	frequency
σ	shielding constant
τ_c	correlation time
ω_0	Lamour frequency

1

Basic Concepts of NMR Spectroscopy

1.1. INTRODUCTION

Nuclear magnetic resonance, known widely as NMR spectroscopy, is a powerful technique applied extensively to the structural elucidation of organic compounds. Since its discovery in the early twentieth century, NMR has been in wide use while evolving to what it is today. Understanding the basic concepts in interpreting NMR spectra is fundamental for the structural analysis of organic compounds. In this chapter we introduce the reader to the basic concepts of NMR data interpretation. The major topics discussed provide information on the chemical structures of organic compounds, and the connectivities and correlations of atoms through bonds and space. Understanding how to interpret NMR data from hyphenated and nonhyphenated NMR instruments is essential. This chapter is not intended to explain the theory of NMR with mathematical equations and algorithms, as these can be found elsewhere [1–4]. In addition, more detailed information from a practical perspective with less focus on mathematical algorithms is available in the literature [5–16].

LC-NMR and Other Hyphenated NMR Techniques: Overview and Applications, First Edition. Maria Victoria Silva Elipe.

1.2. BASIC KNOWLEDGE REGARDING THE PHYSICS OF NMR SPECTROSCOPY

Spectroscopy studies the interaction of matter with electromagnetic radiation, resulting in absorption or emission of energy. When energy is in the radio-frequency (RF) region ($>10^6$ to 10^8 Hz), nonionizing radiation energy is used to quantize the energy levels of spin nuclei (Figure 1-1). Nuclear magnetic resonance is an absorption spectroscopy that involves the magnetic properties of atomic nuclei. Under a magnetic field in the RF region, nuclei with magnetic moments can have different energy levels, and those absorption energy transitions can be measured by NMR. Following are the basic rules regarding nuclei magnetic moments and their nuclear spin based on their nuclear properties.

- Nuclei with an odd mass number have half-integer nuclear spin I (e.g., $I = 1/2$ for ^{1}H, ^{13}C, ^{15}N, ^{31}P, ^{19}F, ^{29}Si; $I = 3/2$ for ^{23}Na, ^{11}B; $I = 5/2$ for ^{17}O).
- Nuclei with an even mass and an even atomic number have zero nuclear spin I (e.g., $I = 0$ for ^{12}C, ^{16}O).
- Nuclei with an even mass number and an odd atomic number have integer nuclear spin I (e.g., $I = 1$ for ^{2}H, ^{14}N; $I = 3$ for ^{10}B).

Table 1-1 displays the nuclear spin properties of the most common nuclei studied in the field of organic molecules. Under a magnetic field, a nucleus with nuclear spin will present a concrete number of energy levels. The number

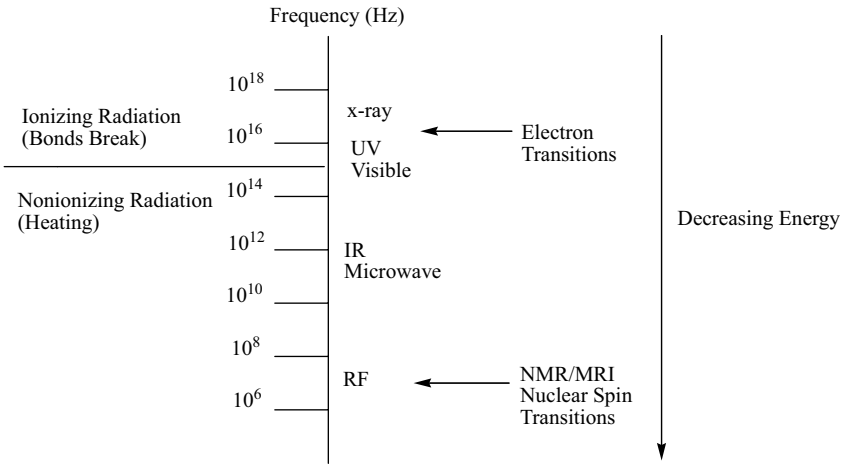

FIGURE 1-1. Electromagnetic radiation energy spectrum as frequency (Hz).

TABLE 1-1. Properties of Some Common Nuclei in Organic Molecules

Nucleus	Spin I	Natural Abundance (%)	Sensitivity (Relative to ^{1}H)	Gyromagnetic Ratio γ (10^7 rad T^{-1} s^{-1}]	Frequency (MHz) at $B_0 = 2.3488$ T
^{1}H	1/2	99.985	1	26.7519	100.0
^{2}H	1	0.015	9.65×10^{-3}	4.1066	15.351
^{10}B	3	19.58	1.99×10^{-2}	2.8747	10.746
^{11}B	3/2	80.42	0.17	8.5847	32.084
^{12}C	0	98.9			
^{13}C	1/2	1.108	1.59×10^{-2}	6.7283	25.144
^{14}N	1	99.63	1.01×10^{-3}	1.9338	7.224
^{15}N	1/2	0.37	1.04×10^{-3}	−2.7126	10.133
^{16}O	0	99.96			
^{17}O	5/2	0.037	2.91×10^{-2}	−3.6280	13.557
^{19}F	1/2	100	0.83	25.1815	94.077
^{23}Na	3/2	100	9.25×10^{-2}	7.0704	26.451
^{29}Si	1/2	4.70	7.84×10^{-3}	−5.3190	19.865
^{31}P	1/2	100	6.63×10^{-2}	10.8394	40.481

Source: Data from references 6 and 24.

of levels depends on the magnetic moment of each nucleus and follows the rule $2I + 1$, where I is the nuclear spin number [e.g., for $I = 1/2$, two is the number of energy levels [$2(1/2) + 1 = 2$] with an α spin state, or $I_1 = +1/2$, for the low energy level and a β spin state or, $I_2 = -1/2$, for the high energy level, for nuclei with a positive gyromagnetic ratio, as indicated below]. For nuclear spin $I = 1/2$ (e.g., ^{1}H and ^{13}C), each nucleus can be displayed as a magnet randomly oriented in any direction (Figure 1-2a). Under the magnetic field, those magnets in the sample have two orientations, aligned or opposite to the direction of the applied magnetic field (Figure 1-2b). The distance between the energy levels depends on the strength of the magnetic field applied and the gyromagnetic ratio for the particular nucleus. For nuclei with $I = 1/2$ and a negative gyromagnetic ratio, such as ^{15}N and ^{29}Si, β is the lower spin state ($I_1 = -1/2$) and α is the higher spin state ($I_2 = +1/2$). The difference in energy (ΔE) for the transition to occur is

$$\Delta E = h\nu = \frac{h\gamma B_0}{2\pi}$$

where ν is the frequency of the transition, γ is the gyromagnetic ratio intrinsic per nucleus (see Table 1-1 for some examples), B_0 is the magnetic field applied, and h is Planck's constant. Figure 1-3 depicts the energy-level separation for a nucleus with half-integer nuclear spin ($I = 1/2$; e.g., ^{1}H and ^{13}C) pointing to the different energy when a magnetic field strength of 300 MHz (7.05 T) or 600 MHz (14.10 T) is applied to the nucleus.

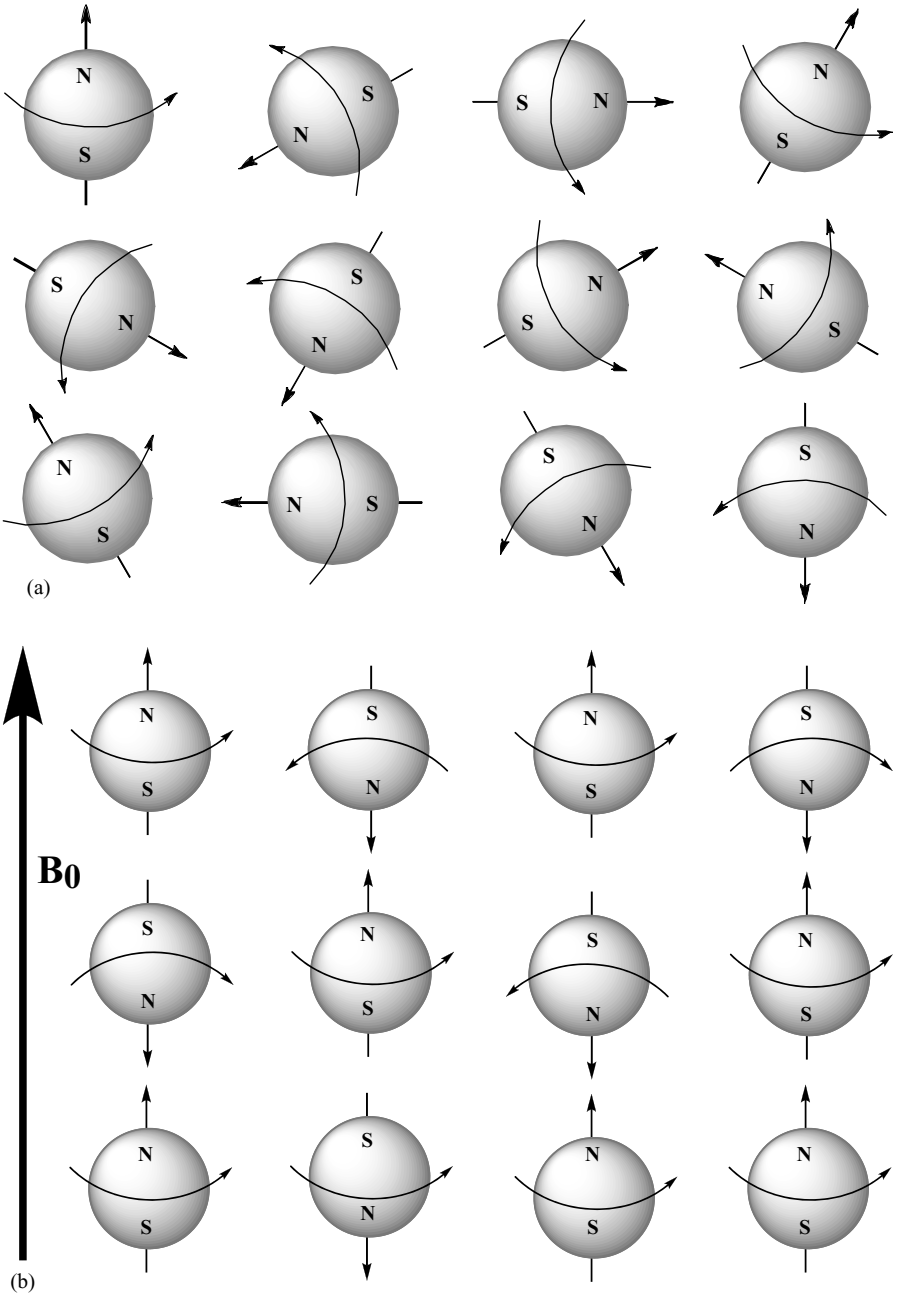

FIGURE 1-2. Orientation of the nuclear spins as simple magnets for $I = 1/2$ in the absence of an external magnetic field (except for the Earth's magnetic field) (a) or the presence (b) of an external magnetic field (different from the Earth's magnetic field).

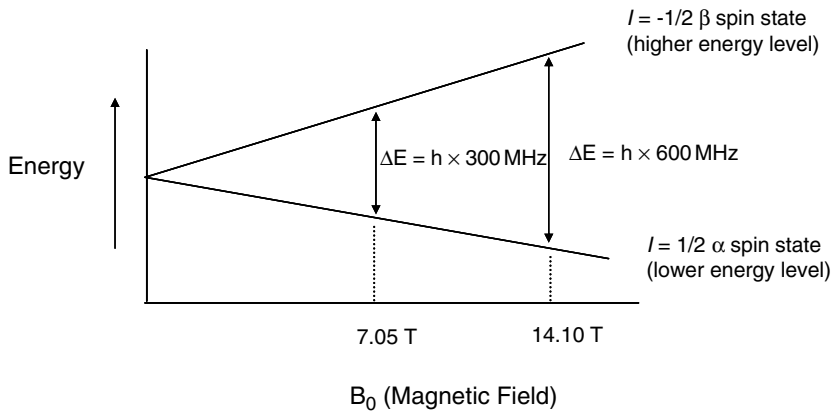

FIGURE 1-3. Graphical relationship between magnetic field (B_0) and frequency (ν) for nuclei with nuclear spin $I = 1/2$ and positive gyromagnetic ratio (e.g., ^{1}H, ^{13}C, ^{31}P, ^{19}F) NMR absorptions. For nuclei with $I = 1/2$ and negative gyromagnetic ratio such as ^{15}N and ^{29}Si, β is the lower spin state and α is the higher spin state. The graph is not to scale.

Conventionally, the frequency unit megahertz is used for proton ^{1}H to denominate the strength of the magnetic field instead of the magnetic field unit tesla. Unfortunately, NMR spectroscopy is a low-sensitivity technique because the energy difference between the levels (ΔE) of the nuclear spin states is much less than the thermal energy (kT, where k is the Boltzmann constant and T is the temperature) at normal or room temperature (around 25°C). This energy difference is also an indication of the small difference in the population of nuclei between the two spin states. The slight excess of population in the lower-energy state is in agreement with the Boltzmann distribution. The energy difference is proportional to the magnetic field applied (B_0); therefore, increasing the strength of the magnetic field increases the population difference of the spin states and the sensitivity (Figure 1-3). The distribution of nuclei between two spin states is given by the Boltzmann equation,

$$\frac{N_\alpha}{N_\beta} = e^{-\Delta E/kT} \approx 1 - \frac{\Delta E}{kT} = 1 - \frac{h\gamma B_0}{2\pi kT}$$

where N_α and N_β are the number of nuclei in the ground state α and the excited state β. For the case of a magnetic field of 60 MHz (1.41 T) and 300 K (27°C), the population ratio for ^{1}H is $N_\alpha/N_\beta \approx 0.9999904$, and for a magnetic field of 300 MHz (7.05 T), $N_\alpha/N_\beta \approx 0.99995$. Figure 1-2b is a simplistic representation of the small excess in the population of nuclei in the lower energy level for nuclei aligned with the external applied magnetic field. Overall, with the small difference in energy level, energy transitions of nuclear spins can occur with a

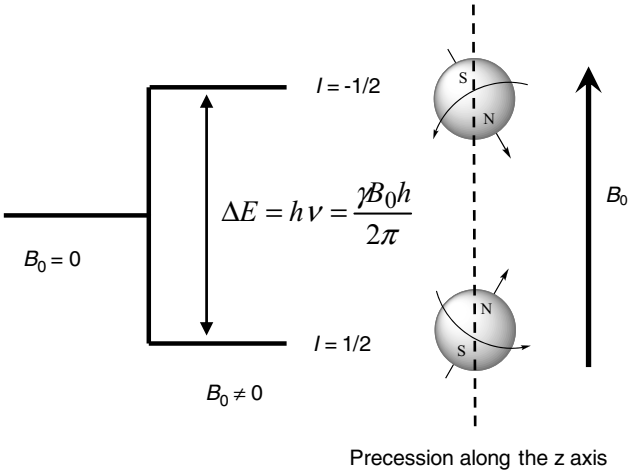

FIGURE 1-4. Classical representation of the energy levels and precession of the two spin states for nuclei with half-integer nuclear spin ($I = 1/2$; e.g., ^{1}H, ^{13}C, ^{31}P, ^{19}F). For nuclei with $I = 1/2$ and negative gyromagnetic ratio such as ^{15}N and ^{29}Si, β is the lower spin state ($I = -1/2$) and α is the higher spin state ($I = 1/2$).

second RF pulse applied to nuclei with a magnetic moment. From a practical perspective, acquiring multiple scans improves the signal-to-noise (*S*/*N*) ratio of a spectrum by the square root of the number of scans (n):

$$\frac{S}{N} = \sqrt{n}$$

Therefore, the number of scans has to increase fourfold to double the signal-to-noise ratio. When nuclei are under an external magnetic field, they precess along the axis of the field, conventionally the z-axis. Figure 1-4 is a pictorial representation of the two energy levels of a nucleus with $I = 1/2$ (e.g., ^{1}H and ^{13}C) under a magnetic field based on its orientation. The nucleus is considered a micromagnet that under a magnetic field can rotate clockwise or counterclockwise. Those two rotations represent the two energy levels of the half-integer nuclear spin. For nuclei with $I = 1/2$ and a negative gyromagnetic ratio, such as ^{15}N and ^{29}Si (see Table 1-1), the energy levels are reversed, with β for the lower spin state ($I = -1/2$) and α for the higher spin state ($I = 1/2$). Having a negative gyromagnetic ratio also decreases the population ratio between the two nuclear spin levels, which contributes to making the nuclei less sensitive.

This book focuses primarily on nuclei with a nuclear spin of half-integer $I = 1/2$ (e.g., ^{1}H, ^{13}C, ^{15}N, ^{19}F, ^{31}P), the major nuclei present in organic

compounds. Under a magnetic field, a nucleus with a half-integer nuclear spin will rotate or precess along the axis of the applied magnetic field (normally the z-axis) at the Lamour frequency $\nu = \gamma B_0$, where ν is the Lamour frequency, γ is the gyromagnetic ratio intrinsic per nucleus, and B_0 is the external magnetic field (Figure 1-4). Transitions occur when a second RF pulse perpendicular to the external magnetic field is applied to the sample within a short time frame. Those transitions are detected by a detector in the xy-plane and converted to an appropriate format for interpretation.

As in any other type of spectroscopy, after radiation to reach a high energy level over a period of time, spin nuclei will return to the ground state through different mechanisms. The NMR signal is termed free induction decay (FID) because it is free of the influence of the particular RF field, it is induced in the coil, and it decays back to equilibrium. Magnetization is the sum of all the magnetic moments in the sample for a particular nucleus (e.g., ^{1}H). In NMR, there are two mechanisms that bring the magnetization to the ground state: spin–lattice or longitudinal (along the z-axis) relaxation (T_1) and spin–spin or transverse (perpendicular to the z-axis and in the xy-plane) relaxation (T_2). T_1 is the time to transfer energy from the magnetization going from the excited to the ground state in the z-axis, and T_2 is the time to transfer energy within the precessing nucleus (e.g., ^{1}H) in the xy-plane to the ground state through dephasing, line broadening, and consequently, loss of signal. More details on those relaxation mechanisms may be found in the literature [1–12,15–17]. T_1 and T_2 values are influenced by the size of the molecule based on molecular weight and affect the quality of the NMR signal. T_1 and T_2 are in the same range ($T_1 \approx T_2$) for small molecules (e.g., methanol) that tumble fast in solution. T_1 is greater than T_2 ($T_1 > T_2$) for large molecules (e.g., proteins, polymers) that tumble more slowly in solution. T_1 is much greater than T_2 ($T_1 \gg T_2$) for solid or crystalline samples in the solid state, which makes the NMR lines much broader than they are in liquids, affecting the resolution due to short T_2's [1–12,15–17].

1.3. BASIC PARAMETERS FOR NMR INTERPRETATION

The NMR spectra of half-integer nuclei ($I = 1/2$; e.g., ^{1}H, ^{13}C, ^{15}N, ^{31}P, and ^{19}F) are the focus of this book and provide structural information on how the atoms are connected to each other through bonds and relative orientations in space. The parameters containing structural information are chemical shifts, spin–spin coupling constants, spin systems, signal intensities, and bond and spatial correlations: the most commonly used parameters for the structural elucidation of organic compounds. These parameters are described below with examples illustrating their significance in the world of structural elucidation in organic chemistry.

1.3.1. Chemical Shift

Since the discovery of NMR, technology has played an important role in its development. From the early electromagnets and permanent magnets to the current superconducting magnets, the magnetic field of NMR instruments has increased from the first 40-MHz instruments to the 900-MHz instruments available at present. At the time of this writing, 1-GHz NMR instruments are almost ready to become available commercially. The most common NMR instruments used in the field of small molecules are between 300 and 600 MHz. Occasionally, 800-MHz NMR instruments are used when sample quantity is limited. By using greater magnetic field instruments with cryogenic probes, increased sensitivity can be achieved. Data from a sample acquired using instruments that have different magnetic fields are difficult to compare on the scale of frequency units because the energy absorption is different with different magnetic fields. Over the years it became obvious that uniformity of scale was needed for NMR spectra, regardless of the strength of the magnetic field of the instrument used to acquire the data. Historically, tetramethylsilane (TMS) was selected as a reference compound because it is chemically inert, volatile [boiling point (bp) 27°C], symmetrical, and soluble in most organic solvents. There were a variety of approaches, but over the years, chemical shift in parts per million (ppm) has been shown the success of the best uniformity on the NMR scale. The chemical shift (δ) is defined as

$$\delta = \frac{\nu_{\text{sample}} - \nu_{\text{standard (TMS)}}}{\nu_{\text{spectrometer}}} \times 10^6$$

where ν_{sample} is the resonance frequency of the protons of the sample, $\nu_{\text{standard(TMS)}}$ is the resonance frequency of TMS as the standard, and $\nu_{\text{spectrometer}}$ is the frequency of the spectrometer where the data are acquired (e.g., 600-MHz instrument). For TMS, the chemical shift of the methyl protons is assigned conventionally to 0.00 ppm, based on the definition of chemical shifts. Figures 1-5 and 1-6 depict the spectra of a 3-vinylphenol compound simulated at frequencies of 60 to 600 MHz in the frequency domain and on the chemical shift scale, respectively. Obviously, comparison of the data for any molecule in the frequency domain becomes difficult, but it is straightforward on the chemical shift scale, which has become the standard scale for NMR spectroscopy. Another observation from Figures 1-5 and 1-6 is that increasing sensitivity and resolution are achieved by increasing the magnetic field. At higher magnetic fields, analysis of the NMR data becomes less cumbersome than analysis at lower fields. For 3-vinylphenol, all the protons have a distinct resonance

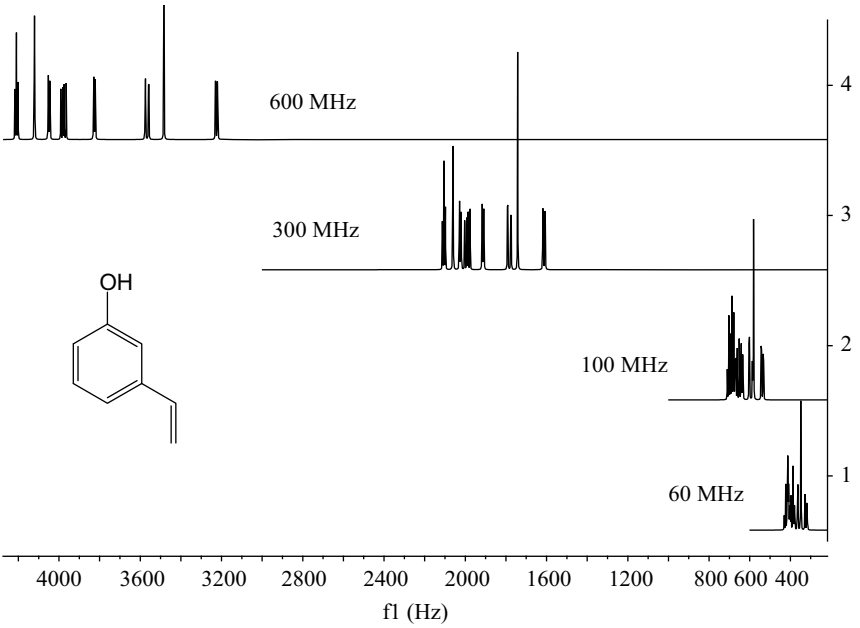

FIGURE 1-5. Simulated ^{1}H NMR spectra of 3-vinylphenol at magnetic fields of 60, 100, 300, and 600 MHz, respectively on the frequency scale (in hertz) from bottom to top.

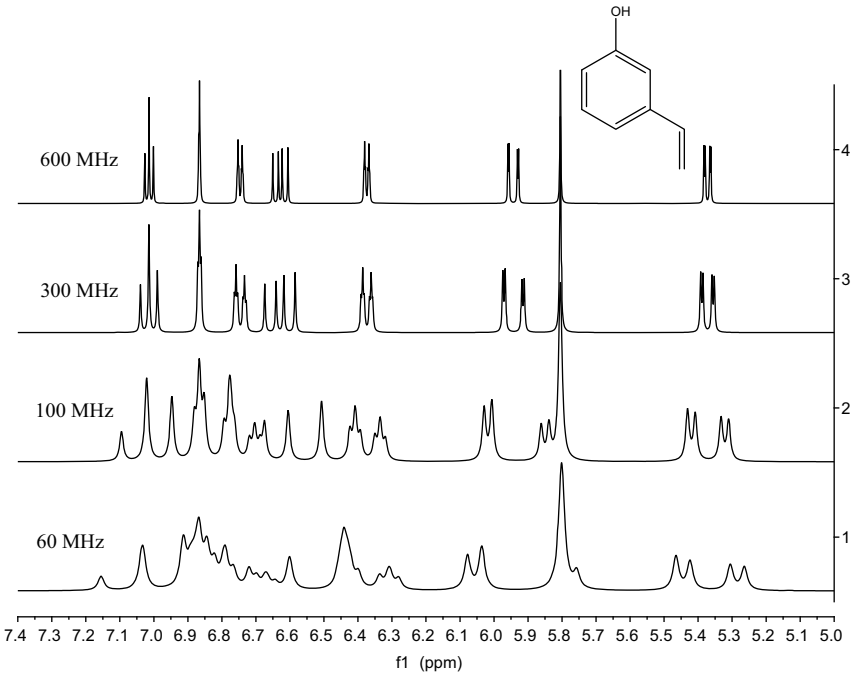

FIGURE 1-6. Simulated ^{1}H NMR spectra of 3-vinylphenol at magnetic fields of 60, 100, 300, and 600 MHz on the chemical shift scale (ppm) from bottom to top, respectively.

TABLE 1-2. Typical Ranges of ^{1}H and ^{13}C Chemical Shifts for Common Functional Groups in Organic Compounds

Functional Group	^{1}H (δ/ppm)	^{13}C (δ/ppm)
TMS (tetramethylsilane)	0.0	0.0
Primary alkyl (RCH_3)	0.7–1.3	0–30
Secondary alkyl (R_2CH_2)	1.2–1.5	15–45
Tertiary alkyl (R_3CH)	1.4–1.7	30–50
Quaternary alkyl (R_4C)		35–70
Allylic (−C=C−CH)	1.6–2.3	
Vinylic/alkene (R_2C=CH)	4.5–6.5	80–145
Acetylenic/alkyne (R−CΞCH)	2.5–3.0	70–90
Benzylic methyl ($ArCH_3$)	2.2–2.8	20–65
Aromatic (CH of Ar)	6.0–9.0	110–170
Alkyl fluoride (F−CH)	4.1–4.7	70–80
Alkyl chloride (F−CH)	3.6–3.8	25–50
Alkyl bromide (Br−CH)	3.4–3.6	10–40
Alkyl iodide (I−CH)	3.1–3.3	0–40
Alcohol/ether (O−CH)	3.1–4.0	50–90
Aldehyde (O=C−H)	9.0–10.0	180–210
Carboxylic acid (O=C−OH)	10.0–13.0	170–180
Carbonyl ketone (R_2C=O)		190–220
Carbonyl ester/amide (R−COOR, $R-CONR_2$)		150–180
Alcohols (R−OH)	2.5–5.0 (variable)	
Phenols (Ar−OH)	5.0–10.0 (variable)	
Amines ($R-NH_2$, R_2-NH)	0.5–4.0 (variable)	
Amines ($Ar-NH_2$, Ar_2-NH)	6.0–9.0 (variable)	
Ammoniums ($R-NH_3^+$, $R_2-NH_2^+$, R_3-NH^+)	2.5–5.0 (variable)	
Ammoniums ($Ar-NH_3^+$, $Ar_2-NH_2^+$, Ar_3-NH^+)	6.0–9.0 (variable)	

Source: Data from references 18 and 24.

frequency. However, in the case of a molecule with equivalent protons, such as the protons of a methyl group, the equivalent protons will resonate at the same frequency.

Table 1-2 shows the typical ranges of ^{1}H and ^{13}C chemical shifts for common functional groups in organic compounds. As shown in the table, carbons resonate at a greater range of frequencies than that of protons and spread their signals over a wider scale (ca. 0 to 13 ppm for ^{1}H and 0 to 220 ppm for ^{13}C), which decreases signal overlapping and facilitates assignments. For any nucleus, the location of the chemical shift signals depends on the local influence of the electronic layer surrounding the functional groups. When an external magnetic field is applied, the electrons surrounding a nucleus (e.g., ^{1}H, ^{13}C) will circulate perpendicular to the field, creating an induced magnetic field opposed to the applied external magnetic field in the area of the nucleus. Therefore, the nucleus is under a weaker magnetic field than the externally applied field and is said to be *shielded*. This is the principle of the diamagnetic

shielding effect. The effective magnetic field (B_{eff}) that the nucleus experiences is described as

$$B_{\text{eff}} = B_0 - \sigma B_0 = (1 - \sigma)B_0$$

where B_0 is the external magnetic field and σ is the shielding constant. Substituting the value of the effective magnetic field in the equation of the energy difference (ΔE) for the transition to occur, the frequency of the transition (ν) can be deduced:

$$\Delta E = h\nu = \frac{h\gamma B_{\text{eff}}}{2\pi} = \frac{h\gamma(1 - \sigma)B_0}{2\pi}$$

$$\nu = \frac{\gamma(1 - \sigma)B_0}{2\pi}$$

The strength of the induced magnetic field is proportional to the applied magnetic field. Therefore, the diamagnetic shielding increases with the strength of the applied external magnetic field. Also, the higher the electron density is around the proton, the higher the diamagnetic shielding and the larger the value of σ. With a larger value of σ, the frequency and effective magnetic field of the transition for the nucleus will be lower, an upfield shift. For a lower value of σ for protons with lower electron density, the frequency of the transition and the effective magnetic field will be greater, a downfield shift. Conventionally, the terms *upfield* and *downfield shift* come from the first generation of NMR instruments, continuous-wave (CW) instruments that operated at a constant RF frequency and variable applied magnetic field strength. The term high field is used when the B_{eff} for the transition to occur is smaller than B_0 (large σ and low frequency). Therefore, to reach B_0 at a constant frequency, a greater field is needed. Following pattern, the same, the term *low field* comes when the B_{eff} for the transition to occur is greater than B_0 (small σ and high frequency). Therefore, to reach B_0 at a constant frequency, a smaller field is needed. In other words, the induced magnetic field generated by the electrons can be aligned or opposed to the applied magnetic field. If the induced field is opposed to the external applied field, the effective magnetic field is lower, with a larger value of σ. Therefore, the proton as an example of a nucleus with nuclear spin is shielded, resonating at a lower frequency, and absorptions are upfield or at lower energy than if no induced field is present. However, if the induced field reinforces the applied field, the proton experiences a greater magnetic or effective field with a smaller σ. Therefore, the proton experiences a deshielding effect, resonating to a higher frequency, and

absorptions are downfield or at higher energy than if no induced field is present.

Electronegativity, hybridization, inductive effect, and ring current effects are the major factors affecting the position in the scale for nuclei with half-integer spin (e.g., ^{1}H and ^{13}C) in functional groups. When a proton or a carbon is bonded to a heteroatom that is less electronegative than the proton or the carbon, the nucleus keeps its electronic cloud closer, producing a shielding effect, which is translated for the nucleus (proton or carbon) to resonate at a lower frequency and appear on the right side of the spectrum. In this case the nucleus is shielded and upfield-shifted on the δ scale. The methyl protons and carbons of TMS are considered some of the most upfield protons and carbons, and they have been positioned at 0 ppm on the δ scale for ^{1}H and ^{13}C NMR conventionally at the right side of the δ scale, at lower ppm values. If the nucleus is bonded to a more electronegative atom such as fluorine, oxygen, or an aromatic ring, the nucleus (proton or carbon) is under a deshielding effect because the electrons have a greater tendency to remain longer closer to the atom or functional group that is more electronegative; therefore, their proton and carbon signals will resonate to a higher frequency, appearing toward the middle left side of the chemical shift in the δ scale. Table 1-2 shows how fluorine affects the chemical shifts to protons and carbons stronger than oxygen, bromine, and iodine, due to fluorine's strong electronegativity properties (see Table 1-2 for chemical shift range variations when electronegative atoms or groups are present in a molecule). Inductive and mesomeric effects are important in these cases. Therefore, the proton or carbon is deshielded and downfield-shifted in the δ scale, where the proton or carbon resonates to a higher frequency than does TMS (see Table 1-2 for cases of multiple bonds). More information on how functional groups affect the proton and carbon chemical shifts may be found in the literature [18].

Ring current effects are important for molecules with aromatic rings and multiple bonds. In general, multiple bonds have electrons in the π molecular orbitals that induce a local magnetic field when being under an external magnetic field. The induced magnetic field opposes the externally applied magnetic field, giving the multiple bonds a particular spatial orientation that affects the resonance frequency of the bonded protons or carbons in proximity to the multiple bonds. Figure 1-7 depicts the preferred orientation for benzene, a carbonyl of an aldehyde functional group, a double bond of the olefinic or vinyl group, and a triple bond of an acetylenic group. Protons (and carbons) in the shielded area will resonate at a lower frequency and be upfield-shifted. On the contrary, protons (and carbons) in the deshielded area will resonate at a higher frequency and be downfield-shifted. Acetylene protons and its carbons are the least deshielded of the multiple-bond functional groups, due to the additional π bonds, which affect how the molecule orients under the magnetic field.

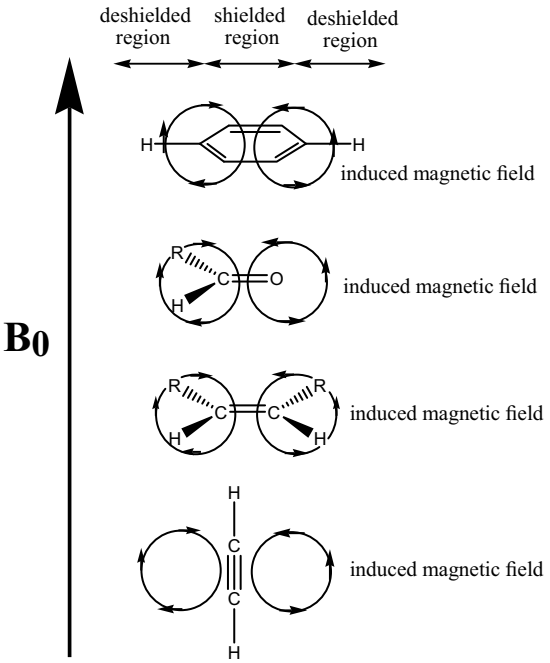

FIGURE 1-7. Shielding and deshielding zones for benzene protons (ring current effect), aldehydic proton, olefinic or vinyl protons, and acetylenic protons based on their preferred aligned orientation under an externally applied magnetic field B_0 from top to bottom, respectively.

Figure 1-7 depicts the distinct orientation of the acetylenic group compared to the vinyl and benzene groups. Table 1-2 shows the trend in the ^{1}H and ^{13}C chemical shifts of most common functional groups with multiple bonds, where protons and carbons of triple bonds are less deshielded than for double bonds and aromatic functional groups. More detailed information on shielding and deshielding and on ^{1}H and ^{13}C chemical shifts for functional groups in organic compounds may be found in the literature [6–8,10,16,18–27].

Figures 1-8 and 1-9 depict the one-dimensional ^{1}H and ^{13}C NMR spectra of sinomenine (Aldrich), an optical isomer of methoxythebaine as a morphine derivative or isoquinoline alkaloid. The numbers depict the atomic positions for protons and carbons in the structure and the position of their corresponding signals in the spectra (Figures 1-8 and 1-9). The proton and carbon chemical shifts follow the trend explained above, also indicated in the ranges in Table 1-2.

1.3.2. Spin–Spin Coupling Constants

The signals in the NMR spectra may split into more than one line if the nuclei interact with others that are bonded directly by one to three bonds. Coupling

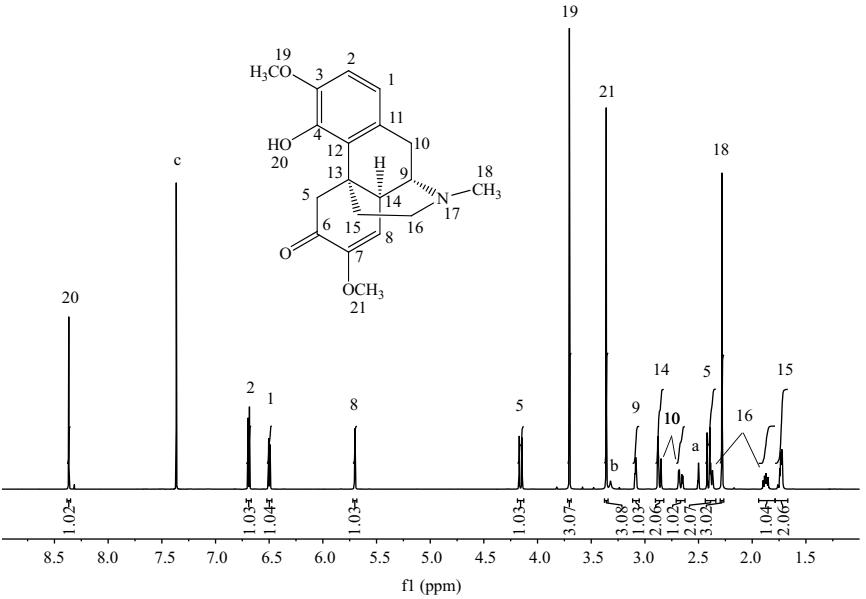

FIGURE 1-8. ^{1}H NMR spectrum of sinomenine in DMSO-*d*6 at 600 MHz with a cryogenic probe. The letters a, b, and c denote information on solvent peak for c, residual protonated water on DMSO-*d*6 (HOD) for b, and residual protonated DMSO-*d*6 (CD_2HSOCD_3) for a. The lines on top of the proton signals are the integrals, and the numbers below are their values, representing the number of protons per signal. The structure of sinomenine is attached for reference.

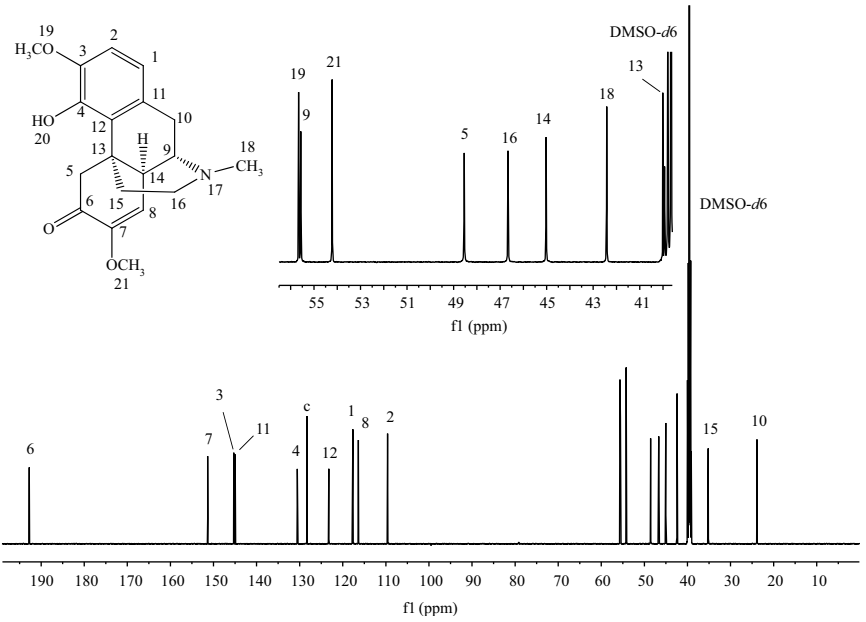

FIGURE 1-9. ^{13}C NMR spectrum of sinomenine in DMSO-*d*6 at 600 MHz with a cryogenic probe. The letter c denotes the signal as a solvent peak. The structure of sinomenine is attached for reference.

beyond three bonds is not common except for the case of ring strain, aromatic or unsaturated bonds connected through a "W" configuration, and coupling with heteroatoms such as ^{19}F and ^{31}P. This phenomenon is called *spin–spin coupling*, *scalar coupling*, or *J-coupling*. In this section we focus primarily on proton–proton spin couplings as the most significant and easiest to obtain, mainly through the one-dimensional ^{1}H NMR spectra of organic compounds. The splitting from spin–spin couplings is due to the interaction of proton nuclear spins with the bonding electrons in the molecule. Based on Pauli's principle, a stable state occurs when the bonding electrons between two nuclei are paired with antiparallel spins. In general, when two vicinal protons have different chemical environments, they affect each other by their two nuclear spin orientations through the bonding electrons, and each proton will appear as two signals or as a doublet separated by the same frequency difference. This frequency difference is the spin–spin coupling constant, J (in hertz).

The number of lines and the intensity of the signals follows Pascal's triangle using the $n+1$ rule, where n is the number of neighboring protons (Table 1-3). For example, in an ethyl group ($-CH_2-CH_3$), the methyl protons appear as a triplet (i.e., three signals) because $n+1=2+1=3$, where the number 2 for n ($n=2$) comes from the two neighboring protons of the CH_2 group. In the triplet, the middle signal has double intensity, as Pascal's triangle indicates. The methylene group shows as a quartet (i.e., four lines) because $n+1=3+1=4$, where the number 3 for n ($n=3$) comes from the three neighboring protons of the CH_3. Figure 1-10 depicts the type of signal described in Table 1-3 that follows Pascal's triangle. Pascal's triangle is applicable to the protons in aliphatic carbon chains (e.g., hydrocarbons). The proton spin coupling constant, vicinal coupling via three bonds (^{3}J coupling for protons separated by three bonds, H−C−C−H, where the number 3 indicates the number of bonds between the protons), for the aliphatic carbon chain is around 7 Hz for free rotation. When the rotation is restricted, the vicinal coupling

TABLE 1-3. Pascal's Triangle of Multiplicities, Relative Intensities, and Signal Types Based on the Number of Neighboring Protons

Number of Neighboring Protons (n)	Multiplicities ($n+1$)	Relative Intensities	Type of Signal (Abbreviation)
0	1	1	singlet (s)
1	2	1 1	doublet (d)
2	3	1 2 1	triplet (t)
3	4	1 3 3 1	quarter (q)
4	5	1 4 6 4 1	quintet (qui)
5	6	1 5 10 10 5 1	sextet (sxt)
6	7	1 6 15 20 15 6 1	septet (spt)
7	8	1 7 21 35 35 21 7 1	octet (oct)

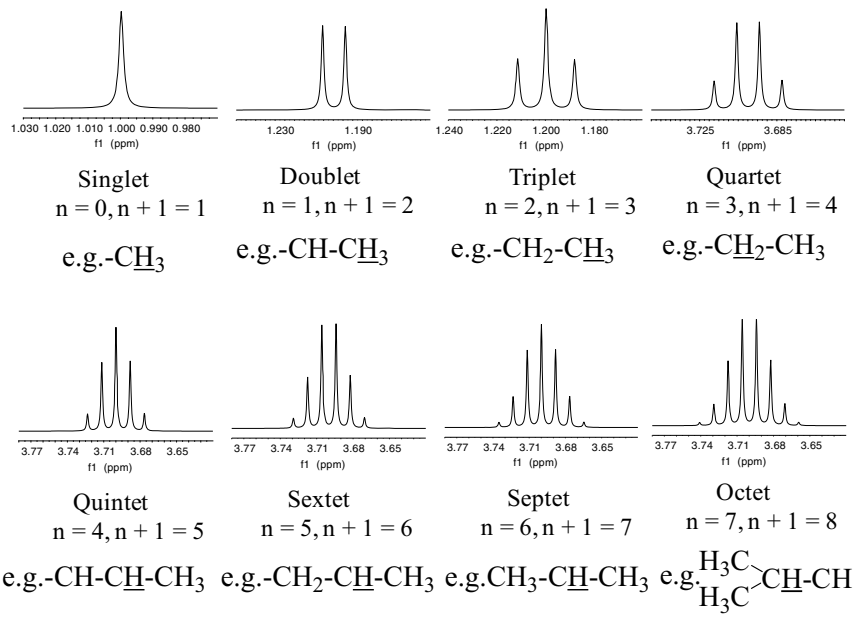

FIGURE 1-10. Simulated representation of the multiplicity of splitting patterns from Pascal's triangle in Table 1-3. The chemical shift scales have been selected arbitrarily. The heights of the individual signals and the multiplets are not in scale relative to each other.

constants vary with the dihedral angle between the protons. The Karplus equations attempt to explain the dependence of the dihedral angles on the value of the coupling constants. For example, for a dihedral angle of 0° or 180°, the coupling constant is greatest (8 to 18 Hz), and when the angle is 90°, the coupling constant reaches a minimum value of zero. Angles in between will be associated with coupling constants in between the highest and lowest values. In the case of enantiotopic geminal protons of a methylene group, the spin proton coupling constant, geminal coupling via two bonds (^2J coupling for protons separated by two bonds, H−C−H), is larger (11 to 14 Hz) than that of vicinal protons (see Table 1-4 for more details). These protons will appear as doublets if no other neighboring protons are present in the molecule.

In the case of aliphatic cyclic rings, the coupling constants depend on the size of the ring. For six-membered rings, the chair conformation is normally the lowest in energy; therefore, axial and equatorial protons interact, giving rise to three types of spin–spin coupling constants for protons in neighboring or vicinal carbons: axial–axial ($^3J_{\text{ax-ax}} \sim 8$ to 13 Hz), axial–equatorial ($^3J_{\text{ax-eq}} \sim 2$ to 6 Hz), and equatorial–equatorial ($^3J_{\text{eq-eq}} \sim 2$ to 5 Hz) (see Table 1-4 for more details). In general, the axial–equatorial couplings are larger than equatorial–equatorial couplings by 1 unit ($^3J_{\text{ax,eq}} \sim {}^3J_{\text{eq,eq}} + 1$).

TABLE 1-4. Typical Absolute Values of Proton–Proton Spin–Spin Coupling Constants (Hz) for the Most Common Functional Groups in Organic Compounds

Type of Protons	^2J (Geminal)	^3J (Vicinal)	^4J	^5J
Aliphatic chain	8–18	~7 (free rotation) 0–18 (restricted rotation)		
Six-membered rings	11–14	8–13 (ax.–ax.) 2–6 (ax.–eq.) 2–5 (eq.–eq.)		
Alkenes (vinyl)	~2.5	7–11 (*cis*.) 12–18 (*trans*)		
Allylic (H−C=C−C−H)			2–3 (cisoide) 3–4 (transoide)	
Homoallylic (H−C−C=C−C−H)				0–3 (cisoide) 0–3 (transoide)
Aromatic rings		6–9 (*ortho*)	1–3 (*meta*)	0–1 (*para*) 0–1 (W-type)
Aromatic rings with nitrogen		4–6 (six-membered rings) 2–3 (five-membered rings)		

Source: Data from references 18 and 24.

More detailed information may be found in the literature for other ring cycles [18].

Double bonds show three types of couplings: geminal for protons attached to the same carbon ($^2J \sim 2.5$ Hz) which are smaller than for methylene protons ($^2J = 11$ to 14 Hz), and *cis* and *trans* coupling constants, where *trans* ($^3J \sim 12$ to 18 Hz) couplings are larger than *cis* ($^3J \sim 7$ to 11 Hz) couplings. Allylic coupling is a four-bond coupling (^4J) from the vinyl proton to the allylic proton (H−C=C−C−H): *cisoide* ($^4J \sim 2$ to 3 Hz) and *transoide* ($^4J \sim 3$ to 4 Hz). Homoallylic coupling is a five-bond coupling (^5J) from the protons bonded to allylic carbons (H−C−C=C−C−H): *cisoide* ($^5J \sim 0$ to 3 Hz) and *transoide* ($^5J \sim 0$ to 3 Hz). Aromatic rings such as benzene have three types of coupling constants—*ortho*, *meta*, and *para*—with *ortho* the largest and *para* the shortest ($^3J \sim 6$ to 9 Hz, $^4J \sim 1$ to 3 Hz, and $^5J \sim 0$ to 1 Hz for *ortho*, *meta*, and *para* coupling, respectively). In aromatic compounds such as fused aromatic rings, five- and even six-bond proton couplings can be observed when protons are in a zig zag or "W" configuration. These couplings are approximately 1 Hz or smaller. For aromatic rings with a nitrogen atom, the *ortho* coupling constants are smaller than for the same ring with only carbon atoms in the ring. For a six-membered ring such as pyridine, the *ortho* coupling constants are about 4 to 6 Hz, and for five-membered rings are about 2 to 3 Hz. Table 1-4 depicts the most typical proton spin–spin coupling constants in organic compounds. More detailed information on coupling constants may be found in the literature [18].

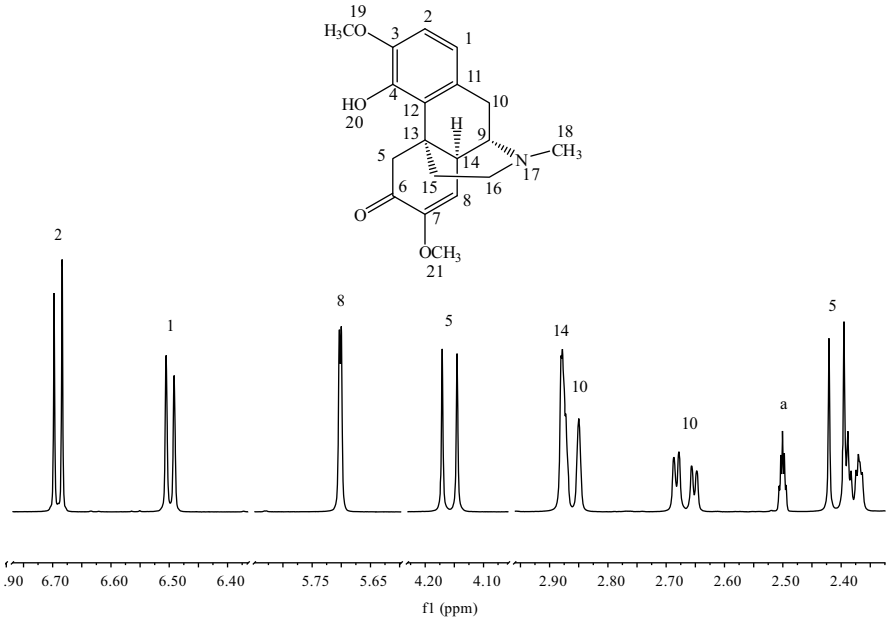

FIGURE 1-11. Expansion of the ^{1}H NMR spectrum of sinomenine. The letter a denotes the residual protonated DMSO-*d*6 (CD_2HSOCD_3). The structure of sinomenine is attached for reference.

Figure 1-11 shows some expansions of the ^{1}H NMR spectrum of sinomenine to visualize the multiplicity and couplings of some of the protons of the molecule. Notice that the proton H-1 is a doublet but broader than proton H-2 because its broadening is caused by the nonresolved small benzylic coupling with the methylene protons H-10. In addition, one of the protons H-10 shows clearly the doublet of a doublet splitting pattern, due to couplings with the other proton H-10 and the proton H-9. The splitting pattern of the solvent peak (methyl group) is a quintet, due to the coupling of deuterium with nuclear spin $I = 1$ and the proton for the residual protonated solvent signal of DMSO-*d*6 as CD_2HSOCD_3 ($2n + 1 = 2 \times 2 + 1 = 5$ signals with $n =$ number of D in the same carbon where H is). Table 1-5 displays the ^{1}H and ^{13}C chemical shifts, the proton–proton spin coupling constants, and the multiplicity of the proton signals for sinomenine extracted from Figures 1-8 and 1-9. Notice the distinct values of the ^{1}H and ^{13}C chemical shifts of methyl groups attached to nitrogen (H/C-18) and oxygen (H/C-19 and H/C-21), being shifted more downfield when they are attached to oxygen, due to oxygen being more electronegative than nitrogen.

Other nuclei, such as ^{19}F, will couple to neighboring protons (and carbons for their ^{13}C nuclei) with larger couplings than those of proton–proton coupling constants. In aliphatic chains, the absolute value ranges from 45 to 80 Hz for geminal proton–fluorine (H−C−F) coupling constants ($^{2}J_{HF}$), and 0 to 30 Hz for vicinal (H−C−C−F) couplings ($^{3}J_{HF}$) depending on the

TABLE 1-5. ^{1}H, ^{13}C, and ^{15}N Chemical Shifts (δ/ppm) of Sinomenine in DMSO-*d6*

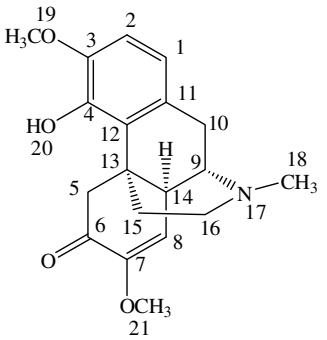

Position	^{1}H (δ/ppm, J/Hz)[a,b]	^{13}C (δ/ppm)[a]	^{15}N (δ/ppm)
1	6.50 (bd, $J = 8.3$ Hz, 1H)	117.7	
2	6.69 (d, $J = 8.3$ Hz, 1H)	109.6	
3		145.3	
4		130.5	
5	4.16 (d, $J = 15.4$ Hz, 1H)	48.5	
	2.41 (d, $J = 15.4$ Hz, 1H)		
6		192.8	
7		151.4	
8	5.70 (d, $J = 1.9$ Hz, 1H)	116.4	37.4
9	3.09 (bt, $J = 3.7$ Hz, 1H)	55.6	
10	2.86 (bd, $J = 18.5$ Hz, 1H)	23.9	
	2.67 (dd, $J = 18.5$, 5.4 Hz, 1H)		
11		145.0	
12		123.2	
13		40.0	
14	2.88 (bd, $J = 1.9$ Hz, 1H)	45.0	
15	1.74 (m, 2H)	35.2	
16	2.38 (ddd, $J = 11.5$, 9.0, 7.5 Hz, 1H)	46.7	
	1.88 (ddd, $J = 11.5$, 9.6, 6.2 Hz, 1H)		
17			
18	2.28 (s, 3H)	42.4	
19	3.70 (s, 3H)	55.7	
20	8.37 (s, 1H)		
21	3.36 (s, 3H)	54.2	

[a]Chemical shift references are assigned to the residual solvent peak to 2.50 ppm for CD_2HSOCD_3 for ^{1}H and 39.51 ppm for the methyl group of CD_3SOCD_3 for ^{13}C.

[b]Signal splitting patterns: s, singlet; d, doublet; dd, doublet of doublets; ddd, doublet of doublet of doublets; bd, broad doublet; bt, broad triplet; m, multiplet.

conformation of the molecule (0 to 5 Hz for synclinal and 10 to 25 Hz for antiperiplanar). In aromatic rings, the proton–fluorine coupling constants are somehow larger than the proton–proton couplings ($^{3}J_{HF} = 6$ to 10 Hz for *ortho*, $^{4}J_{HF} = 4$ to 8 Hz for *meta*, and $^{5}J_{HF} = 0$ to 3 Hz for *para*) [18].

TABLE 1-6. Typical Values of Proton–Carbon Spin–Spin Coupling Constants (Hz) for the Most Common Functional Groups in Organic Compounds

Type of Bond	$^1J_{C-H}$	$^2J_{C-H}$	$^3J_{C-H}$
Single bond	120–160	1–6	0–8
Double bond	160–180	0–16	6–13
Triple bond	~250	40–60	
Aromatic ring	160–170	1–4	6–11

Source: Data from references 18 and 24.

Due to the low natural abundance of ^{13}C (see Table 1-1) and how large ^1H–^{13}C couplings are, ^{13}C NMR spectra are normally acquired using proton-decoupling techniques to simplify their interpretation and increase sensitivity on the carbon signals for carbons attached directly to protons by eliminating their splitting patterns and collapsing them to singlets (nuclear Overhauser effect). Table 1-6 depicts the typical ranges of ^1H–^{13}C coupling constants in common functional groups of organic compounds [18,24]. Nonetheless, the general value of those coupling constants are used to acquire specific two-dimensional ^1H–^{13}C NMR experiments that provide information on protons and carbons bonded via one to three bonds (discussed later in the chapter). Carbon–carbon (^{13}C–^{13}C) coupling constants are not observable, due to the low natural abundance of carbon 13 unless the compound of interest has been synthesized with labeled carbon 13.

1.3.3. Spin Systems

The spin systems are a group of nuclei with nuclear spins that show spin–spin interactions. The spin systems have been classified using Pople notation and are labeled by letters. Spins can interact through strong or weak coupling. Spins with weak coupling are well separated in the δ scale and follow the multiplicity of the splitting patterns described in Section 1.3.2; they are considered first-order spectra. The spins are designated AX for a well-separated two-spin system and AM for an intermediate range of separation, AXY for a well-separated three-spin system and AMX when one of them (M) is in an intermediate position, and so on. ABX is a three-spin system with two spins (A and B) strongly coupled close to each other on the δ scale and coupled weakly with the third spin (X), which is farther from the other two on the δ scale. The spins with the first letters of the alphabet are the more deshielded spins. Strong spin systems show splitting patterns under second-order spectra because the NMR signals of the spins are so close on the δ scale that the spin system is distorted and the center of the multiplet is not in the middle. This follows the second-order spectra because $\Delta\delta/J < 10$, where $\Delta\delta = \delta_{Ha} - \delta_{Hb}$

TABLE 1-7. Major Differences Between First- and Second-Order Spectra

First-Order Spectra	Second-Order Spectra
The splitting patterns follow the $n+1$ multiplicity rule	The $n+1$ multiplicity rule is not valid, due to the increase in multiplicity of the splitting patterns
The relative intensities of the signals of multiplets follow Pascal's triangle	No rules can be applied to determine the intensity of the signals of multiplets because their intensity distribution is altered
Spectra are simple	Spectra are complex to analyze
Spectra are analyzed directly	Spectra are difficult to analyze and require computer algorithms for their analysis

with the $J = J_{a\text{-}b}$ being the spin–spin coupling constant between spins a and b. Table 1-7 highlights the main points that distinguish the first- and second-order spectra. A simple inspection of Figure 1-6 shows that the spectra at 60 and 100 MHz are not easily interpreted by the rules given in Section 1.3.2, but the spectra at 300 and 600 MHz follow the rules of interpretation well. In conclusion, spectra acquired in higher field instruments possess higher resolution whose analysis fits the common rules of interpretation without or with less intervention by computer algorithms. More details of the spin system notation are given in the literature [7,16,24–26].

A simple demonstration of the distortion of multiplet signals when $\Delta\delta/J < 10$ occurs for two geminal or vicinal protons of a methylene group with no other coupling, where the intensity of the lines of the two sets of doublets is affected by how close they are on the δ or chemical shift scale. If the difference in frequency of the center of the two doublets is less than 10 ($\Delta\delta/J < 10$), the inner lines of the doublets are larger than the outer lines. When distorted, the center of each multiplet is not the middle point between the lines of each multiplet, a circumstance termed the *roofing effect*. Figure 1-12 illustrates methylene protons ranging from an AX ($\Delta\delta/J > 10$) to an AB ($\Delta\delta/J \leq 10$) notation system. Figures 1-8 and 1-11 show the roofing effects for the spin systems of protons H-1/H-2, and methylene protons H-10, but the roofing effect is barely noticeable for the methylene protons H-5 because they are far apart on the chemical shift scale.

1.3.4. Signal Intensities

In the ^{1}H NMR spectra, the areas of the signals associated with the individual protons or spin systems provide information on the ratio of protons for these spin systems in the molecule. The ratio is more accurate when the spectra are collected with enough delay time between scans or recycle delay to minimize possible long relaxation times that some protons (e.g., aromatic, aldehydic) may have. Therefore, the integrated areas of the signals are directly proportional

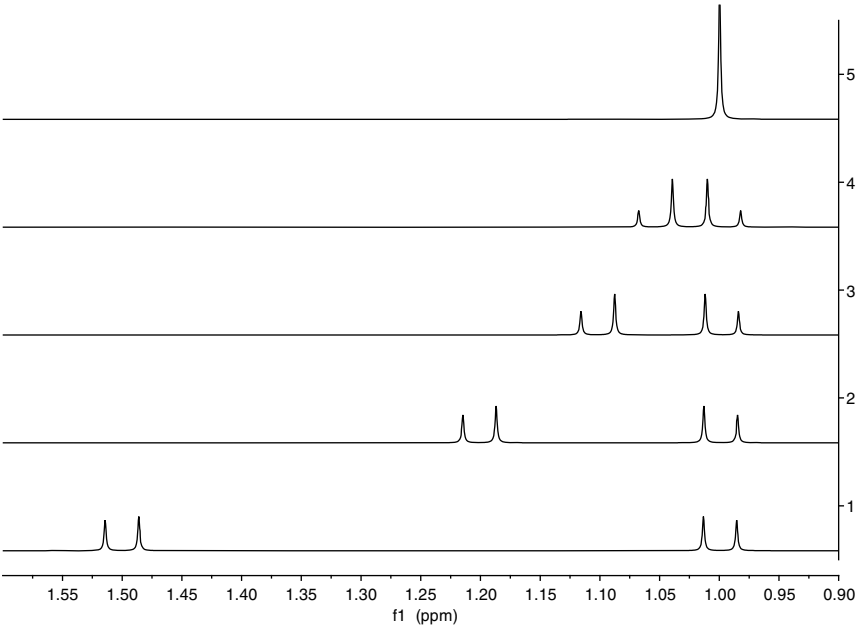

FIGURE 1-12. Simulated spectra of a methylene with the geminal coupling constant set at 14 Hz and at different chemical shifts, showing the roofing effect.

to the number of nuclei or protons in the molecule. The only exception is that of the exchangeable protons, such as the OH of alcohols and carboxylic acid and the NH or NH_2 of amino and amide groups, which may exchange with the residual water of the deuterated NMR solvents more rapidly than the time required for the NMR spectra. Figure 1-8 shows the ratios of the protons for sinomenine. For example, the signal for the methyl protons H-19 integrates for three protons and the signal for the vinyl proton H-8 integrates for one proton; therefore, the ratio of the areas of these two proton signals is 3 : 1, respectively (see Figure 1-8).

A one-dimensional ^{1}H NMR experiment using a 90° pulse and recycle delay for about a three- to fivefold T_1 (longitudinal relaxation time) or even a 30° pulse with around about a two- to threefold T_1 for recycle delay is commonly used for quantitation studies. If a sample has two components, the ratio of the areas of the signals from each component will provide a molar ratio for both components in the sample as long as each area is divided by the appropriate number of protons for the signals selected for the calculation. To calculate accurate weigh percentages, an internal standard of known purity must be added to the NMR solution. Overall, the process of calculating weigh percentages (w/w%) is becoming common practice in many laboratories in industry and academia. More information on the methodology of quantitation by NMR or qNMR may be found in the literature [28].

In ^{13}C NMR, the typical spectrum acquired with broadband proton decoupling to simplify the multiplets into singlets is not appropriate for qNMR. The carbons attached to protons are simplified to singlets and the intensity of the singlets is increased by the number of protons attached to the carbon, termed the *nuclear Overhauser effect* (NOE). However, quaternary carbons are not affected by the NOE effect, due to the lack of protons attached to those carbons. Besides, the relaxation times of carbons are greater than those of protons, and having a short recycle delay between pulses (or scans) will affect the intensity of those carbons with longer relaxation times, such as aromatics or downfield carbons such as carbonyls. Figure 1-9 shows the ^{13}C NMR spectrum of sinomenine, where each signal represents one carbon of the molecule and none of them have the same intensity and area. Gated decoupling is the common experiment used to achieve quantitation by ^{13}C NMR. In this experiment, the areas of the carbon signals are proportional to the number of carbons associated with each signal. The process used to perform the quantitation analysis is the same as for ^{1}H NMR, but only on special cases is quantitation carried out by ^{13}C NMR if it cannot be done by proton or other nuclei (e.g., fluorine) that are more abundant in nature and more sensitive than carbon (e.g., ^{13}C nuclei).

1.3.5. Bond Correlations

Coupling constants give information as to how the nuclei are related through bonds. The proton–proton spin couplings indicate how the protons of each spin system are connected through the backbone of the molecule. The heteronuclear coupling constants, such as between protons and carbons, provide information on how the protons and the carbons are located in the molecule. However, one-dimensional ^{1}H NMR spectra do not always provide sufficient information on how the nuclei are connected by bonds, due to the overlapping of proton signals by ^{1}H NMR, which makes coupling measurements difficult and time consuming. In ^{13}C NMR, the complex overlapping of coupled proton–carbon signals causes collecting coupled one-dimensional ^{13}C NMR spectra to take longer, making the measurement impractical. Expanding the data to a second dimension decreases the overlapping of signals, facilitating the structural analysis of organic compounds. There are two major types of NMR experiments that give information through bonds: homonuclear and heteronuclear two-dimensional NMR experiments. The focus of this chapter is on interpretating NMR data, not the theory behind these experiments, which is explained thoroughly in the literature [1–6,11,13]. Below is a brief description and interpretation of the most common two-dimensional (2D) homo- and heteronuclear experiments used for structural analysis.

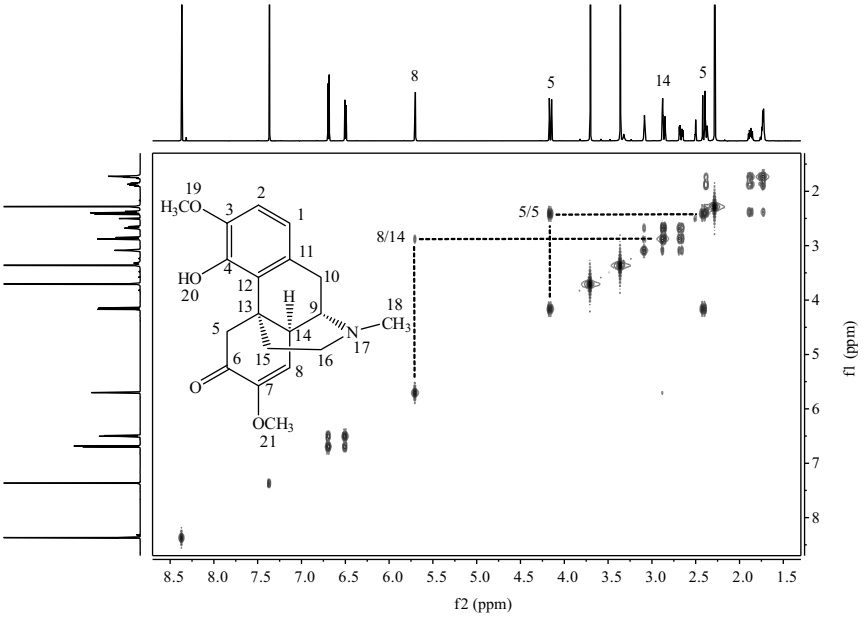

FIGURE 1-13. 2D ^{1}H–^{1}H COSY spectrum of sinomenine in DMSO-*d*6. The dashed lines show the correlations via bonds of the methylene protons H-5 and of the vinyl proton H-8 with the methine proton H-14. The horizontal and vertical traces are the 1D ^{1}H NMR spectrum of sinomenine from Figure 1-8. The structure of sinomenine is attached for reference.

The most typical 2D homonuclear NMR experiments are 2D correlation spectroscopy (COSY) and 2D total correlation spectroscopy (TOCSY). 2D COSY gives information on the correlation of protons mainly via three bonds. Figure 1-13 depicts the 2D ^{1}H–^{1}H COSY spectrum of sinomenine in DMSO-*d*6. The diagonal trace represents the one-dimensional (1D) ^{1}H spectrum, with the cross-peaks in the diagonal located at the chemical shifts of the proton signals of sinomenine as shown in the 1D ^{1}H NMR spectrum (Figure 1-8). The cross-peaks outside the diagonal give information on the proton nuclear spins with two-, three-, and sometimes four-bond correlations: H−C−H, H−C−C−H, and H−C−C−C−H, respectively. The dashed lines between the vinyl proton H-8 and the methine proton H-14 in Figure 1-13 indicates their three-bond correlations to be H−C−C−H, and the dashed lines between the methylene protons H-5 indicate their two-bond correlation to be H−C−H. The intensity of the cross-peaks outside the diagonal are related directly to the value of the coupling constant. Therefore, the most intense cross-peaks have the largest coupling constants, and vice versa. The 2D TOCSY spectrum gives rise to information similar to that of 2D COSY, but it connects all the protons of each spin system at the appropriate mixing time. The 1D version, 1D TOCSY, is a useful experiment that will require only minutes instead of over an hour of acquisition time for a concentrated sample,

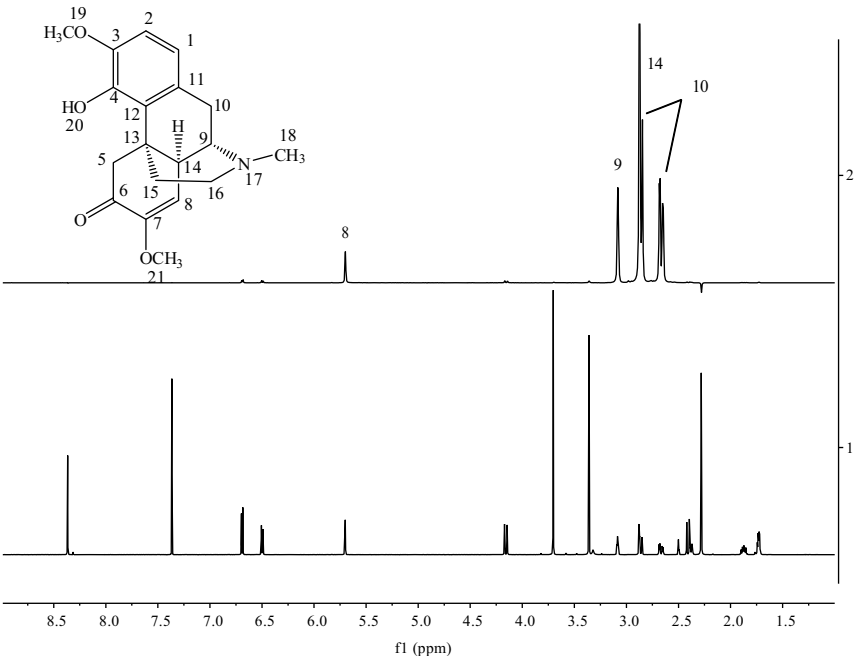

FIGURE 1-14. 1D ^{1}H NMR (bottom) and 1D TOCSY (top) spectra of sinomenine in DMSO-*d*6. Proton H-9 was irradiated at 80 ms of mixing time to provide information about the proton signals for its spin system with protons H-8, H-10, and H-14. The structure of sinomenine is attached for reference.

and it provides specific information on one spin system at a time. Figure 1-14 depicts the stacked spectra of the 1D ^{1}H NMR (bottom) and the 1D TOCSY (top) of sinomenine in DMSO-*d*6, where irradiating the signal of proton H-9 elicited TOCSY signals with all the protons of its spin system: H-8, H-14, and H-10.

The most common 2D heteronuclear experiments are 2D heteronuclear single quantum coherence (HSQC) and 2D heteronuclear multiple-bond correlation (HMBC). In organic molecules the most abundant nuclei with nuclear spin are protons and carbons. Therefore, the information obtained from these experiments can provide the carbon skeleton of the molecule or part of it. A 2D ^{1}H–^{13}C HSQC experiment provides information on the C−H one-bond correlations. Typically, the value around 140 Hz is used as a low-pass filter for the average value of the one-bond C−H coupling constant for organic compounds to obtain information on the protons and carbons attached by one bond. Figure 1-15 shows the 2D ^{1}H–^{13}C gradient HSQC spectrum of sinomenine with all the one-bond C−H cross-peaks assigned for the individual C−H bond of the molecule. Notice that for nonequivalent methylene protons, where the protons have different chemical shifts, both protons are attached to the same carbon, showing only one carbon chemical shift for both proton signals as for the methylenes in positions 5, 10, and 16 in the molecule.

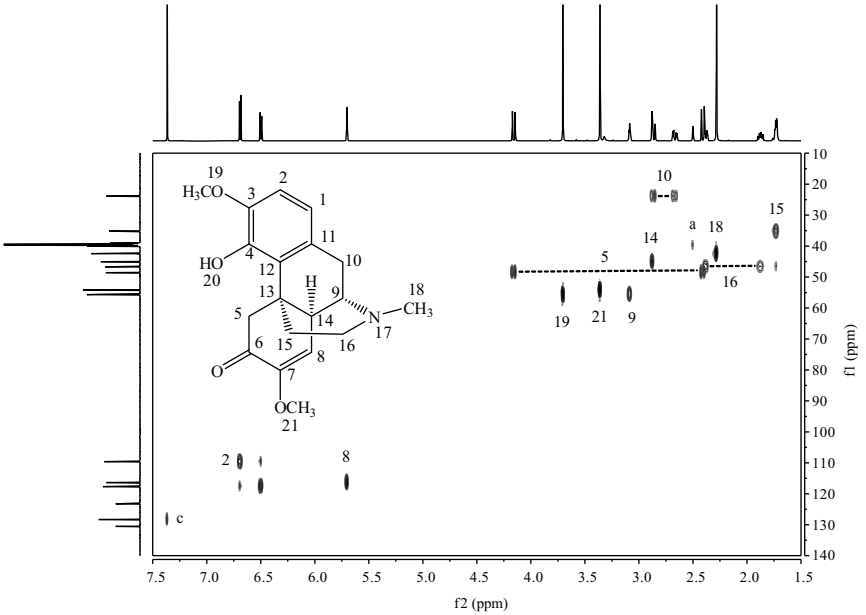

FIGURE 1-15. 2D ^{1}H–^{13}C gradient HSQC spectrum of sinomenine in DMSO-*d*6. The assignments are provided by the number positions of the C−H atoms in the molecule. The dashed lines indicate methylene C−H groups. The horizontal and vertical traces are the 1D ^{1}H and ^{13}C NMR spectra of sinomenine from Figures 1-8 and 1-9, respectively. The structure of sinomenine is attached for reference.

A 2D ^{1}H–^{13}C HMBC experiment provides information on the carbons and protons through two, three, and four bonds. However, the experiment is optimized for the three-bond C−H correlations, where the typical value for the long-range C−H coupling constant is anywhere in the range 5 to 10 Hz. Figure 1-16 shows the 2D ^{1}H–^{13}C gradient HMBC spectrum of sinomenine. The dashed lines show the C−H correlations of the hydroxyl proton H-20 with carbons C-3 and C-12 via three-bond C-H correlations and with carbon C-4 via two-bond C−H correlation. The carbonyl carbon C-6 shows a two-bond C−H correlation with the methylene proton H-5 and a three-bond C−H correlation with the vinyl proton H-8 (Figure 1-16). These 2D homo- and heteronuclear experiments are well described in the literature [1–13,15,16,22–27,29]. Today, with the availability of cryogenic probes, the sensitivity of instruments has improved tremendously, and it is becoming part of a routine analysis to detect less sensitive nuclei, such as ^{15}N. These two inverse detection experiments, HSQC and HMBC, can be applied to ^{1}H–^{15}N bonds as long as the molecule has a nitrogen atom and protons one to three or even four bonds apart. Normally, the one-bond low-pass filter is around 90 Hz for the ^{1}H–^{15}N one-bond coupling constant, and the long-range ^{1}H–^{15}N coupling constant is the same as in ^{1}H–^{13}C, about 5 to 10 Hz. The example featured in this chapter, sinomenine, has one nitrogen atom as a tertiary amino; therefore, ^{1}H–^{15}N HMBC is the

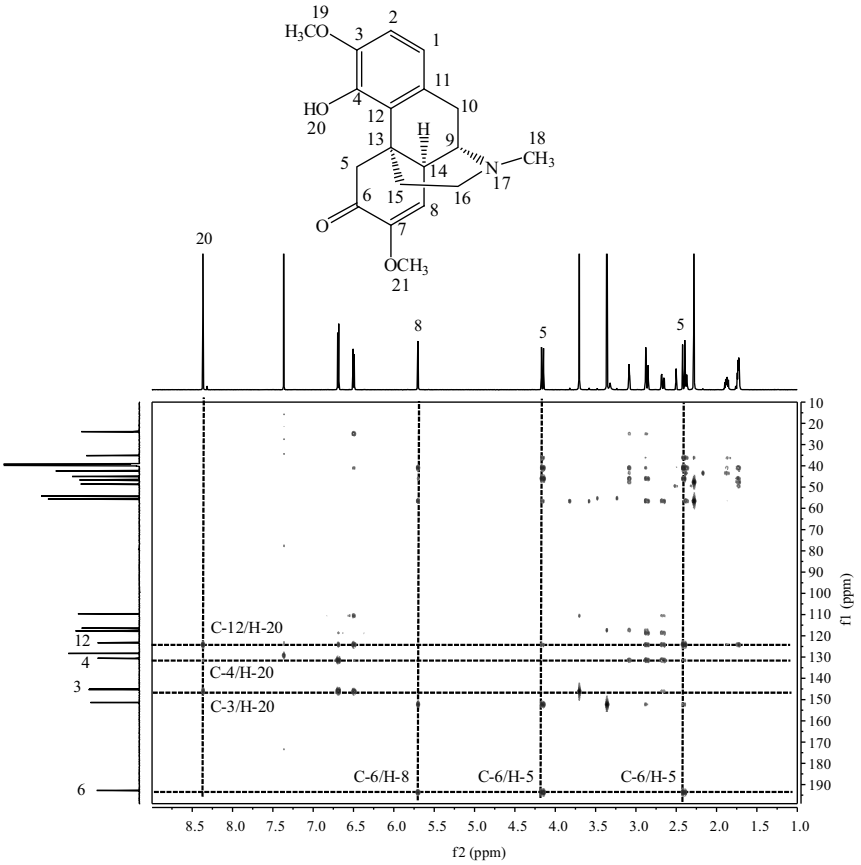

FIGURE 1-16. 2D ^{1}H–^{13}C gradient HMBC spectrum of sinomenine in DMSO-*d*6. The dashed lines show the two- and three-bond C−H correlations for the protons and carbons numbered in the figure and explained in the text. The horizontal and vertical traces are the 1D ^{1}H and ^{13}C NMR and spectra of sinomenine from Figures 1-8 and 1-9, respectively. The structure of sinomenine is attached for reference.

experimental method that should provide the chemical shift of that nitrogen through correlations with the neighboring protons. Figure 1-17 depicts a 2D ^{1}H–^{15}N gradient HMBC spectrum with the nitrogen N-17 showing two-bond N−H correlations with the methyl protons H-18, methylene protons H-16, and methine proton H-9, and three-bond N−H correlations with the methylene protons H-10 and the methylene protons H-15. The chemical shift of nitrogen N-17 is included in the table of chemical shift assignments for sinomenine (Table 1-5).

1.3.6. Spatial Correlations

Molecules are three-dimensional in space, and knowing how the atoms are related to each other in the distance is helpful in structural analysis. One- and

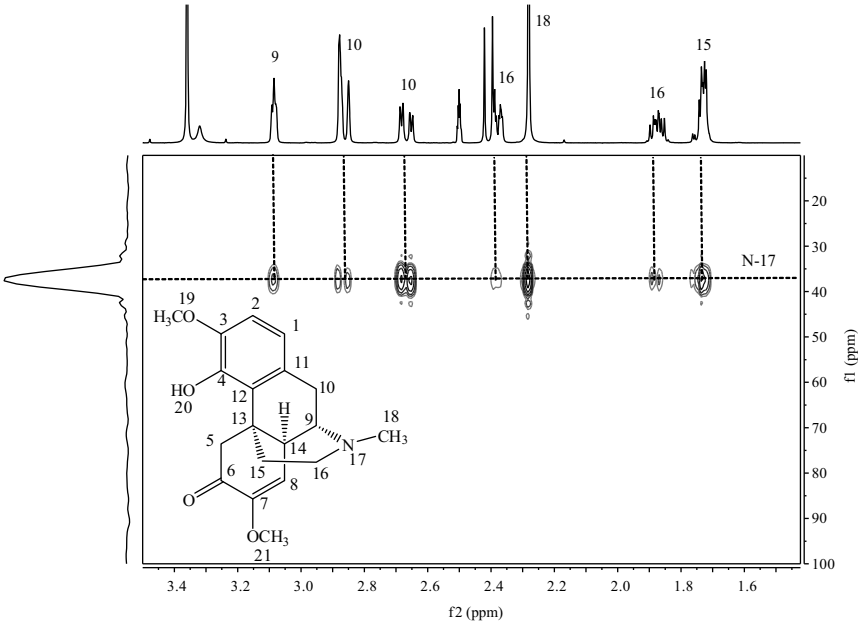

FIGURE 1-17. 2D ^{1}H–^{15}N gradient HMBC spectrum of sinomenine in DMSO-*d*6. The dashed lines show the two- and three-bond N−H correlations for the protons and nitrogen numbered in the figure and explained in the text. The horizontal and vertical traces represent the 1D ^{1}H NMR spectrum from Figure 1-8 and the ^{15}N trace from the 2D ^{1}H–^{15}N gradient HMBC spectrum NMR of sinomenine. The structure of sinomenine is attached for reference.

two-dimensional nuclear Overhauser effect spectroscopy (NOESY) and rotating frame Overhauser effect spectroscopy (ROESY) experiments provide information on the protons in spatial proximity in less than 5 Å. In general, molecules in solution tumble at different rates, depending on their size and molecular weight. Small molecules (e.g., methanol) tumble faster and large molecules (e.g., proteins, polymers) tumble more slowly. In addition, relaxation affects the intensity of the NOEs and their signs. Small molecules (e.g., methanol) tumble faster with $\tau_c \leq 10^{-11}$s (τ_c is the correlation time or the time for a molecule to rotate 1 rad) and the transitions responsible for the NOE are positively compliant with $\omega\tau_c < 1$ (ω is the Lamour frequency, expressed in Section 1.2 as $\nu = \gamma B_0$). When a molecule becomes large, $\omega\tau_c \sim 1$ and no NOE signal is detected because the relaxation becomes very efficient via double quantum transitions. When molecules are larger, they tumble slowly, with $\omega\tau_c > 1$, and the NOEs are negative. To observe the correlations through space for the case of $\omega\tau_c \sim 1$, a ROESY experiment is performed. ROESY uses a spin-locking field, which makes the magnetization go through a different mechanism than in NOESY. In ROESY, the effective precession frequencies or Lamour frequencies (ω) are very small and all the molecules (small *and* large) tumble

faster, compliant with $\omega\tau_c \ll 1$. Therefore, the NOEs (or better said, the ROEs) are all positive, regardless of the size and molecular weight of the molecule in the 1D and 2D ROESY spectra. The main drawback of the ROESY experiment is the fact that some neighboring proton signals will give TOCSY peaks caused by the same spin-lock pathway that is used in both experiments, TOCSY and ROESY. Detailed information on these experiments may be found in the literature [1–13,15,16,22–27,29].

Sinomenine, the example used in this chapter, has a molecular weight of 329.39 Da and in a 600-MHz NMR instrument will show positive NOEs. Figure 1-18 depicts the stacked spectra of the 1D ^{1}H NMR (bottom) and the 1D NOE (top) of sinomenine in DMSO-*d*6, where irradiating the signal of the vinyl proton H-8 elicited NOE signals with the methoxy protons H-21, the methylene protons H-10, and the methine protons H-9 and H-14. Figure 1-19 depicts the 2D ^{1}H–^{1}H NOESY spectrum, which shows the same information as for the 1D NOE, but with all the possible NOEs in the molecule. The dashed lines indicate the NOE signals between the vinyl proton H-8 with the methoxy protons H-21 and the aromatic proton H-2 with the other methoxy protons H-19, facilitating the assignment of the individual methoxy groups and their

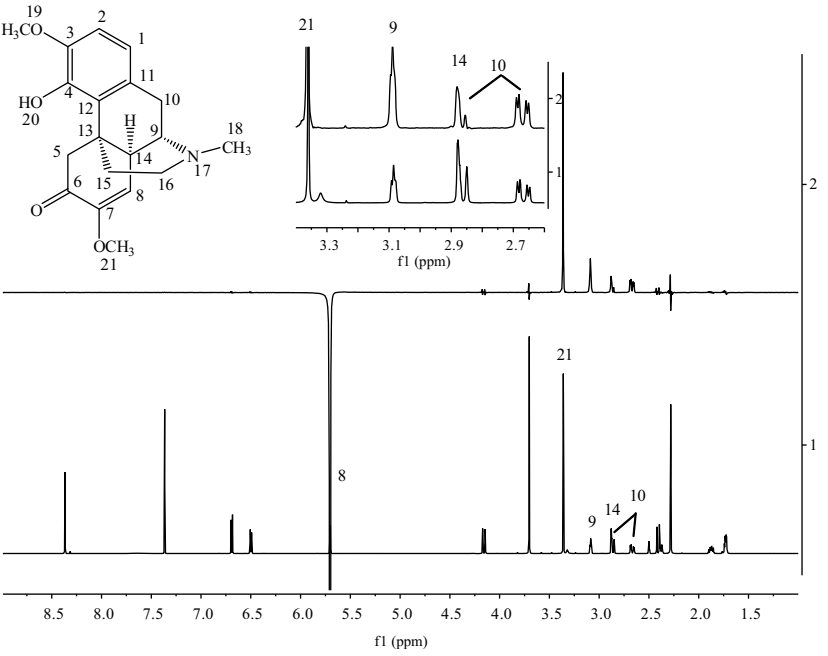

FIGURE 1-18. 1D ^{1}H NMR (bottom) and 1D NOE (top) spectra of sinomenine irradiating at the vinyl proton H-8 in DMSO-*d*6. The expansion of both spectra provides a better view of the aliphatic region between 3.4 and 2.6 ppm. The structure of sinomenine is attached for reference.

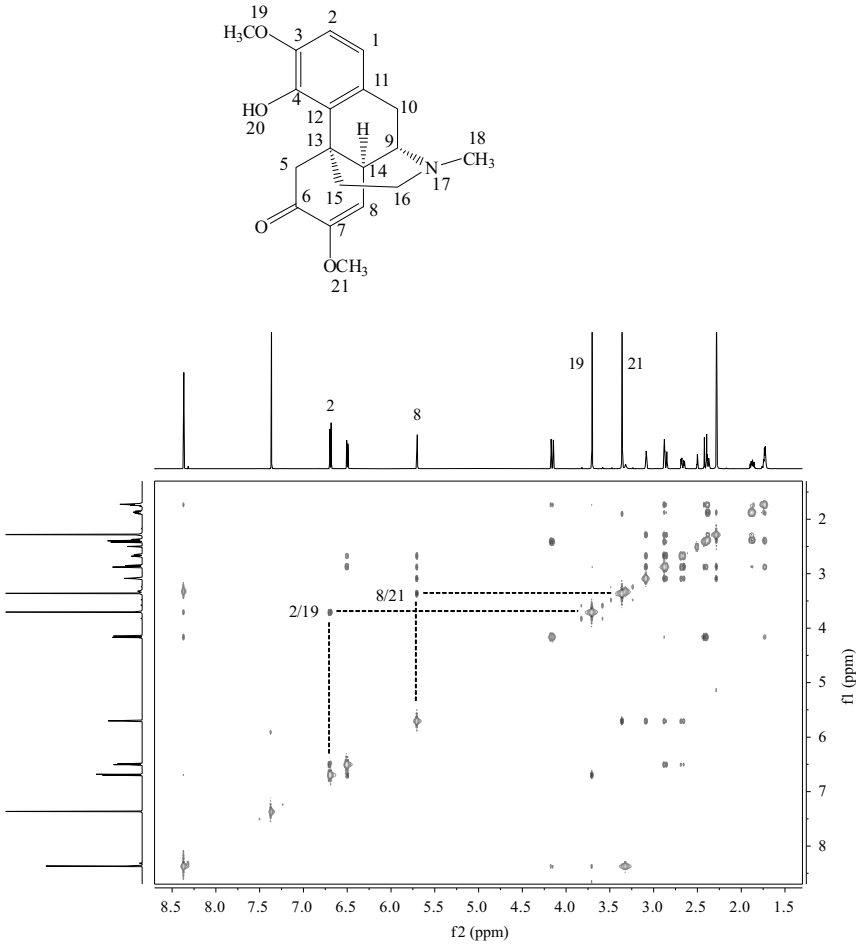

FIGURE 1-19. 2D ^{1}H–^{1}H NOESY spectrum of sinomenine in DMSO-*d*6. The horizontal and vertical traces are the 1D ^{1}H NMR spectrum of sinomenine from Figure 1-8. The dashed lines show the spatial correlations of the two methoxy groups and their corresponding *ortho* proton described in the text. The structure of sinomenine is attached for reference.

location in the molecule. The use of 1D NOE data instead of the 2D NOESY version is advantageous when only particular NOE information is needed. Acquiring 1D data requires only minutes, whereas 2D data require several hours. When resolution is needed, especially in the case of overlapping signals, 1D NMR experiments are preferred because the second dimension in 2D NMR experiments results in much lower resolution.

1.3.7. Other Topics

In previous sections the NMR experiments most commonly used for structural elucidation have been described. Obviously, many other experiments are

available that can provide additional information. However, the majority of cases are solved by the experiments described above. On some occasions, other approaches can be carried out to determine specific information, such as the presence of solvent signals that do not belong to the major component of the sample or the presence of exchangeable protons in the molecule. In the case of the presence of solvent peaks that can cause ambiguities in assignments, a 1D diffusion-ordered spectroscopy (DOSY) experiment can take a few minutes in a concentrated sample and help to determine which signals belong to the major component of the sample as long as the other components have a different molecular weight and shape. Figure 1-20 shows the difference between the conventional 1D ^{1}H NMR (bottom) spectrum with the 1D DOSY (top) spectrum of sinomenine in DMSO-*d*6. The letters c, b, and a in the 1D ^{1}H NMR (bottom) spectrum denote information on the solvent peak, residual protonated water on DMSO-*d*6 (HOD), and residual protonated DMSO-*d*6 (CD_2HSOCD_3), respectively. These solvent peaks disappear in the 1D DOSY experiment with the appropriate parameters. Because those peaks belong to molecules with much smaller molecular weight

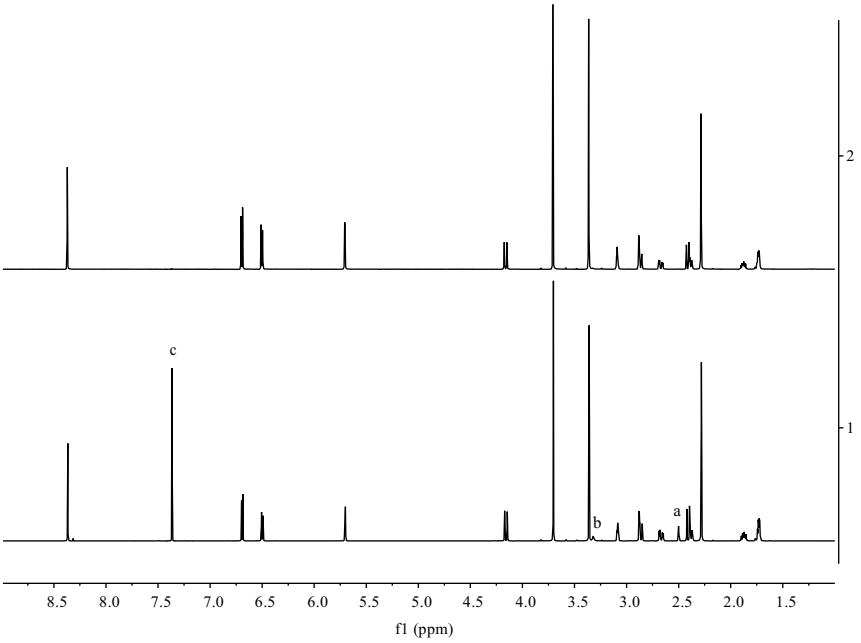

FIGURE 1-20. 1D ^{1}H NMR (bottom) and 1D DOSY (top) spectra of sinomenine in DMSO-*d*6. The letters c, b, and a denote the information of solvent peak, residual protonated water on DMSO-*d*6 (HOD), and residual protonated DMSO-*d*6 (CD_2HSOCD_3), respectively. These solvent peaks disappear in the 1D DOSY experiment.

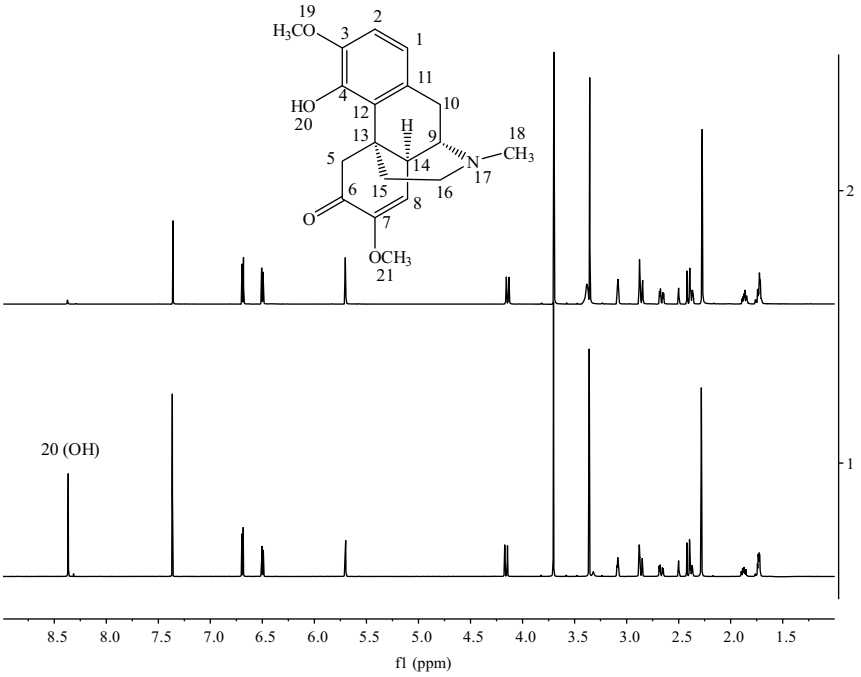

FIGURE 1-21. 1D ^{1}H NMR spectra of sinomenine in DMSO-*d*6 (bottom) and in DMSO-*d*6 with a drop of D_2O (top). The structure of sinomenine is attached for reference.

than that of sinomenine, the diffusion experiment "filters" the signals from low-molecular-weight components such as solvents at the appropriate delay time for the diffusion time and gradient strength: 300 ms and 60%, respectively, in this case. This is a simple way to assure which signals belong to the analyte of interest in the sample and which are solvent peaks, as long as there is enough difference as to the molecular weight of the various components in the sample mixture. Figure 1-21 shows the 1D ^{1}H NMR spectra in DMSO-*d*6 (bottom) and after adding approximately 1 drop of D_2O (top). The downfield proton signal at 8.37 ppm almost disappears when D_2O is added, indicating that this signal is assigned to the hydroxyl proton that exchanges in the presence of D_2O.

At present, 2D ^{1}H–^{13}C HSQC experiments are used routinely to determine the protons attached to carbons by one bond. Before inverse detection experiments became routine, a simple 1D ^{13}Cdistortionless enhancement by polarization transfer (DEPT) experiment was used to give that information. Figure 1-22, the ^{13}C DEPT-135 spectrum of sinomenine shows the methyl and methine carbon signals positive (up), the methylene carbon signals negatives (down), and the quaternary carbons canceled out (null). The

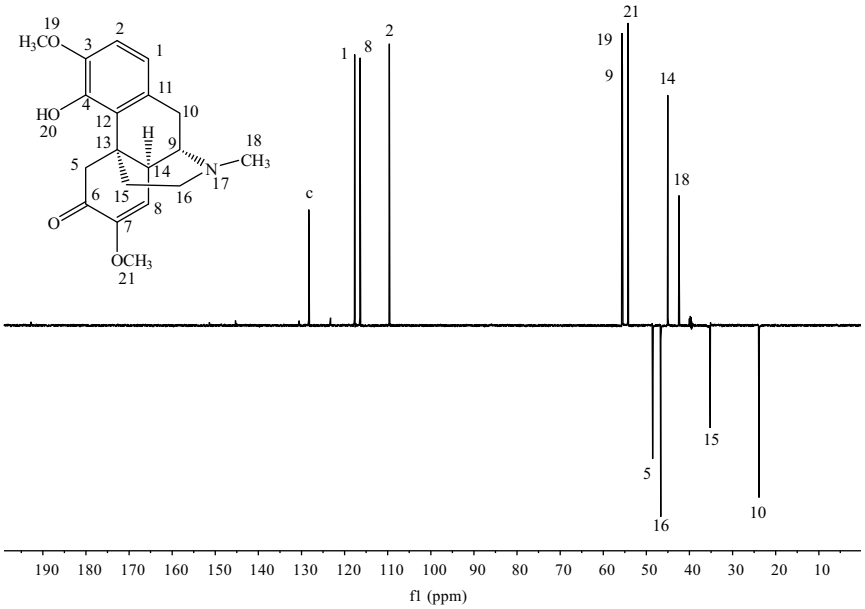

FIGURE 1-22. ^{13}C DEPT-135 spectrum of sinomenine in DMSO-*d*6. The structure of sinomenine is attached for reference.

advantage of ^{13}C DEPT-135 compared to 2D ^{1}H–^{13}C HSQC is the enhanced resolution of the carbon signals in one dimension. A 2D ^{1}H–^{13}C HSQC has much lower cross-peaks signal resolution in the second dimension. Therefore, when two signals are too close, it may be possible to have ambiguity in the assignments of those carbon signals. On the contrary, 2D ^{1}H–^{13}C HSQC can facilitate the assignment of the carbon signals attached to protons if the proton assignments are known preliminarily. ^{13}C DEPTQ is a modern version of ^{13}C DEPT-135 that includes the quaternary carbons as shown in Figure 1-23 for sinomenine. The quaternary carbons in a ^{13}C DEPTQ spectrum are negative (down). Sinomenine has a proton and carbon signal that does not belong to the compound, with proton and carbon chemical shifts of 7.36 and 128.4 ppm, respectively. Gottlieb et al. [30] provided the proton and carbon chemical shifts list of common laboratory solvents when they are trace impurities in samples where the data are acquired in routinely used deuterated solvents. Based on that list, the solvent that is closed in proton and carbon chemical shift numbers to that impurity solvent in the sinomenine sample used is benzene (7.37 ppm for proton and 128.3 ppm for carbon in DMSO-*d*6 from reference 30). The diffusion experiment in Figure 1-20 provided information that the proton signal at 7.36 ppm was a solvent peak, and the 2D ^{1}H–^{13}C HSQC in Figure 1-15 provided information on

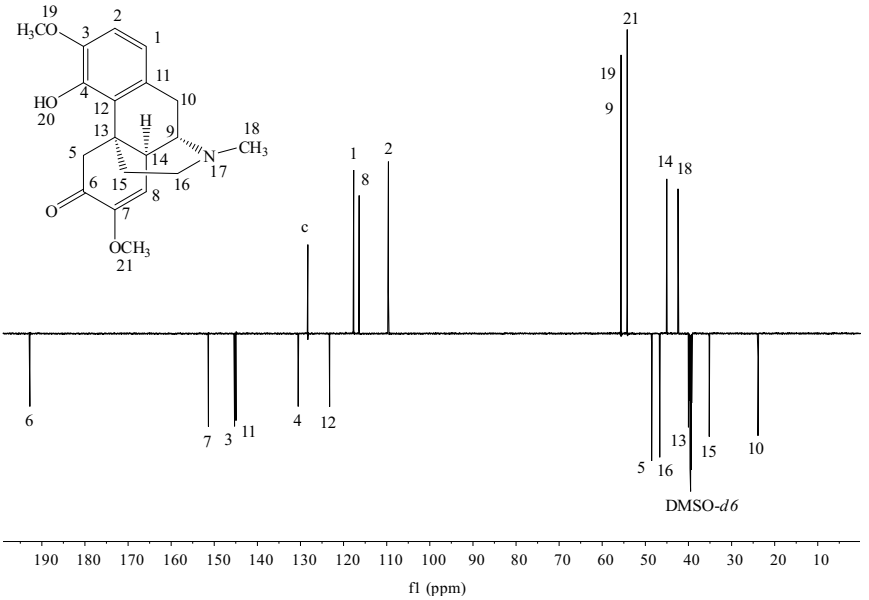

FIGURE 1-23. ^{13}C DEPTQ spectrum of sinomenine in DMSO-*d*6. The structure of sinomenine is attached for reference.

the chemical shift of the carbon attached to that proton at 128.4 ppm. The ^{13}C DEPT-135 and ^{13}C DEPTQ spectra indicated that the attached carbon was an aromatic CH. With all that information, it is possible to discriminate the most commonly used solvent peaks present in the sample and avoid ambiguity assignments on the proton and carbon signals of the analyte of interest.

One more experiment less commonly used, but simple to acquire and with useful information, is the combination of 2D $^{1}H–^{13}C$ HSQC and 2D $^{1}H–^{1}H$ TOCSY spectra in a 2D $^{1}H–^{13}C$ HSQC–TOCSY experiment. Figure 1-24 illustrates the 2D $^{1}H–^{13}C$ HSQC–TOCSY spectrum of sinomenine in DMSO-*d*6 with 80 ms of spin-lock mixing time. The information extracted from a 2D $^{1}H–^{13}C$ HSQC–TOCSY experiment is the proton and carbon chemical shifts of each individual spin system of the molecule with the appropriate spin-lock mixing time. The dashed lines on Figure 1-24 show the proton H-14 having correlations to all the carbons of its spin system: C-8, C-9, C-10, and C-14.

The literature cited in this chapter covers topics other than those discussed here, which are beyond our focus. The objective here is to bring the reader up to speed from a practical perspective on the NMR experiments most commonly used for structural elucidation of organic compounds.

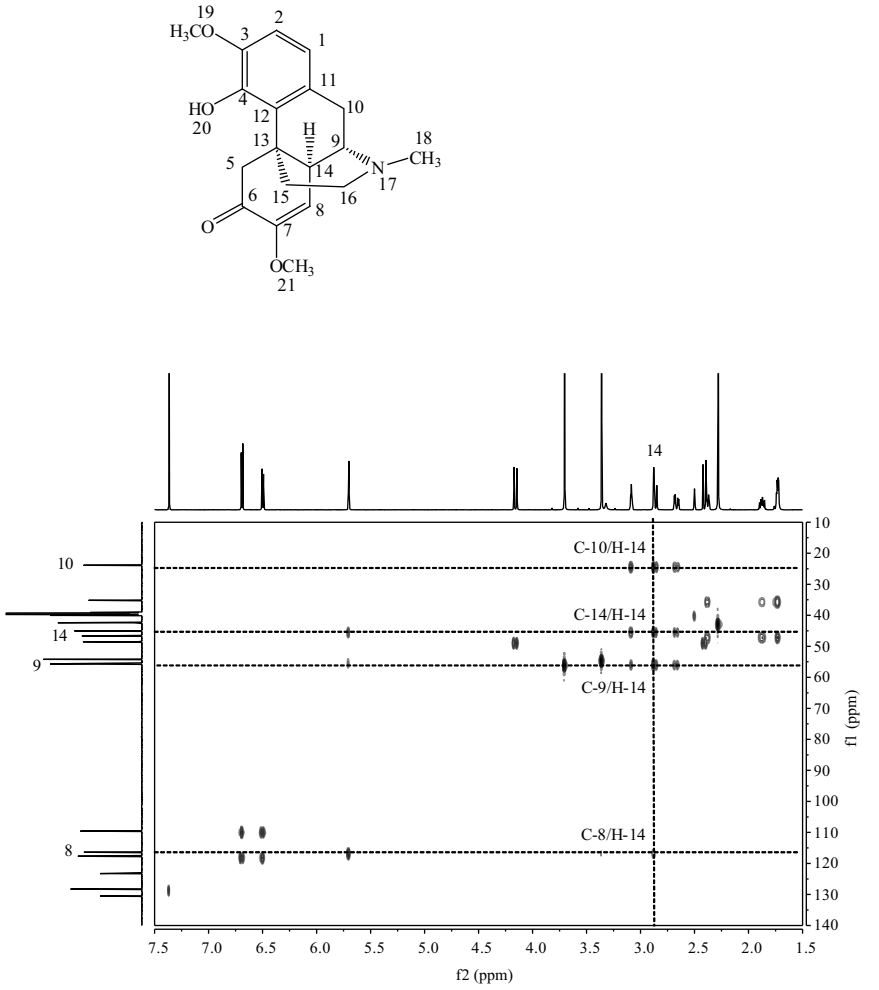

FIGURE 1-24. 2D ^{1}H–^{13}C HSQC–TOCSY with 80 ms of mixing time of sinomenine in DMSO-*d*6. The dashed lines show the correlations of proton H-14 and the carbons in its spin system explained in the text. The structure of sinomenine is attached for reference.

1.4. CONCLUSIONS

Nuclear magnetic resonance or NMR spectroscopy is a powerful technique employed extensively for the structural elucidation of organic compounds. In this chapter we have given a simplistic description of the basic physics behind the theory of NMR without elaborating on theory. The major focus of this chapter is on the basic concepts and the routine use of 1D and 2D homo- and heteronuclear NMR experiments from a practical perspective to elucidate the structure of organic compounds. Other topics are covered in the literature provided.

REFERENCES

[1] A. Abragam, *Principles of Nuclear Magnetism*, Oxford University Press, Oxford, England, 1961.

[2] R.R. Earnst, G. Bodenhausen, and A. Wokaun, *Principles of Nuclear Magnetic Resonance in One and Two Dimensions*, Clarendon Press, Oxford, England, 1987.

[3] F.J.M. van de Ven, *Muldimensional NMR in Liquids: Basic Principles and Experimental Methods*, Wiley-VCH, New York, 1995.

[4] D. Canet, *Nuclear Magnetic Resonance: Concepts and Methods*, Wiley, Chichester, England, 1996.

[5] A.E. Derome, *Modern NMR Techniques for Chemistry Research*, Pergamon Press, Oxford, England, 1987.

[6] R.K. Harris, *Nuclear Magnetic Resonance Spectroscopy: A Physicochemical View*, Longman Scientific & Technical, Harlow, England, 1987.

[7] F.A. Bovey, L. Jelinkski, and P.A. Mirau, *Nuclear Magnetic Resonance Spectroscopy*, 2nd ed., Academic Press, San Diego, CA, 1988.

[8] R.J. Abraham, J. Fisher, and P. Loftus, *Introduction to NMR Spectroscopy*, Wiley, New York, 1988.

[9] S.W. Homans, *A Dictionary of Concepts in NMR*, Clarendon Press, Oxford, England, 1989.

[10] J.D. Roberts, *ABCs of FT-NMR*, University Science Books, Sausalito, CA, 1990.

[11] J.K.M. Sanders and B.K. Hunter, *Modern NMR Spectroscopy: A Guide for Chemists*, 2nd ed., Oxford University Press, Oxford, England, 1993.

[12] P.J. Hore, *Nuclear Magnetic Resonance* (Oxford Chemistry Primers series), Oxford University Press, Oxford, England, 1995.

[13] G.E. Martin and A.S. Zekter, *Two-Dimensional NMR Methods for Establishing Molecular Connectivity: A Chemist's Guide to Experiment, Selection, Performance, and Interpretation*, VCH, New York, 1988.

[14] P.J. Hore, J.A. Jones, and S. Wimperis, *NMR: The Toolkit* (Oxford Chemistry Primers series), Oxford University Press, Oxford, England, 2000.

[15] M.H. Levitt, *Spin Dynamics: Basics of Nuclear Magnetic Resonance*, 2nd ed., Wiley, Chichester, England, 2008.

[16] R.S. Macomber, *A Complete Introduction to Modern NMR Spectroscopy*, Wiley, New York, 1998.

[17] V.I. Blakhmutov, *Practical NMR Relaxation for Chemists*, Wiley, Chichester, England, 2004.

[18] E. Pretsch, P. Bühlmannm, and C. Affolter, *Structure Determination of Organic Compounds: Tables of Spectral Data*, 3rd ed., Springer-Verlag, Berlin, Germany, 2000.

[19] F.W. Wehrli and T. Wirthlin, *Interpretation of Carbon-13 NMR Spectra*, Heyden, London, England, 1980.

[20] T.J. Batterham, *NMR Spectra of Simple Heterocycles*, Robert E. Krieger, Malabar, FL, 1982.

[21] H.-O. Kalinowski, S. Berger, and S. Braun, *Carbon-13 NMR Spectroscopy*, Wiley, Chichester, England, 1988.

[22] E. Breitmaier, *Structure Elucidation by NMR in Organic Chemistry: A Practical Guide*, Wiley, Chichester, England, 1993.

[23] G. Batta, K.E. Kövér, and C. Szántay, Jr., *Methods for Structure Elucidation by High Resolution NMR*, Elsevier, Amsterdam, The Netherlands, 1997.

[24] H. Friebolin, *Basic One and Two-Dimensional NMR Spectroscopy*, 3rd ed., Wiley-VCH, Weinheim, Germany, 1998.

[25] R.M. Silverstein, F.X. Webster, and D.J. Kiemle, *Spectrometric Identification of Organic Compounds*, 7th ed., Wiley, Hoboken, NJ, 2005.

[26] M. Balci, *Basic* $^{1}H - {}^{13}C$*-NMR Spectroscopy,* Elsevier, Amsterdam, The Netherlands, 2005.

[27] T.N. Mitchel and B. Costisella, *NMR—From Spectra to Structures: An Experimental Approach*, Springer-Verlag, Berlin, Germany, 2007.

[28] U. Holzgrabe, I. Wawer, and B. Diehl, *NMR Spectroscopy in Pharmaceutical Analysis*, Elsevier, Oxford, England, 2008.

[29] J.H. Simpson, *Organic Structure Determination Using 2-D NMR Spectroscopy: A Problem-Based Approach*, Academic Press, San Diego, CA, 2008.

[30] H.E. Gottlieb, V. Kotlyar, and A. Nudelman, NMR Chemical Shifts of Common Laboratory Solvents as Trace Impurities, *J. Org. Chem.* **62** (1997), 7512–7515.

2

Historical Development of NMR and LC-NMR

2.1. INTRODUCTION

In the first part of this section we provide the reader with a historical overview of NMR and a brief description of the evolution of the most typical experiments used in NMR for the structural elucidation of organic compounds. In the second part we focus mainly on the improvements carried out in NMR as a hyphenated analytical technique for the elucidation of organic compounds, with an understanding of the need to develop LC-NMR for the analysis of complex mixtures.

2.2. HISTORICAL DEVELOPMENT OF NMR

NMR spectroscopy started with the introduction of the Zeeman effect, discovered in 1896, on the splitting of spectral lines in the presence of an external magnetic field for nuclei with angular moment. In addition, in 1924, Pauli explained the hyperfine structure as further splitting of the energy levels due to the interaction of nuclei with an intrinsic angular momentum or spins that orient them parallel and antiparallel under a magnetic field, indicating the existence of a magnetic moment. The first attempts to measure NMR signals

LC-NMR and Other Hyphenated NMR Techniques: Overview and Applications, First Edition. Maria Victoria Silva Elipe.

were unsuccessful. In 1936, Gorter attempted to detect ^{7}Li nuclei in crystalline lithium fluoride and ^{1}H nuclei in crystalline potassium alum in the solid state as condensed matter [1]. In 1942, Gorter and Broer attempted the same detection of ^{7}Li nuclei but in solid lithium chloride and ^{19}F nuclei in solid potassium fluoride [2]. The unsuccessful attempts were due to the long T_1 relaxation of the crystalline forms of those compounds and the low signal-to-noise level of detection in the apparatus used for those experiments, which resulted in saturation, low detection, and no observation of the NMR signal.

Successful attempts by two different groups occurred in 1945, when NMR signals in condensed phases were detected by physicists Bloch [3] at Stanford and Purcell [4] at Harvard, who received the first Nobel Prize in Physics for NMR research in 1952. Bloch measured the nuclear magnetic moment of protons in water and Purcell measured it in parafilm. Bloch named the phenomenon *nuclear induction* because his group had the water sample induced under a magnetic field for some time before measurement [3]. However, Purcell considered the technique to be *nuclear magnetic resonance absorption*, due to the relationships among the energy levels [4]. Both groups of scientists realized that the phenomena they described were the same, and the name adopted for the technique become *nuclear magnetic resonance* (NMR) *spectroscopy.*

Work on solids dominated the early years of NMR because of the limitations of instruments and incomplete development of its theory. The interest in anisotropic interaction such as dipolar couplings in solids attached attention because of the tremendous amount of structural information. Work on liquids was confined to relaxation studies. A later development was the discovery of the chemical shift and the spin–spin coupling constant. Physicists lost interest in NMR because magnetic moments could not be measured with precision. Any nucleus is affected by the local chemical environment, and its magnetic moment will vary according to the molecular structure. The discovery of the chemical shifts came due to that variation. The interest of chemists grew over time with the demonstration of the influence of chemical shifts and coupling constants on the structure of compounds. In fact, in 1951 the proton spectrum of ethanol with three distinct resonances at 30 MHz showed the potential of NMR for the structural elucidation of organic compounds [5]. Images of the oscilloscope screen taken using Polaroid cameras were the only way to record the spectra permanently and to establish the reference point of the chemical shift of the water at 0 ppm as standard. A second photograph was taken for the sample under analysis after the standard water sample. The time needed between spectra was short, to minimize the magnetic field drift of those magnets, which was relatively fast. Coupling constants or scalar couplings presented additional information on the structure of the molecule through the splitting patterns. Scalar coupling provides information on spins that are

connected by bonds, offering another tool to detail the structure of molecules at the bonding stage of the atomic level. Another technique that presented additional information was the double-resonance experiment. Spin decoupling, or double resonance, which removes the spin–spin splitting by a second RF field, was developed to obtain information about the scalar couplings in molecules by simplifying the NMR spectrum [6]. Later, the spin decoupling technique was employed to study chemical exchange and the nuclear Overhauser effect, mentioned below. Initial manipulation of the nuclear spin carried out by Hahn [7] was essential for further development of experiments such as insensitive nuclei enhanced by polarization transfer (INEPT) [8], which is the basis of many modern pulse sequence experiments. Hahn's spin-echo experiment, used to detect very low abundance nuclear spins, known as the *Hartmann–Hahn experiment* [9], was applied initially to solids before being widely used on liquids.

Working with permanent magnets gave more field stability than with electromagnets, but the field strength was limited to no more than 20,000 G (2 T or 85.16 MHz). Higher magnetic field strength provided greater chemical shift dispersion and sensitivity; therefore, electromagnets were the best choice for 60- and 100-MHz instruments. However, electromagnets were not an option for future work at fields higher than 100 MHz to increase resolution, chemical shift dispersion, and sensitivity. During the 1960s and 1970s the development of superconducting magnets and computers improved the sensitivity and broadened the application of NMR spectrometers in the field of organic chemistry. With superconducting magnets, where the coil is submerged in liquid He to maintain its superconducting status without resistance, a field strength of 1 GHz has been achieved for commercial NMR instruments at the time of this writing. The development of magnets is central to the history of the principal NMR vendors. The Varian brothers, Russell and Sigurd, founded Varian Associates in 1948 as a combination of Russell's invention of the klystron tube for the airborne radar used during World War II in navigation and air defense systems, and the development of scientific innovation in the area of NMR. The Varian brothers envisioned the future of NMR after learning of the discoveries made by Felix Bloch at Stanford as a potential application to the field of chemistry. The funding dedicated to the research and development of NMR instruments and their applications came from the sale of klystron tubes for military and commercial uses. The first prototype instrument was the HR-30, a high-resolution 30-MHz instrument with an electromagnet. With incorporated improvements, the HR-40 was available commercially in 1955, and the HR-60 came in 1958, with both instruments using electromagnets. In 1957, Varian focused on the development of the A-60 as an analytical 60-MHz instrument with an electromagnet, an affordable instrument

sized appropriately for an organic chemistry laboratory. The A-60 incorporated a locked-frequency device invented by Wes Anderson to lock the frequency to the precession of the protons of water as the control sample. This device facilitated the use of recalibrated charts. The A-60 was in production for six years. In 1967, the T-60, which had a permanent magnet, and in 1973 the EM-360, reached the market. The HR-100 came in the 1960s. In 1962 the first superconducting magnet was being tested with the coil submerged in liquid He to maintain its superconductive properties of no resistance.

With superconducting coils, there was no need of a power supply once the coil reached the superconducting status, with perpetual motion in the flow of electrons in the coil, due to the no-resistance status. Therefore, the magnet could live forever unless its superconducting status were lost due to some external heat increasing the temperature of the liquid He in which the coil is submerged. It was observed that with a continued supply of liquid He, the homogeneity of the field increases considerably without significant decay over time. The homogeneity improved after the current shims were redesigned. The prototype 200-MHz instrument had a 2.7-fold better sensitivity than that of the 100-MHz instrument. In addition, improvements in resolution, sensitivity, chemical shift dispersion, and stability opened a new era of technical development for NMR and terminated the future for instruments with electromagnets and permanent magnets.

Connecting a console to the magnet and redesigning the probes to be cylindrical with sample spinning provided an important step in the NMR technology. With superconducting coils, the next field strength that reached the market was 200 MHz in 1965. In 1969 the German company Bruker GmbH began to compete with Varian in the NMR business. Bruker came out with its WH-270 in the 1970s, which featured improvements in the dewar design of the magnets and the state-of-the-art minicomputers offering Fourier transform NMR. In fact, in the 1970s, a European company, Oxford Instruments, entered the superconducting magnet market. During that decade it was thought that a 500-MHz magnet would be the maximum field for niobium–tin coils. The high price of the instrument made it available primarily for biological NMR studies rather than for organic chemistry. In the 1980s and early 1990s, 600 MHz was the highest field commercially available [10,11]. At present, 600 MHz is considered a routine instrument. Higher field instruments, such as those of 800 MHz and above, are commonly used for biomolecular NMR. Bruker has already offered a 1-GHz instrument to customers.

The development of computers was initially a limiting factor in the advancement of the NMR field because of the difficulties of data processing without appropriate computerized tools. An important gain in sensitivity came from the use of a multichannel storage device termed a *computer of averaging*

transients (CAT), which accumulated several consecutives spectra with exact frequency registration for later processing. With CAT, it was possible to analyze diluted samples instead of pure liquids, melted solids, or liquefied gases, expanding the applications of NMR in chemistry. A CAT provided an increase in signal-to-noise ratio, with the signal increase related directly to the square root of the number of transients or scans of consecutive spectra. Continued development of computers moved the processing time for NMR data from overnight to a few seconds. Pulse Fourier transform (FT) revolutionized the field of NMR by applying a short and intense pulse to excite the nuclei over the entire spectral width. The FT technique was implemented in the instruments of Ernst and Anderson [12] in the 1960s, but it took time to become the standard method of acquiring spectra. Initially, the free induction decay (FID) was digitized and converted to IBM punched paper cards with one data point per card. Those cards were processed overnight using an IBM 7090 computer. If spectrum needed to be phased, the process would have to be repeated with another overnight processing. The process became faster when computers were better developed and made part of NMR spectrometers, but it still took many minutes to process the data. The processing time was reduced to seconds when the fast Fourier transformation algorithm was available and became a routine procedure [13]. The fast-FT algorithm restricts the data points to a factor of 2^n, n being an integer. FT provided a tenfold increase in the signal-to-noise ratio, allowing the measurement of low-abundance nuclear spins such as ^{13}C [14].

Some technical developments went into the area of permanent spectral recording. This development went from taking photographs of the oscilloscope screen to high-speed chart recorders, similar to the way that infrared spectra were recorded in the 1940s and 1950s. Some instrumental improvements affected the resolution and stability of the data and the field. Improvements in the resolution of the NMR spectra came from the sample spinner. Spinning the sample produces motional averaging, with all the molecules in solution in the NMR tube under the influence of the same average magnetic field. With sample spinning, the homogeneity of the field was improved. In addition, another component was developed to reach better consistency in the magnetic field homogeneity: the shims, or electrical shimming currents. Adjusting the shims around a sample provides fine-tuning of the distribution of the magnetic field around the sample and increases the resolution of the spectra [10,11].

Another milestone that increased the signal-to-noise (*S*/*N*) ratio was Overhauser's [15] discovery of the nuclear Overhauser effect (NOE), which improves *S*/*N* in less sensitive nuclei by polarization transfer. The threefold enhancement generally observed for the weak ^{13}C signals was a major factor in stimulating research on this important nuclide. Several years later, the

proton–proton Overhauser effect was applied to identify protons that are within 5 Å of each other.

In 1971, Jeener came up with the idea of applying two pulses to a sample with various delays in between pulses. The data were collected as a two-dimensional matrix of signal intensity and as a function of two frequency parameters in two dimensions after applying FT to their time-domain FIDs. Jeener expected to find information on relaxation properties; instead, he observed connectivities through patterns of couplings between spins. The same information could be acquired through a sequence of double-resonance experiments. However, the two-dimensional technique gave a clear picture of all those connectivies at once with sensitivity similar to that of the one-dimensional technique. Unfortunately, Jeener did not publish these results early in his research. In the 1970s, Ernst and co-workers [16] implemented Jeener's idea of acquiring a two-dimensional spectrum by applying two separate RF pulses with different increments between the pulses, and after two Fourier transformations the two-dimensional spectrum was created. Two-dimensional experiments opened up a new direction for the development of NMR, and Ernst was awarded the second Nobel prize for NMR work in 1991.

Two-dimensional correlation experiments are of special value because they connect signals through bonds. Examples of these correlation experiments are correlation spectroscopy (COSY) [16], total correlation spectroscopy (TOCSY) [17], heteronuclear correlation spectroscopy (HETCOR) [18], and their variations. Other two-dimensional experiments, such as nuclear Overhauser effect spectroscopy (NOESY) [19] and rotating frame Overhauser effect spectroscopy (ROESY) [20], provide information on protons that are connected through space to establish molecular conformations. In 1979, Müller [21] developed a novel two-dimensional experiment that correlates the chemical shift of two spins, one with a strong and the other with a weak magnetic moment. Initially, the experiment was applied to detect the weak ^{15}N nuclei in proteins, but it was later modified to detect the chemical shift of ^{13}C nuclei through detection of protons attached directly to carbons [22]. The heteronuclear multiple quantum correlation (HMQC) experiment gives the same data as HETCOR but with greater sensitivity. Heteronuclear single quantum coherence (HSQC) [23] is another widely used experiment that provides the same information as HMQC and uses two successive INEPT sequences to transfer the polarization from protons to ^{13}C or ^{15}N. Heteronuclear multiple-bond correlation (HMBC) [24] gives correlations through long-range couplings which allow two and three ^{1}H–^{13}C connectivities to be observed for organic compounds.

In 1981, two-dimensional incredible natural abundance double quantum transfer experiment (INADEQUATE) [25] was developed, which defines all

the carbon–carbon bonds, thus establishing the complete carbon skeleton in a single experiment. However, due to the low natural abundance of adjacent ^{13}C nuclei, this experiment is not very practical. All of these experiments became available with the development of computers in the 1980s. With the accelerated improvements in electronics, computers, and software in the 1990s, the use of pulsed field gradients as part of the pulse sequences was developed [26] and used to improve solvent suppression and decrease the time required to acquire two-dimensional experimental data.

Resolution and sensitivity have been the drivers of technical advancement in NMR. Going forward, Styles et al. [27] designed a probe where the coil and the preamplifier are cooled to cryogenic temperatures using liquid helium. The cryogenic probe shows improved performance by minimizing the noises coming from the resistance of the receiver coil when cooling the electronics of the NMR probe to 20 to 25 K. In this system, the sample is maintained at room temperature. ^{1}H and ^{13}C NMR spectra were obtained that demonstrated an increase in sensitivity of about fourfold compared to standard room-temperature probes [27]. In the last few years, cryogenic probes have become more accessible, and many laboratories can afford the additional expense to improve sensitivity and expand the analysis of samples in the submicrogram range.

This brief historical introduction is intended to provide a simplified overview of some of the critical milestones of NMR, mainly in chemical applications, excluding innovations in the field of protein, solid-state, and magnetic resonance imaging in clinical medicine. For more details, see the articles by Emsley and Feeney [28], Shoolery [10,11], and Freeman [29,30] and the references therein. Figure 2-1 depicts the major milestones in the history of NMR, including Nobel prizes in 2002 to K. Wüthrich for his work in the protein world and in 2003 to P.C. Lauterbur and P. Mansfield for their work in magnetic resonance imaging (MRI), areas not covered in this chapter. Figure 2-2 depicts the progression over time of the magnetic field from the first 30-MHz instrument in 1951 to today's 1-GHz instrument.

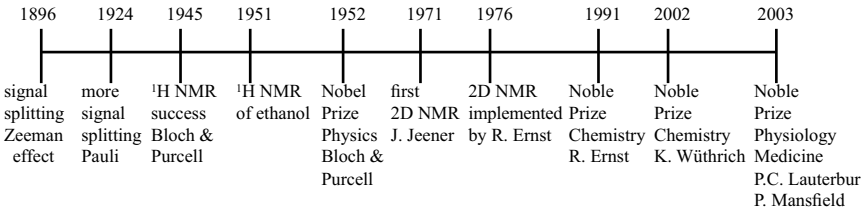

FIGURE 2-1. Major milestones in the history and discovery of NMR [10,11,28–30].

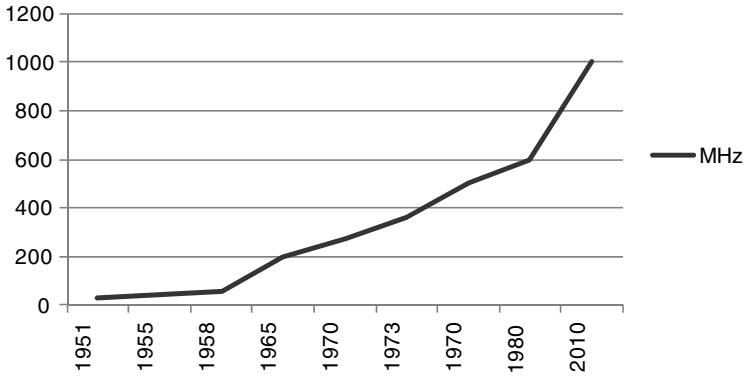

FIGURE 2-2. Increase in magnetic field (in MHz) for NMR instruments over the years, based on the literature [10,11,28–30].

2.3. HISTORICAL DEVELOPMENT OF LC-NMR

NMR is one of the most powerful analytical techniques available for the structural elucidation of organic compounds. On the other hand, separation of the individual components by chromatography is required before undertaking NMR analysis of complex mixtures. Traditionally, liquid chromatography–mass spectrometry (LC-MS) is applied routinely to analyze mixtures without prior isolation of its components. In many cases, however, NMR is needed for unambiguous identification of the structure of compounds. The need to target the analysis of the structure of components from mixtures prompted development of the hyphenation of NMR to analytical techniques with major emphasis on separation.

Even though hyphenated high-pressure liquid chromatography (HPLC) and NMR, known as LC-NMR, has been known since the late 1970s [31–41], the technique was not implemented widely until the last 15 to 20 years [42–50]. The first paper on LC-NMR was published in 1978 by Watanabe and Niki [31] using a stop-flow mode to analyze a mixture of two or three known compounds as a potential analytical technique for qualitative analysis. At that time, the limitations on the NMR side (e.g., sensitivity; available NMR deuterated solvents compatible with HPLC; software and hardware; resolution achieved only with sample spinning) made direct coupling to HPLC equipment difficult. Watanabe and Niki [31] modified the NMR probe to make it more sensitive by introducing a thin-walled Teflon tube 1.4 mm in inner diameter and transforming it into a flow-through structural design. The effective length and volume of this probe were about 1 cm and 15 μL, respectively. Two three-way valves connected this probe to the HPLC dielectric constant detector. This connection needed to be short to minimize

broadening of the chromatographic peaks. During the stop-flow mode, the time to acquire an NMR spectrum on each peak was limited to 2 h to avoid excess broadening of the remaining chromatographic peaks. The authors also mentioned that use of tetrachloroethylene or carbon tetrachloride as solvents and ETH–silica as the normal-phase column limited the applications for this technique.

Because solvent suppression techniques were not available at that time, Watanabe and Niki [31] recognized that more development was required in the software and hardware on the NMR side to include the use of reversed-phase columns and suitable NMR solvents, which in turn would broaden the range of applications. A year later, Bayer et al. [32] carried out on-flow and stop-flow experiments on standard compounds with a different flow-probe design. They used normal-phase columns and carbon tetrachloride as solvent. An external lock arrangement was carried out by placing an ampoule filled with D_2O (deuterated water) near the flow cell to provide field-frequency stability. One of their observations was that the resolution of the NMR spectra in the LC-NMR system was poorer than in an uncoupled NMR system, which made the measurement of small coupling constants more challenging.

The first application of on-flow LC-NMR was carried out in 1980 to analyze mixtures of several jet fuel samples using the refractive index as the HPLC detector and adding tetramethylsilane (TMS) for reference purposes [33]. Deuterated chloroform, Freon 113, and normal-phase columns were the common conditions used for LC-NMR [34–38], limiting the use of this technique. In an attempt to maximize the chromatographic efficiencies compared to those of conventional analytical detectors such as ultraviolet detectors, in 1980, Laude and Wilkins [39] placed a stainless column inside the bore of a wide-bore 300-MHz instrument. In this setup, the transfer line from the column to the flow cell is minimized, and with the use of a 30-μL flow cell, the authors claimed that the sensitivity and resolution achieved were similar to those of conventional NMR, where the sample is placed inside an NMR tube for analysis [39]. Unfortunately, this type of system, with the column inside the bore of the magnet, has not been popular, and technology has developed in a different direction.

In 1987, Curran and Williams [40] were the pioneers of flow injection analysis (FIA)/NMR or FIA-NMR. The authors designed an NMR flow cell to be used in commercial high-resolution ^1H NMR probes where the sample flows from the injector to the NMR flow cell without passing through an HPLC column for separation purposes. The system is more suitable for rapid kinetic analysis or unstable samples, due to the short time from injection to the beginning of analysis compared with conventional methods that place the sample in an NMR tube, or LC-NMR.

To minimize the dynamic range of the solvent and the analyte, the use of deuterated solvents and selected solvent peak suppression techniques to suppress the solvent signal was recommended. The authors developed a 50-μL NMR flow cell with a flow rate of 1 mL/min and indicated that spectroscopic resolution was better for a flowing system than for a static sample [40]. The focus of LC-NMR is to detect high-abundance nuclei such as ^{1}H. However, in 1994, Stevenson and Dorn [41] explored ^{13}Cdynamic nuclear polarization (DNP) as a detector for continuous-flow NMR as HPLC-^{13}C DNP. The instruments consisted of an HPLC, a low magnetic field region with a low-field electron paramagnetic resonance (EPR) flow cell with a silica-phase immobilized nitroxide radical as the unpaired electron source for the DNP experiment, and transfer poly(ether ether ketone) (PEEK) tubing going to the NMR flow cell inside the magnet of an NMR instrument. PEEK tubing connected the system from the HPLC to the NMR. The sample mixture was separated in the HPLC, polarized in the EPR source, and transferred to the NMR for analysis. The types of samples analyzed were organic compounds with halogens bonded covalently. One drawback for LC-DNP is that not all the molecules can be polarized by DNP; however, ^{13}C signal enhancement could increase the Boltzmann magnetization up to 50-fold in a particular magnetic field. The technique is also suitable for other low-abundance nuclide as long as the sample responds to DNP [41].

The use of reversed phase columns in LC-NMR complicates the NMR analysis because of (1) the use of more than one protonated solvent, which will very likely interfere with the sample; (2) the change in solvent resonances during the course of the chromatographic run when using solvent gradients; and (3) the presence of small analyte signals relative to those of the solvent. In 1995, Smallcombe et al. [51] overcame these problems by developing a solvent-suppression technique, which greatly improved the quality of the spectra obtained by on-flow or stop-flow experiments. Optimization of the WET (water suppression enhanced through T_1 effects) solvent suppression technique generates high-quality spectra and effectively obtains one-dimensional on-flow and stop-flow spectra and two-dimensional spectra for the stop-flow mode, such as WET-TOCSY, WET-COSY, WET-NOESY, and others [51].

In addition to the exploratory measurement of ^{13}C through DNP enhancement as HPLC-^{13}C DNP [41], proton has become the most common nucleus for LC-NMR analysis. However, since the early 1990s, there has been some use of LC-NMR measuring ^{19}F as LC-^{19}F NMR. The main applications have been in the pharmaceutical industry for the identification of metabolites and impurities [52–54]. Scarfe et al. [54] pointed out an interesting application of hyphenated LC-^{19}F NMR for the metabolism work, eliminating the need of

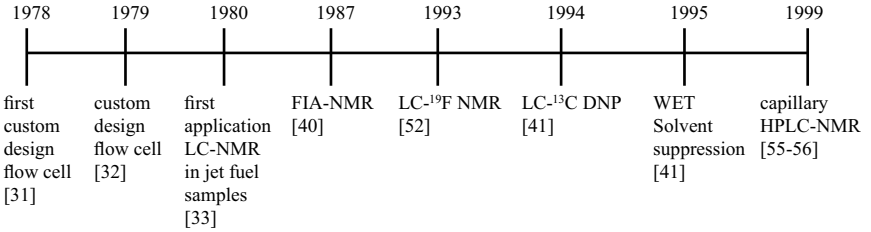

FIGURE 2-3. Major milestones in the history and discovery of LC-NMR.

radiolabeling because ^{19}F is 100% naturally occurring, with half-integer spin, and has a sensitivity of 0.83 related to ^{1}H.

Over the years, the issue of low sensitivity in NMR has prompted the development of other technologies. There have been two primary approaches: the development of smaller flow cells to the capillary level and the increase in sensitivity with cryogenic probes. In the late 1990s, Sweedler et al. [55,56] developed probes with a microcoil flow cell volume of 1.1 μL connected to capillary HPLC through capillary tubing. In those cases, the sample volume injected into the system is about 5 μL, injecting less than 5 μg of sample with 750 ng as the amount minimally detectable by NMR. In the case of cryogenic probes, the sensitivity, increased by cooling the electronics of the NMR probe to 20 to 25 K, is around fourfold in the case of standard conditions (no-flow conditions) [27]. In the last few years, cryogenic probes have become more accessible, and many laboratories can afford the additional cost. Figure 2-3 depicts the major milestones of the history and discovery of LC-NMR as they appear in the literature. More detailed information on their applications and references is provided in Chapter 4.

2.4. HISTORICAL DEVELOPMENT OF OTHER ANALYTICAL TECHNIQUES HYPHENATED WITH NMR

During the last decade, the need to solve structural problems in complex mixtures and small quantities has extended the development of hyphenated NMR to other analytical techniques in the areas of separation and structural information. In the area of separation, capillary and solid-phase extraction techniques have focused on small quantities and trace analysis. In the area of structural information, mass spectrometric techniques have been the best developed and most commonly used to solve structural problems.

An early attempt at online coupling of gas chromatography and nuclear magnetic resonance (GC-NMR) was performed by Tsuda et al. in 1972 [57].

Tsuda's group designed three different flow cells inserted in the magnet to test the technology with a mixture of methyl ethyl ketone (MEK) and *p*-xylene. The gases were trapped in a small condenser to be mixed with deuterated solvent before entering the NMR flow cell [57]. What is today considered direct hyphenation of GC-NMR was introduced in the early 1980s by Herzog and Buddrus [58,59], who also designed a flow cell to trap the gases and condense them for NMR analysis. The group evaluated their GC-NMR system with mixtures of components with low boiling points (50°C) and up to 200°C for high-boiling-point samples [58,59].

In 1988, Hatada et al. measured the molecular weight of polymers by gel permeation chromatography (GPC) coupled to NMR (GPC-NMR) without the need to perform calibration curves as done when using GPC alone [60]. The advantage that NMR presents is based on reliable measurement of the molar ratios of the signal for the end group of the polymer and the monomeric units. The authors developed a flow cell for the online GPC-NMR instrument. The data obtained from the proton of GPC-NMR were in the same range as the data measured from the GPC calibrated technique [60]. In 1998, in a similar fashion, Hatada et al. [61] applied size-exclusion chromatography (SEC) hyphenated to NMR (SEC-NMR) to analysis of the molecular weight distribution of mixtures of poly(methyl methacrylate) polymers in complex mixtures.

In 1988, Allen et al. described the direct coupling of supercritical fluid chromatography (SFC) with NMR (SFC-NMR) [62]. The group built an NMR flow cell probe with variable temperature and pressure capabilities to operate at temperatures as high as 100°C with pressures around 3000 psi, required to couple with the SFC system [62]. The authors tested the SFC-NMR system on a model mixture of fuels. In 1994, Albert et al., in collaboration with Bruker GmbH [63], developed a system with an SFC probe head using a 5-mm sapphire tube that allowed 120 μL of active volume in the flow cell, a dimension typical for commercial LC-NMR flow cell systems. The SFC-NMR system was tested with a mixture of phthalates. The authors indicated that the major advantage of SFC-NMR is that no solvent suppression techniques are needed when using CO_2 as the solvent system [63]. Supercritical fluid extraction (SFE) hyphenated with NMR (SFE-NMR) works in a manner similar to SFC-NMR, with the difference that the SFE flow cell handles the high pressures needed for SFE. SFE-NMR was reported by Braumann et al. in 1995 [64].

Capillary electrophoresis (CE) is an analytical technique capable of separating small sample volumes in the nanoliter range. In 1994, Wu et al. [65] coupled CE to NMR (CE-NMR), designing a 5-nL limit in the detection cell to expand the ability of NMR in a nanoliter sample volume. In 1998, capillary HPLC (CHPLC or capLC), capillary electrophoresis (CE),

capillary electrochromatography (CEC), and capillary zone electrophoresis (CZE) were coupled to NMR to explore their capabilities [66]. Capillary electrochromatography (CEC) and capillary zone electrophoresis (CZE) were tested for the identification of known metabolites of paracetamol from human urine [67,68]. The authors claimed that the analysis was carried out on approximately 10 ng of metabolite detected by NMR. A recent new development in the capillary chromatography arena is the hyphenation of capillary isotachophoresis (cIPT) with NMR (cIPT-NMR), developed in 2001 by Sweedler's group [69]. The group demonstrated a twofold increase in sensitivity using cIPT-NMR [69].

Since early 2000, solid-phase extraction hyphenated with NMR (SPE-NMR) has become a powerful combination for the structural elucidation of minor components of mixtures, including trace analysis. SPE concentrates the analytes of interest in cartridges in several injections and without the need of deuterated solvents, followed by drying under N_2 prior to online NMR analysis in the appropriate deuterated solvent. In 2001, Nyberg et al. [70] explored the application of SPE-NMR to fractions from a plant extract, Habanero pepper, to determine the structures of their components.

During the last few years, more progress has been achieved by hyphenating LC-NMR with MS for a more complete structural analysis of components of complex mixtures. The LC-NMR-MS or LC-NMR/MS (called LC-MS-NMR in this book) has expanded the structure-solving capabilities by obtaining simultaneous MS and NMR data from the same chromatographic peak. There are some compromises that have to be taken into account because of the differences between MS and NMR, such as sensitivity, solvent compatibility, and destructive versus nondestructive techniques, among others discussed in Chapter 3. LC-MS has been used for many years as a preferred analytical technique. However, with the development of electrospray ionization techniques, LC-MS has been used routinely for the analysis of complex mixtures in the pharmaceutical industry. LC-MS-NMR is a combination of LC-MS with electrospray in many cases, and LC-NMR is presented in Chapter 3. In the late 1990s, LC-MS-NMR has been used successfully primarily in drug metabolism [71,72]. An extension of this technique is the hyphenation of NMR and MS with SPE (SPE-MS-NMR). A common trend is by splitting the flow between the MS and NMR and having the SPE unit prior to the NMR for further concentration of analytes of interest for NMR analysis. SPE-MS-NMR has been employed mainly in the area of natural products and in drug metabolism in the last few years [73,74].

Figure 2-4 depicts the major milestones of various analytical separation techniques coupled with NMR as they appear in the literature. More detailed information on their applications and references is provided in Chapters 5 and 6.

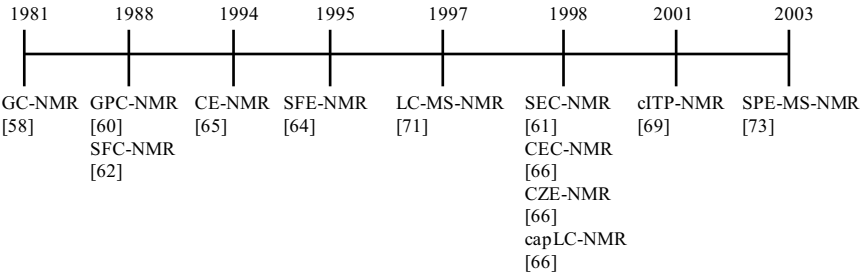

FIGURE 2-4. Major milestones in the history and discovery of other analytical techniques hyphenated with NMR.

2.5. CURRENT TRENDS

The brief history of NMR and hyphenated NMR given in this chapter demonstrates the importance of the NMR technique as part of complex analytical techniques to pursue the structural elucidation of components of complex mixtures. Many analytical techniques have been hyphenated to NMR to facilitate the analysis of samples from complex mixtures. The application and hyphenation of NMR are still evolving; not all the current hyphenated analytical techniques may show the same development, depending on factors such as cost, engineering needs, and user friendliness to analysts with different backgrounds. The classical approach of isolation prior to NMR analysis in an NMR tube is still a commonly used methodology that may not necessarily disappear with emerging analytical hyphenated techniques in coming years. Through the coming years, existing and emerging hyphenated NMR techniques will be evaluated by analysts in academia and industry based on practicality.

REFERENCES

[1] C.J. Gorter, Negative Results of an Attempt to Detect Nuclear Magnetic Spins, *Physica* **3** (1936), 995–998.

[2] C.J. Gorter and L.F.J. Broer, Negative Results of an Attempt to Observed Nuclear Magnetic Resonance, *Physica* **9** (1942), 591–595.

[3] F. Bloch, W.W. Hansen, and M.E. Packard, Nuclear Induction, *Phys. Rev.* **69** (1946), 127.

[4] E.M. Purcell, H.C. Torrey, and R.V. Pound, Resonance Absorption by Nuclear Magnetic Moments in a Solid, *Phys. Rev.* **69** (1946), 37–38.

[5] J.T. Arnold, S.S. Dharmatti, and M.E. Packard, Chemical Effects on Nuclear Induction Signals from Organic Compounds, *J. Chem. Phys.* **19** (1951), 507.

[6] W.A. Anderson, Nuclear Magnetic Resonance Spectra of Some Hydrocarbons, *Phys. Rev.* **102** (1956), 151–167.

[7] E.L. Hahn, Spin Echoes, *Phys. Rev.* **80** (1950), 580–594.

[8] G.A. Morris and R. Freeman, Enhancement of Nuclear Magnetic Resonance Signals by Polarization Transfer, *J. Am. Chem. Soc.* **101** (1979), 760–762.

[9] S.R. Hartmann and E.L. Hahn, Nuclear Double Resonance in the Rotating Frame, *Phys. Rev.* **128** (1962), 2042–2053.

[10] J.N. Shoolery, NMR Spectroscopy in the Beginning, *Anal. Chem.* **55** (1993), 731A–741A.

[11] J.N. Shoolery, The Development of Experimental and Analytical High Resolution NMR, *Prog. Nucl. Magn. Reson. Spectrosc.* **28** (1995), 37–52.

[12] R.R. Ernst and W.A. Anderson, Application of Fourier-Transform Spectroscopy to Magnetic Resonance, *Rev. Sci. Instrum.* **37** (1966), 93–102.

[13] J.W. Cooley and J.W. Tukey, An Algorithm for the Machine Calculation of Complex Fourier Series, *Math. Comput.* **19** (1965), 297–301.

[14] R. Freeman and S. Whittekoek, Selective Determination of Relaxation Times in High Resolution NMR, *J. Magn. Reson.* **1** (1969), 238–276.

[15] A.W. Overhauser, Polarization of Nuclei in Metals, *Phys. Rev.* **92** (1953), 411–415.

[16] W.P. Aue, E. Bartholdi, and R.R. Ernst, Two-Dimensional Spectroscopy: Application to Nuclear Magnetic Resonance, *J. Chem. Phys.* **64** (1976), 2229–2246.

[17] L. Braunschweiler and R.R. Ernst, Coherence Transfer by Isotropic Mixing: Application to Proton Correlation Spectroscopy, *J. Magn. Reson.* **53** (1983), 521–528.

[18] R. Freeman and G. A Morris, Experimental Chemical Shift Correlation Maps in Nuclear Magnetic Resonance, *J. Chem. Soc. Chem. Commun.* (1978), 684–686.

[19] J. Jeener, B.H. Meier, P. Bachmann, and R.R. Ernst, Investigation of Exchange Processes by Two-Dimensional NMR Spectroscopy, *J. Chem. Phys.* **71** (1979), 4546–4553.

[20] A. Bax and D.G. Davis, Practical Aspect of Two-Dimensional Transverse NOE Spectroscopy, *J. Magn. Reson.* **63** (1985), 207–213.

[21] L. Müller, Sensitivity Enhanced Detection of Weak Nuclei Using Heteronuclear Multiple Quantum Coherence, *J. Am. Chem. Soc.* **101** (1979), 4481–4484.

[22] A. Bax and S. Subramanian, Sensitivity-Enhanced Two-Dimensional Heteronuclear Shift Correlation NMR Spectroscopy, *J. Magn. Reson.* **67** (1986), 565–569.

[23] G. Bodenhausen and D.J. Ruben, Natural Abundance Nitrogen-15 NMR by Enhanced Heteronuclear Spectroscopy, *Chem. Phys. Lett.* **69** (1980), 185–189.

[24] A. Bax and M.F. Summer, ^{1}H and ^{13}C Assignments from Sensitivity-Enhanced Detection of Heteronuclear Multiple-Bond Connectivity by 2D Multiple Quantum NMR, *J. Am. Chem. Soc.* **108** (1986), 2093–2094.

[25] A. Bax, R. Freeman, and T.A. Frenkiel, An NMR Technique for Tracing Out the Carbon Skeleton of an Organic Molecule, *J. Am. Chem. Soc.* **103** (1981), 2102–2104.

[26] R.E. Hurd, Gradient-Enhanced Spectroscopy, *J. Magn. Reson.* **87** (1990), 422–428.

[27] P. Styles, N.F. Soffe, C.A. Scott, D.A. Crag, F. Row, D.J. White, and P.C.J. White, A High-Resolution NMR Probe in Which the Coil and Preamplifier Are Cooled with Liquid Helium, *J. Magn. Reson.* **60** (1984), 397–404.

[28] J.W. Emsley and J. Feeny, Progress Milestone in the First Fifty Years of NMR, *Nucl. Magn. Reson. Spectrosc.* **28** (1995), 1–9.

[29] R. Freeman, The Fourier Transform Revolution in NMR Spectroscopy, *Anal. Chem.* **65** (1993), 743A–753A.

[30] R. Freeman, Pioneers of High-Resolution NMR, *Concepts Magn. Reson.* **11** (1999), 61–70.

[31] N. Watanabe and E. Niki, Direct-Coupling of FT-NMR to High Performance Liquid Chromatography, *Proc. Jpn. Acad. Ser. B* **54** (1978), 194–199.

[32] E. Bayer, K. Albert, M. Nieder, E. Grom, and T. Keller, On-Line Coupling of High-Performance Liquid Chromatography and Nuclear Magnetic Resonance, *J. Chromatogr.* **186** (1979), 497–507.

[33] J.F. Haw, T.E. Glass, D.W. Hausler, E. Motell, and H.C. Dorn, Direct Coupling of a Liquid Chromatograph to a Continuous Flow Hydrogen Nuclear Magnetic Resonance Detector for Analysis of Petroleum and Synthetic Fuels, *Anal. Chem.* **52** (1980), 1135–1140.

[34] J.F. Haw, T.E. Glass, and H.C. Dorn, Continuous Flow High Field Nuclear Magnetic Resonance Detector for Liquid Chromatography Analysis of Fuel Samples, *Anal. Chem.* **53** (1981), 2327–2332.

[35] J.F. Haw, T.E. Glass, and H.C. Dorn, Analysis of Coal Conversion Recycle Solvent by Liquid Chromatography with Nuclear Magnetic Resonance Detection, *Anal. Chem.* **53** (1981), 2332–2336.

[36] J.F. Haw, T.E. Glass, and H.C. Dorn, Conditions for Quantitative Flow FT-^{1}H NMR Measurements Under Repetitive Pulse Conditions, *J. Magn. Reson.* **49** (1982), 22–31.

[37] E. Bater, K. Albert, M. Nieder, and E. Grom, On-Line Coupling of Liquid Chromatography and High-Field Nuclear Magnetic Resonance Spectrometry, *Anal. Chem.* **54** (1982), 1747–1750.

[38] J.F. Haw, T.E. Glass, and H.C. Dorn, Liquid Chromatography/Proton Nuclear Magnetic Resonance Spectrometry Average Composition Analysis of Fuels, *Anal. Chem.* **55** (1983), 22–29.

[39] D.A. Laude, Jr. and C.L. Wilkins, Direct-Linked Analytical Scale High-Performance Liquid Chromatography/Nuclear Magnetic Resonance Spectrometry, *Anal. Chem.* **56** (1984), 2471–2475.

[40] S.A. Curran and D.E. Williams, Design and Optimization of an NMR Flow Cell for a Commercial NMR Spectrometer, *Appl. Spectrosc.* **41** (1987), 1450–1454.

[41] S. Stevenson and H.C. Dorn, ^{13}C Dynamic Nuclear Polarization: A Detector for Continuous-Flow, On-Line Chromatography, *Anal. Chem.* **66** (1994), 2993–2999.

[42] K. Albert, Liquid Chromatography–Nuclear Magnetic Resonance Spectroscopy, *J. Chromatogr. A* **856** (1999), 199–211.

[43] J.C. Lindon, J.K. Nicholson, and I.D. Wilson, Directly Coupled HPLC-NMR and HPLC-NMR-MS in Pharmaceutical Research and Development, *J. Chromatogr. B* **748** (2000), 233–258.

[44] R.P. Hicks, Recent Advances in NMR: Expanding Its Role in Rational Drug Design, *Curr. Med. Chem.* **8** (2001), 627–650.

[45] J.C. Lindon, J.K. Nicholson, and I.D. Wilson, Direct Coupling of Chromatography to NMR Spectroscopy, *Prog. Nucl. Magn. Reson. Spectrosc.* **29** (1996), 1–49.

[46] M.V. Silva Elipe, LC-NMR and LC-MS-NMR: Recent Technological Advancements, in J. Cages (ed.), *Encyclopedia of Chromatography*, Marcel Dekker, New York, 2002, pp. 1–13.

[47] K. Albert, *On-Line LC-NMR and Related Techniques*, Wiley, Chichester, England, 2002.

[48] M.V. Silva Elipe, Advantages and Disadvantages of Nuclear Magnetic Resonance Spectroscopy as Hyphenated Technique, *Anal. Chim. Acta* **497** (2003), 1–25.

[49] M.V. Silva Elipe, LC-NMR Overview and Pharmaceutical Applications, in Y. Kazakevich and R. LoBrutto (eds.), *HPLC for Pharmaceutical Scientists*, Wiley, Hoboken, NJ, 2007, pp. 901–936.

[50] M.V. Silva Elipe, LC/NMR and LC/MS/NMR, in J. Cages (ed.), *Encyclopedia of Chromatography* 3rd ed., Vol. 1, 2009, pp. 1337–1351.

[51] S.H. Smallcombe, S.L. Patt, and P.A. Keifer, WET Solvent Suppression and Its Applications to LC NMR and High-Resolution NMR Spectroscopy, *J. Magn. Reson. Ser. A* **117** (1995), 295–303.

[52] M. Spraul, M. Hofmann, I.D. Wilson, E. Lenz, J.K. Nicholson, and J.C. Lindon, Coupling of HPLC with ^{19}F- and ^{1}H-NMR Spectroscopy to Investigate the Human Urinary Excretion of Flurbiprofen Metabolites, *J. Pharm. Biomed. Anal.* **11** (1993), 1009–1015.

[53] E.A. Crowe, J.K. Roberts, and R.J. Smith, ^{1}H and ^{19}F LC/NMR: Application to the Identification of Impurities in Compounds of Pharmaceutical Interest, *Pharm. Sci.* **1** (1995), 103–105.

[54] G.B. Scarfe, B. Wright, E. Clayton, S. Taylor, I.D. Wilson, J.C. Lindon, and J.K. Nicholson, ^{19}F-NMR and Directly Coupled HPLC-NMR-MS Investigations into the Metabolism of 2-Bromo-4-trifluoromethylaniline in Rat: A Urinary Excretion Balance Study Without the Use of Radiolabelling, *Xenobiotica* **28** (1998), 373–388.

[55] M.E. Lacey, R. Subramanian, D.L. Olson, A.G. Webb, and J.V. Sweedler, High-Resolution NMR Spectroscopy of Sample Volumes from 1 nL to 10 μL, *Chem. Rev.* **99** (1999), 3133–3152.

[56] R. Subramanian, W.P. Kelley, P.D. Floyd, Z.J. Tan, A.G. Webb, and J.V. Sweedler, A Microcoil NMR Probe for Coupling Microscale HPLC with On-Line NMR Spectroscopy, *Anal. Chem.* **71** (1999), 5335–5339.

[57] T. Tsuda, Y. Ojika, M. Izuda, I. Fujishima, and D. Ishii, The Combination of Gas Chromatography and Nuclear Magnetic Resonance Spectroscopy, *J. Chromatogr.* **69** (1972), 194–197.

[58] J. Buddrus and H. Herzog, Coupling of Chromatography and NMR: 3. Study of Flowing Gas Chromatography Fractions by Proton Magnetic Resonance, *Org. Magn. Reson.* **15** (1981), 211–213.

[59] H. Herzog and J. Buddrus, Coupling of Chromatography and NMR: 5. Analysis of High-Boiling Gas Chromatographic Fractions by On-Line Nuclear Magnetic Resonance, *Chromatographia* **18** (1984), 31–33.

[60] K. Hatada, K. Ute, Y. Okamoto, M. Imanari, and N. Fujii, On-Line GPC/NMR Experiments Using the Isotactic Poly(methyl methacrylate) with Well Defined Chemical Structure, *Polym. Bull.* **20** (1988), 317–321.

[61] K. Ute, R. Niimi, S.-Y. Hongo, and K. Hatada, Determination of Molecular Weight Distribution by Size Exclusion Chromatography with 750 MHz ^{1}H NMR Detection (On-Line SEC-NMR), *Polym. J.* **30** (1998), 439–443.

[62] L.A. Allen, T.E. Glass, and H.C. Dora, Direct Monitoring of Supercritical Fluids and Supercritical Chromatographic Separations by Proton Nuclear Magnetic Resonance, *Anal. Chem.* **60** (1988), 390–394.

[63] K. Albert, U. Braumann, L.-H. Tseng, G. Nicholson, E. Bayer, M. Spraul, M. Hofmann, C. Dowle, and M. Chippendale, On-Line Coupling of Supercritical Fluid Chromatography and Proton High-Field Nuclear Magnetic Resonance Spectroscopy, *Anal. Chem.* **66** (1994), 3042–3046.

[64] U. Braumann, H. Händel, K. Albert, R. Ecker, and M. Spraul, On-Line Monitoring of the Supercritical Fluid Extraction Process with Proton Nuclear Magnetic Resonance Spectroscopy, *Anal. Chem.* **67** (1995), 930–935.

[65] N. Wu, T.L. Peck, A.G. Webb, R.L. Magin, and J.V. Sweedler, Nanoliter Volume Sample Cells for ^{1}H NMR Application to On-Line Detection in Capillary Electrophoresis, *J. Am. Chem. Soc.* **111** (1994), 7929–7930.

[66] K. Pusecker, J. Schewitz, P. Gfrörer, L.-H. Tseng, K. Albert, and E. Bayer, On-Line Coupling of Capillary Electrochromatography, Capillary Electrophoresis, and Capillary HPLC with Nuclear Magnetic Resonance Spectroscopy, *Anal. Chem.* **70** (1998), 3280–3285.

[67] J. Schewitz, P. Gfrörer, K. Pusecker, L.-H. Tseng, K. Albert, E. Bayer, I.D. Wilson, N.J. Bailey, G.B. Scarfe, J.K. Nicholson, and J.C. Lindon, Directly Coupled CZE-NMR and CEC-NMR Spectroscopy for Metabolite Analysis: Paracetamol Metabolites in Human Urine, *Analyst* **123** (1998), 2835–2837.

[68] K. Pusecker, J. Schewitz, P. Gfrörer, L.-H. Tseng, K. Albert, E. Bayer, I.D. Wilson, N.J. Bailey, G.B. Scarfe, J.K. Nicholson, and J.C. Lindon, On-Flow Identification of Metabolites of Paracetamol from Human Urine Using Directly

Coupled CZE-NMR and CEC-NMR Spectroscopy, *Anal. Commun.* **35** (1998), 213–215.

[69] R.A. Kautz, M.E. Lacey, A.M. Wolters, F. Foret, A.G. Webb, B.L. Karger, and J.V. Sweedler, Sample Concentration and Separation for Nanoliter-Volume NMR Spectroscopy Using Capillary Isotachophoresis, *J. Am. Chem. Soc.* **123** (2001), 3159–3160.

[70] N.T. Nyberg, H. Baumann, and L. Kenne, Application of Solid-Phase Extraction Coupled to an NMR Flow-Probe in the Analysis of HPLC Fractions, *Magn. Reson. Chem.* **39** (2001), 236–240.

[71] G.B. Scarfe, I.D. Wilson, M. Spraul, M. Hofmann, U. Brauman, J.C. Lindon, and J.K. Nicholson, Application of Directly Coupled High-Performance Liquid Chromatography–Nuclear Resonance–Mass Spectrometry to the Detection and Characterisation of the Metabolites of 2-Bromo-4–trifluoromethylaniline in Rat Urine, *Anal. Commun.* **34** (1997), 37–39.

[72] K.I. Burton, J.R. Everett, M.J. Newman, F.S. Pullen, D.S. Richards, and A.G. Swanson, On-Line Chromatography Coupled with High Field NMR and Mass Spectrometry (LC-NMR-MS): A New Technique for Drug Metabolite Structure Elucidation, *J. Pharm. Biomed. Anal.* **15** (1997), 1903–1912.

[73] V. Exarchou, M. Godejohann, T.A. Van Beek, I.P. Gerothanassis, and J. Vervoort, LC-UV-Solid-Phase Extraction-NMR-MS Combined with a Cryogenic Flow Probe and Its Application to the Identification of Compounds Present in Greek Oregano, *Anal. Chem.* **75** (2003), 6288–6294.

[74] M. Godejohann, L.-H. Tseng, U. Braumann, J. Fuchser, and M. Spraul, Characterization of a Paracetamol Metabolite Using On-Line LC-SPE-NMR-MS and Cryogenic NMR Probe, *J. Chromatogr. A* **1058** (2004), 191–196.

3

Basic Technical Aspects and Operation of LC-NMR and LC-MS-NMR

3.1. INTRODUCTION

NMR is one of the most powerful techniques for the structural elucidation of organic compounds. Separation and isolation of the individual components of a sample mixture are the normal steps before analyzing their structures by NMR. Prior to isolation, LC/MS is used routinely to analyze the components of the mixture to evaluate the need to isolate the compound(s) of interest. In many cases, however, NMR is necessary for the identification of ambiguous structures. Even though hyphenated LC-NMR has been known since the late 1970s [1–4], the technique was not implemented widely until the last two decades [5–10]. For a more complete structural analysis, LC-MS and LC-NMR have been combined (LC-MS-NMR) in the last decade, with its efficacy demonstrated successfully. In this chapter we discuss primarily technical considerations regarding LC-NMR and LC-MS-NMR.

3.2. TECHNICAL CONSIDERATIONS REGARDING LC-NMR

The decision to use either NMR or LC-NMR for the analysis of components from mixtures depends on factors related to their chromatographic separation

LC-NMR and Other Hyphenated NMR Techniques: Overview and Applications, First Edition. Maria Victoria Silva Elipe.

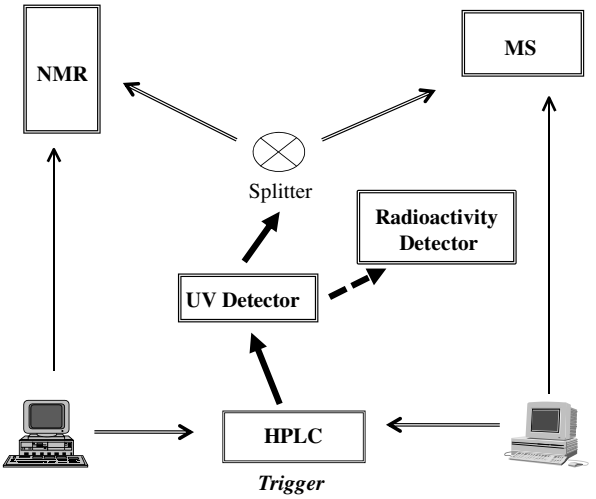

FIGURE 3-1. Schematic setup of an LC-NMR and LC-MS-NMR system with the addition of a radioactive detector when needed for the identification of radioactive metabolites.

and the ability of NMR to elucidate the structure of organic compounds, whether or not HPLC and NMR are hyphenated. Figure 3-1 shows the schematic setup of an LC-NMR system that can also be connected to other devices, such as a radioactivity detector and a mass spectrometer. The sample mixture is injected into the injector port of the HPLC unit for separation under specific conditions (e.g., solvent system, column, temperature) before arriving at the NMR instrument. Commonly, the separation is monitored by an ultraviolet (UV) detector, but other detectors, such as a photodiode array, a refractive index detector, a radioactive detector, or even an MS instrument, can be used for that purpose. The HPLC is connected to the NMR flow cell through red poly(ether ether ketone) (PEEK) tubing. The major technical considerations of LC-NMR, discussed below, are solvent compatibility, solvent suppression, the NMR flow cell, and LC-NMR sensitivity.

3.2.1. Solvent Compatibility

Liquid NMR requires the use of deuterated solvents to minimize the dynamic range between the solvent(s) and the solute or analyte. Conventionally, the sample is analyzed as a solution using a 3- or 5-mm NMR tube, depending on the NMR probe or amount of sample, which require, respectively, about 150 or 500 μL of deuterated solvents. The increased solvent requirements for LC-NMR make this technique costly compared to other analytical techniques using nondeuterated solvents. Deuterium oxide (D_2O) is the most readily available, reasonably priced solvent (over $300 per liter). The cost of

deuterated acetonitrile (CD_3CN) has been decreasing over the years and varies depending on the percentage of D_2O included, but is still over $1000/per liter. Deuterated methanol (CD_3OD) is even more expensive. Deuterated solvents for normal-phase columns are highly expensive, if available. This restriction necessitates the use of reversed-phase columns for LC-NMR. With the recent development of solid-phase extraction (SPE) as SPE-NMR and capillary-based HPLC as capLC-NMR or microflow NMR (see Chapter 6 for more information on those techniques), the amount of deuterated solvents needed to pump the analyte of interest to the flow cell for NMR analysis is much less and stays in the microliter to milliliter range. These developments make the hyphenated NMR techniques economically more accessible. However, in the case of columnless LC-NMR, such as flow injection analysis NMR (FIA-NMR) and direct injection NMR (DI-NMR) (discussed briefly in Section 3.6), other deuterated solvents can be used as solvent systems as a way to transport the sample to the flow cell without the need for separation by HPLC. Due to the low volume used in columnless LC-NMR, the use of protonated solvents helps reduce the costs of the technique tremendously.

3.2.2. Solvent Suppression

Commonly, a system of at least two solvents is used in HPLC to separate the analytes of the sample mixture. During an LC-NMR run, the signals of the solvents in the chromatographic peak are much larger than those of the analyte of interest and need to be suppressed. This applies even with deuterated solvents because they have a percentage of protonation that is larger than the analytes in the sample mixture for the typical millimolar concentration of samples. In the early days of LC-NMR, solvent suppression was the downside of the technique. In the case of acetonitrile, a commonly used solvent for reversed-phase separations and accessible as deuterated solvent, the two ^{13}C satellite peaks of either the protonated or residual protonated methyl group for CH_3CN or CD_3CN also require suppression because they are typically much larger than signals from the sample. The natural abundance of ^{13}C is 1.108%, which indicates the enormous difference in dynamic range in molar concentrations between the solvent and the millimolar sample concentration. In the 1990s, the first increment of presaturation NOESY was used successfully. It suppresses the solvent signals better than presaturation; however, the spectrum is less accurate for quantitation. With optimization of the WET (water suppression enhanced through T_1 effects) solvent suppression technique by Smallcombe et al. [11] in 1995, the quality of spectra generated during LC-NMR has been improved significantly and is now routine. The WET solvent suppression technique is the standard technique for LC-NMR because compared with other techniques, such as presaturation or watergate, it has the

capability of suppressing several solvent lines with only minimal baseline distortions. One disadvantage of suppressing the solvent lines is that any nearby analyte signal will also be suppressed, resulting in loss of structural information. Completely unknown structures are more difficult to analyze by LC-NMR than by conventional tube NMR, due to the possibility of having signals from the analyte suppressed if they are in the same region of the solvent lines. This factor makes LC-NMR more appropriate for partially unknown structures than for totally unknown compounds. With the development of solid-phase extraction NMR (SPE-NMR) and capillary-HPLC NMR (capLC-NMR) or microflow NMR (see Chapter 6), solvent suppression is not the major requirement as it is for conventional LC-NMR because less solvent is needed for NMR analysis of these systems. For samples that do not require separation prior to NMR analysis, flow injection analysis NMR (FIA-NMR) and direct injection NMR (DI-NMR) are nonchromatographic NMR techniques in which the sample is injected directly and pumped to the NMR flow cell without passing through a chromatographic column [12]. In those cases, the dynamic range between the analyte and the solvent signals is less dramatic than for conventional LC-NMR, due to the absence of a chromatographic column, which would require a greater quantity of solvent. With the WET suppression technique, favorable results in the microgram range have been obtained using protonated or deuterated solvents [12].

3.2.3. NMR Flow Cell

There are three aspects to consider regarding a flow cell inserted in an NMR probe: the connection to the HPLC, the filling factor, and the homogeneity of the solution in the flow cell. The flow cell must have an inlet port attached to capillary tubing (e.g., red PEEK tubing) to be connected to the HPLC system and an outlet port to go to waste. The filling factor refers to having the receiver coil around the flow cell, which must have an optimized volume to allow most of the chromatographic peak to occupy the cell for best NMR sensitivity. Finally, the homogeneity of the solution must be maximized to avoid distortions in the spectrum due to bubble formation and inhomogeneous solution caused by variations in the flow rate of the HPLC gradient solvent system over time. Based on these considerations, the flow cells are designed to have the inlet line entering the flow cell from the bottom and the outlet line exiting from the top (Figure 3-2). Conventional NMR flow cells have an active volume of 60 μL (i.e., corresponding to the length of the receiver coil around the flow cell) and a total volume of 120 μL. These commercial flow cells are comparable to 3-mm NMR tubes in diameter. Based on the design, this means that NMR will "see" only 60 μL of the chromatographic peak. If the flow rate in the HPLC is 1 mL/min when 4.6-mm columns are used, only 3.6 s of the

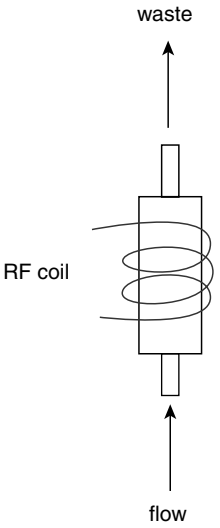

FIGURE 3-2. Schematic representation of a typical NMR flow cell (not to scale). The flow goes through the NMR flow cell from the botton (inlet) to the top (outlet), toward waste. The RF coil is the receiver coil.

chromatographic peak will be seen by NMR. Chromatographic peaks are generally much wider than 4 s, indicating that less than half of the chromatographic peak will be detected (Figure 3-3). This is one of the disadvantages of LC-NMR compared with conventional 3-mm NMR probes, where the amount of sample seen by the NMR receiver coil is independent of the width of the chromatographic peak. In addition, NMR flow cells with active volumes of 10, 30, 60, and 120 μL are available commercially. Applications using solid-

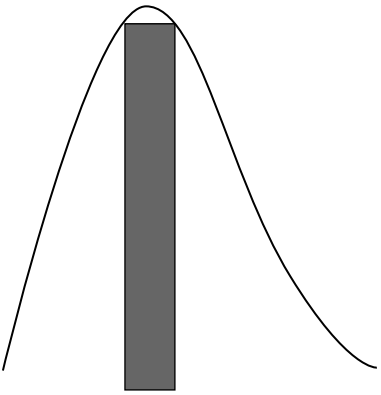

FIGURE 3-3. Schematic representation of a chromatographic peak where what the RF coil will be able to detect is shown in gray (not to scale).

phase extraction (SPE-NMR) are more appropriate for 10- or 30-μL flow cells (see Chapter 6). Microcoil NMR flow cells for capLC-NMR or microflow NMR have available typical active volumes of 1.5, 5, and 10 μL, but also volumes ranging from 30 μL to 5 nL for samples in low concentration (see Chapter 6). In recent years, with the development of cryogenic probes, commercial flow cells have also been available to perform LC-NMR and gain sensitivity by means of cooling the electronics of cryogenic probes.

3.2.4. LC-NMR Sensitivity

NMR is less sensitive than other analytical techniques, such as MS, and hence requires much larger samples for structural analysis. MS analysis is carried out routinely in the picogram range. Modern high-field NMR spectrometers (400 MHz and higher) can detect proton signals from pure demonstration samples well into the nanogram range (molecular weight 300 Da). However, samples in the high microgram or low milligram range are adequate to perform structural analysis. Smaller amounts are more appropriate for simple structures and larger amounts for complex molecules in their structure and molecular size. With cryoprobes (for Bruker NMR instruments) or cold probes (for Varian NMR instruments, now a division of Agilent Technologies), depending on the NMR vendor currently available, the sensitivity of NMR improves markedly: at least fourfold for proton (^{1}H) compared to room-temperature probes. Samples in the low nanogram range can be detected but are not appropriate for structural analysis. In the high nanogram range, structural analysis can be carried out for cryogenic probes. For real-world samples, however, purity problems become more intrusive with diminishing sample size and can be overwhelming in the submicrogram domain even as a result of interference by impurities in the deuterated solvent used for NMR studies. This places a current practical lower limit on most structural elucidation by NMR, which is estimated by the writer to be close to 500 ng (molecular weight 300 Da) for cryogenic probes.

Although several other important nuclides can be detected by NMR, proton (^{1}H) remains the most widely used because of its high sensitivity, high isotopic natural abundance (99.985%), and ubiquitous presence in organic compounds. Of comparable importance is carbon (^{13}C), 1.108% natural abundance, which, because of substantial improvements in instrument sensitivity, is now utilized as routinely as protons by direct or indirect detection probes. Fluorine (^{19}F), 100% natural abundance, is used less since it is present in only about 10% of pharmaceutical compounds; however, compared to proton, fluorine displays important properties: its chemical shift dispersion and high chemical shift sensitivity to moderate structural changes. Another consequence of the intrinsic low sensitivity of NMR is that virtually all samples

require signal averaging to reach an acceptable signal-to-noise level. Depending on sample size and amount of sample for structural analysis, signal averaging time may range anywhere from several minutes to several days. For metabolites in the range 1 to 10 μg, for example, overnight experiments are generally necessary. For that amount, only proton experiments are performed in partially unknown structures such as metabolites.

3.3. TECHNICAL CONSIDERATIONS REGARDING LC-MS-NMR

Analysis of complex mixtures in a chromatographic run by the hyphenation of several analytical techniques, such as NMR and MS with HPLC, is becoming more popular in the pharmaceutical industry and in natural products chemistry. NMR and MS data on the same analyte are crucial for structural elucidation. When different isolates, such as natural products, metabolites, in-process impurities, or degradation products, are analyzed by NMR and MS, one cannot always be certain that the NMR and MS data apply to the same analyte, especially in MS and NMR analysis when the analytes have been isolated using analytical columns and prep columns, respectively. HPLC conditions are not always reproducible when analytical and prep-HPLC columns are used to isolate different amounts of the analytes of interest for separate MS and NMR analysis. To avoid this ambiguity, LC-MS and LC-NMR are combined. MS data should be obtained initially because NMR data collection in the stop-flow mode can take hours or days, depending on the complexity of the structure and the amount of sample. This is why it is advisable from the author's perspective to designate this operation as LC-MS-NMR or LC/MS/NMR rather than LC-NMR-MS or LC-NMR/MS. In the literature, LC-NMR-MS is more common, but it does not follow the sample pathway in the hyphenated MS and LC-NMR system.

Since MS is considerably more sensitive than NMR, a splitter is incorporated after the HPLC to direct the sample separately to the MS and NMR units. As indicated below, the author used a custom-made system [8]. The MS used in the examples presented here is a classic LCQ instrument (ThermoFinnigan, San Jose, CA). A custom-made splitter was used with a splitting ratio of 1/100 (Acurate, LC Packings, Sunnyvale, CA). It was designed to deliver 1% of the sample initially to the MS and the balance 20 s later to the NMR. With a flow rate of 1 mL/min, the final flow rate going to the NMR will be 0.990 mL/min and to the MS will be 0.010 mL/min. Electrospray is the only source of ionization that will work with such a low flow rate (10 μL/min) in LCQ. Figure 3-1 depicts the scheme of the LC-MS-NMR system used in the example for this book. The technical considerations regarding LC-MS-NMR are the

same as those for LC-NMR (see Section 3.2), plus the effect of using deuterated solvents for the MS of LC-MS-NMR.

For the last decade, the LC-MS-NMR (or LC-NMR-MS as designated by NMR vendors) system has been available commercially from both major NMR vendors: Bruker BioSpin Corp., and Varian, Inc. (now Agilent Technologies). The work presented here has been carried out by the author using a custom design of an LC-MS-NMR system on a Varian NMR instrument, as explained in Sections 3.4.2 and 3.5.

3.3.1. Deuterated Solvents

An important consideration for an LC-MS-NMR system is the use of deuterated solvents needed for the NMR part. Analytes with exchangeable or "active" hydrogens can exchange (i.e., equilibrate) with deuterium (^{2}H) from the deuterated solvent system at different rates. The analyst should be alert to this possibility since it could result in the appearance of several closely spaced molecular ions with pseudo molecular ions increased, depending on the number of exchangeable hydrogens being deuterated. If the compound of interest exchanges all the active hydrogens for deuteriums, the pseudo molecular ion will be $[M + {}^2H]^+$ or $[M - {}^2H]^-$ in the positive or negative mode, respectively, where M is the molecular weight with all the exchangeable hydrogens deuterated. When buffers or other compatible solvents for MS are needed, it is recommended that deuterated buffers be used to avoid the suppression of additional solvent lines in the NMR spectra, which can also suppress signals from the analyte of interest if those signals are under the suppressed solvent signals (see Section 3.2.2).

With a splitter near the mass spectrometer, Burton et al. [13] used a second pump to inject methanol–acetic acid, with the purpose of exchanging the deuteriums for protons to obtain fully protonated molecular ions. In general, injecting water or aqueous buffer via a syringe pump to the MS effluent flow in a 1 : 4 ratio will carry out the D–H back-exchange, providing typical information on the molecular ions: $[M + H]^+$ or $[M - H]^-$ for the positive or negative mode, respectively, where M is the molecular weight with all the exchangeable hydrogens protonated [7].

3.4. MODES OF OPERATION OF LC-NMR

The HPLC system is connected by red poly(ether ether ketone) (PEEK) tubing to the NMR flow cell, which is inside the magnet. With shielded cryomagnets the HPLC can be as close as 30 to 50 cm to the magnet, rather than 1.5 to 2 m for conventional nonshielded magnets. Normally, an ultraviolet detector is

used in the HPLC system to monitor the chromatographic run. However, radioactivity or fluorescent detectors can also be used to trigger stopping the flow when the chromatographic peak(s) of interest are in the NMR flow cell for analysis.

There are four general modes of operation for LC-NMR: on-flow, stop-flow, time-sliced, and loop collection. These modes, described below, are automated by software that controls the valves of the HPLC to stop the flow when needed, depending on the mode of operation selected for the LC-NMR system.

3.4.1. On-Flow Mode

The simplest method of performing LC-NMR is in the on-flow mode. In the on-flow or continuous-flow mode, the chromatographic run continues without the run stopping at any point. The chromatographic peaks are flowing through the NMR flow cell while NMR spectra are being acquired over time. In this mode, NMR experiments require more to analyze "on the fly" because the resident time in an NMR flow cell is very short (3.6 s at 1 mL/min) during the chromatographic run, which limits this approach to one-dimensional NMR spectra acquisition only, typically one-dimensional ^{1}H NMR. This mode can be used to analyze the main components and to rapidly identify the major known compounds of the mixture. ^{19}F NMR can provide a simplified pseudo-two-dimensional LC-NMR spectrum compared to ^{1}H NMR for the on-flow mode [14]. If only one fluorine atom or one trifluoromethyl group is present in each component of the mixture, the number of components can be accounted for by the number of individual separate ^{19}F signals when each component has a different retention time or by a distinct chemical shift in the ^{19}F signals if two components have similar retention times.

3.4.2. Stop-Flow Mode

Knowledge of the retention time of the chromatographic peak of interest for NMR analysis is required prior to an LC-NMR run to perform in the stop-flow mode. In this mode the chromatographic peak is analyzed under static conditions. The chromatographic peak of interest is submitted directly from the HPLC to the NMR flow cell. Therefore, stop-flow requires accurate calibration of the delay time, which is the time required for the sample to travel from the UV detector of the HPLC to the NMR flow cell. The delay time depends on the flow rate and on the length and width of the tubing connecting the HPLC with the NMR. If the analyte of interest in the sample mixture has no UV chromophore or has other characteristics, other detectors can be used in the HPLC system instead of the typical UV detector, such as radioactive,

fluorescence, MS, and others. In any case, accurate calibration of the delay time has to be performed prior to NMR analysis.

Because the chromatographic run is stopped automatically when the peak of interest is in the NMR flow cell, the amount of sample required for the analysis can be reduced compared to the on-flow mode, and two-dimensional NMR experiments such as WET-COSY, WET-TOCSY, and others [11] can be obtained since the sample can remain inside the flow cell for days. A common practice is to connect a back-pressure regulator valve at the outlet tubing coming out the NMR probe to avoid any possible loss of sample due to some flow in the system affected by back-pressure effects. It is possible to obtain NMR data on a number of chromatographic peaks in a series of stops during the chromatographic run without on-column diffusion that causes loss of resolution, but only if the NMR data for each chromatographic peak can be acquired in a short time (ideally, 30 min or less if more than four peaks have to be analyzed, but less than 2 h for the analysis for no more than three peaks). The use of commercially available cryogenic probes (cryoprobes or cold probes) improves the sensitivity of the stop-flow mode as it does for the general tube and tubeless NMR modes (see Section 3.2.4).

To perform analysis on a limited amount of sample, such as for the structure elucidation of metabolites, stop-flow is the preferred mode when the chromatography is reasonable or the metabolite is unstable for isolation. The analysis of the major metabolites of compound I (Figure 3-4) illustrates the capabilities of the stop-flow mode. Compound I is a *ras* farnesyl transferase inhibitor in rats and dogs [15]. Preliminary studies by LC-NMR using a linear solvent gradient [5 to 75% B 0 to 25 min, 75 to 95% B 25 to 35 min, A: D_2O, B: ACN (acetonitrile), 1 mL/min, 235 nm, BDS Hypersil C18 column 15 cm × 4.6 cm, 5 μm] indicated that even with the use of protonated acetonitrile in the solvent mixture, all the resonances were visible for compound I (Figure 3-5). Figures 3-6 and 3-7 are UV chromatograms from a small injection of dog bile and dog urine for metabolites M9 (retention time 10 min) and M11 (retention time 21 min), respectively. These small injections were carried out to identify the UV chromatographic peaks of the analytes of interest and to determine any possible interference coming from other chromatographic peaks that could cause overlapping of signals from different analytes during stop-flow NMR analysis. Metabolite M11 was also found in rat urine. To analyze the structures of M9 and M11 by NMR, larger injections of dog bile, dog urine, and rat urine were carried out to perform the stop-flow experiments. The ^{1}H NMR spectrum in the LC-NMR system (Varian Inova 500 MHz equipped with a ^{1}H–^{13}C pulse field gradient indirect detection microflow NMR probe with a 60-μL flow cell; Palo Alto, CA) of M9 (Figure 3-8) revealed the presence of a 1,2,4-trisubstituted aromatic ring in the 3-chlorophenyl ring and the glucuronide moiety. Neither of the two possibilities for the position of the glucuronide moiety ring,

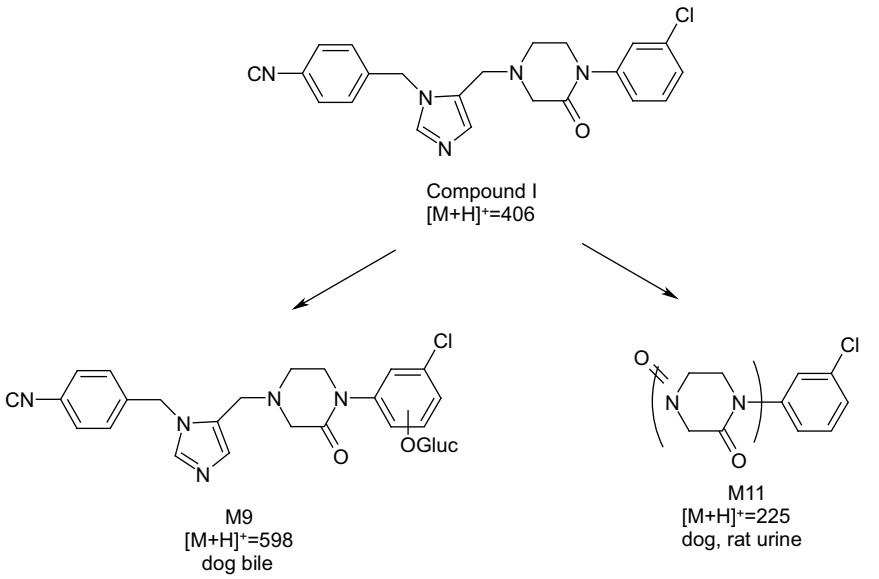

FIGURE 3-4. Structure of compound I, a *ras* farnesyl transferase inhibitor in rats and dogs, and proposed structures by MS of its major metabolites in dog bile (M9) and in dog and rat urine (M11). (Reprinted from reference 8; copyright © 2003, with permission from Elsevier.)

position 4 or 6 (see Figure 3-8), could be distinguished. NOE experiments on the LC-NMR were not successful because of problems with solvent suppression. The sample was collected and the NOE was performed in the tube NMR mode (Varian Unity 400 MHz, equipped with a 3-mm ^{1}H–^{13}C pulse field gradient indirect detection Nalorac probe, Palo Alto, CA) over a weekend (Figure 3-9). Even though the sample collected contained more impurities, the NOE experiment showed that the glucuronide moiety was attached at C-4 by irradiating the methylene protons at the i position, which elicited NOE signals from protons H-2 and H-6, thus eliminating the C-6 possibility (Figure 3-9). LC-MS analysis of M11 indicated it to be only the 1-(3-chlorophenyl) piperazinone moiety with additional oxidation on the piperazinone ring. The stop-flow ^{1}H NMR spectrum in the LC-NMR system of M11 lacked the isolated methylene signal on the piperazine ring (Figure 3-10), indicating it to be 1-(3-chlorophenyl)piperazine-2,3-dione.

The following case required the use of an alternative detector in the HPLC system to assure NMR analysis on the chromatographic peak of interest. Stop-flow is an ideal mode to use to analyze the structure of volatile analytes. In the case of radiolabeled metabolites, the use of a radioactive detector is recommended to monitor the run and determine which peak in the UV chromatogram is the radiolabeled metabolite. The NMR analysis of the radioactive

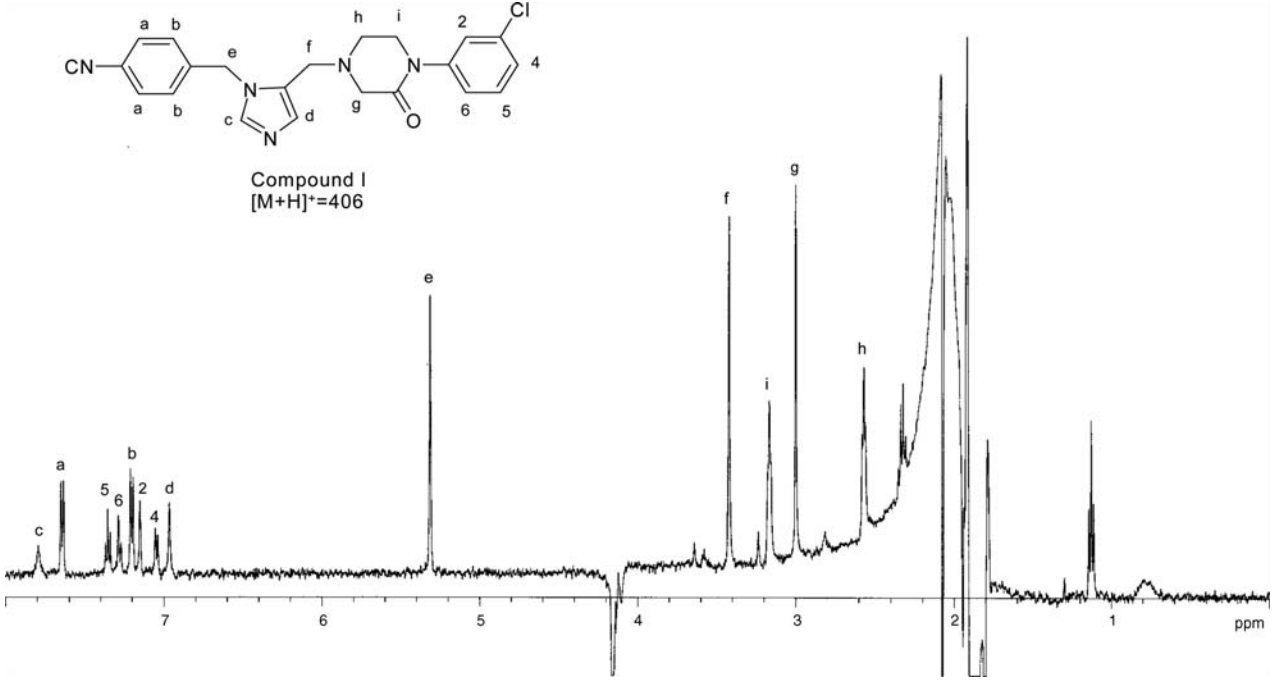

FIGURE 3-5. ^{1}H NMR spectrum of compound I in stop-flow mode. (Reprinted from reference 8; copyright © 2003, with permission from Elsevier.)

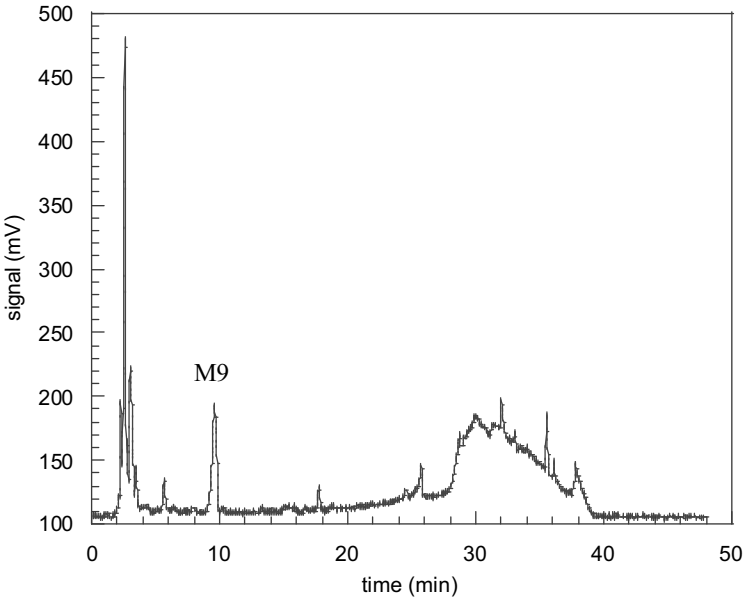

FIGURE 3-6. UV chromatogram from a small injection of dog bile containing metabolite M9. (Reprinted from reference 8; copyright © 2003, with permission from Elsevier.).

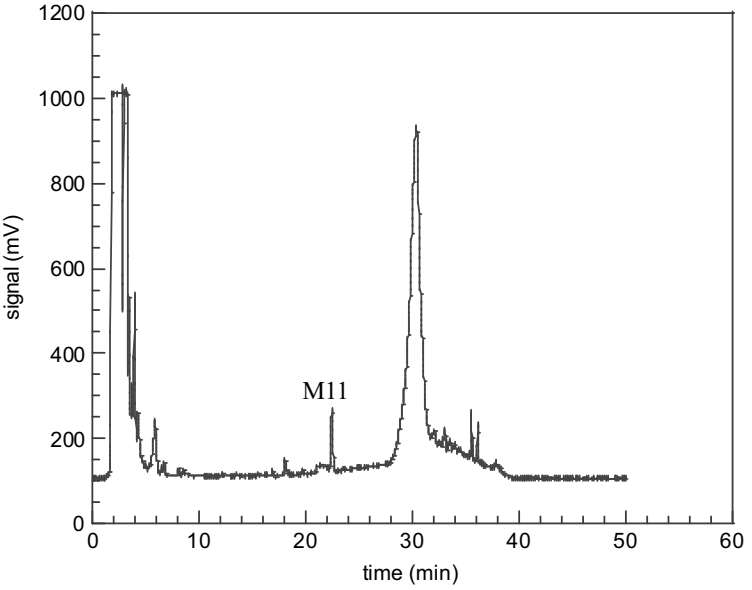

FIGURE 3-7. UV chromatogram from a small injection of dog urine containing metabolite M11. (Reprinted from reference 8; copyright © 2003, with permission from Elsevier.)

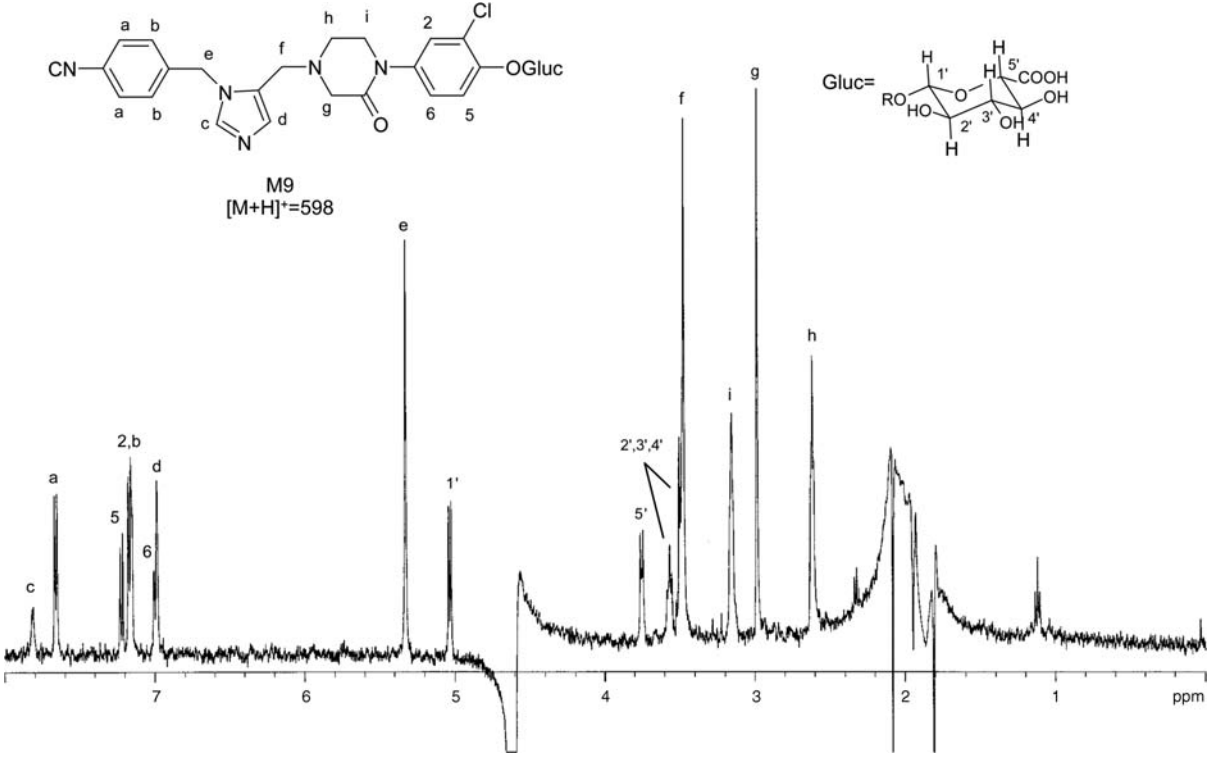

FIGURE 3-8. ^{1}H NMR spectrum of metabolite M9 from dog bile in the stop-flow mode. (Reprinted from reference 8; copyright © 2003, with permission from Elsevier.)

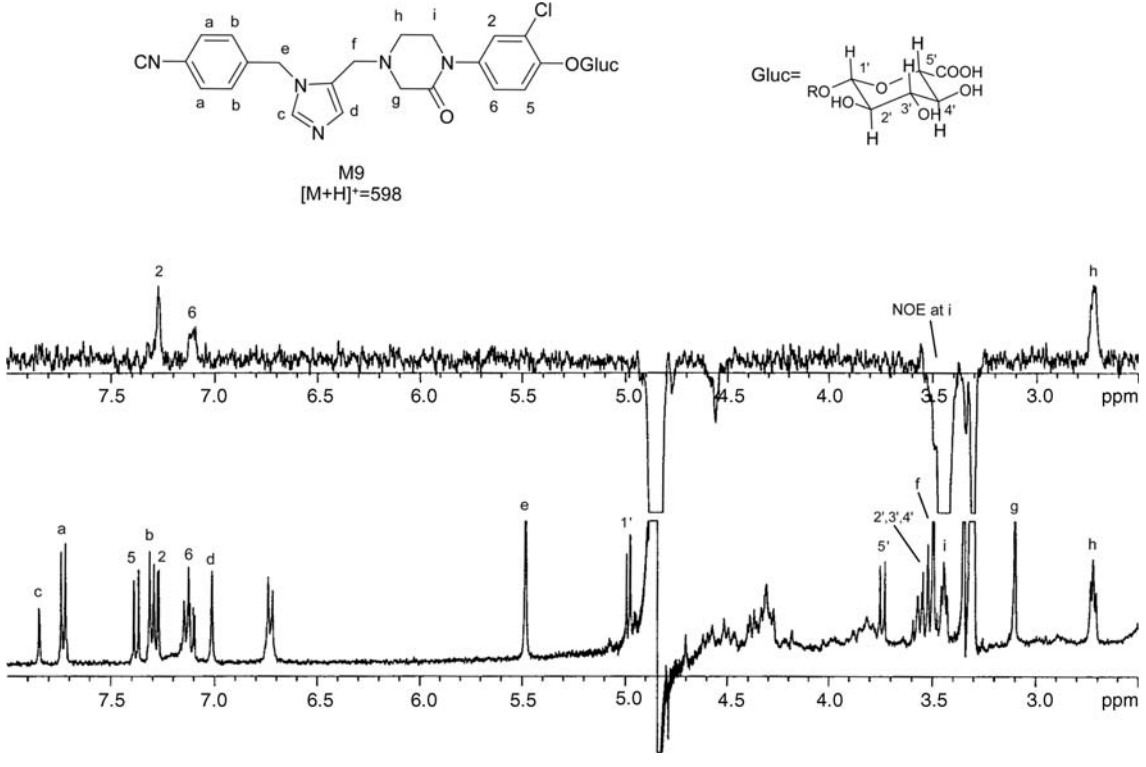

FIGURE 3-9. ^{1}H NMR (bottom) and 1D NOE spectra at i (top) of M9 from dog bile recovered from LC-NMR. (Reprinted from reference 8; copyright © 2003, with permission from Elsevier.)

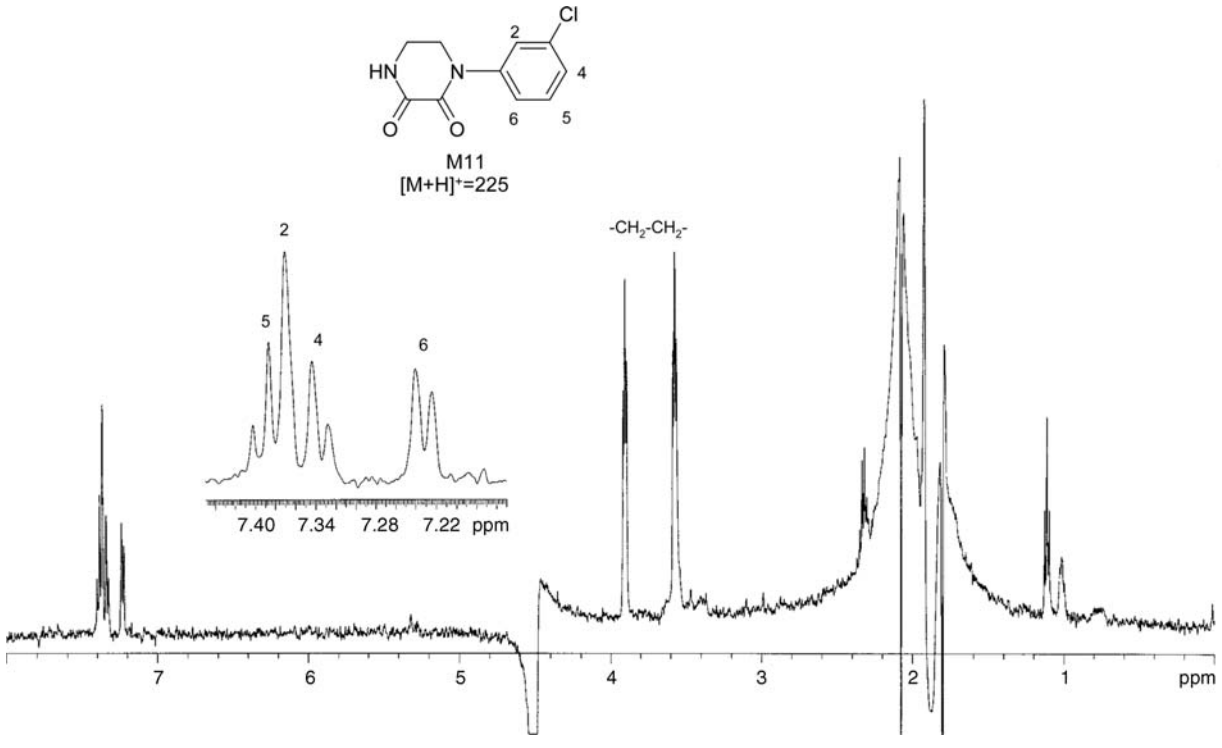

FIGURE 3-10. ^{1}H NMR spectrum of metabolite M11 from dog urine in the stop-flow mode. (Reprinted from reference 8; copyright © 2003, with permission from Elsevier.)

volatile metabolite M3 with small molecular weight illustrates application of the stop-flow mode to LC-NMR studies [16]. Conventional NMR was not possible because the radioactivity of the sample was lost when the fraction containing the metabolite was evaporated to dryness prior to the NMR studies. In this example, the LC-MS was not informative, suggesting a molecular weight below 200 Da. LC-NMR was the alternative used to solve this structural problem. To be able to identify the UV chromatographic peak corresponding to the radioactive metabolite, a radioactivity detector equipped with a liquid cell (Radiomatic C150TR, Packard, Meriden, CT) was connected online to the LC-UV system of an LC-NMR. Figure 3-1 shows the schematic diagram for this setup. Small injections were carried out initially to identify the metabolite UV chromatographic peak with the radioactive peak prior to the stop-flow experiments (Figure 3-11). Stop-flow experiments were triggered by UV because the transfer delay from the UV to the NMR was shorter than from the radioactive detector to the NMR, due to the thicker tubing used in the liquid cell of the radioactivity detector. The ^{1}H NMR spectrum revealed the presence of the *p*-fluorophenyl ring with the characteristic splitting pattern, indicating that the compound was drug related. The downfield shift of the *ortho* protons at 7.91 ppm suggested the presence of a carbonyl substituent (Figure 3-12). The presence of a singlet at 4.85 ppm, integrating for

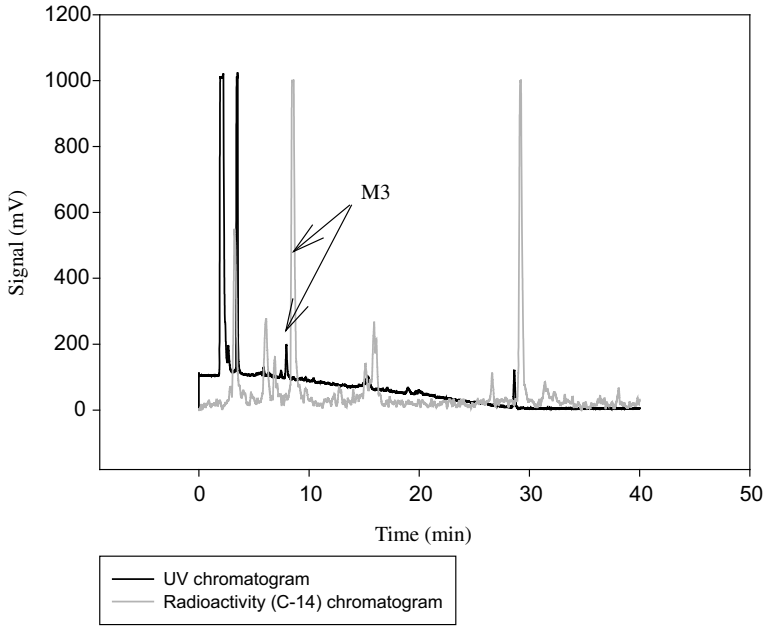

FIGURE 3-11. UV and radioactive (C-14) chromatograms of a fraction containing metabolite M3 [16].

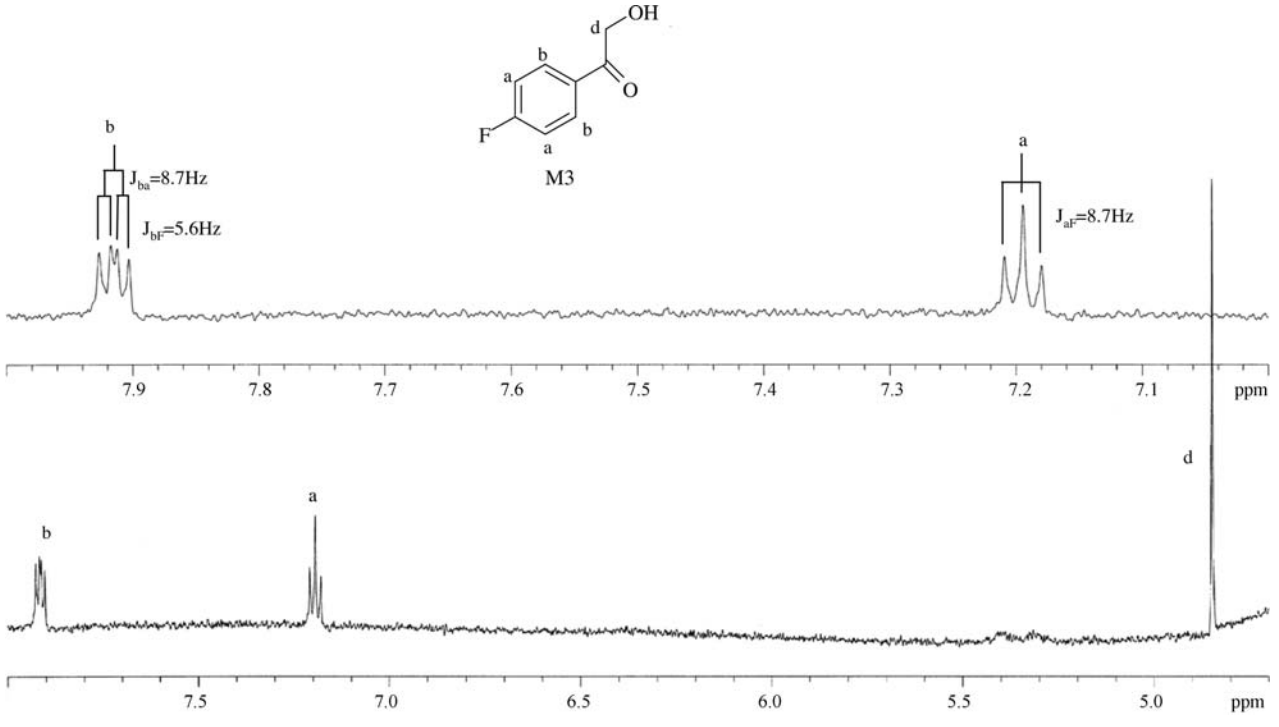

FIGURE 3-12. Expanded sections of the ^{1}H NMR spectrum of metabolite M3 acquired for one day [16].

approximately two protons, was consistent with a methylene that was flanked by the carbonyl and a hydroxyl group (Figure 3-12). These features thus led to proposing the structure for M3 as *p*-fluoro-α-hydroxyacetophenone (Figure 3-12).

3.4.3. Time-Sliced Mode

The time-sliced mode involves a series of stops during elution of the chromatographic peak of interest. The time-sliced mode is used when two analytes elute together, when they elute with close retention times, or when the separation is poor. In addition, this mode is used when the analytes of interest have poor or non-UV absorption and no other detector is available to trigger the stop-flow NMR run automatically. The time-sliced mode can be performed automatically by the software controlling the HPLC run, or manually, depending on the difficulty of the case and the preference of the analyst.

3.4.4. Loop Collection Mode

In the loop collection mode, the chromatographic peaks of interest are stored automatically in separate loops controlled by the software for later off-line NMR analysis. During the process of collecting the chromatographic peaks in loops, the chromatogram is not disturbed, as when sequential stops are performed during stop-flow NMR experiments. Later, the stored chromatographic peaks are transferred to the NMR flow cell individually for NMR studies. The software is designed to send the stored chromatographic peaks to the NMR flow cell in the same or different order as that in which they were stored from the chromatographic run. Loop collection can be used when there is more than one chromatographic peak of interest in the same run, to avoid carryover contamination if the analytes have close retention times and if the amount or concentration of the analytes of interest shows a diverse dynamic range. In the loop collection mode, the analytes must be stable inside the loops during the extended period of analysis for all the peaks stored in the loops. Capillary tubing should be used to avoid peak broadening with concomitant loss of analyte "seen" by the NMR spectrometer based on the dimensions of the NMR flow cell. Loop collection can be used in connection with SPE for SPE-NMR analysis (see Sections 6.12 and 6.13).

3.5. MODES OF OPERATION OF LC-MS-NMR

As mentioned in Section 3.4, with the use of shielded cryomagnets, the location of the MS instrument will follow the same rule as for the HPLC, to be

as close as 30 to 50 cm to the magnet. The most common modes of operation for LC-MS-NMR are on-flow and stop-flow. With stop-flow, the MS instrument can also trigger stopping the flow on the chromatographic peak of interest that will be analyzed by NMR. These two modes are presented here by an example. In the loop collection mode, the MS of the LC-MS-NMR system may also monitor the trapping of the chromatographic peak inside the loop for cases when the UV detector is not the most appropriate, due to a lack of chromophores in the sample. The limitations of triggering stop-flow by MS are based on the quality of the ionization of the molecular ion or fragment ions of the analyte of interest. Poor ionization of ions of the analyte of interest limits the capabilities of MS to control the stop-flow modality in the LC-MS-NMR system. The time-sliced mode is not practical for LC-MS-NMR, due to interruption of the chromatographic flow, which makes it difficult to detect MS data consistently while acquiring NMR data during the time the flow is stopped.

In the past decade, there have been relatively few cases in the literature dealing with the application of LC-MS-NMR, mainly in the pharmaceutical industry. In this chapter, an evaluation of this technology is presented to determine the pros and cons and to decide which cases are suitable for this application. To illustrate the on-flow and stop-flow modes of operation, a group of eight flavonoids was chosen [8]. Flavonoids are natural products with important biological functions that act as antioxidants, free-radical scavengers, and metal chelators, and are important to the food industry. The eight flavonoids chosen were selected to mimic a real complex mixture of compounds of similar structures that may present some ambiguity in their analysis that can be resolved by this hyphenated technique versus the individual nonhyphenated techniques. Figure 3-13 shows the eight flavonoids (Aldrich) chosen to illustrate the capabilities of LC-MS-NMR. These compounds have simple structures composed primarily of aromatic protons; some have low-field aliphatic protons which would not be hidden under NMR solvent peaks. Phenolic protons exchange rapidly with D_2O so that each compound will show only one pseudo molecular ion with all phenolic protons deuterated.

The chromatographic conditions are as follows: 35 to 50% B 0 to 10 min, 50 to 80% B 10 to 15 min, A: D_2O, B: ACN, 1 mL/min, 287 nm, Discovery C18 column 15 cm × 4.6 cm, 5 μm. Stock solutions of each compound were prepared at 1 μg/μL in ACN–MeOH 1 : 1 [8].

A Varian Unity Inova 600-MHz NMR instrument (Palo Alto, CA) equipped with a $^{1}H(^{13}C/^{15}N)$ pulse field gradient triple-resonance microflow NMR probe (flow cell 60 μL; 3 mm o.d.) was used. Reversed-phase HPLC analysis of the samples was carried out on a Varian modular HPLC system (a 9012 pump and a 9065 photodiode array UV detector). The Varian HPLC software was also equipped with the capability for programmable stop-flow experiments

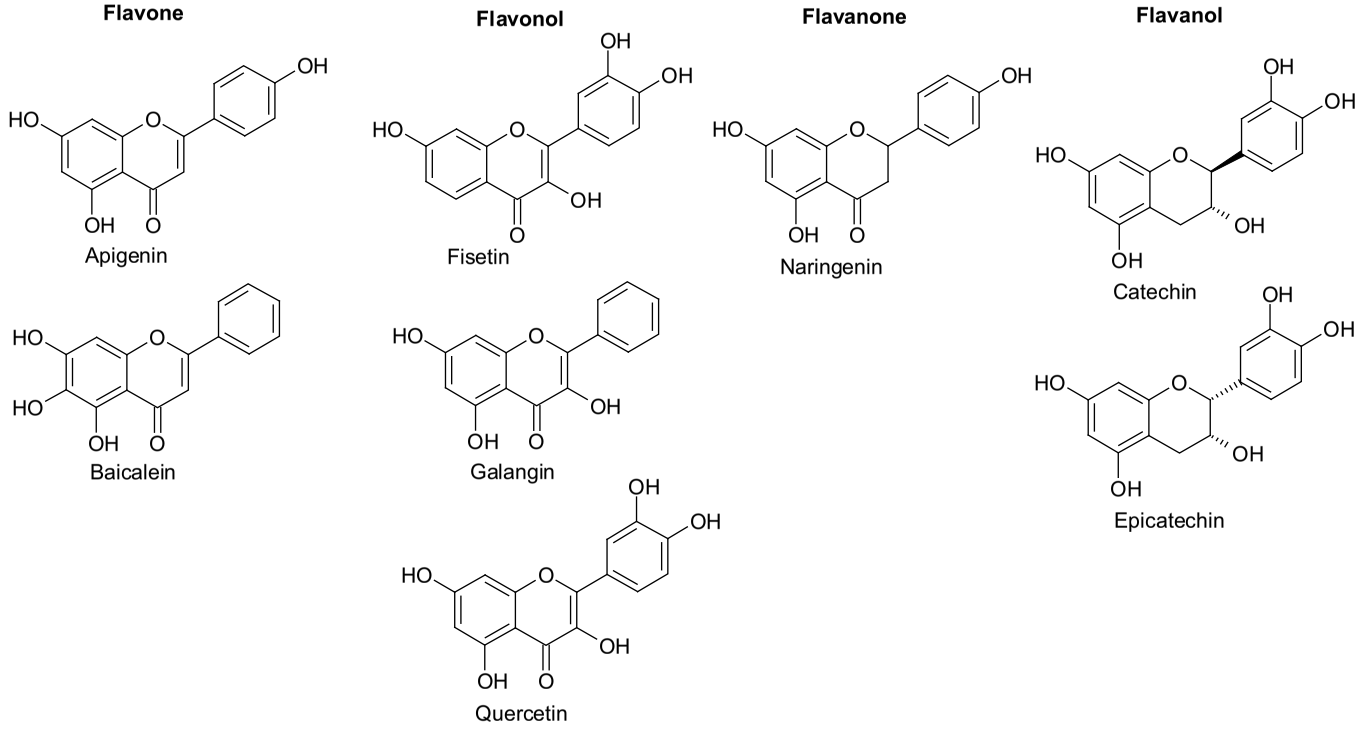

FIGURE 3-13. Structures of eight flavonoids used for LC-MS-NMR technology development studies. (Reprinted from reference 8; copyright © 2003, with permission from Elsevier.)

based on UV peak detection. An LCQ classic MS instrument (mentioned in Section 3.3) was connected online to the HPLC-UV system of an LC-NMR by contact closure. The ^{2}H resonance of the D_2O was used for field-frequency lock, and the spectra were centered on the ACN methyl resonance. Suppression of the resonances from HOD, the methyl of ACN, and its two ^{13}C satellites was accomplished using a train of four selective WET pulses, each followed by a B_0 gradient pulse and a composite 90° read pulse as described by Smallcombe et al. [11]. The on-flow and stop-flow modes of operation for this example are described below [8].

3.5.1. On-Flow Mode

As indicated previously, the on-flow experiment was carried out on a mixture of eight flavonoids (Figure 3-13) in a prepared mixture of 20 μg each. MS and NMR data were obtained during this on-flow experiment [8]. The UV chromatogram is depicted in Figure 3-14. Table 3-1 and Figures 3-16 to 3-19 show the pseudo molecular ion information $[M - {}^{2}H]^{-}$ in the negative mode for the eight flavonoids obtained in this on-flow experiment, where M is the molecular weight with all the hydroxyl protons deuterated. Figure 3-15

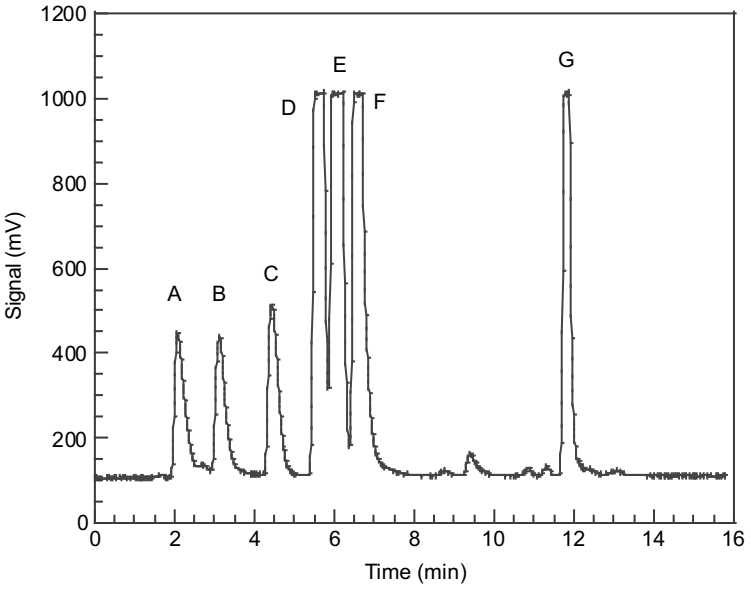

FIGURE 3-14. UV chromatogram of an on-flow experiment involving injection of a mixture of eight flavonoids (A: catechin + epicatechin; B: fisetin; C: quercetin; D: apigenin; E: naringenin; F: baicalein; G: galangin). (Reprinted from reference 8; copyright © 2003, with permission from Elsevier.)

is a two-dimensional data set (time versus chemical shift), where each ^{1}H NMR spectrum was acquired for 16 scans, decreasing the delays (total time per spectrum of 20 s) to obtain more spectra during the chromatographic run and to acquire more data points for the ^{1}H NMR spectra of the various components of the chromatography. Figures 3-16 to 3-19 depict the ^{1}H NMR traces of each flavonoid extracted from the two-dimensional data set of Figure 3-15. Notice that catechin and epicatechin coelute under these chromatographic conditions (peak A of the UV chromatogram of Figure 3-14), due to the similarity of their structures (see Figure 3-13). Distinguishing these diastereomers by MS alone is not feasible (Table 3-1 and Figure 3-16) because both have the same pseudo molecular ion information. Differences in the NMR spectra would be expected between diasteromers and are, in fact, observed clearly, even as a mixture (Figure 3-16). The ability of LC-MS-NMR to distinguish signals from the individual diastereomers is illustrated in Figure 3-16. Protons H-2 and H-3 in catechin and H-2a and H-3a in epichatechin show different chemical shifts because of the slightly different local chemical environment around chiral centers C-2 and C-3 for catechin and C-2a and C-3a for epicatechin as diasteromers. Those differences are sufficient for NMR to be able to distinguish between the diasteromers of organic molecules. The ^{1}H NMR spectrum of naringenin in Figure 3-18 shows the ability of NMR to analyze a mixture of two components in different ratios (X denotes the signals coming from apigenin as the minor component of this chromatographic peak). In this particular case, NMR shows clearly the presence of the two components of the mixture. Assignments can be carried out simply based on the different ratio of the NMR signals for the two compounds because proton signals are in the molar ratio for the individual components of the mixture. This is another advantage of NMR versus MS [8].

3.5.2. Stop-Flow Mode

TABLE 3-1. MS Data of Flavonoids in the Negative Mode from the On-Flow Run in an LC-MS-NMR Instrument

Peak	Compound	MW[a]	M[b]	m/z, $[M - {}^2H]^-$
A	Catechin + epicatechin	290	295	293
B	Fisetin	286	290	288
C	Quercetin	302	307	305
D	Apigenin	270	273	271
E	Naringenin	272	275	273
F	Baicalein	270	273	271
G	Galangin	270	273	271

[a] Molecular weight.

[b] Molecular weight with all the hydroxyl protons deuterated.

Source: Reference 8;

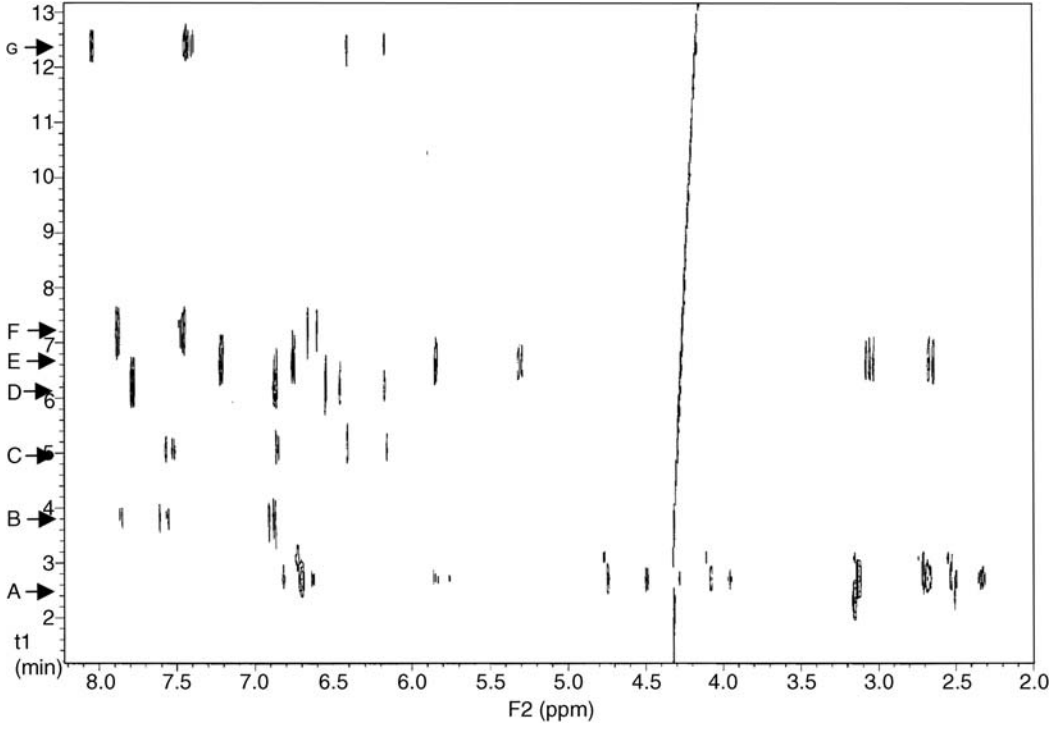

FIGURE 3-15. Two-dimensional data set (time/min versus chemical shift/ppm) for an on-flow experiment injecting a mixture of eight flavonoids (A: catechin + epicatechin; B: fisetin; C: quercetin; D: apigenin; E: naringenin; F: baicalein; G: galangin). (Reprinted from reference 8; copyright © 2003, with permission from Elsevier.)

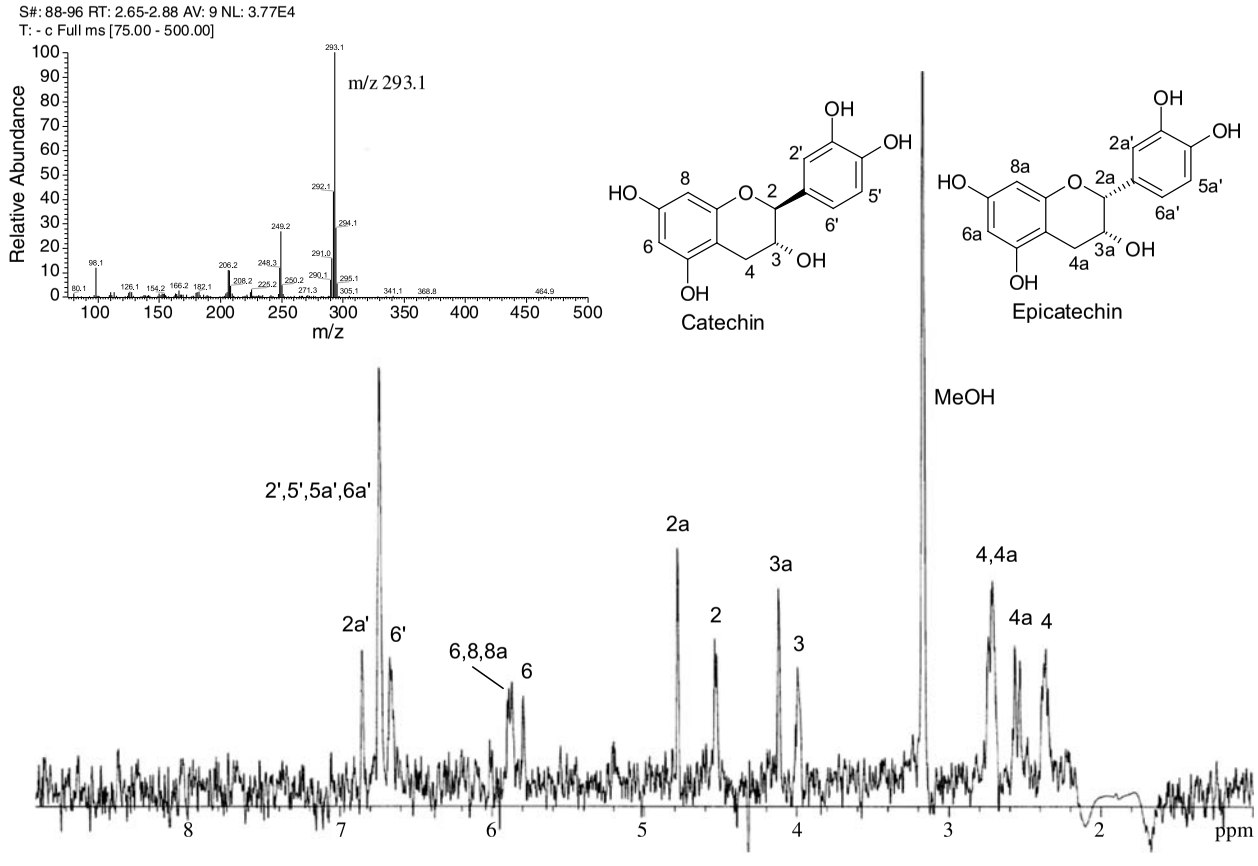

FIGURE 3-16. MS and ^{1}H NMR spectra from a two-dimensional data set from an on-flow experiment of catechin and epicatechin. (Reprinted from reference 8; copyright © 2003, with permission from Elsevier.)

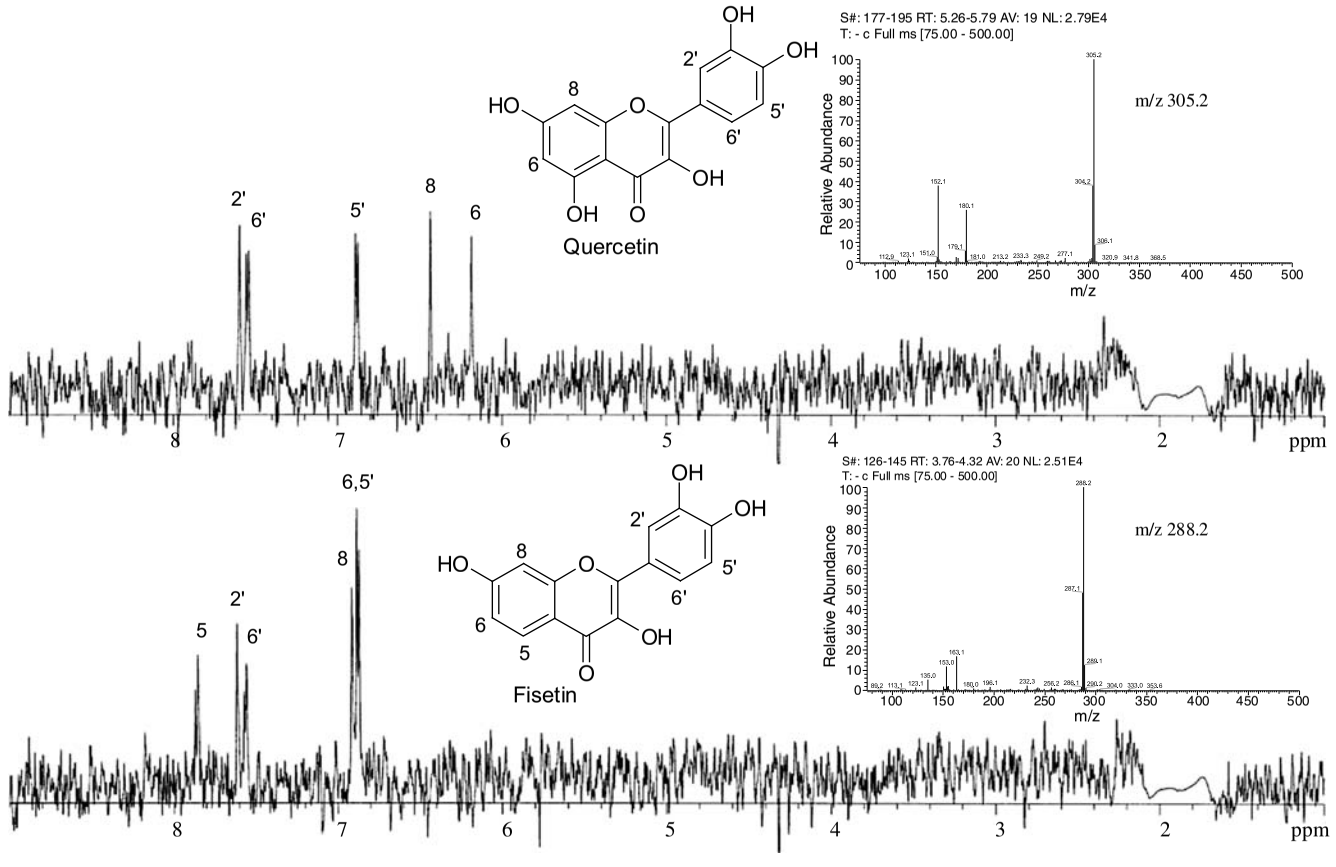

FIGURE 3-17. MS and ^{1}H NMR spectra from a two-dimensional data set from an on-flow experiment of fisetin (bottom) and quercetin (top). (Reprinted from reference 8; copyright © 2003, with permission from Elsevier.)

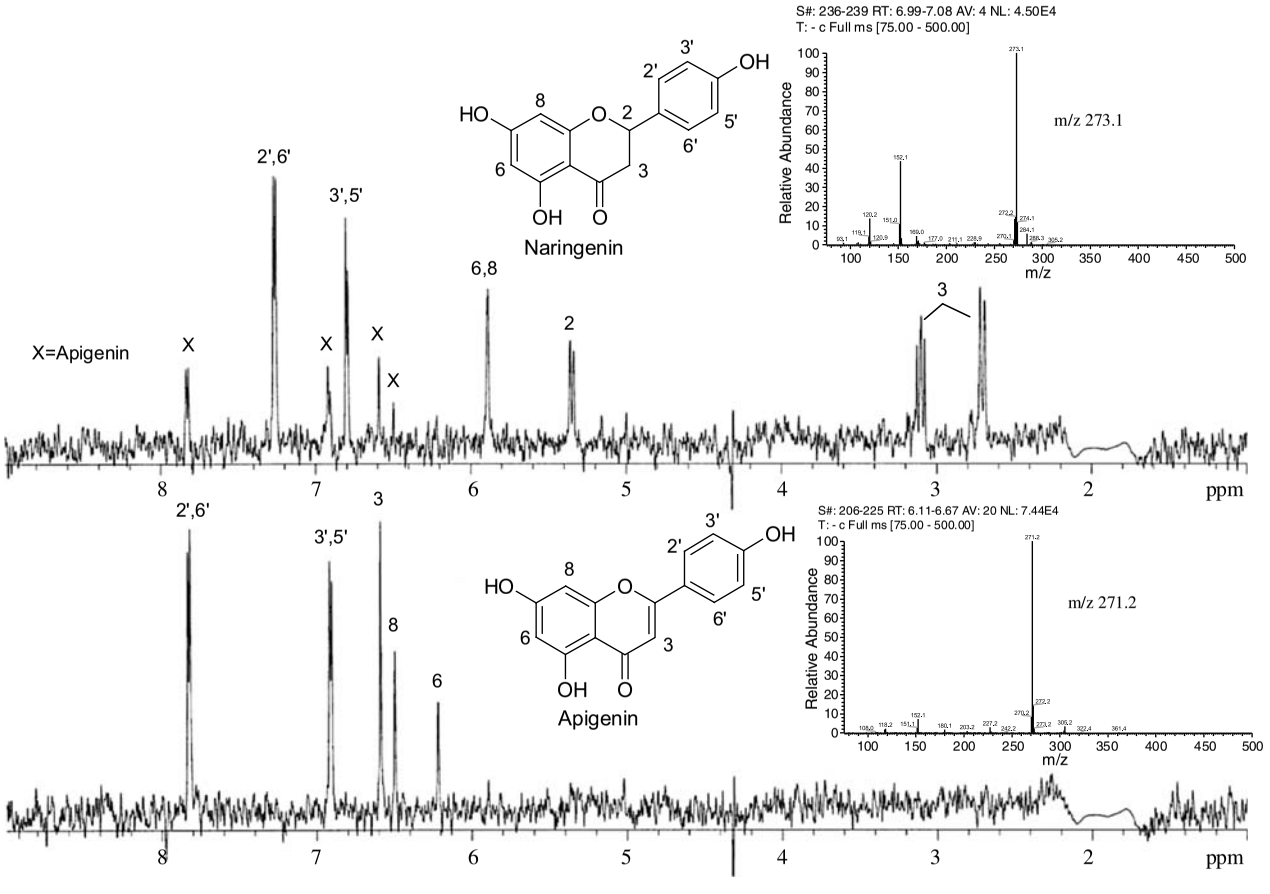

FIGURE 3-18. MS and ^{1}H NMR spectra from a two-dimensional data set from an on-flow experiment of apigenin (bottom) and naringenin (top). (Reprinted from reference 8; copyright © 2003, with permission from Elsevier.)

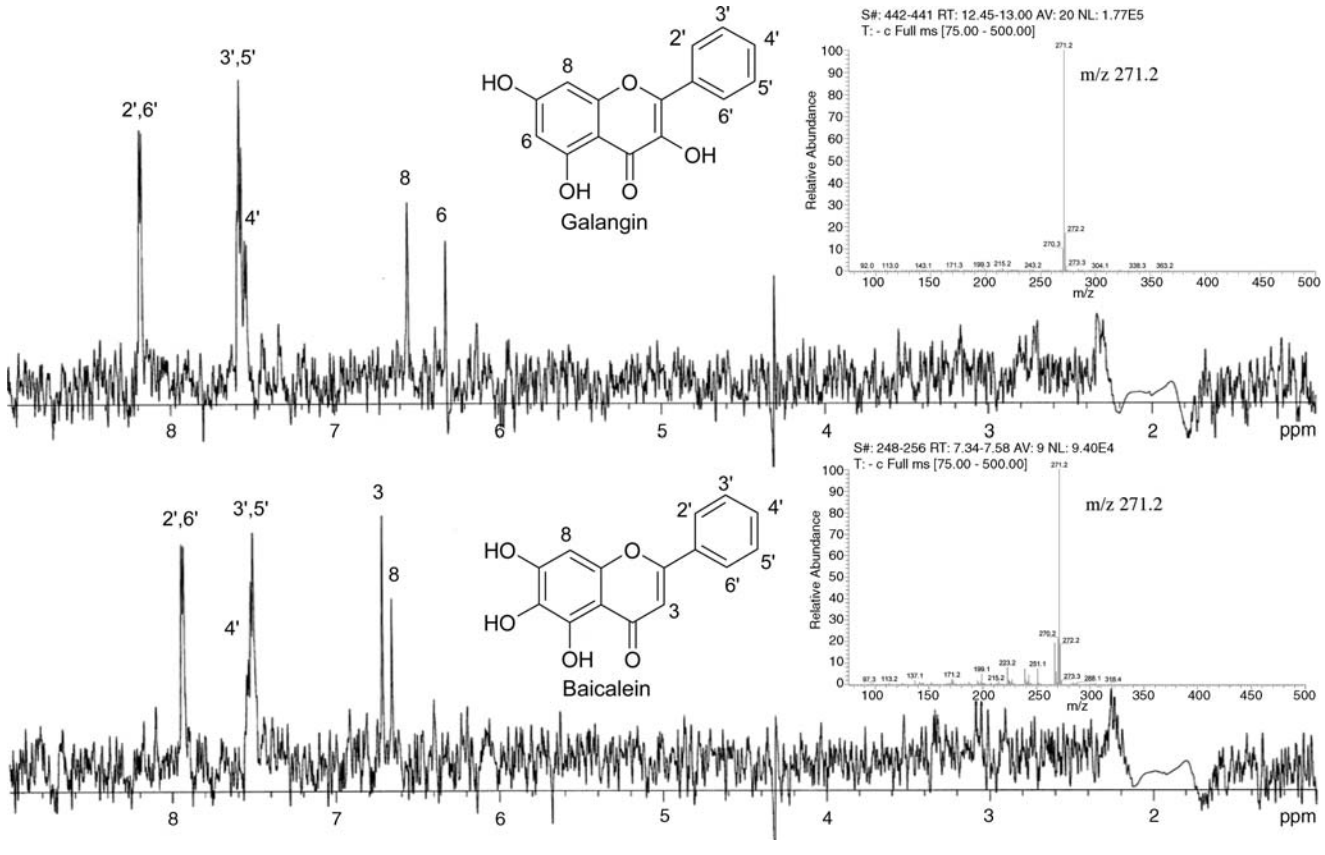

FIGURE 3-19. MS and ^{1}H NMR spectra from a two-dimensional data set from an on-flow experiment of baicalein (bottom) and galangin (top). (Reprinted from reference 8; copyright © 2003, with permission from Elsevier.)

Two stop-flow experiments were carried out injecting a solution containing 10 μg on apigenin (Figure 3-13) using, independently, the UV peak maximum or the pseudo molecular ion of the chromatographic peak seen in the total ion chromatogram for the MS instrument to trigger the stop-flow mode [8]. Since the Varian software automatically triggers the stop-flow mode with the UV peak, this mode was used as a reference point to stop the flow at the correct position of the analyte of interest in the chromatogram. When the MS was used to trigger the stop-flow, it was carried out manually with a chronometer while monitoring the molecular ion of apigenin in the negative mode (*m*/*z* 275). After peak detection in the UV or MS and a time delay of about 52 s or 20 s, respectively, the HPLC pump was stopped, trapping the peak of interest in the flow cell of the LC-NMR microprobe. ^{1}H NMR stop-flow spectra were acquired using an acquisition time of 1.5 s, a delay between the successive pulses of 0.5 s, a spectral width of 9000 Hz, and 32-K time-domain data points. The methyl resonance of ACN was referenced to 1.94 ppm. These two experiments were carried out injecting 10 μg of apigenin and acquiring ^{1}H NMR spectra for about 4.5 min (128 scans), giving rise to the same quality of ^{1}H NMR spectra of apigenin (Figure 3-20) [8].

These experiments indicated that for sample mixtures, the on-flow mode of LC-MS-NMR is useful for obtaining structural information of the major components. If more detailed analysis is required, or the amount of sample is small and the compound(s) cannot be isolated because of instability or volatility, stop-flow is the mode of choice. The LC-MS and LC-NMR chromatographic conditions must be compatible. In addition, prior evaluation of the LC conditions in an LC-MS-NMR system is required to assure consistency with the chromatographic resolution needed in the LC-NMR part of the system. The sample must ionize well by electrospray to obtain MS data. When the stop-flow mode is triggered by MS, prior MS information on the chromatographic peak(s) of interest is needed in deuterated solvent(s) to evaluate the suitability of the system to provide structural information. When exchangeable protons are present in the molecule of interest, an evaluation of the possibility of the presence of multiple pseudo molecular ions in the deuterated solvent system due to different exchange rates is required to consider how practical and successful a hyphenated LC-MS-NMR system will be to perform stop-flow on those conditions for the analyte of interest.

3.6. OTHER MODES OF OPERATION

The focus of this book is on chromatographic flow NMR. However, nonchromatographic flow NMR methods are becoming popular as optional modes of operation for hyphenated flow NMR techniques. An excellent

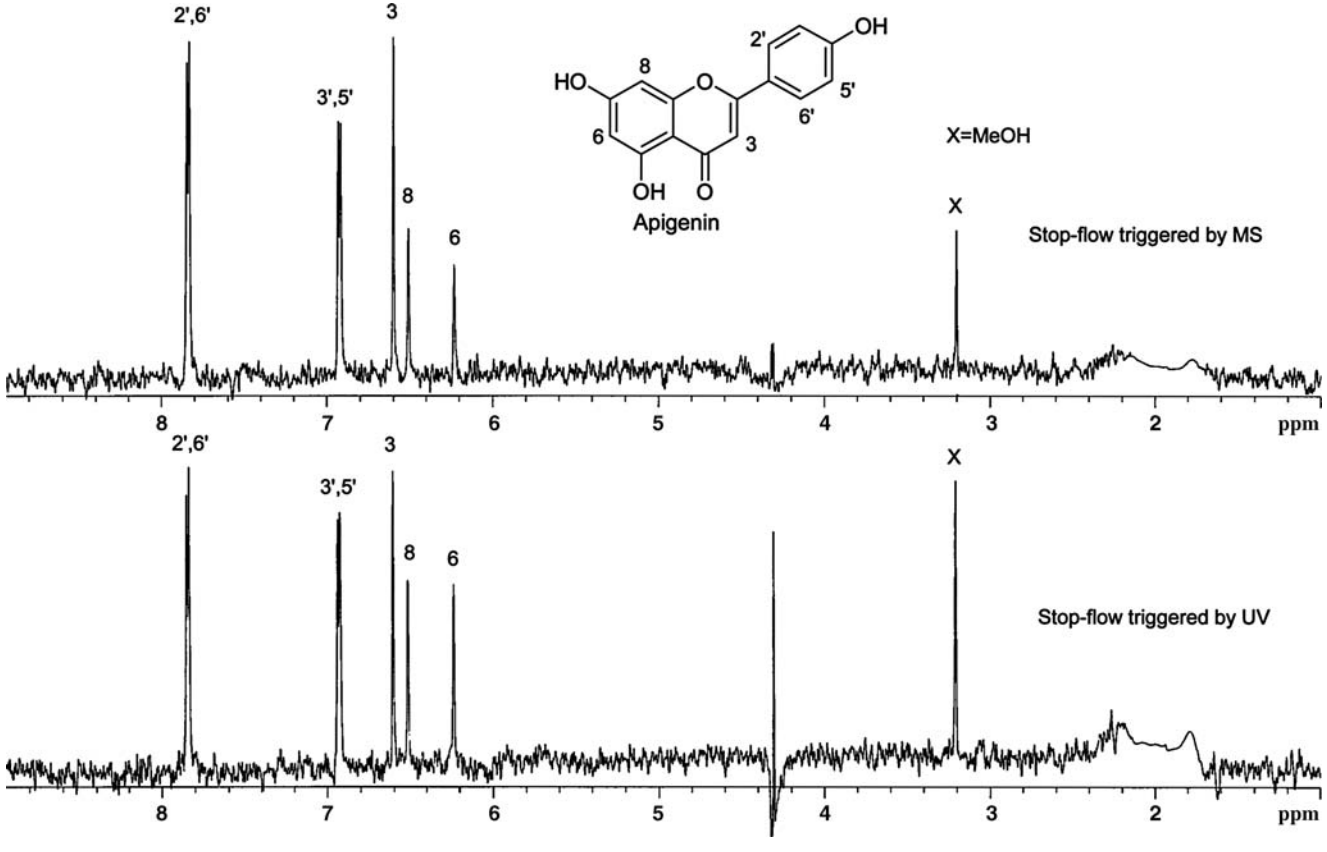

FIGURE 3-20. ^{1}H NMR spectra of apigenin triggering the stop-flow by UV (bottom) and by MS (top). (Reprinted from reference 8; copyright © 2003, with permission from Elsevier.)

review article by Keifer describes flow injection analysis NMR (FIA-NMR) and direct injection NMR (DI-NMR) as two nonchromatographic flow NMR techniques [12]. In these techniques, separation of components of mixtures is performed somewhere else, as no HPLC is connected to the system. An LC pump with reservoirs holding the mobile phase is attached directly to the NMR flow cell by the appropriate tubing for FIA-NMR. A UV detector is an optional tool to monitor the flow. On-flow and stop-flow operating modes are also applied to these columnless LC-NMR techniques. The on-flow mode can be triggered by a UV signal or by the calibrated delay time from the injector port to the NMR flow cell at a particular flow rate. DI-NMR is a simplified version of FIA-NMR in which a simplified pump with no mobile phase attached is connected directly to the NMR flow cell. The only solvent used is to dissolve the sample and wash the tubing of the system but at a different injection time, which explains the absence of mobile phase in the system. DI-NMR is more appropriate for automated repetitive analysis. Keifer's article and its references provide more information on those columnless techniques [12].

3.7. CHALLENGING CONSIDERATIONS

Hyphenated flow NMR techniques have some limitations that need to be considered to maximize their applications. The challenges described below are air bubbles, carryover (especially in autosampler devices), sample solubility and precipitation, flow cell and system cleaning, flow rate and magnetic susceptibility, and quantitation. Those challenges are absent in the conventional tube NMR version, except for sample solubility and precipitation.

3.7.1. Air Bubbles

Air bubbles come from inhomogeneous mixing of solvents. Degassing solvents prior to their utilization in an LC-NMR system will prevent or minimize their presence in the NMR flow cell. Air bubbles inside the NMR flow cell cause distortions in the NMR line shape, line broadening, and even loss of the NMR signal during the NMR acquisition time. Eliminating the air bubbles inside the NMR flow cell is not trivial, and the most common solution to that problem is to flush the flow cell and begin the analysis over again with a new sample injection. As indicated above, the best option is to avoid the formation of air bubbles before injecting the sample for NMR analysis by carefully degassing the solvents.

3.7.2. Carryover with and Without an Autosampler

Carryover is a common problem in flow NMR techniques as a result of continuous injections of several samples for analysis. Washing the LC-NMR system between injections will avoid the problem. In the conventional operating mode of an LC-NMR, where each sample is manually injected for NMR analysis, carryover can be avoided by flushing the system toward the end of the chromatographic run by changing the gradient of solvent system and allowing enough chromatographic time to wash the system. The use of methanol as a solvent during the chromatographic run and for washing the system can cause carryover because methanol is absorbed into the PEEK tubing. Flushing methanol from the system can take hours. Therefore, minimizing the use of methanol will avoid the problem. In addition, cracks in the system, such as in the tubing or the NMR flow cell, will also produce carryover. Analysis of small components of a chromatogram will present carryover when the small components are part of the tailing of larger leading components in the chromatogram. Carryover is more pronounced in autosamplers. The needle in an autosampler requires washing in between injections to minimize carryover from samples injected previously. Not enough washing time will increase carryover during subsequent injections. The time increase for washing a system between injections will prolong the total time of the analysis of all the samples but will minimize the carryover issues.

3.7.3. Sample Solubility and Precipitation

The solubility of the sample is critical to avoid precipitation and clogging of the tubing in an LC-NMR system. The ideal situation is to have the sample soluble in the solvent system used for the chromatography of the LC-NMR. If the chromatographic separation requires the use of an HPLC gradient solvent system instead of isocratic elution, the sample should ideally be soluble in different compositions of the solvent mixture during the chromatographic run and be very soluble in the solvent composition used at the beginning of the chromatographic run during the injection time. If the sample is not soluble in the chromatographic solvent mixture, another solvent must be used to inject the sample into the system. However, there is a higher risk of precipitation in these conditions, due to lack of solubility of the sample under the chromatographic solvent conditions. If the sample precipitates, the tubing will clog and the NMR flow cell will become dirty, with a high probability of carryover on the next injection. Clogging can increase the back pressure, due to blockage of the tubing. Samples may be filtered before injecting them into an LC-NMR system to minimize clogging due to the presence of particles in

the sample, but filtering will not solve the problem if solubility is an issue. Changing the guard column can also help to prevent clogging if the sample contains solid particles such as silica gel particles from a previous separation, but it cannot increase the sample solubility if this is the main problem. Clogging is a bigger issue for chromatographic systems that use capillary tubing. Therefore, filtering and guard columns are a requirement in these systems to minimize the need to change the tubing for the entire system, due to clogging, which makes the use of hyphenated NMR techniques less practical for the analysis of sample mixtures.

3.7.4. Flow Cell and System Cleaning

As indicated in Section 3.7.3, clogging the tubing and the NMR flow cell of the LC-NMR system is a major problem that may require replacing the system's tubing. The recommendation to prevent or minimize clogging is that after every chromatographic run, the entire system be washed with a solvent mixture on a regular basis. If residual sample remains in the NMR flow cell, the proton lineshape will be compromised and degraded if contamination persists. The recommendation is to wash the NMR flow cell monthly using aggressive solvent mixtures such as 3% hydrogen peroxide in water. In recent years, technology has improved with the commercial availability of interchangeable or removable NMR flow cells, even for cryogenic NMR systems. Those flow cells provide a longer life and utilization of the LC-NMR system.

3.7.5. Flow Rate and Magnetic Susceptibility

Another factor that raises concern is the compatibility of the flow rate of an HPLC gradient solvent system with NMR operations. An HPLC gradient solvent system with a flow rate greater than 2 to 3% per minute causes problems in optimizing the magnetic field homogeneity (shimming), due to gradient solvent mixing along the flow cell. With a flow rate greater than 3% per minute, it may take days for the mixture to equilibrate in the flow cell before NMR experiments can be carried out. Poor mixing in an HPLC gradient solvent system affects the quality of the NMR spectra, due to nonuniformed magnetic susceptibility across the area where the coil is located in the NMR flow cell. Under these conditions, resolution and lineshape will degrade, providing low-quality NMR spectra. When these systems are used, the solvent composition presents another challenge for NMR operations. Each solvent has its own optimal shimming conditions that affect the quality of the NMR lineshape. If two solvents are mixed in an approximate 1 : 1 ratio, shimming the sample in the NMR flow cell becomes a problem. The recommendation is

to use mixtures that do not exceed a ratio of 2 : 3 for the mixture of two solvents and to avoid a 1 : 1 ratio, to minimize major shimming issues and degradation of the lineshape, which will render NMR analysis of sample mixtures difficult.

3.7.6. Quantitation

With tube-based NMR as the classic methodology, accurate quantitation is obtained by introducing an internal standard of known purity to calculate the weight percentage of the analyte of interest in the sample. ERETIC is a methodology in which a calibrated electronic signal is created that is used as a standard for quantitation. ERETIC is more appropriate for the quantitation of a greater number of samples, such as in 96-well plates and provides a reasonable but less accurate measurement than when using an internal standard. These techniques become difficult to implement in LC-NMR settings. An internal standard would have to elute at the same retention time as the analyte of interest, and its concentration should not be modified during the chromatographic run. ERETIC is also in question because it is not an accurate method for quantitation, so its use is still under debate. In conventional LC-NMR, quantitation becomes less reliable with the use of solvent suppression techniques. Quantitation with FIA-NMR and DI-NMR may be more feasible using an internal standard methodology, but this approach is still under investigation [12].

3.8. CONCLUSIONS

Structural analysis of mixtures by the hyphenated techniques LC-NMR and LC-MS-NMR requires careful consideration of HPLC solvent systems, solvent suppression and sensitivity for NMR analysis, and possible deuterium exchange if exchangeable protons are present, because they affect interpretation of the molecular ions of analytes for MS analysis. In addition, air bubbles, carryover, solubility and precipitation, flow rate, system cleanliness, and quantiation are factors that will affect the results of NMR analysis if they are not controlled. The most common modes of operation in hyphenated NMR techniques are on-flow and stop-flow, depending on the amount of sample available for the investigation. Other optional operational modes are time-sliced and loop collection, depending on the chromatographic conditions and the number of chromatographic peaks in the sample mixture that require NMR analysis. Careful evaluation of those factors will provide the proper strategy to use to carry out structural analysis of the components of sample mixtures.

REFERENCES

[1] N. Watanabe and E. Niki, Direct-Coupling of FT-NMR to High Performance Liquid Chromatography, *Proc. Jpn. Acad. Ser. B* **54** (1978) 194–199.

[2] E. Bayer, K. Albert, M. Nieder, E. Grom, and T. Keller, On-Line Coupling of High-Performance Liquid Chromatography and Nuclear Magnetic Resonance, *J. Chromatogr.* **186** (1979) 497–507.

[3] J.F. Haw, T.E. Glass, D.W. Hausler, E. Motell, and H.C. Dorn, Direct Coupling of a Liquid Chromatograph to a Continuous Flow Hydrogen Nuclear Magnetic Resonance Detector for Analysis of Petroleum and Synthetic Fuels, *Anal. Chem.* **52** (1980) 1135–1140.

[4] J.F. Haw, T.E. Glass, and H.C. Dorn, Continuous Flow High Field Nuclear Magnetic Resonance Detector for Liquid Chromatography Analysis of Fuel Samples, *Anal. Chem.* **53** (1981) 2327–2332.

[5] J.C. Lindon, J.K. Nicholson, and I.D. Wilson, Directly Coupled HPLC-NMR and HPLC-NMR-MS in Pharmaceutical Research and Development, *J. Chromatogr. B* **748** (2000) 233–258.

[6] R.P. Hicks, Recent Advances in NMR: Expanding Its Role in Rational Drug Design, *Curr. Med. Chem.* **8** (2001) 627–650.

[7] K. Albert, *On-Line LC-NMR and Related Techniques*, Wiley, Chichester, England, 2002.

[8] M.V. Silva Elipe, Advantages and Disadvantages of Nuclear Magnetic Resonance Spectroscopy as Hyphenated Technique, *Anal. Chim. Acta* **497** (2003) 1–25.

[9] M.V. Silva Elipe, LC-NMR Overview and Pharmaceutical Applications, in Y. Kazakevich and R. LoBrutto (eds.), *HPLC for Pharmaceutical Scientists*, Wiley, Hoboken, NJ, 2007, pp. 901–936.

[10] M.V. Silva Elipe, LC/NMR and LC/MS/NMR, in J. Cages (ed.), *Encyclopedia of Chromatography* 3rd ed., Vol. **1**, Marcel Decker, New York, 2009 pp. 1337–1351.

[11] S.H. Smallcombe, S.L. Patt, and P.A. Keifer, WET Solvent Suppression and Its Applications to LC NMR and High-Resolution NMR Spectroscopy, *J. Magn. Reson. Ser. A* **117** (1995) 295–303.

[12] P.A. Keifer, Flow Techniques in NMR Spectroscopy, *Annu. Rep. NMR Spectrosc.* **62** (2007) 1–47.

[13] K.I. Burton, J.R. Everett, M.J. Newman, F.S. Pullen, D.S. Richards, and A.G. Swanson, On-Line Liquid Chromatography Coupled with High Field NMR and Mass Spectrometry (LC-NMR-MS): A New Technique for Drug Metabolite Structure Elucidation, *J. Pharm. Biomed. Anal.* **15** (1997), 1903–1912.

[14] E.A. Crowe, J.K. Roberts, and R.J. Smith, ^{1}H and ^{19}F LC/NMR: Application to the Identification of Impurities in Compounds of Pharmaceutical Interest, *Pharm. Sci.* **1** (1995), 103–105.

[15] R. Singh, I.-W. Chen, L. Jin, M.V. Silva, B.H. Arison, J.H. Lin, and B.K. Wong, Pharmacokinetics and Metabolism of *RAS* Farnesyl Transferase Inhibitor in Rats and Dogs: In Vitro–In Vivo Correlation, *Drug Metab. Dispos.* **29** (2001) 1578–1587.

[16] M.V. Silva Elipe, S.-E. W. Huskey, and B. Zhu, Application of LC-NMR for the Study of the Volatile Metabolite of MK-0869, a Substance P Receptor Antagonist, *J. Pharm. Biomed. Anal.* **30** (2003) 1431–1440.

4

Applications of LC-NMR

4.1. INTRODUCTION

Analysis of complex mixtures has created a need for hyphenated techniques to determine the structures of the components of mixtures. NMR has been used successfully in the field of organic chemistry since its discovery to determine the structure of organic compounds. In many cases, isolating compounds for NMR analysis may be time consuming and present difficulties, especially for unstable compounds. The difficulties have prompted the need to develop alternatives to use to solve structural problems. NMR is a technique that provides low sensitivity but is powerful because it provides detailed information on the structure of compounds. With the development of pulse field gradients, solvent suppression, new probe designs, and digital signal processing, NMR has become capable of working with HPLC solvents, in many cases in their deuterated form, as a hyphenated technique. Those developments have made LC-NMR a handy methodology for the analysis of sample mixtures. LC-NMR has become a standard tool in many laboratories as a hyphenated technique to approach determining the structures of compounds present in mixtures that may present some issues during isolation or due to instability. In this chapter we give an overview of applications of LC-NMR in a

LC-NMR and Other Hyphenated NMR Techniques: Overview and Applications, First Edition. Maria Victoria Silva Elipe.

variety of fields, as well as cases to demonstrate the applicability and extensive use of this hyphenated technique.

4.2. APPLICATIONS OF LC-NMR

LC-NMR has been applied extensively to the field of structural elucidation of organic compounds in many areas, including natural products, drug metabolism, drug discovery, impurity characterization, degradation products, food analysis, polymers, metabolomics and metabonomics, and isomers, including tautomers and chiral compounds. The diversity of applications of LC-NMR makes it a routine technique commonly used in academic and industrial laboratories, particularly in the pharmaceutical area. Below is a description of examples of LC-NMR applied successfully in these areas.

4.2.1. Natural Products

LC-NMR has been widely applied in the field of natural products chemistry. Two principal approaches have been used: examination of crude extracts and determination of the structure of unknowns. In the case of crude extracts, the main focus is to screen these extracts for rapid determination of the presence of known major components of the extracts and of unknown components, for further investigation of their structures. The mode of operation for the screening methodology is on-flow LC-NMR, which makes possible rapid analysis of complex mixtures for recognition of major known components. If structural elucidation is needed mainly for the unknown components, stop-flow is more appropriate. In addition, preliminary pre-purification of the analytes of interest may be necessary to eliminate or minimize other interferences from other components present in the mixture that may affect the structural elucidation analysis when they have retention times similar to those of the components of interest [1–4].

Traditionally, after HPLC and LC-MS screening of crude extracts from plant, marine, or microbial sources, analytes of interest have been isolated to determine their structures. The process is lengthy and requires isolation of a few milligrams to carry out NMR analysis normally in 3- or 5-mm NMR tubes. In many cases, unnecessary time is consumed isolating known structures; therefore, better methodology to identify them has been a need with natural products. Dereplication is a process of quick identification of known and undesired compounds from natural product extracts as a means of using resources wisely by isolating only unknown compounds of interest. LC-MS has for many years been the method of choice for dereplication. However, lack of ionization of some compounds and information on a molecular ion that can

generate several possible molecular formulas are drawbacks to identifying the known compound in many cases. LC-NMR has been employed as a screening method in natural products from plants, marine, life, and microorganisms to discriminate known components and identify the presence of unknown components of interest. On-flow is the method used for screening, and stop-flow or loop collection is used to determine the structure of unknown components of interest by performing other experiments, including two-dimensional NMR experiments.

Wolfenger et al. [5] performed screening by on-flow LC-NMR on *Swertia calycina*, a plant from the Gentianaceae family, to identify antifungal agents in the extract without isolation. The LC-UV profile was simple, with three major components in the extract. Two of them were proposed by LC-MS: sweroside, a secoiridoid type, and decussatin, a polyphenol, and were confirmed by LC-NMR (Figure 4-1). The third component was proposed by LC-MS to be a quinonic compound, but it was not possible to pinpoint its final structure. Based on the chemical shifts and splitting patterns of the proton signals from the online LC-^{1}H NMR spectrum, the structure was proposed to be 2-methoxy-1,4-naphthoquinone (Figure 4-1), a naphthoquinone first reported in the Gentianaceae family at that time. Stop-flow LC-NMR was applied to

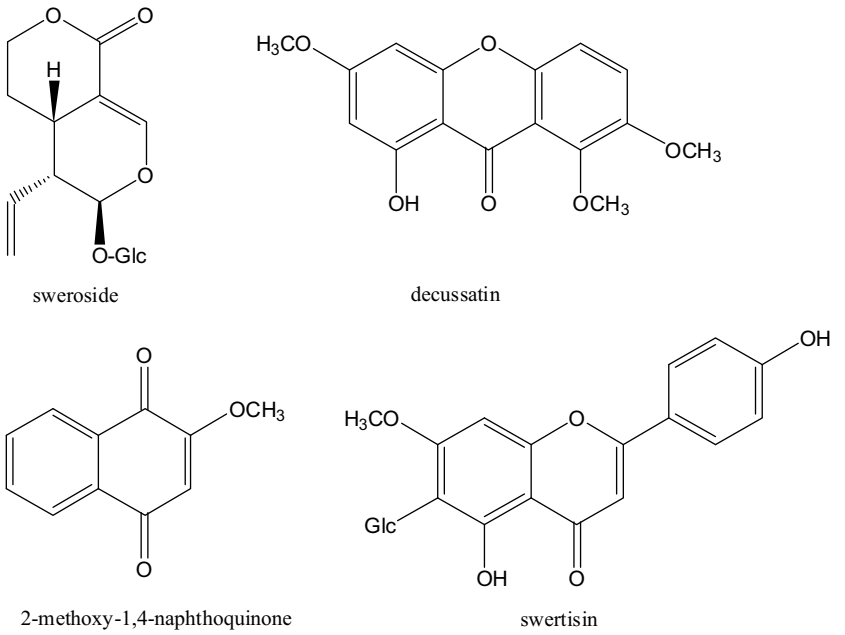

FIGURE 4-1. Structures of four components of two Gentianaceae plants indentified by LC-NMR. The three major components of *Swertia calycina* were identified by on-flow LC-NMR as sweroside, decussatin, and 2-methoxy-1,4-naphthoquinone. The structure of swertisin or 5,4′-dihydroxy-7-methoxy-6-C-glucosylflavone from *Gentiana ottonis* was identified by stop-flow LC-NMR together with LC-MS/MS [5].

another extract of a Gentianaceae plant, *Gentiana ottonis*, because it presented a more complex LC-UV profile and to increase the sensitivity of LC-NMR. The stop-flow LC-NMR and the LC-MS/MS experiments facilitated determination of the position of C-glycosylation of a flavone C-glycoside, not possible by conventional LC-MS, as the known 5,4′-dihydroxy-7-methoxy-6-*C*-glucosyl-flavone or swertisin (Figure 4-1). LC-NMR was performed using a WET solvent suppression technique on the methyl group and its two ^{13}C satellites of MeCN and the residual HOD peak. The authors indicated that the detection limits of the LC-NMR stop-flow mode carried out on their 500-MHz instrument was approximately 0.05 μmol per chromatographic peak, and it was lowered by a factor of 100 in the LC-NMR stop-flow mode, with acquisition times of several hours without significant dispersion of the chromatography in the flow cell [5].

Renukappa et al. [6] performed on-flow and stop-flow LC-NMR on the crude plant extract *of Bacopa monniera* W. (Scrophulariaceae) to determine the major active saponin components of the extract. To fully determine their spin-system connectivities of the three major components as P1, P3, and P4, WETGCOSY and WETTOCSY experiments in the stop-flow LC-NMR mode were performed due to the complexity of their structures. The major components identified were bacoside A_3 or 3-β-[*O*-β-D-glucopyanosyl-(1 → 3)-*O*-[α-L-arabinofuranosyl-(1 → 2)]-*O*-β-D-glucopyranosyl)oxy]jujubogenin for P1, 3-β-[*O*-β-D-glucopyanosyl-(1 → 3)-*O*-[α-L-arabinofuranosyl-(1 → 2)]-*O*-β-D-arabinopyranosyl)oxy]jujubogenin for P3, and bacopasaponin C or 3-β-[*O*-β-D-glucopyanosyl-(1 → 3)-*O*-[α-L-arabinofuranosyl-(1 → 2)]-*O*-β-D-arabinopyranosyl)oxy]pseudojujubogenin for P4 (Figure 4-2). LC-NMR was performed using MeCN/D_2O and MeOH/D_2O solvent systems with a WET solvent suppression technique on the methyl groups and their two ^{13}C satellites of MeCN and MeOH, and the residual HOD peak. The structures were also confirmed by comparing the spectroscopical data with authentic samples. The authors concluded that when other types of NMR data, such as from NOESY, ^1H-^{13}C HSQC, and ^1H-^{13}C HMBC experiments, are needed to clarify structural features, isolation of the chromatographic peak of interest is a requirement because the amount that can be analyzed by LC-NMR is not sufficient to perform those experiments [6].

In the last decade, LC-NMR has been applied to plants and marine natural products, and also to extracts from microorganisms as a dereplication technique by the on-flow mode. Stop-flow is employed predominantly when more structural information is needed than just from the one-dimensional traces of the on-flow LC-NMR mode by acquiring two-dimensional homonuclear experiments. Two-dimensional COSY spectrum on stop-flow mode was the key experiment for unambiguous identification of δ-tocotrienol from a crude palm oil extract (Figure 4-3) [7]. After on-flow LC-NMR carried out to screen naphthylisoquinoline alkaloids in plants from the

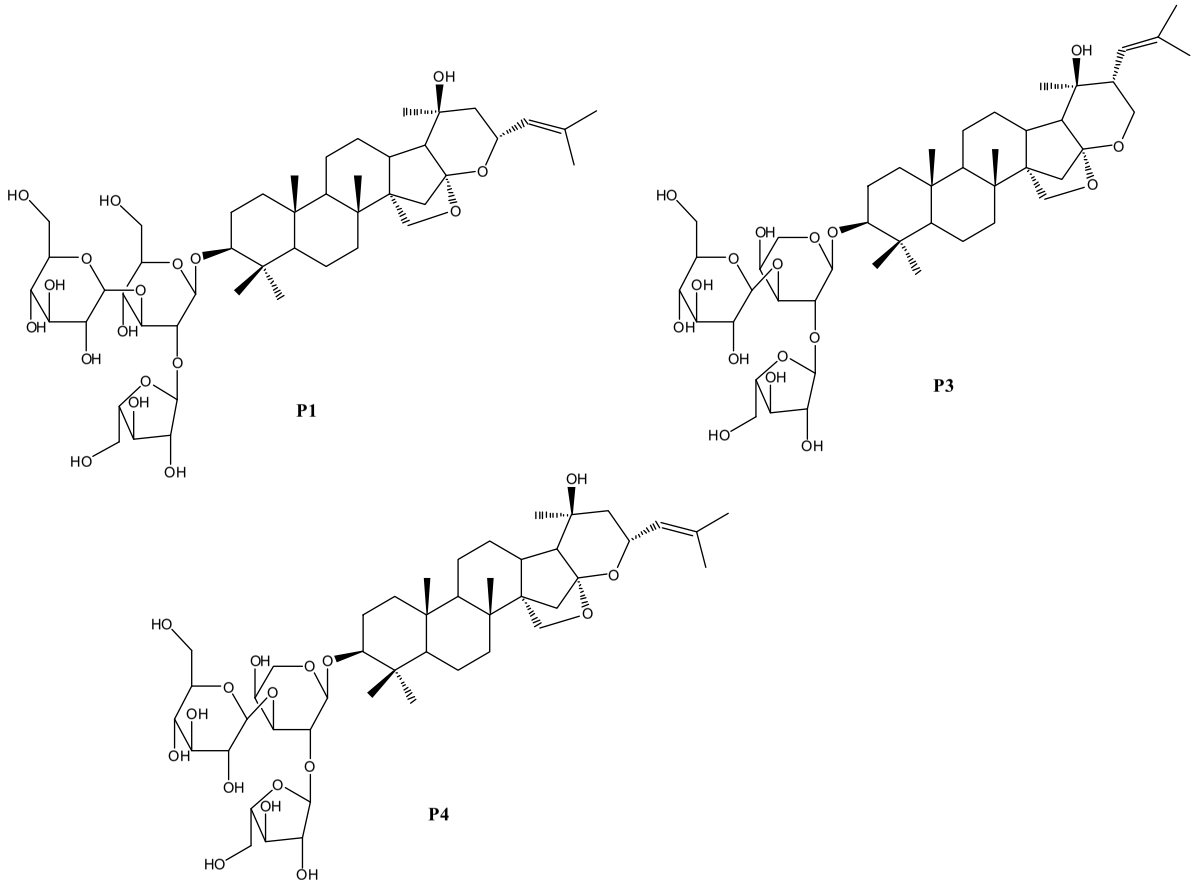

FIGURE 4-2. Structures of the three major components identified from the crude plant extract *of Bacopa monniera* W. (Scrophulariaceae) as P1, P3, and P4 in on-flow and stop-flow LC-NMR. The structures are bacoside A_3 or 3-β-[*O*-β-D-glucopyanosyl-(1 → 3)-*O*-[α-L-arabinofuranosyl-(1 → 2)]-*O*-β-D-glucopyranosyl)oxy]jujubogenin for P1, 3-β-[*O*-β-D-glucopyanosyl-(1 → 3)-*O*-[α-L-arabinofuranosyl-(1 → 2)]-*O*-β-D-arabinopyranosyl)oxy]jujubogenin for P3, and bacopasaponin C or 3-β-[*O*-β-D-glucopyanosyl-(1 → 3)-*O*-[α-L-arabinofuranosyl-(1 → 2)]-*O*-β-D-arabinopyranosyl)oxy]pseudojujubogenin for P4 [6].

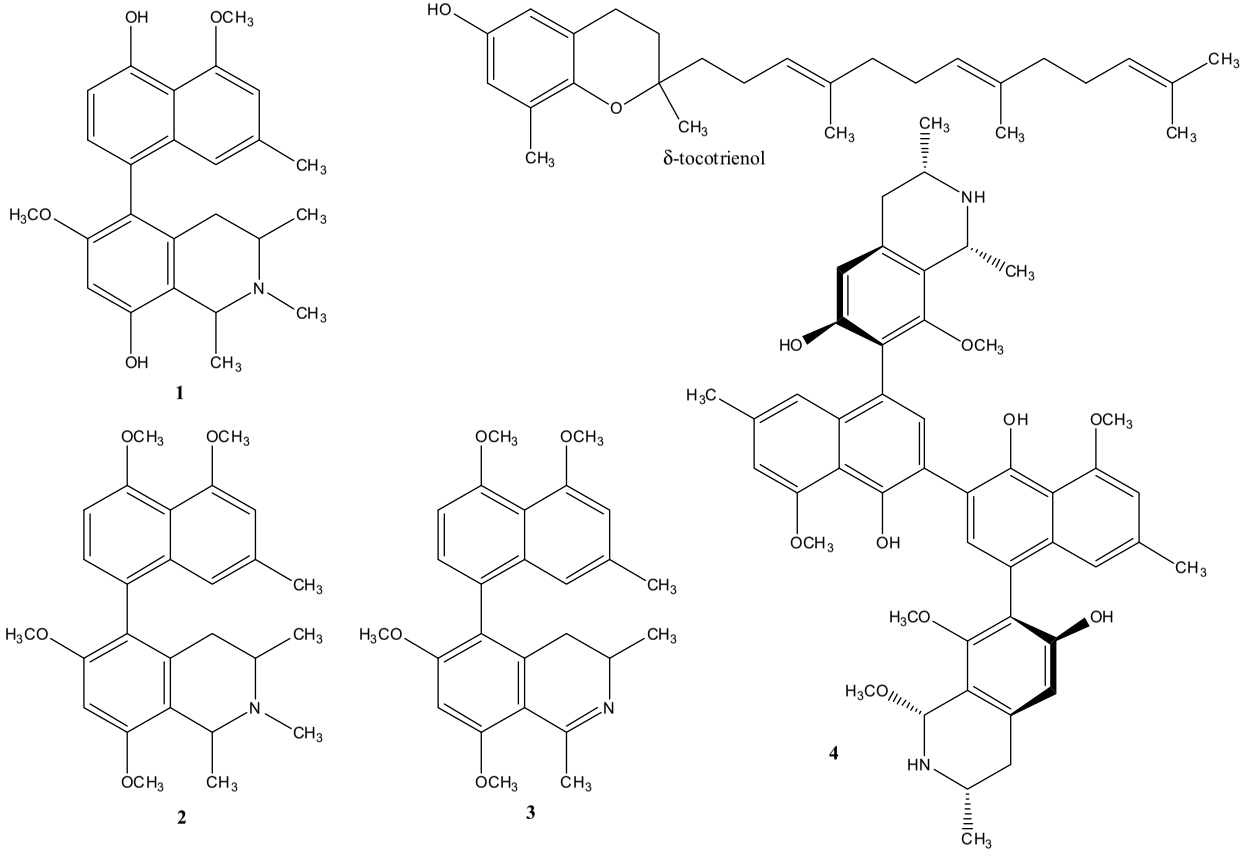

FIGURE 4-3. Structures of δ-tocotrienol [7], monomer naphthylisoquinoline alakoids 1, 2, and 3 [8], and dimer naphthylisoquinoline alkaloid 4 [9].

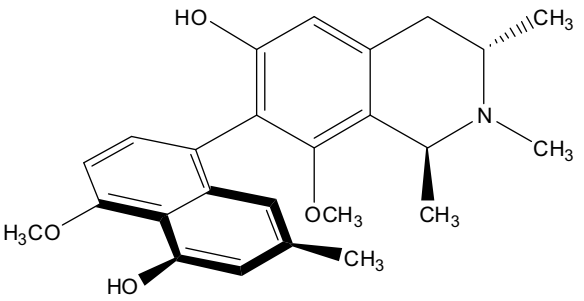

5

FIGURE 4-4. Structure of the monomer naphthylisoquinoline alkaloid 5 from *Ancistrocladus griffithi*, an Ancistrocladaceae plant [10].

Ancistrocladaceae family, two-dimensional TOCSY and two-dimensional ROESY in the stop-flow mode were used to identify unequivocally the spin systems and spatial correlations to establish their relative configuration of unknown naphthylisoquinoline alkaloids for the monomer alkaloids 1, 2, and 3 [8] and the dimer alkaloid 4 [9]. However, sometimes isolation of the compound of interest is necessary to confirm unambiguously the structure of compounds by two-dimensional ROESY and two-dimensional heteronuclear NMR techniques such as $^{1}H–^{13}C$ HMBC to perform carbon assignments and proton–carbon correlations. Isolation of the monomer naphthylisoquinoline alkaloid 5 from *Ancistrocladus griffithi*, a Ancistrocladaceae plant, was needed to confirm and fully characterize the structure proposed by online LC-NMR (Figure 4-4) [10].

Other examples in the literature follow the same trend as noted above in the common practice of performing stop-flow LC-NMR after dereplication through on-flow LC-NMR analysis, to identify the structure of specific compounds in a mixture of crude extracts from plants [11–14], marine life [15,16], and microorganisms [17–21]. Queroiz et al. [19] approached on-flow LC-NMR differently by reducing the flow rate to 0.1 mL/min to run NMR spectra per chromatographic peak, acquiring 120 increments of 256 transients each for a total chromatographic duration of 19 h. The authors consider this technique a low-flow LC-NMR method because they were able to obtain the same separation as with a flow rate of 1 mL/min but with the advantages of having more transients (or scans) per chromatographic peak. The advantage of a lower flow rate is that the limit of detection is lowered under these conditions. The authors were able to obtain NMR data from more than 10 LC peaks from the injected crude extract during a period of 19 h [19].

In addition to on-flow and stop-flow LC-NMR techniques, trapping chromatographic peaks on loop collectors has been used to overcome the low

sensitivity of NMR [22,23]. The chromatographic column may be overloaded with concentrated sample to collect each individual peak in a loop for later analysis. The loop used is capillary tubing, to avoid diffusion and dilution of the analyte of interest in the loop. Normally, the stop-flow LC-NMR mode is employed on selected peaks of interest after loop storage, and not necessarily in the order of elution in which they have been collected from the chromatographic run. However, the loop collector method may fail if the concentration of the analytes of interest is insufficient for NMR analysis. Traditional isolation on those peaks is needed for off-line NMR analysis [23]. Shaha et al. [22] used superheated deuterium oxide (D_2O) instead of water as the mobile phase of the HPLC to minimize any interference from other solvents present in conventional HPLC organic–aqueous eluents, which often contain modifiers. This method is appropriate when isothermal conditions give poor separation and the temperature gradient yields good separation of the components of the extract, as found in the analysis of ginger extracts, which are thermally unstable during GC and GC-MS analysis [22].

4.2.2. Drug Metabolism

LC-NMR has been employed extensively and successfully in the field of drug metabolism. Conventionally, NMR spectroscopy has been used off-line for the structural determination of metabolites through isolation from their biological matrices (e.g., urine, bile, feces, brain, and other tissues, including in vitro transformations from microsome and hepatocyte incubations). However, isolation is time consuming, and with the development of better NMR probe designs, solvent suppression techniques to accommodate reversed-phase common deuterated HPLC solvent systems, high-field magnets, and better electronics in the NMR instruments coupled to common personal computers, used of LC-NMR has become routine in many laboratories. Currently, isolation of metabolites is pursued for cases where the complexity of the structure requires more detailed information from ^{1}H and ^{13}C chemical shift data through two-dimensional inverse detection NMR experiments (e.g., HSQC, HMBC). These experiments are more complex to perform in an LC-NMR setting, due to the need for solvent suppression and limitations in increasing the concentration of the metabolites of interest from the chromatographic peak of the HPLC run. However, LC-NMR has not replaced the isolation process, especially for complex matrices such as bile samples. Preliminary separation of the major components of the matrix is a requirement for LC-NMR to eliminate any other endogenous materials that may elute with the chromatographic peak of interest and interfere with the NMR analysis. NMR will detect anything above the NMR detection limit that has protons or whatever nuclei of study on the chromatographic peak that is in the flow cell

where the RF receiver coil is located. Therefore, overlapping of signals from components in the same chromatographic peak will complicate the analysis, providing ambiguous results. Common modes of operation for LC-NMR analysis of metabolites are on-flow, stop-flow, and loop collection. On-flow gives an overview of the major metabolites present in the sample mixture; stop-flow makes it possible to obtain data from major and minor metabolites that are above the threshold of detection and to obtain two-dimensional NMR experiments if a sufficient amount of analyte is in the flow cell; and loop collection provides another mode of separating metabolites into capillary loops for later NMR analysis [2,24,25].

Tocopherols are components of vitamin E and are sensitive to light and air, which makes them difficult to analyze from toothpaste and gingival samples after isolation, due to possible degradation with light and air. Tocopherol homologs were analyzed successfully by on-flow LC-NMR from human samples to determine the effect of the enrichment of vitamin E in gingival tissue after the treatment of toothpastes containing α-tocopherol acetate [26]. Studies have shown that decreasing the flow rate to 0.3 mL/min when performing on-flow LC-NMR provides higher NMR sensitivity but with lower resolution, due to peak broadening. The lower resolution is sufficient to identify the proton signals of each chromatographic peak [27]. Unfortunately, when several hydroxylated metabolites are formed, each positional isomer cannot be easily distinguished from simple inspection in an on-flow NMR experiment [27]. Murai et at. [27] collected WETNOESY data in the stop-flow mode to assign the hydroxylation correctly in each positional isomer for metabolites M1 and M2 (Figure 4-5) [27]. Another way to determine the number of metabolites in a biological sample is by performing on-flow LC-^{19}F NMR before stop-flow LC-^{1}H NMR analysis to determine the structure of the metabolites of interest [28]. If the parent drug has ^{19}F, LC-^{19}F NMR has the advantage of not interfering with signals from the matrix because only drug-related compounds, and not endogenous compounds, will have ^{19}F in their structures [28].

Stop-flow mode is the most common approach to determining the structure of metabolites by simple inspection of an ^{1}H NMR spectrum acquired with a sufficient signal-to-noise ratio compared to the spectrum of the parent drug to determine the difference in the structure of the metabolite [29–39]. LC-NMR plays an important role in the structural analysis of volatile or unstable metabolites because they cannot be isolated successfully for off-line NMR analysis [33,36,37]. Dear et al. [33] used ion-exchange HPLC in an LC-NMR system as a tool to identify the structure of a highly polar radioactive metabolite that did not have a significant UV chromophore and was unretained in reversed-phase HPLC, due to its highly hydrophilic nature [33]. After cleaning up the sample with solid-phase extraction, ion-exchange LC-NMR

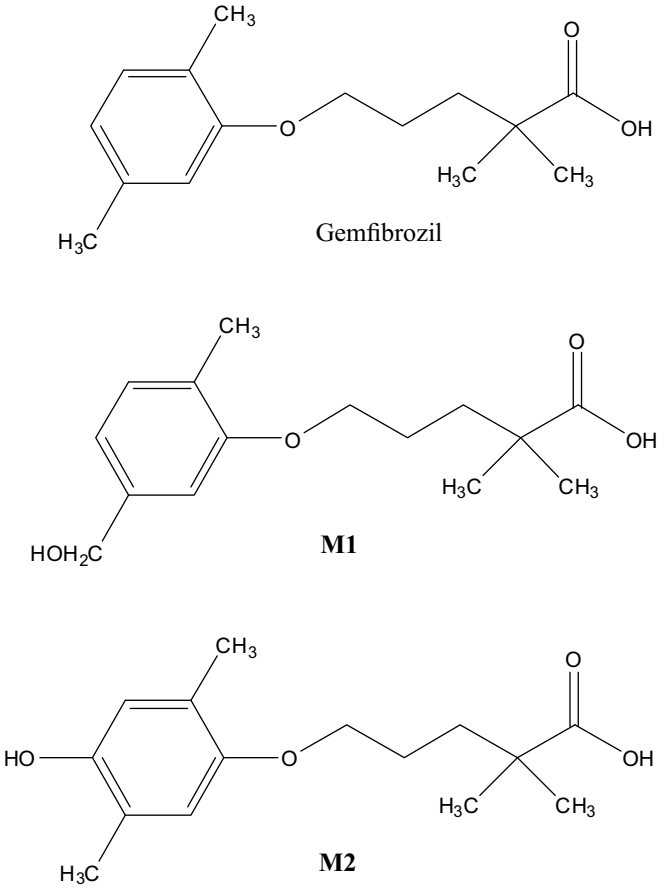

FIGURE 4-5. Structure of gemfibrozil and its M1 and M2 hydroxylated metabolites as positional isomers [27].

was employed. Performing stop-flow LC-NMR on the chromatographic peak of interest provided most of the information regarding the structure of the metabolite. Unfortunately, the presence of *N*-acetyl was not confirmed, due to overlapping of the signals with the acetonitrile signal from the LC-NMR solvent system. Therefore, recovering the peak trapped in the flow cell was necessary to confirm its structure, which also included ^{13}C data through the HMBC experiment (Figure 4-6) [33].

Identification of the structures of metabolites in different incubations with microsomes containing recombinant human cytochrome P450 enzymes (CYP) also provides information on the metabolic pathway of metabolites [37]. Identification of the polar metabolite M3 by HPLC and LC-NMR from the incubations of [^{14}C]M1 and [^{14}C]M2 metabolites of the drug MK-0869 with microsomes containing human recombinant CYP1A2, CYP2A6, CYP2B6,

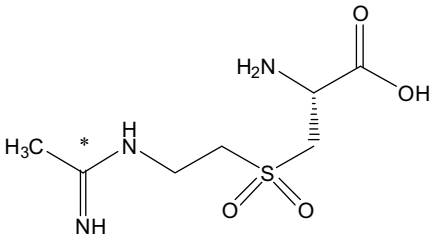

FIGURE 4-6. Structure of the *N*-acetyl highly polar metabolite *N*-acetyl-3-{[2-(ethanimidoylamino) ethyl]sulfonyl}alanine. The asterisk indicates the radioactive ^{14}C labeled position [33].

CYP2C8, CYP2C9, CYP2C19, CYP2D6, CYP 2E1, or CYP3A4 was crucial to determine the CYPs enzymes involved in the *O*-dealkylation mechanism pathway. Only human recombinant CYP2C19, CYP1A2, and CYP3A4 metabolized M1 and M2 to the very polar metabolite M3. These findings suggest that M1 or M2 converted to M3 via *O*-dealkylation of the 1-(3,5-bis(trifluoromethylphenyl)ethanol moiety, followed by equilibrium of the corresponding hemiacetal–aldehyde forms of the morpholine ring (Figure 4-7). The aldehyde or open ring of the morpholine ring could either lose the aminoethanol tether after oxidation on the benzylic position in the case of M1 or hydrolysis in the case of M2, giving rise to *p*-fluorophenylglyoxal, which could be further reduced to the *p*-fluoro-α-hydroxyacetophenone or M3 (Figure 4-7) [37]. In the case of ambiguities on assignments of the one-dimensional ^{1}H NMR from an LC-NMR run, two-dimensional WETCOSY/TOCSY experiments under stop-flow conditions will facilitate the proton assignments [32]. Storing the chromatographic peaks of interest in loops is another option that can be used to pursue the NMR analysis of more than one analyte from biological samples. The NMR analysis can be performed in a different order than that used to collect chromatographic peaks in loop collectors [40]. Recently, with the use of cryogenic probes, improvement in sensitivity is at least fourfold, facilitating the analysis of mixtures in the drug metabolism world [41]. Cloarec et al. [41] also used statistical correlation spectroscopy to deconvolute the overlapping mixture of components on a single UV chromatographic peak.

An important metabolic pathway is the formation of conjugates of acyl glucuronide and its acyl migration species, depending on the pH of the media [42–49]. β-Glucuronidation is a major metabolic pathway for drugs containing a carboxylic acid or hydroxyl group. In the case of carboxylic acid, the β-1-*O*-acylglucuronide adduct formed is labile in vivo and in vitro to mutarotation or acyl migration under physiological pH and mild basic conditions, yielding a series of positional isomers for both α- and β-anomers (Figure 4-8). LC-^{19}F NMR has been used in the on-flow mode to observe the separation in the chromatography of the various acyl migrated components based on their retention times for fluorine-containing parent drug

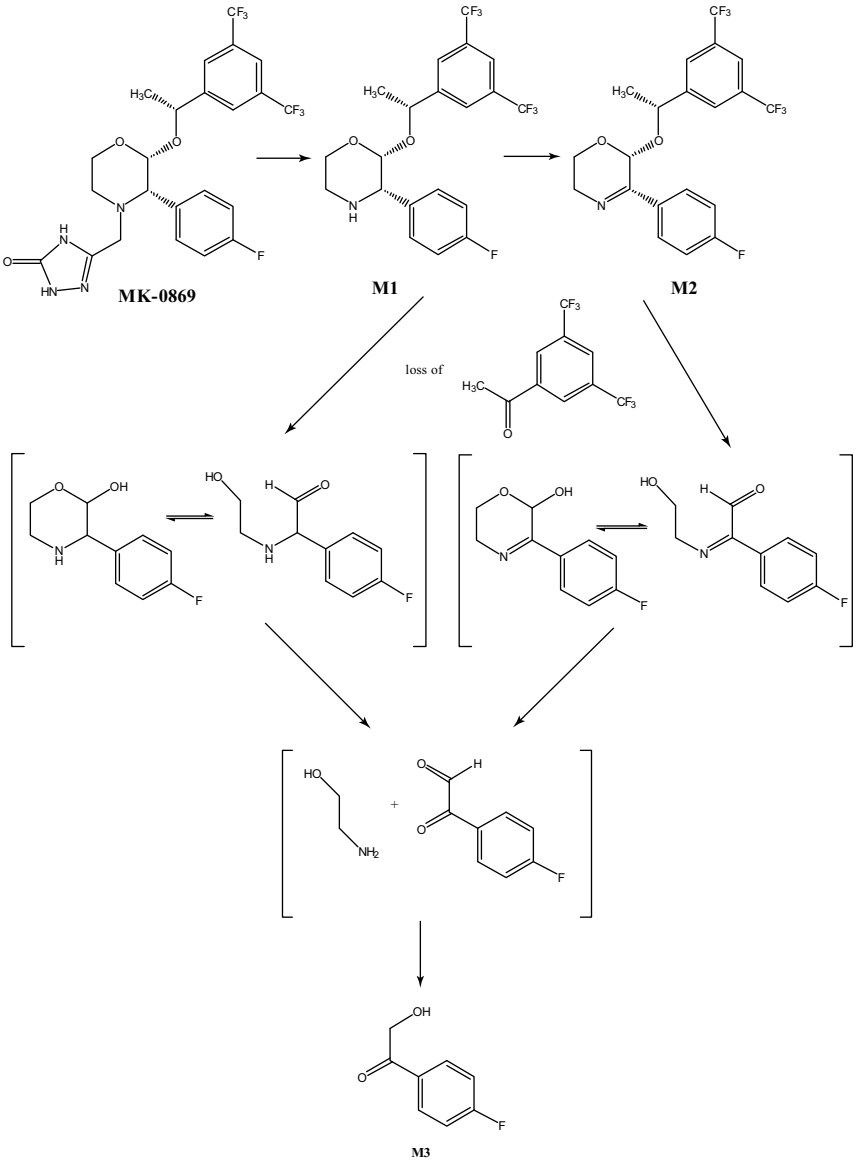

FIGURE 4-7. Proposed mechanism of formation for the metabolic pathway of the metabolite M3 of MK-0869 from incubations of [^{14}C]M1 and [^{14}C]M2 metabolites with microsomes containing recombinant human CYP2C19, CYP1A2, or CYP3A4 [37].

molecules [45]. The greater chemical shift dispersion of ^{19}F simplifies analysis of the mixture versus the LC-^{1}H NMR version because of the low number of ^{19}F atoms in the parent drug compared to ^{1}H atoms in the molecule and the lack of interference with endogenous compounds in the

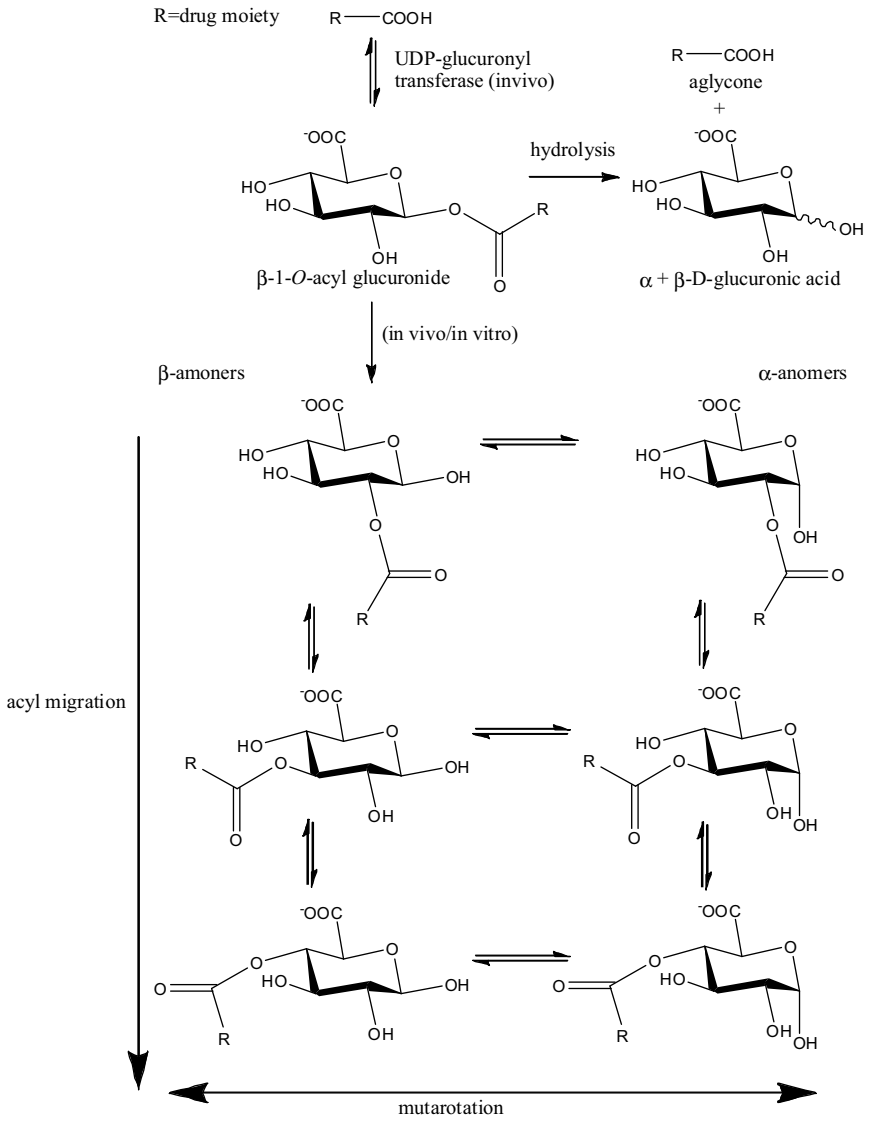

FIGURE 4-8. General scheme of formation of any drug with carboxylic acid into a 1-*O*-acyl glucuronide drug adduct, its hydrolysis, and the reaction products arising from internal acyl migration and mutarotation.

sample without fluorine [45]. It has been accepted that the acyl migration reactions are reversible except for formation of the α- and β-1-*O*-acyl isomers, probably due to the high energy barrier to form the C-O bond of the anomeric position (Figure 4-8). However, the presence of the α-1-*O*-acyl glucuronide as a minor component has brought the hypothesis of its formation from equilibrium with the α-2-*O*-acyl glucuronide (Figure 4-9) [47].

To demonstrate that hypothesis, Nicholson's group applied LC-^{1}H NMR to *S*-naproxen β-1-*O*-acyl glucuronide during acyl migration and obtained kinetic information [47,49]. The authors demonstrated that the α-1-*O*-acyl isomer is formed from the α-2-*O*-acyl glucuronide isomer through a postulated intramolecular rearrangement where the 1,2-*cis*-(*ax*,*eq*) fused intermediate has a lower energy barrier formation than the 1,2-*trans*-(*eq*,*eq*) fused intermediate, favoring the back reaction of α-2-*O*-acyl glucuronide to α-1-*O*-acyl isomer (Figure 4-10) [47]. In addition, the α-1-*O*-acyl isomer is thermodynamically more stable and kinetically more unstable than its counterpart, β-1-*O*-acyl glucuronide [47].

4.2.3. Drug Discovery

Earlier in the process of discovering drug candidates with potential biological activities for future development, hyphenated analytical techniques can be employed in two main areas to assess and determine the components of complex mixtures in drug discovery: medicinal chemistry and combinatorial chemistry. LC-MS has been the traditional technique used to analyze the components of complex mixtures in those areas, due to its high sensitivity. However, MS has some drawbacks for complete structure determination. Problems with the ionization and reliability of the molecular ions of analytes of mixtures in determining their structures can make structural assignments tentative or impossible, especially to distinguish molecules of the same molecular weight or between regioisomers [2,50]. In medicinal chemistry, determination of the components in reaction mixtures, such as by-products or impurities, is required early in the process to modify the synthesis for better yield. In addition, identification of degradation products from dosage formulations early in the process provides information on the stability of drug candidates for future animal studies and in the selection of the drug formulations for development stages [2,50]. Impurity characterization and degradation products are discussed in detail in the following sections. The identification of drug metabolites early in the process is critical in drug discovery to design better drug candidates with higher efficacy, bioavailability, and minimum toxicity [2,50]. The application of LC-NMR in drug metabolism was discussed in Section 4.2.2. Shapira et al. [51] applied ultrafast two-dimensional TOCSY experiments in a custom-made NMR flow cell connected directly to an ongoing chromatographic separation to determine in situ the structure of the components of the mixture as a potential application to mixture analysis in drug discovery. In combinatorial chemistry, the analysis of reaction mixture from high-throughput reaction screening in combinatorial libraries is critical to the design of better drug candidates [2,50,52]. The use of LC-NMR has been tested on a mixture of peptides [2,50,52]. Direct flow

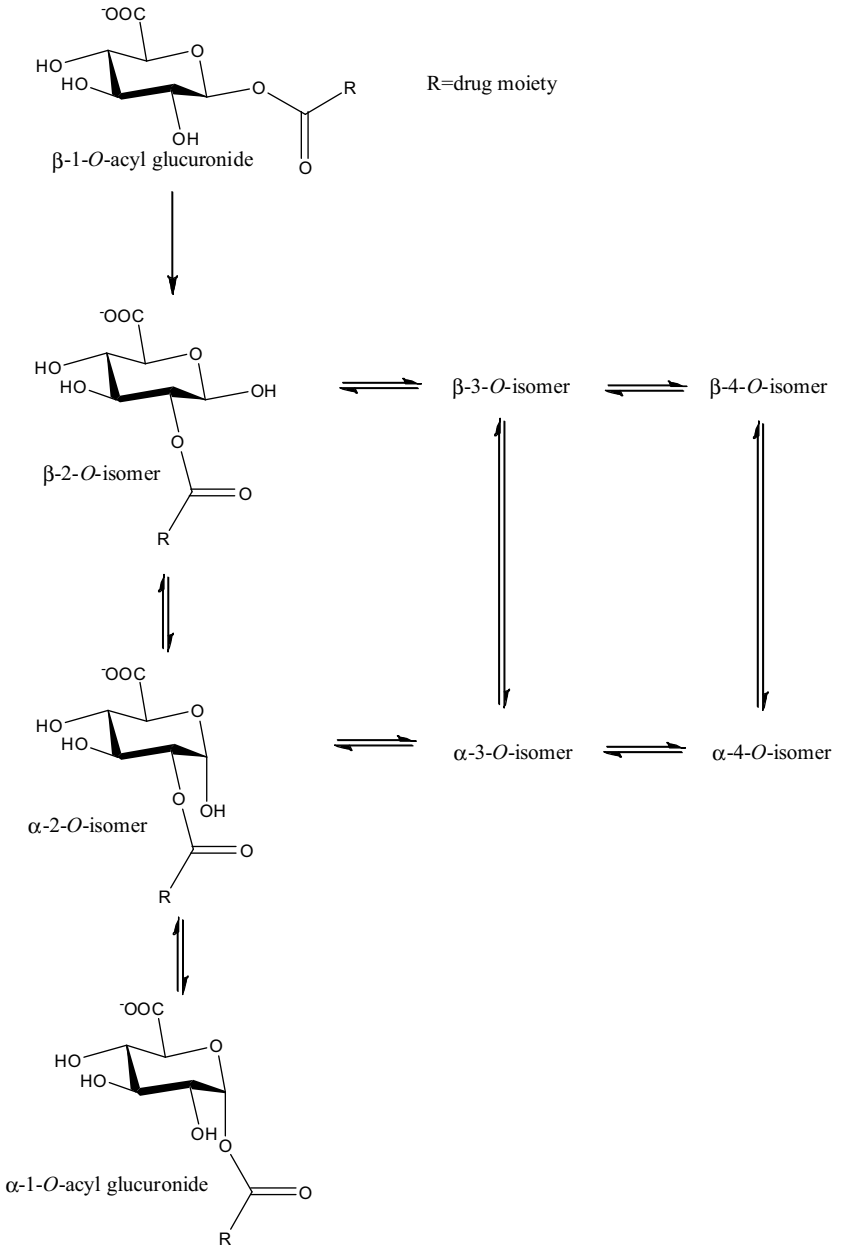

FIGURE 4-9. Accepted scheme of formation of α-1-*O*-acyl glucuronide isomer from β-2-*O*-acyl glucuronide through equilibrium with α-2-*O*-acyl glucuronide [47].

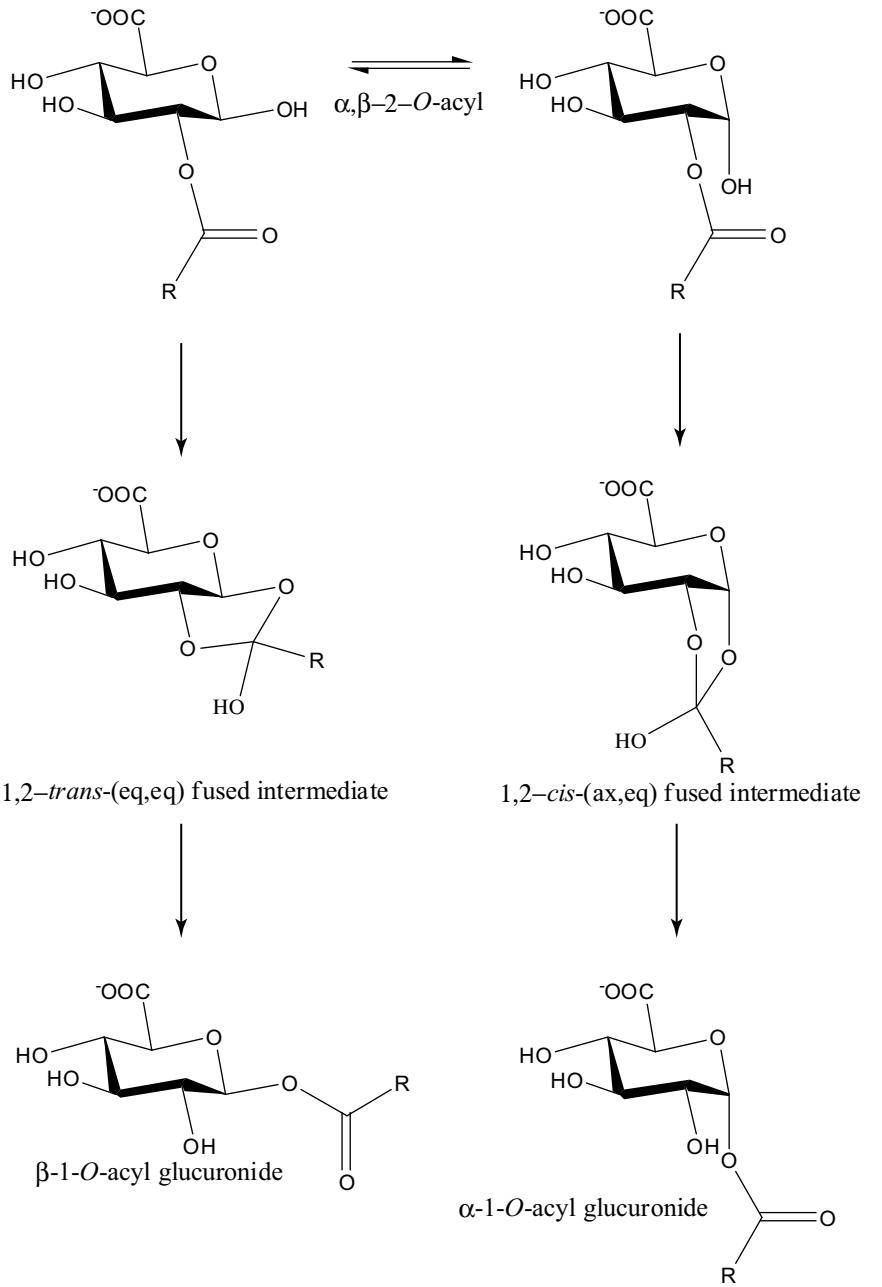

FIGURE 4-10. Postulated mechanism of formation of the α-1-*O*-acyl glucuronide isomer as an intramolecular rearrangement of α-2-*O*-acyl glucuronide [47].

NMR techniques without the presence of the HPLC instrumental component have also been used, but that is beyond the scope of this book [53].

4.2.4. Impurity Characterization

Impurity characterization by LC-NMR has been employed primarily in the pharmaceutical industry. During the development of drug candidates, the structures of impurities present in drug substances and drug products, which are formulated drug substances, have to be characterized when their levels are equal or greater than 0.1% of the UV peak area based on HPLC analysis. Knowledge of their structures can provide an assessment of their potential toxicological effects and is a requirement of regulatory agencies worldwide. Impurity characterization is also important when impurities are formed during the reactions that form the drug substance or active principal ingredient (API) to understand and optimize chemical reactions and know their potential formation mechanisms so as to avoid or minimize their presence [50,54]. Traditionally, MS and LC-MS have been the techniques used to characterize impurities in both drug substances and drug products, but the structural information obtained by MS is not sufficient to determine their structures without ambiguity, especially in cases of regioisomers or complex structures such as dimers, which can have a greater number of possible molecular formulas for a particular molecular ion. In those cases, isolation is used to carry out NMR analysis to determine their structures. With the improvements in electronics, probe design, cryogenic systems, and sensitivity in modern NMR instruments, LC-NMR has become capable of analyzing complex mixtures, eliminating or decreasing the number of steps during the impurity isolation process [50,54]. Early in the 1990s, on-flow and stop-flow NMR experiments were carried out on simulated mixtures to demonstrate the sensitivity of LC-NMR for ^{1}H and ^{19}F NMR analysis [55,56]. The time-sliced operation mode has been used less frequently, but a successful example is its application to fluticasone propionate (Figure 4-11) to determine any evidence of the presence of other components in the same chromatographic peak [57]. In addition, the authors were able to determine the structures of four impurities as dimers that were at a level of 2% or below without the need of isolation [57].

In recent years, the common trend toward impurity structural determination is to pursue isolation after initial LC-NMR and LC-MS analysis. LC-NMR analysis using on-flow and stop-flow modalities provides proposals of potential structures for impurities of interest. Thereafter, isolation of those analytes and sometimes synthesis of those proposed structures are carried out to confirm their definitive structures by MS and NMR, obtaining one- and two-dimensional NMR data with ^{1}H and ^{13}C connectivities [58–64].

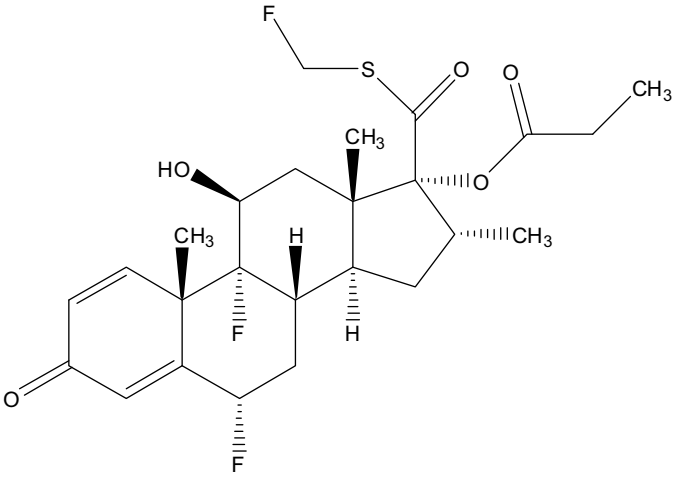

Fluticasone propionate

FIGURE 4-11. Structure of fluticasone propionate [57].

Sharma and Jones [60] indicated that LC-NMR is a powerful technique but is more appropriate for pursuing the structure determination of major rather than minor components, such as a low level of impurities due to low sensitivity, easy loss of sample in the flow system, relying on a small percentage of the chromatographic peak detected by the RF coil, and the difficulty of acquiring two-dimensional homonuclear and, especially, two-dimensional heteronuclear NMR experiments with the need of water suppression. The authors believe that isolation of impurities is no more time consuming than redevelopment of the chromatography to make it compatible with the LC-NMR requirements, such as using deuterated solvents and appropriate flow rates, minimizing broadening of chromatographic peaks, increasing the concentration of analyte in the peak, and other requirements [60].

4.2.5. Degradation Products

The characterization of degradation products is important during the drug discovery and development processes. In drug discovery, the identification of degradation products in dosage formulations provides information on the stability of drug candidates to develop better formulations, increasing drug stability. In drug development, the drug candidate by itself and in solution is stressed under specific conditions of temperature, humidity, and pH for a certain period of time, based on the International Conference of Harmonisation of Technical Requirements or ICH guidelines for the registration of pharmaceuticals for human use [65]. Forced degradation testing is a

requirement from regulatory agencies to register pharmaceuticals for human use with the purpose of identifying and quantifying degradation products in formulated drugs that may cause undesirable side effects in patients. LC-MS has been the method of choice for the characterization of degradation products in forced degradation testing of drug substances and drug products, due to its high sensitivity and fast analysis. However, LC-MS has limitations for the ambiguous determination of the structures of degradants that have complex molecular structures with large molecular weight that have a greater number of possible molecular formulas for their molecular ions. With the improvements in electronics, probe design, cryogenic systems, and sensitivity in modern NMR instruments, LC-NMR is capable of analyzing complex mixture of degradation products by eliminating or decreasing the number of steps in the isolation process [66–79].

Peng et al. [66] characterized six degradation products from a dosage formulation of the protease inhibitor PGE4410186, *N*-hydroxy-1,3-di-[4-ethoxybenzenesulfonyl]-5,5-dimethyl-[1,3]cyclohexyldiazine-2-carboxamide, during the drug discovery process by LC-MS and LC-NMR (Figure 4-12). LC-NMR data were acquired in the stop-flow mode. The drug degraded quickly in a dosage formulation designed for an animal model study. Rapid identification of the structures of the degradation products by LC-MS and LC-NMR was useful to its drug discovery process [66]. Fukutsu et al. [71] presented the typical stressed study or forced degradation study of the drug substance cefpodoxime proxetil to investigate the stability characteristic and degradation profile of the drug. The forced degradation study was carried out in solid and in solution. The drug in the solid state as a drug substance and in its formulation was treated under a dry and a humid atmosphere at 40°C. In solution, the drug was exposed to various pH solutions [71]. Three degradation products were characterized by LC-MS and LC-NMR in stop-flow mode without the need of isolation (Figure 4-13) [71]. Even though LC-NMR is intended to avoid the purification process of degradation products to carry out their structural analysis in less time, it is a common practice to isolate them to confirm their structures further by two-dimensional inverse detection NMR experiments such as ^{1}H-^{13}C HMBC [70,72,75,77]. Murakami et al. [73] used pre-concentration column trapping to concentrate the fractions with degradation products of stressed commercial tablets of amlodipine maleate (Figure 4-14) to obtain two-dimensional LC-DQF-COSY and LC-^{1}H-^{13}C-HMBC data through the stop-flow LC-NMR mode for their structural determination without the need of isolation. Shah et al. [78,79] collected the individual chromatographic peaks of the degradation products from the forced degradation studies of irbesartan and telmisartan (Figure 4-14) in fraction loops to acquire two-dimensional LC-COSY and two-dimensional LC-HMBC data to facilitate their structure analysis.

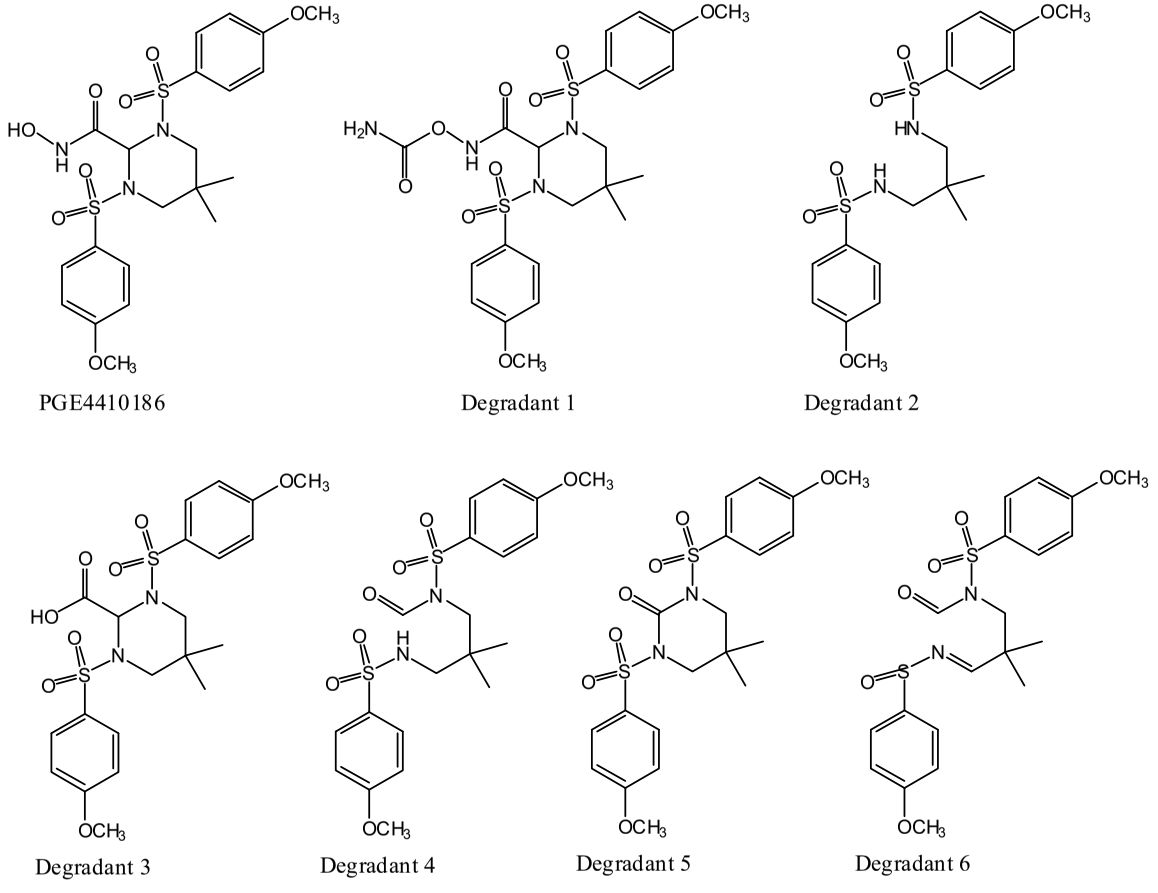

FIGURE 4-12. Structures of PGE4410186 and its six degradation products [66].

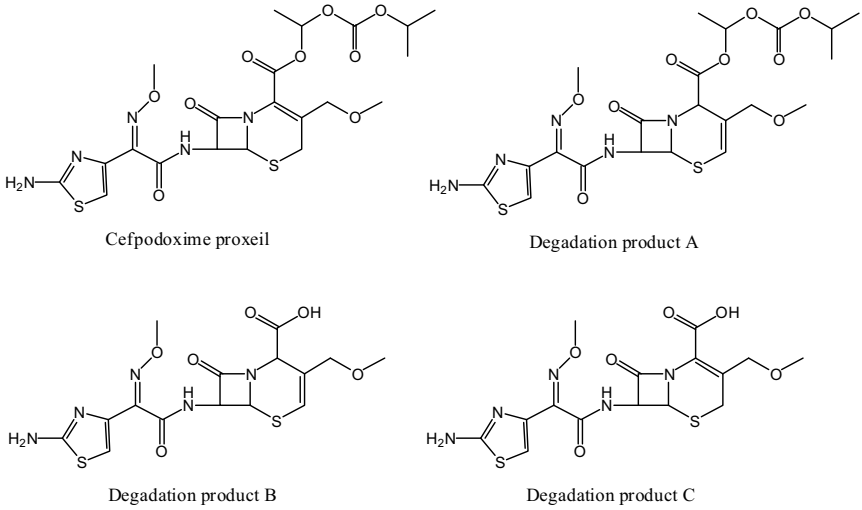

FIGURE 4-13. Structures of cefpodoxime proxetil and its three degradation products [71].

4.2.6. Food Analysis

LC-NMR has not been applied extensively to food analysis. However, there are few cases in recent years that provide interesting applications in this field [2,7,80–87]. The four modalities of LC-NMR—on-flow, stop-flow, time-sliced, and loop collection—have been applied in those cases. On-flow mode is practical when looking simultaneously at all the components of the particular food being analyzed to determine the major components of the mixture [7,80–82,84,86]. An example of the use of stop-flow is in the analysis of crude extracts from mango [80], beer [81], grape juice [82], and wine [82] to determine the major components of the extracts and to follow the biochemistry on the effects of ripening, processing, and microbial growth [80,84]. Stop-flow is applied to individual components of the mixture to confirm their structure with better signal-to-noise data, especially for minor components, and to be able to acquire some two-dimensional NMR experiments, such as WETGCOSY [7,81,83,85–87]. Examples of stop-flow applications are determination of the lutein and zeaxanthin steroisomers in sweet corn and spinach (Figure 4-15) [83], polymethoxylated flavonoids, and an acetylated tetranortriterpenoid with limonoid structure as proceranone from molecular distillation of orange peel oils (*Citrus sinensis*) (Figure 4-15) [85], and in the analysis of carotenoids in tomato juice, palm oil, and Satsuma mandarin orange juice [87]. The time-sliced mode is used to determine the composition of a particular chromatographic peak and to increase the signal-to-noise ratio compared to the on-flow mode but faster than the stop-flow mode, minimizing the distortion of the chromatography by stopping the flow for short periods of

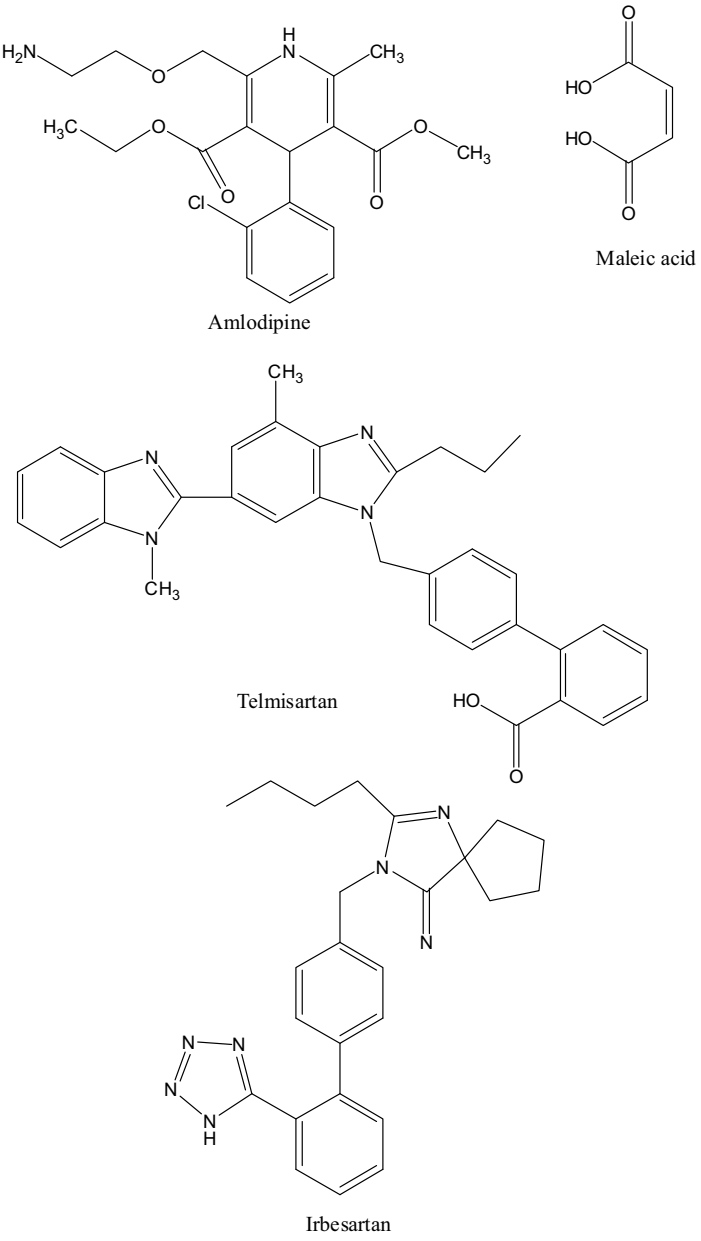

FIGURE 4-14. Structures of amlodipine maleate [73], telmisartan [78], and irbesartan [79].

time in the same chromatographic peak [82]. An example of the use of the time-sliced mode is the analysis of the aromatic composition of beer, grape juice, and wine extracts [82]. A loop collector is used to analyze chromatographic peaks at a later time, and not necessarily in the order of their

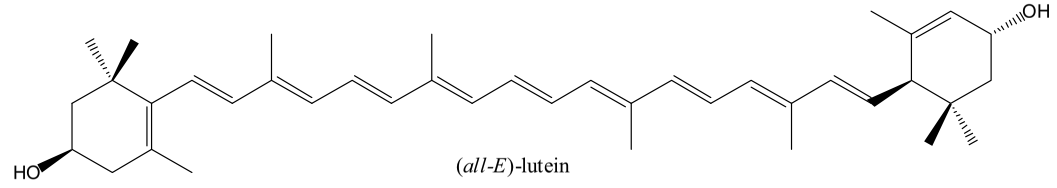

(*all-E*)-lutein

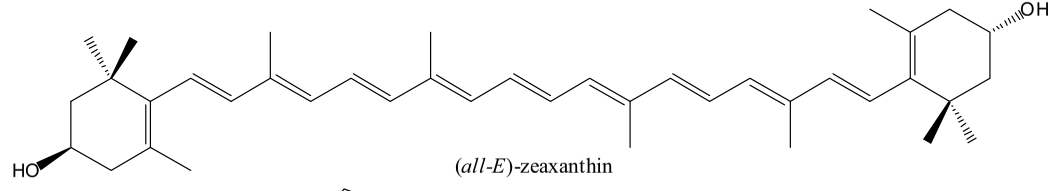

(*all-E*)-zeaxanthin

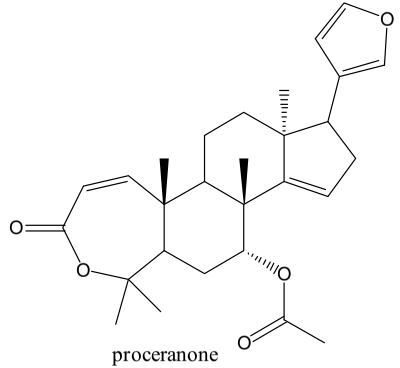

proceranone

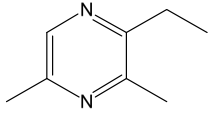

2-ethyl-3,5-dimethylpyrazine

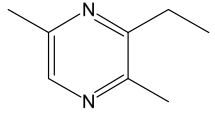

2-ethyl-3,6-dimethylpyrazine

FIGURE 4-15. Structures of lutein and zeaxanthin from sweet corn and spinach [83], proceranone from orange peel oils (*Citrus sinensis*) [85], and two isomers of ethyldimethylpyrazine, 2-ethyl-3,5-dimethylpyrazine, and 2-ethyl-3,6-dimethylpyrazine, as a food-flavoring agent [86].

chromatographic elution, with the advantage of acquiring one- and two-dimensional NMR data for a longer period, as in the stop-flow mode. A loop collector has the advantage of analyzing many chromatographic peaks stored in loops individually without disrupting the chromatography [2,80–82,84,86]. Examples of loop collector applications are the determination of the two isomers of ethyldimethylpyrazine, 2-ethyl-3,5-dimethylpyrazine and 2-ethyl-3,6-dimethylpyrazine, as food-flavoring agents (Figure 4-15) [86].

4.2.7. Polymers

There are few examples in the literature of the use of LC-NMR with polymers, using on-flow LC-NMR as the main mode in their analysis [88–94]. The behavior of the C_{30} bonded interphases has been measured indirectly through the separation of five different isomers of vitamin A acetate at different temperatures by on-flow LC-NMR [88]. At high temperatures the C_{30} polymer chains have higher mobility, making the insertion of different vitamin A isomers into the interphase alkyl chain difficult, restricting the gauche conformations for the C_{30} bonded interphases. Under lower-temperature conditions, the retention times are longer and separation of the different isomers of vitamin A acetate improves, due to the lower mobility of the C_{30} interphase alkyl change, increasing the number of *trans* conformations, which favors contacts between the alkyl chains of the polymer and the different vitamin A acetate isomers. Two chromatographic peaks were separated at 50°C and four at 2°C [88]. On-flow LC-NMR has been applied to poly (ethylene oxide) to determine the chemical structure and degree of polymerization; to oligostyrene to analyze the end group structure, the degree of polymerization, and its tacticity; and to random poly(styrene-*co*-ethyl acrylate) to determine the chemical composition and chemical heterogenecity at a high level of conversion [89]. Silicone analysis has been possible by ^{1}H and ^{29}Si LC-NMR on-flow and stop-flow modes [90,91], including inverse detection experiments of ^{29}Si through the ^{1}H in stop-flow mode [91]. On-flow LC-NMR has been used for the analysis of block copolymers such as PC-*b*-PMMA and P2EHA-*b*-PMA to determine their chemically heterogenecity, composition, and tacticity [92–94].

4.2.8. Metabolomics and Metabonomics

In the last decade, the concept of metabolic profiling in plants, animals, and human beings has opened new areas of interpreting the data acquired by various analytical techniques with the application of chemometrics. Metabolomics and metabonomics are concepts that have emerged from these studies. Metabolomics and metabonomics refer to metabolic profiling of

metabolites in plants, microorganisms, animal and human biofluids, and tissues of organisms. *Metabolomics* is applied mostly to the metabolic profiling of plants, and *metabonomics* is applied more to the analysis of animal and human biofluids and tissues. In the analysis of biofluids, especially for animals and humans in the pharmaceutical world, metabonomics also refers to the changes in metabolic profiling over a period of time. Through analysis of the metabolic composition of biofluids by ^{1}H NMR, pattern recognitions are used with chemoinformatic tools to attempt the interpretation of the data as a toxicological assessment, a genomic approach to evaluate altered gene expression after drug exposure, and to assess health and influence therapies [95,96].

A large portion of the NMR data acquired for metabolomic or metabonomic analysis is not found using hyphenated NMR techniques. The most common experiment is the one-dimensional ^{1}H NMR of biofluid samples with 5 to 10% D_2O to lock in D_2O. There are few cases in the literature where LC- NMR is used in this type of application. On-flow and stop-flow LC-NMR have been used to perform metabolic profiling on plant crude extracts and rapid identification of natural products for dereplication and quality control. To date, metabolomics have been applied to nonhyphenated NMR to classify and characterize different species of medicinal plants for quality control, especially when the active ingredients are unknown [97]. On-flow and stop-flow LC-NMR modes are valuable tools to identify succinyltaurine as a novel endogenous urinary taurine-related metabolite for the metabonomic study of hypertension in rats [98].

4.2.9. Isomers, Tautomers, and Chiral Compounds

The traditional method of analyzing isomers, tautomers, and chiral compounds by NMR is off-line in the NMR tube, but the analysis has been performed under LC-NMR settings in some cases. In the case of positional isomers or regioisomers, LC-NMR has been applied to drug metabolism to assign the correct hydroxylation position on two isomer metabolites in the stop-flow mode (Figure 4-5) [27] to a mixture of three regioisomers combining on-flow LC-NMR with principal component analysis to determine their individual structures [99], and in drug discovery for the characterization of two regioisomer products from the synthesis of 1,5-diarylpyrazoles [100]. Stop-flow LC-NMR has been used to identify *cis* and *trans* isomers of isomerized tretinoin, which is related to retionic acid [101]. Zhou and Hill [102] have applied LC-NMR in the stop-flow mode to study the ketonization kinetics of the keto-enol tautomerization of ethyl butyryl acetate using a cryogenic LC-NMR probe. LC-NMR has been used for determination of the absolute configuration of secondary alcohols coupled to (*R*)- and

(*S*)-9-anthrylmethoxyacetic acid (9-AMA) as 9-AMA esters [103], and to a new tetrahydrophenanthrene through its Mosher ester derivative in stop-flow LC-NMR mode isolated from the aerial parts of the plant *Heliotropium ovalifolium* [104]. Recently, LC-CD (circular dichroism) and LC-NMR have been combined (LC-CD-NMR) for the determination in situ of the absolute configuration of the individual enantiomeric chromatographic peaks of a pyridylananine derivative mixture in the stop-flow mode [105].

4.2.10. Others Areas

LC-NMR has been applied to other type of compounds and areas to explore their capability. Tran et al. [106] have investigated the effects of chromatographic peak broadening when executing in the stop-flow mode in isocratic and gradient elution on each individual peptide of a sample mixture with a different number of amino acids and at different temperatures. The authors observed different behaviors depending on the shape and molecular weight of the peptides in terms of the degradation of the resolution of the chromatographic peaks with subsequent stops and with the length of time acquiring NMR data on each peak during stop-flow. The authors concluded that 30 min of stopping the flow provided a safer margin with less degradation on the chromatography [106]. In the environmental arena, LC-NMR has been used to identify components for on-flow and time-sliced modes in a leachate from an industrial landfill holding industrial toxic and hazardous wastes from different sources [107] and highly polar nitroaromatic compounds for on-flow mode from leachate and groundwater samples obtained from a former TNT-contaminated waste site [108].

4.3. CONCLUSIONS AND FUTURE TRENDS

LC-NMR has provided a combination of separation and structural elucidation analysis of the components of complex mixtures. The application of LC-NMR to natural product extracts; drug metabolites, including the areas of metabolomics and metabonomics; synthetic samples from drug discovery and development processes, including their impurities and degradation products; food components; polymers; and leachates from wasted materials has demonstrated its validity due to the improvements in NMR technology. Those applications have demonstrated the capability of LC-NMR methodology for the analysis of sample mixtures. Therefore, NMR has become a standard tool in many laboratories as a hyphenated technique for the structural elucidation of the components of complex mixtures that may present some problems during isolation or instability. However, LC-NMR has not replaced the option of

isolating the analytes of interest for further NMR studies as the classical option for determining their structures, especially when additional NMR data are necessary to eliminate any ambiguity from simple NMR experiments in the LC-NMR settings. Two-dimensional heteronuclear NMR experiments with ^{13}C in the second dimension are still preferred with isolated materials due to the low natural abundance of ^{13}C, which limits the use of LC-NMR for those cases. The analysis of ^{1}H and ^{19}F nuclei present in organic molecules has been demonstrated successfully by LC-NMR, but off-line analysis of isolated materials is still preferred when ^{13}C NMR data are required. The trend to LC-NMR use is toward the analysis of complex mixtures to obtain information as to their profiles, such as in natural products and drug metabolism, and on the structural analysis of compounds that do not present ambiguity issues, with high natural abundance and sensitive nuclei, mainly for ^{1}H NMR data. Therefore, off-line NMR of isolated materials is applied to small components that are in the limit of detection of LC-NMR, and to compounds with complex molecular structures that require multiple nuclei analysis by NMR to eliminate ambiguity in their analysis.

REFERENCES

[1] J.-L. Wolfender, K. Ndjoko, and K. Hostettmann, The Potential of LC-NMR in Phytochemical Analysis, *Phytochem. Anal.* **12** (2001), 2–22.

[2] K. Albert, *On-Line LC-NMR and Related Techniques*, Wiley, Chichester, England, 2002.

[3] K. Hostettman and A. Marston, Twenty Years of Research into Medicinal Plants: Results and Perspectives, *Phytochem. Rev.* **1** (2002), 275–285.

[4] J.-L. Wolfender, E. F. Queiroz, and K. Hostettmann, Development and Application of LC-NMR Techniques to the Identification of Bioactive Natural Products in S. M. Colegate, R. J. Molyneux (eds.), *Bioactive Natural Products: Detection, Isolation and Structural Determination*, 2nd ed., CRC Press, Boca Raton, FL, 2008, pp. 143–190.

[5] J.-L. Wolfender, S. Rodriguez, and K. Hostettman, Liquid Chromatography Coupled to Mass Spectrometry and Nuclear Magnetic Resonance Spectroscopy for the Screening of Plant Constituents, *J. Chromatogr. A* **794** (1998), 299–316.

[6] T. Renukappa, G. Ross, I. Klaiber, B. Vogler, and W. Kraus, Appliaction of High-Performance Liquid Chromatography Coupled to Nuclear Magnetic Resonance Spectrometry, Mass Spectrometry and Bioassay for the Determination of Active Saponins from *Bacopa monniera* Weetst, *J. Chromatogr. A* **847** (1999), 109–116.

[7] S. Strohschein, C. Rentel, T. Lacker, E. Bayer, and K. Albert, Separation and Identification of Tocotrienol Isomers by HPLC-MS and HPLC-NMR Coupling, *Anal. Chem.* **71** (1999), 1780–1785.

[8] G. Bringmann, M. Rückert, W. Saeb, and V. Mudogo, Characterization of Metabolites in Plant Extracts of *Ancistrocladus likoko* by High-Performance Liquid Chromatography Coupled On-Line with ^{1}H NMR Spectroscopy, *Magn. Reson. Chem.* **37** (1999), 98–102.

[9] G. Bringmann, M. Wohlfarth, H. Rischer, M. Heubes, W. Saeb, S. Diem, M. Herderich, and J. Schlauer, A Photometric Screening Method for Dimeric Naphthylisoquinoline Alkaloids and Complete On-Line Structural Elucidation of a Dimer in Crude Plant Extract, by the LC-MS/LC-NMR/LC-CD Triad, *Anal. Chem.* **73** (2001), 2571–2577.

[10] G. Bringmann, M. Wohlfarth, H. Rischer, M. Heubes, J. Schlauer, and R. Brun, Extract Screening by HPLC Coupled to MS-MS, NMR, and CD: A Dimeric and Three Monomeric Naphtylisoquinoline Alkaloids from *Ancistrocladus griffithii*, *Phytochemistry.* **61** (2002), 195–204.

[11] F.D.P. Andrade, L.C. Santos, M. Datchler, K. Albert, and W. Vilegas, Use of On-Line Liquid Chromatography–Nuclear Magnetic Resonance Spectroscopy for the Rapid Investigation of Flavonoids from *Sorocea bomplandii*, *J. Chromatogr. A* **953** (2002), 287–291.

[12] J.-L. Wolfender, E.F. Queiroz, and K. Hostettmann, Phytochemistry in the Microgram Domain-A LC-NMR Perspective, *Magn. Reson. Chem.* **43** (2005), 697–709.

[13] J. Qu, Y.-H. Wang, J.-B. Li, S.-S. Yu, Y. Li, and Y.-B. Liu, Rapid Structural Determination of New Trace Cassaine-Type Diterpenoid Amides in Fractions from *Erythrophleum fordii* by Liquid Chromatography–Diode-Array Detection/Electrospray Ionization Tandem Mass Spectrometry and Liquid Chromatography/Nuclear Magnetic Resonance, *Rapid Commun. Mass Spectrom.* **21** (2007), 2109–2119.

[14] S.W. Kang, M.C. Kim, C.Y. Kim, S.H. Jung, and B.H. Um, The Rapid Identificaiton of Isoflavonoids from *Belamcanda chinensis* by LC-NMR and LC-MS, *Chem. Pharm. Bull.* **56** (2008), 1452–1454.

[15] S.C. Bobzin, S. Yang, and T.P. Kasten, LC-NMR: A New Tool to Expedite the Dereplication and Identification of Natural Products, *J. Ind. Microbiol. Biotechnol.* **25** (2000), 342–345.

[16] S.C. Bobzin, S. Yang, and T.P. Kasten, Application of Liquid Chromatography–Nuclear Magnetic Resonance Spectroscopy to the Identification of Natural Products, *J. Chromatogr. B* **748** (2000), 259–267.

[17] C.B.L. Abel, J.C. Lindon, D. Noble, B.A.M. Rudd, P.J. Sidebottom, and J.K. Nicholson, Characterization of Metabolites in Intact *Streptomyces citricolor* Culture Supernatants Using High-Pressure Liquid Chromatography–Nuclear Magnetic Resonance Spectroscopy, *Anal. Biochem.* **270** (1999), 220–230.

[18] P. Kleinwächter, K. Martin, I. Groth, and K. Dornberger, Use of Coupled HPLC/^{1}H NMR and HPLC/ESI-MS for the Detection and Identification of (2*E*,4*Z*)-Decadienoic Acid, a New *Agromyces* Species, *J. High Resolut. Chromatogr.* **23** (2000), 609–612.

[19] E.F. Queiroz, J.-L. Wolfender, K.K. Atindehou, D. Traore, and K. Hostettmann, On-Line Identification of the Antifungal Constituents of *Erythrina vogelii* by Liquid Chromatography with Tandem Mass Spectrometry, Ultraviolet Absorbance Detection and Nuclear Magnetic Resonance Spectroscopy Combined with Liquid Chromatographic Micro-Fractionation, *J. Chromatogr. A* **974** (2002), 123–134.

[20] M.W. Sumarah, J.D. Miller, and B.A. Blackwell, Isolation and Metabolite Production by *Penicilium roqueforti, P. paneum* and *P. crustosum* Isolated in Canada, *Mycopathologia* **159** (2005), 571–577.

[21] L. Pharm, J. Vater, W. Rotard, and C. Mügge, Identification of Secondary Metabolites from *Streptomyces violaceoruber* TU22 by Means of On-Flow LC-NMR and LC-DAD-MS, *Magn. Reson. Chem.* **43** (2005), 710–723.

[22] S. Saha, R.M. Smith, E. Lenz, and I.D. Wilson, Analysis of a Ginger Extract by High-Performance Liquid Chromatography Coupled to Nuclear Magnetic Resonance Spectroscopy Using Superheated Deuterium Oxide as the Mobile Phase, *J. Chromatogr. A* **991** (2003), 143–150.

[23] P. Chen, C. Li, S. Liang, G. Song, Y. Sun, Y. Shi, S. Xu, J. Zhang, S. Sheng, Y. Yang, and M. Li, Characterization and Quantification of Eight Water-Soluble Constituents in Tuber of *Pinellia ternate* and in Tea Granules from the Chinese Multiherb Remedy Xiaochaihu-Tang, *J. Chromatogr. B* **843** (2006), 183–193.

[24] J.C. Lindon, J.K. Nicholson, and I.D. Wilson, Direct Coupling of Chromatographic Separations to NMR Spectroscopy, *Prog. NMR Spectrosc.* **29** (1996), 1–49.

[25] J.C. Lindon, J.K. Nicholson, U.G. Sidelmann, and I.D. Wilson, Direct Coupled HPLC-NMR and Its Application to Drug Metabolism, *Drug Metab. Rev.* **29** (1997), 705–746.

[26] A. Lienau, T. Glaser, M. Krucker, D. Zeeb, F. Ley, F. Curro, and K. Albert, Qualitative and Quantitative Analysis of Tocopherol in Toothpastes and Gingival Tissue Employing HPLC NMR and HPLC MS Coupling, *Anal. Chem.* **74** (2002), 5192–5198.

[27] T. Murai, H. Iwabuchi, and T. Ikeda, Identification of Gemfibrozil Metabolites, Produced as Positional Isomers in Human Liver Microsomes, by On-Line Analyses Using Liquid Chromatography/Mass Spectrometry and Liquid Chromatography/Nuclear Magnetic Resonance Spectroscopy, *J. Mass Spectrom. Soc. Jpn.* **52** (2004), 277–283.

[28] M. Tugnait, E.M. Lenz, M. Hofmann, M. Spraul, I.D. Wilson, J.C. Lindon, and J.K. Nicholson, The Metabolism of 2-Trifluoromethylaniline and Its Acetanilide in the Rat by ^{19}F NMR Monitored Enzyme Hydrolysis and ^{1}H/^{19}F HPLC-NMR Spectroscopy, *J. Pharm. Biomed. Anal.* **30** (2003), 1561–1574.

[29] A.E. Mutlib, J.T. Strupczewski, and S.M. Chesson, Application of Hyphenated LC/NMR and LC/MS Techniques in Rapid Identification of *In Vitro* and *In Vivo* Metabolites of Iloperidine, *Drug Metab. Dispos*. **23** (1995), 951–964.

[30] J.P. Shockcor, I.S. Silver, R.M. Wurm, P.N. Sanderson, R.D. Farrant, B.C. Sweatman, and J.C. Lindon, Characterization of In Vitro Metabolites from Human Liver Microsomes Using Directly Coupled HPLC-NMR: Application to a Phenoxanthiin Monoamine Oxidase-A Inibitor, *Xenobiotica* **26** (1996), 41–48.

[31] N. Feng, Z. Zhang, D. An, W. Huang, G. Wang, X. Han, and X. Bao, Investigation of the Metabolism of 7-(4-Chlorobenzyl)-7,8,13,13a-tetrahydroberberine Chloride in the Rat, *Eur. J. Drug Metab. Pharmacokinet.* **23** (1998), 41–44.

[32] W.J. Ehlhardt, J.M. Woodland, T.M. Baughman, M. Vandenbranden, S.A. Wrighton, J.A. Kroin, B.H. Norman, and S.R. Maple, Liquid Chromatography/Nuclear Magnetic Resonance Spectroscopy and Liquid Chromatography/Mass Spectrometry Identification of Novel Metabolites of the Multidrug Resistance Modulator LY335979 in Rat Bile and Human Liver Microsomal Incubations, *Drug Metab. Dispos.* **26** (1998), 42–51.

[33] G.J. Dear, R.S. Plumb, B.C. Sweatman, P.S. Parry, A.D. Roberts, J.C. Lindon, J.K. Nicholson, and I.M. Ismail, Use of Directly Coupled Ion-Exchange Liquid Chromatography–Mass Spectrometry and Liquid Chromatography–Nuclear Magnetic Resonance Spectroscopy as a Strategy for Polar Metabolites, *J. Chromatogr. B* **748** (2000) 295–309.

[34] K.E. Zhang, B. Hee, C.A. Lee, B. Liang, and B.C.M. Potts, Liquid Chromatography–Mass Spectrometry and Liquid Chromatography–NMR Characterization of In Vitro Metabolites of a Potent and Irreversible Peptidomimetic Inhibitor of Rhinovirus 3C Protease, *Drug Metab. Dispos.* **29** (2001), 729–734.

[35] R. Singh, I.-W. Chen, L. Jin, M.V. Silva, B.H. Arison, J.H. Lin, and B.K. Wong, Pharmacokinetics and Metabolism of a *Ras* Farnesyl Transferase Inhibitor in Rats and Dogs: In Vitro–In Vivo Correlation, *Drug Metab. Dispos.* **29** (2001), 1578–1587.

[36] M.B. Fisher, D. Jackson, A. Kaerner, S.A. Wrighton, and A.G. Borel, Characterization by Liquid Chromatography–Nuclear Magnetic Resonance Spectroscopy and Liquid Chromatography–Mass of Two Coupled Oxidative–Conjugative Metabolic Pathways for 7-Ethoxycoumarin in Human Liver Microsomes Treated with Alamethicin, *Drug Metab. Dispos.* **30** (2002), 270–275.

[37] M.V. Silva Elipe, S.-E.W. Huskey, and B. Zhu, Application of LC-NMR for the Study of the Volatile Metabolite of MK-0869, a Substance P Receptor Antagonist, *J. Pharm. Biomed. Anal.* **30** (2003) 1431–1440.

[38] K.-Y. Sohda, T. Minematsu, T. Hashimoto, K.-I. Suzumura, M. Funatsu, K. Suzuki, H. Imai, and H. Kamimura, Application of LC-NMR for Characterization of Rat Urinary Metabolites of Zonampanle Monohydrate (YM872), *Chem. Pharm. Bull.* **52** (2004), 1322–1325.

[39] C. Tang, R. Subramanian, Y. Kuo, S. Krymgold, P. Lu, S.D. Kuduk, C. Ng, D.-M. Feng, C. Elmore, E. Soli, J. Ho, M.G. Bock, T.A. Baillie, and T. Prueksaritanont, Bioactivation of 2,3-Diaminopyridine-Containing Bradykinin B_1

Receptor Antagonist: Irreversible Binding to Liver Microsomal Proteins and Formation of Glutathione Conjugates, *Chem. Res. Toxicol.* **18** (2005), 934–945.

[40] G.J. Dear, I.M. Ismail, P.J. Mutch, R.S. Plumb, L.H. Davies, and B.C. Sweatman, Urinary Metabolites of a Novel Quinoxaline Non-nucleoside Reverse Transcriptase Inhibitor in Rabbit, Mouse and Human: Identification of Fluorine NIH Shift Metabolites Using NMR and Tandem MS, *Xenobiotica* **4** (2000), 407–426.

[41] O. Cloarec, A. Campbell, L.-H. Tseng, U. Braumann, M. Spraud, G. Scarfe, R. Weaver, and J.K. Nicholson, Virtual Chromatography Resolution Enhancement in Cryoflow LC-NMR Experiments via Statistical Total Correlation Spectroscopy, *Anal. Chem.* **79** (2007), 3304–3311.

[42] U.G. Sidelmann, C. Gavaghan, H.A.J. Carless, R.D. Farran, J.C. Lindon, I.D. Wilson, and J.K. Nicholson, Identification of the Positional Isomers of 2-Fluorobenzoic Acid 1-*O*-Acyl Glucuronide by Directly Coupled HPLC-NMR, *Anal. Chem.* **67** (1995), 3401–3404.

[43] U.G. Sidelmann, C. Gavaghan, H.A.J. Carless, M. Spraul, M. Hofmann, J.C. Lindon, I.D. Wilson, and J.K. Nicholson, 750-MHz Directly Coupled HPLC-NMR: Application to the Sequential Characterization of the Positional Isomers of 2-, 3-, and 4-Fluorobenzoic Acid Glucuronides in Equilibrium Mixtures, *Anal. Chem.* **67** (1995), 4441–4445.

[44] E.M. Lenz, D. Greatbanks, I.D. Wilson, M. Spraul, M. Hofmann, J. Troke, J.C. Lindon, and J.K. Nicholson, Direct Characterization of Drug Glucuronide Isomers in Human Urine by HPLC-NMR Spectroscopy: Application to the Positional Isomers of 6,11-Dihydro-11-oxodibenz[*b,e*]oxepin-2-acetic Acid Glucuronide, *Anal. Chem.* **68** (1996), 2832–2837.

[45] U.G. Sidelmann, A.W. Nicholls, P.E. Meadows, J.W. Gilbert, J.C. Lindon, I.D. Wilson, and J.K. Nicholson, High-Performance Liquid Chromatography Directly Coupled to ^{19}F and ^{1}H NMR for the Analysis of Mixtures of Isomeric Ester Glucuronide Conjugates of Trifluoromethylbenzoic Acids, *J. Chromatogr. A* **728** (1996), 377–385.

[46] R. Rühl, R. Thiel, T.S. Lacker, S. Stroshchein, K. Albert, and H. Nau, Synthesis, High-Performance Liquid Chromatography–Nuclear Magnetic Resonance Characterization and Pharmacokinetics in Mice of CD271 Glucuronide, *J. Chromatogr. B* **757** (2001) 101–109.

[47] O. Corcoran, R.W. Mortensen, S.H. Hansen, J. Troke, and J.K. Nicholson, HPLC/^{1}H NMR Spectroscopic Studies of the Reactive α-1-*O*-Acyl Isomer Formed During Acyl Migration of *S*-Naproxen β-1-*O*-Acyl Glucuronide, *Chem. Res. Toxicol.* **14** (2001), 1363–1370.

[48] R.W. Mortensen, O. Corcoran, C. Cornett, U.G. Sidelmann, J. Troke, J.C. Lindon, J.K. Nicholson, and S.H. Hansen, LC-^{1}H NMR Used for Determination of the Elution Order of *S*-Naproxen Glucuronide Isomers in Two Isocratic Reversed-Phase LC-Systems, *J. Pharm. Biomed. Anal.* **24** (2001), 477–485.

[49] R.W. Mortensen, O. Corcoran, C. Cornett, U.G. Sidelmann, J.C. Lindon, J.K. Nicholson, and S.H. Hansen, *S*-Naproxen-β-1-*O*-Acyl Glucuronide Degradation Kinetic Studies by Stopped-Flow High-Performance Liquid Chromatography–^{1}H NMR and High-Performance Liquid Chromatography–UV, *Drug Metab. Dispos.* **29** (2001), 375–380.

[50] S.X. Peng, Hyphenated HPLC-NMR and Its Applications in Drug Discovery, *Biomed. Chromatogr.* **14** (2000), 430–441.

[51] B. Shapira, A. Karton, D. Aronzon, and L. Frydman, Real-Time 2D NMR Identification of Analytes Undergoing Continuous Chromatography Separation, *J. Am. Chem. Soc.* **126** (2004), 1262–1265.

[52] J.C. Lindon, J.K. Nicholson, and I.D. Wilson, Directly Coupled HPLC-NMR and HPLC-NMR-MS in Pharmaceutical Research and Development, *J. Chromatogr. B* **748** (2000), 233–258.

[53] P.A. Keifer, Flow Techniques in NMR Spectroscopy, *Annu. Rep. NMR Spectrosc.* **62** (2007) 1–47.

[54] F. Qiu and D.L. Norwood, Identification of Pharmaceutical Impurities, *J. Liq. Chromatogr. Relat. Technol.* **30** (2007), 877–935.

[55] J.K. Roberts and R.J. Smith, Use of Liquid Chromatography–Nuclear Magnetic Resonance Spectroscopy for the Identification of Impurities in Drug Substances, *J. Chromatogr. A* **677** (1994), 385–389.

[56] E.A. Crowe, J.K. Roberts, and R.J. Smith, ^{1}H and ^{19}F LC/NMR: Application to the Identification of Impurities in Compounds of Pharmaceutical Interest, *Pharm. Sci.* **1** (1995), 103–105.

[57] N. Mistry, I.M. Ismail, M.S. Smith, J.K. Nicholson, and J.C. Lindon, Characterization of Impurities in Bulk Drug Batches of Fluticasone Propionate Using Directly Coupled HPLC-NMR Spectroscopy and HPLC-MS, *J. Pharm. Biomed. Anal.* **16** (1997), 697–705.

[58] S.D. McCrossen, D.K. Bryant, B.R. Cook, and J.J. Richards, Comparison of LC Detection Methods in the Investigation of Non-UV Detectable Organic Impurities in a Drug Substance, *J. Pharm. Biomed. Anal.* **17** (1998), 455–471.

[59] B.C.M. Potts, K.F. Albizati, M.O. Johnson, and J.P. James, Application of LC-NMR to the Identification of Bulk Drug Impurities in GART Inhibitor AG2034, *Magn. Reson. Chem.* **37** (1999), 393–400.

[60] G.J. Sharma and I.C. Jones, Critical Investigation of Coupled Liquid Chromatography–NMR Spectroscopy in Pharmaceutical Impurity Identification, *Magn. Reson. Chem.* **41** (2003), 448–454.

[61] K.M. Alsante, P. Boutros, M.A. Couturier, R.C. Friedmann, J.W. Harwood, G.J. Horan, A.J. Jensen, Q. Liu, L.L. Lohr, R. Morris, J.W. Raggon, G.L. Reid, D.P. Santafianos, T.R. Sharp, J.L. Tucker, and G.E. Wilcox, Pharmaceutical Impurity Identification: A Case Study Using a Multidisciplinary Approach, *J. Pharm. Sci.* **93** (2004), 2296–2309.

[62] P. Novak, M. Cindrić, P. Tepeš, S. Dragojević, M. Ilijaš, and K. Mihaljević, Identification of Impurities in Acarbose by Using an Integrated Liquid

Chromatography–Nuclear Magnetic Resonance and Liquid Chromatography–Mass Spectrometry Approach, *J. Sep. Sci.* **28** (2005), 1442–1447.

[63] P. Novak, P. Tepeš, M. Ilijaš, I. Fistrić, I. Bratŏs, A. Avdagić, Z. Hameršak, V.G. Marković, and M. Dumić, LC-NMR and LC-MS Identification of an Impurity in a Novel Antifungal Drug Icofungipen, *J. Biomed. Pharm. Anal.* **50** (2009), 68–72.

[64] S. Provera, G. Guercio, L. Turco, O. Curcuruto, G. Alvaro, T. Rossi, and C. Marchioro, Application of LC-NMR to the Identification of Bulk Drug Impurities in NK1 Antagonist GW597599 (Vestipitant), *Magn. Reson. Chem.* **48** (2010), 523–530.

[65] ICH, Harmonised Tripartite Guideline Q1A(R2), Stability Testing of New Drug Substances and Products, *Proceedings of the International Conference on Harmonisation (ICH)*, EMEA, London, 2003 (available at http://www.ich.org).

[66] S.X. Peng, B. Borah, R.L.M. Dobson, Y.D. Liu, and S. Pikul, Application of LC-NMR and LC-MS to the Identification of Degradation Products of a Protease Inhibitor in Dosage Formulations, *J. Pharm. Biomed. Anal.* **20** (1999), 75–89.

[67] W. Feng, H. Liu, G. Chen, R. Malchow, F. Bennett, E. Lin, B. Pramanik, and T.-M. Chan, Structural Characterization of the Agent SCH 54592 by LC-NMR and LC-MS, *J. Pharm. Biomed. Anal.* **25** (2001), 545–557.

[68] N. Wu, W. Feng, E. Lin, G. Chen, J. Patel, T.-M. Chan, and B. Pramanik, Quantitative and Structural Determination and Its Related Compounds in Pharmaceutical Preparations Using High-Performance Liquid Chromatography, *J. Pharm. Biomed. Anal.* **30** (2002), 1143–1155.

[69] J.-L. Wolfender, L. Verotta, L. Belvisi, N. Fuzzati, and K. Hostettmann, Structural Investigations of Isomeric Oxidised Forms of Hyperforin by HPLC-NMR and HPLC-$MS^{n,}$ *Phytochem. Anal.* **14** (2003), 290–297.

[70] P. Novak, P. Tepeš, M. Cindrić, M. Ilijaš, S. Dragojević, and K. Mihaljević, Combined Use of Liquid Chromatography–Nuclear Magnetic Resonance Spectroscopy and Liquid Chromatography–Mass Spectrometry for the Characterization of an Acarbose Degradation Product, *J. Chromatogr. A* **1033** (2004), 299–303.

[71] N. Fukutsu, T. Kawasaki, K. Saito, and H. Nakazawa, Application of High-Performance Liquid Chromatography Hyphenated Techniques for Identification of Degradation Products of Cefpodoxime Proxetil, *J. Chromatogr. A* **1129** (2006), 153–159.

[72] L. Wu, T.Y. Hong, and G.G. Vogt, Structural Analysis of Photo-Degradation in Thiazole-Containing Compounds by LC-MS/MS and NMR, *J. Pharm. Biomed. Anal.* **44** (2007), 763–772.

[73] T. Murakami, N. Fukutsu, J. Kondo, T. Kawasaki, and F. Kusu, Application of Liquid Chromatography–Two-Dimensional Nuclear Magnetic Resonance Spectroscopy Using Pre-concentration Column Trapping and Liquid Chromatography–Mass Spectrometry for the Identification of Degradation Products in Stressed Commercial Amlodipine Maleate Tablets, *J. Chromatogr. A* **1181** (2008), 67–76.

[74] T. Murakami, H. Konno, N. Fukutsu, M. Onodera, T. Kawasaki, and F. Kusu, Identification of a Degradation Product in Stressed Tablets of Olmesatan Medoxomil by the Complementary Use of HPLC Hyphenated Techniques, *J. Pharm. Biomed. Anal.* **47** (2008), 553–559.

[75] R.V. Dev, G.S.U. Kiran, B.V. Subbaiah, B.S. Babu, J.M. Babu, P.K. Dubey, and K. Vyas, Identification of Degradation Products in Stressed Tablets of Rabeprazole Sodium by HPLC-Hyphenated Techniques, *Magn. Reson. Chem.* **47** (2009), 443–448.

[76] Y. Kawaguchi-Murakami, N. Fukutsu, T. Kajiro, T. Araki, T. Murakami, T. Kawasaki, N. Kishi, and M. Konno, A Prediction System of Oxidation Reaction as a Solid-State Stress Condition: Applied to a Pyrrole-Containing Pharmaceutical Compound, *J. Pharm. Biomed. Anal.* **50** (2009) 328–335.

[77] F.G. Vogt, L. Wu, M.A. Olsen, and W.M. Clark, A Spectroscopic and Computational Study of an Electrocyclized Photo-degradation Product of 6-(2-(5-Chloro-2-(2,4-difluorobenyzloxy)phenyl)cyclopent-1-enyl)picolinic Acid, *J. Mol. Struct.* **984** (2010), 246–261.

[78] R.P. Shah, A. Sahu, and S. Singh, Identification and Characterization of Degradation Products of Irbesartan Using LC-MS/TOF, $MS^{n,}$ On-Line H/D Exchange and LC-NMR, *J. Pharm. Biomed. Anal.* **51** (2010), 1037–1046.

[79] R.P. Shah and S. Singh, Identification and Characterization of a Photolytic Degradation Product of Telmisartan Using LC-MS/TOF, LC-$MS^{n,}$ LC-NMR and On-Line H/D Exchange Mass Studies, *J. Pharm. Biomed. Anal.* **53** (2010), 755–761.

[80] I.F. Duarte, I. Delgadillo, M. Spraul, E. Humpfer, and A.M. Gil, An NMR Study of the Biochemistry of Mango: The Effects of Ripening, Processing and Microbial Growth, *Magn. Reson. Food Sci.* **262** (2001), 259–266.

[81] I.F. Duarte, M. Spraul, M. Godejohann, U. Braumann, and A. M. Gil, Application of NMR and Hyphenated NMR Spectroscopy for the Study of Beer Components, *Magn. Reson. Food Sci.* **286** (2002), 151–157.

[82] A.M. Gil, I.F. Duarte, M. Godejohann, U. Braumann, M. Maraschin, and M. Spraul, Characterization of the Aromatic Composition of Some Liquid Food by Nuclear Magnetic Resonance Spectroscopy and Liquid Chromatography with Nuclear Magnetic Resonance and Mass Spectrometric Detection, *Anal. Chim. Acta* **488** (2003), 35–51.

[83] R. Aman, J. Biehl, R. Carle, J. Conrad, U. Beifuss, and A. Schieber, Application of HPLC Coupled with DAD, APCI-MS and NMR to the Analysis of Lutein and Zeaxanthin Stereoisomers in Thermally Processed Vegetables, *Food Chem.* **92** (2005), 753–763.

[84] I.F. Duarte, B.J. Goodfellow, A.M. Gil, and I. Delgadillo, Characterization of Mango Juice by High-Resolution NMR, Hyphenated NMR, and Diffusion-Ordered Spectroscopy, *Spectrosc. Lett.* **38** (2005), 319–342.

[85] B. Weber, B. Hartmann, D. Stöckigt, K. Schreiber, M. Roloff, H.-J. Bertram, and C.O. Schmidt, Liquid Chromatography/Mass Spectrometry and Liquid

Chromatography/Nuclear Magnetic Resonance as Complementary Analytical Techniques for Unambiguous Identification of Polymethoxylated Flavones in Residues from Molecular Distillation of Orange Peel Oils (*Citrus sinensis*), *J. Agric. Food Chem.* **54** (2006), 274–278.

[86] N. Sugimoto, C. Yomota, N. Furusho, K. Sato, T. Yamazaki, and K. Tanamoto, Application of Liquid Chromatography–Nuclear Magnetic Resonance Spectroscopy for the Identification of Ethyldimethylpyrazine, a Food Flavouring Agent, *Food Addit. Contam. A* **23** (2006), 1253–1259.

[87] C. Tode, T. Maoka, and M. Sugiura, Application of LC-NMR to Analysis of Carotenoids in Foods, *J. Sep. Sci.* **32** (2009), 3659–3663.

[88] M. Pursch, S. Strohschein, H. Händel, and K. Albert, Temperature-Dependent Behaviour of C_{30} Interphases: A Solid-State NMR and LC-NMR Study, *Anal. Chem.* **68** (1996), 386–393.

[89] W. Hiller and H. Pasch, On-Line HPLC-NMR of Polymers, in H.N. Cheng and A.D. English (eds.), *NMR Spectroscopy of Polymers in Solution and in the Solid State*, American Chemical Society, Washington, DC, 2003, pp. 338–343.

[90] V. Blechta, J. Sỳkora, J. Hetflejš, S. Šabata, and J. Schraml, ^{29}Si NMR in LC-NMR Analysis of Silicones, *Magn. Reson. Chem.* **44** (2006), 7–10.

[91] V. Blechta, M. Kurfürst, J. Sỳkora, J. Hetflejš, and J. Schraml, High-Performance Liquid Chromatography with Nuclear Magnetic Resonance Detection Applied to Organosilicon Polymers: 2. Comparison with Other Methods, *J. Chromatogr. A* **1145** (2007), 175–182.

[92] W. Hiller, P. Sinha, and H. Pasch, On-Line HPLC-NMR of PS-*b*-PMMA and Blends of PS and PMMA: LCCC-NMR at Critical Conditions of PS, *Macromol. Chem. Phys.* **208** (2007), 1966–1978.

[93] W. Hiller, P. Sinha, and H. Pasch, On-Line HPLC-NMR of PS-*b*-PMMA and Blends of PS and PMMA: 2. LCCC-NMR at Critical Conditions of PMMA, *Macromol. Chem. Phys.* **210** (2009), 605–613.

[94] J.-A. Raust, L. Houillot, M. Save, B. Charleux, C. Moire, C. Farcet, and H. Pasch, Two Dimensional Chromatographic Characterization of Block Copolymers of 2-Ethylhexyl Acrylate and Methyl Acrylate, P2EHA-*b*-PMA, Produced Via RAFT-Mediate Polymeriation in Organic Dispersion, *Macromolecules* **43** (2010), 8755–8765.

[95] J.C. Lindon, J.K. Nicholson, E. Holmes, and J.R. Everett, Metabonomics: Metabolic Processes Studied by NMR Spectroscopy of Biofluids, *Concepts Magn. Reson.* **12** (2000), 289–320.

[96] F. Dieterle, B. Riefke, G. Scholtterbeck, A. Ross, H. Senn, and A. Amber, NMR and MS Methods for Metabonomics, in J.-C. Gautier (ed.), *Drug Safety Evaluation: Methods and Protocols* (Methods in Molecular Biology), Springer-Verlag, New York, 2011, Vol. **691**, pp. 385–415.

[97] J.-L. Wolfender, G. Marti, and E.F. Queiroz, Advances in Techniques for Profiling Crude Extracts and for the Rapid Identification of Natural Products: Dereplication, Quality Control and Metabolomics, *Curr. Org. Chem.* **14** (2010), 1808–1832.

[98] K. Akira, H. Mitome, M. Imichi, Y. Shida, H. Miyaoka, and T. Hashimoto, LC-NMR Identification of a Novel Taurine-Related Metabolite Observed in ^{1}H NMR-Based Metabonomics of Genetically Hypertensive Rats, *J. Pharm. Biomed. Anal.* **51** (2010), 1091–1096.

[99] C.Y. Airiau, H. Shen, and R.G. Brereton, Principal Component Analysis in Liquid Chromatogrpahy Proton Nuclear Magnetic Resonance: Differentiation of Three Regio-Isomers, *Anal. Chim. Acta* **447** (2001), 199–210.

[100] S.K. Singh, M. Srinivasa, S. Shivaramakrishna, D. Kavitha, R. Vasudev, J.M. Babu, A. Sivalakshmidevi, and Y.K. Rao, Modified Reaction Conditions to Achieve High Regioselectivity in the Two Component Synthesis of 1,5-Diarylpyrazoles, *Tetrahedron Lett*. **45** (2004), 7679–7682.

[101] S. Strohschein, G. Scholotterbeck, J. Richter, M. Pursch, L.-H. Tseng, H. Händel, and K. Albert, Comparison of the Separation of *cis*/*trans* Isomers of Tretinoin with Different Stationary Phases by Liquid Chromatography–Nuclear Magnetic Resonance Coupling, *J. Chromatogr. A* **765** (1997), 207–214.

[102] C.C. Zhou and D.R. Hill, The Keto–Enol Tautomerization of Ethyl Butyryl Acetate Studied by LC-NMR, *Magn. Reson. Chem.* **45** (2007), 128–132.

[103] J.M. Seco, L.-H. Tseng, M. Godejohann, E. Quiñoa, and R. Riguera, Simultaneous Enantioresolution and Assignment of Absolute Configuration of Secondary Alcohols by Directly Coupled HPLC-NMR of 9-AMA Esters, *Tetrahedon Asymmetry* **13** (2002), 2149–2153.

[104] D. Guilet, A. Guntern, J.-R. Loset, E.F. Queiroz, K. Ndjoko, C.M. Foggin, and K. Hostettmann, Absolute Configuration of a Tetrahydrophenenthrene from *Heliotropium ovalifolium* by LC-NMR of Its Mosher Esters, *J. Nat. Prod.* **66** (2003), 17–20.

[105] T. Tokunaga, M. Okamoto, K. Tanaka, C. Tode, and M. Sugiura, Chiral Liquid Chromatography–Circular Dichroism–NMR for Estimating Separation Conditions of Chiral HPLC Without Authentic Samples, *Anal. Chem.* **82** (2010), 4293–4297.

[106] B.Q. Tran, E. Lundanes, and T. Greibrokk, The Influence of Stop-Flow on Band Broadening of Peptides in Micro-Liquid Chromatography, *Chromatographia* **64** (2006), 1–5.

[107] E. Benfenati, P. Pierucci, R. Fanelli, A. Preiss, M. Godejohann, M. Astratov, K. Levsen, and D. Barceló, Comparative Studies of the Leachate of an Industrial Landfill by Gas Chromatography–Mass Spectrometry, Liquid Chromatography–Nuclear Magnetic Resonance and Liquid Chromatography–Mass Spectrometry, *J. Chromatogr. A* **831** (1999), 245–256.

[108] A. Preiss, M. Elend, S. Gerling, E. Berger-Preiss, and K. Steinbach, Indentification of Highly Polar Nitroaromatic Compounds in Leachate and Ground Water Samples from TNT-Contaminated Waste Site by LC-MS, LC-NMR, and Off-Line NMR and MS Investigations, *Anal. Bioanal. Chem.* **389** (2007), 1979–1988.

5

Applications of LC-MS-NMR

5.1. INTRODUCTION

Development of the combination of HPLC as a major analytical separation technique with structural elucidation techniques such as MS as LC-MS and NMR as LC-NMR has provided a niche in the structural analysis of complex mixtures. As indicated in Chapter 4, LC-NMR has been demonstrated to be an important tool in many areas in academia and industry and has become a routine instrument in many laboratories. However, due to the different requirements on sensitivity in MS and NMR, the sample load in the chromatography is not in the same concentration range for LC-MS and LC-NMR. This issue creates ambiguity as to the assurance of providing accurate information on MS and NMR for the same chromatographic peak when LC-MS and LC-NMR are run separately. Further developments on these hyphenated techniques have brought together a combination of LC-MS and LC-NMR (LC-MS-NMR or LC-NMR-MS) as one technique that overcomes the issue of uncertainty in obtaining MS and NMR data from each component of complex mixtures when analyzed separately using LC-MS and LC-NMR. As mentioned in Chapter 3, a splitter after the HPLC provides different sample loads to the MS and the NMR in the same chromatographic run. LC-MS-NMR does not require that additional designs in the NMR technology, such as

LC-NMR and Other Hyphenated NMR Techniques: Overview and Applications, First Edition. Maria Victoria Silva Elipe.

special NMR flow cells, probes, and experiments, be executed. The main consideration is the use of deuterated solvents for the MS analysis, which provides deuterated molecular ions when exchangeable protons are present. The option of having an additional pump to exchange back to protons for the compounds of interest in the sample mixture before the sample enters the MS has provided another aspect of the analysis, as explained in Chapter 3. Those developments have made LC-MS-NMR a handy methodology for the analysis of complex sample mixtures. LC-MS-NMR has become a standard tool in many laboratories as a hyphenated technique to approach the structural determination of compounds in mixtures that may present problems during isolation or instability and eliminates the ambiguity of different chromatographies when MS and NMR are performed separately. In this chapter we provide an overview of applications of LC-MS-NMR in a variety of fields as well as examples to demonstrate the applicability and extensive use of this hyphenated technique.

5.2. APPLICATIONS OF LC-MS-NMR

LC-MS-NMR has been applied to the field of structural elucidation of organic compounds in many areas, including natural products, drug metabolism, drug discovery and development, including combinatorial chemistry and impurity profiling, and metabolomics and metabonomics. The diversity in the use of LC-MS-NMR has positioned it as another optional technique employed in academic and industrial laboratories, particularly in the pharmaceutical area. Below we discuss briefly cases in which LC-MS-NMR was applied successfully in these areas.

5.2.1. Natural Products

LC-MS-NMR is used in the field of natural products chemistry primarily to examine crude extracts and to determine the structures of unknowns in sample mixtures. Screening is used to examine crude extracts to determine rapidly the presence of known and unknown components for further investigation of their structures, which is an important application in the dereplication analysis of natural products. The on-flow mode of operation used for screening in the LC-MS-NMR methodology provides a rapid analysis of complex mixtures for the recognition of major known components. Stop-flow triggered by MS provides another option for analyzing chromatographic peaks by NMR which it may not be possible to trigger by UV, due to the lack of chromophores and for peaks of interest with a particular molecular ion or fragment ion [1–5].

LC-MS-NMR is not often used in the field of natural products, but the few examples found in the literature maximize the potential of LC-MS-NMR when performing on-flow and stop-flow assays triggered by MS [6,7]. Sandvoss et al. [6] performed rapid screening on the starfish *Asterias rubens* by LC-MS-NMR after applying matrix solid-phase dispersion extraction (MSPD) to facilitate the identification of unknowns in the presence of known compounds. The authors performed stop-flow triggered by MS in an LC-MS-NMR system successfully to further analyze the structure of the main components of the chromatographic peaks of interest, including acquiring two-dimensional WETTOCSY data for their analysis [6]. In a similar fashion, Fritsche at al. [7] used LC-MS-NMR and CD to analyze the structures of two secoisolariciresinol diglucosides (SDGs) (Figure 5-1): [*2R,2′R*]-2,3-bis[(4-hydroxy-3-methoxyphenyl)methyl]-1,4-butanediyl-bis-β-glucuropyranoside and [*2R,2′S*]-2,3-bis[(4-hydroxy-3-methoxyphenyl) methyl]-1,4-butanediyl-bis-β-glucuropyranoside, extracted from flaxseed. Recently, LC-MS-NMR has been applied—not directly to crude extracts [6,8–10]—but to fractions of crude extracts previously fractionated through MSPD [6]. Following this trend, LC-MS-NMR has been applied to solid-phase extraction fractions of an extract from the cyanobacterium *Fischerella ambigua*, dried and reconstituted in small volume, for automatic injection in a capillary NMR flow cell [8]. In addition, LC-MS-NMR has been used as an incomplete separation strategy applied to plant crude extracts combined with NMR and LC-MS (NMR/LC-MS) in parallel dynamic spectroscopy or NMR/LC-MS PDS [9], and to other plant extracts [10].

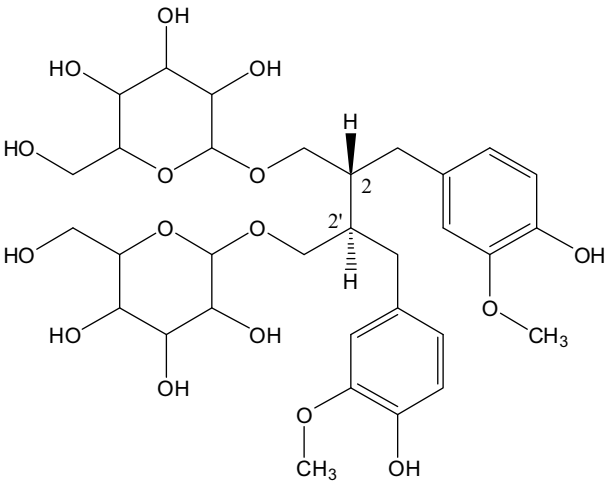

FIGURE 5-1. Structure of secoisolariciresinol diglucoside extracted from flaxseed [7].

5.2.2. Drug Metabolism

During the last decade, LC-MS-NMR has been employed in the field of drug metabolism as an extension of the successful use of LC-NMR (see Section 4.2.2). Obtaining both MS and NMR information on metabolites from the same chromatogram presents advantages over performing LC-MS and LC-NMR separately. When carried out separately, sample loading in the column requires overloading in the LC-NMR system, due to the lower sensitivity of NMR than that of an LC-MS system. Retention time shifting and chromatographic peak broadening are common effects of column overloading when running LC-MS and LC-NMR chromatographies separately. This problem is overcome when the two instrumentations are combined into one technique, LC-MS-NMR, for identification of the correct chromatographic peak by MS and NMR, which is critical in determining structural information on metabolites and other analytes. LC-MS-NMR has the same limitations as LC-NMR in obtaining two-dimensional heteronuclear NMR data. Therefore, isolation of metabolites is still pursued where the complexity of a structure requires more detailed information from ^{1}H and ^{13}C chemical shift data through inverse detection NMR experiments (e.g., HSQC, HMBC). These two-dimensional heteronuclear NMR experiments are more complex when carried out using hyphenated techniques because of limited amounts of metabolite concentration and the need for solvent suppression. Another consideration is the deuteration of molecular ions detected by MS when considering the typical chromatographic run in LC-MS-NMR using deuterated solvents. The problem is solved by attaching another pump before the MS to reverse-exchange deuteriums for protons. Similar to LC-NMR, common modes of operation for LC-MS-NMR analysis of metabolites are on-flow, stop-flow, and loop collection. On-flow gives an overview of the major metabolites present in a sample mixture. Stop-flow makes it possible to obtain data from major and minor metabolites that are above the threshold of detection and to run two-dimensional NMR experiments if a sufficient amount of analyte is inside the flow cell. However, MS data cannot possibly be acquired in this mode, but MS can be used to trigger the stop-flow mode. Finally, loop collection provides another mode of separating metabolites into capillary loops for later NMR analysis and of using MS to trigger the storage of chromatographic peaks in loops if they do not have UV chromophores [1,3,4].

On-flow and stop-flow are the most common methodologies in LC-MS-NMR analysis [11–20]. However, other modes, such as loop collector [21] and column trapping [22], are also used. The most common configuration of the system is to place NMR and MS in parallel in the settings [3,4,11–13,15–22]. However, Dear at al. [14] used serial configuration, having the sample travel from the HPLC to the NMR and ending in the MS before going to the

waste area. The flow going to the NMR was split into a 1 : 12 ratio when entering the electrospray interface of the MS at 50 μL/min [14]. To provide a sufficient sample for MS and NMR analysis due to the different sensitivities of the techniques, the flow rate from the HPLC is split. Even though a splitting ratio of 95 : 5 [11,13,15,17–21] for the flow rate entering the NMR and MS, respectively, is the most commonly used, researchers also use other ratios in their systems, such as 50 : 1 [12], 12 : 1 [14], and 20 : 1 [16,22]. In the drug metabolism world, electrospray in either a positive or a negative mode is the most common source of ionization for MS analysis [11–16,18–22]. Occasionally, other sources, such as atmospheric pressure ionization (API), are employed [17]. H/D back-exchange is another alternative mode used with MS data to eliminate the ambiguity of having partial deuterated/protonated (H/D) molecular or fragment ions [12,14]. A pump is equipped with a T-connection to create a flow with protonated solvents to back-exchange the deuteriums in the solvent system coming from the LC-NMR portion of the system [12,14]. Drug candidates with fluorine in their structures are excellent candidates for alternative use of radiolabeling metabolism studies. Fluorine (^{19}F) occurs in 100% abundance in nature, with a relative sensitivity of 0.83 related to ^{1}H, and considering that fluorinated drugs will have a few fluorine atoms in the molecule, makes ^{19}F NMR a suitable method for pharmacokinetics studies in drug metabolism or PKDM studies [11,13,15,16]. On-flow ^{19}F NMR as part of an LC-MS-NMR system helps to determine more easily the number of metabolites with ^{19}F, their ^{19}F chemical shifts, and their retention times, due to the simplicity of the data [11,13,15,16]. Overall, the combination of LC-MS and LC-NMR (LC-MS-NMR; frequently termed LC-NMR-MS) can provide detailed structural information on particular metabolites of interest. The two metabolites for the HIV-I reverse transcriptase inhibitor BW935U83, its glucuronide conjugate and 3-fluororibolactone analyzed by ^{1}H and ^{19}F NMR in an LC-MS-NMR system (Figure 5-2), are examples of detailed structure information [16]. In addition, LC-MS-NMR can give overall information on the metabolic fate of drugs such as paracetamol or acetaminophen (Figure 5-3) [12].

5.2.3. Drug Discovery and Development

LC-MS-NMR has been employed in two major drug discovery and development areas: combinatorial chemistry and impurity profiling [1,3,23]. Combinatorial libraries are an essential tool in the drug discovery process, with LC-MS as the traditional analytical technique for the analysis of complex mixtures in an automated mode. With the development of NMR probes, including cryogenic probes, that perform better solvent suppression with more

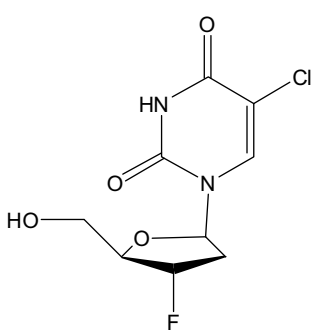

BW935U83

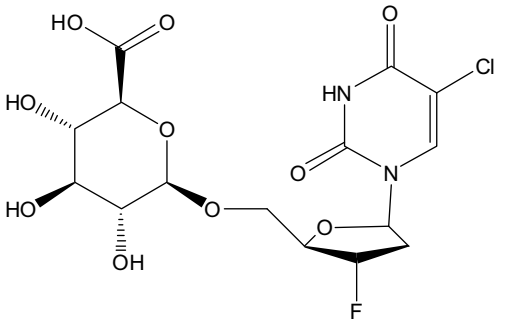

BW935U83 glucuronide conjugate

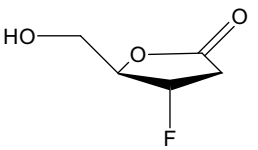

3-fluororibolactone

FIGURE 5-2. Structures of BW935U83 or 5-chloro-1-(2′-3′-dideoxy-3′-fluoro-*erythro*-pentofuranosyl) uracil, its glucuronide conjugate, and 3-fluororibolactone [16].

sensitivity and better electronics, LC-NMR has become another tool for combinatorial chemistry. LC-NMR-MS combines both analytical tools that can provide structural information on combinatorial chemistry samples simultaneously without the ambiguity of having separate chromatographic runs with different column loads, due to the different sensitivities of MS and NMR. However, few peer-reviewed articles are published on this particular application of LC-MS-NMR [3,23–26]. Holt et al. [24] demonstrated the power of LC-MS-NMR as an analytical technique, obtaining UV, NMR, and MS data from individual components of a complex mixture of peptides from a single LC run. Impurity profiling is another area for which LC-MS-NMR has potential [3,27,28]. However, the examples in the literature of which this author is aware are hypothetical cases used to demonstrate the validity and utility of the hyphenated technique.

5.2.4. Metabolomics and Metabonomics

In metabonomics, fingerprinting analysis of biofluids is essential for the reproducibility of results. Sample preparation has to be simple to maximize the advantages of high throughput and fast analysis. Commonly, non-hyphenated analytical techniques such as MS and NMR are used for metabonomic analysis. HPLC introduces more variables, due to the need

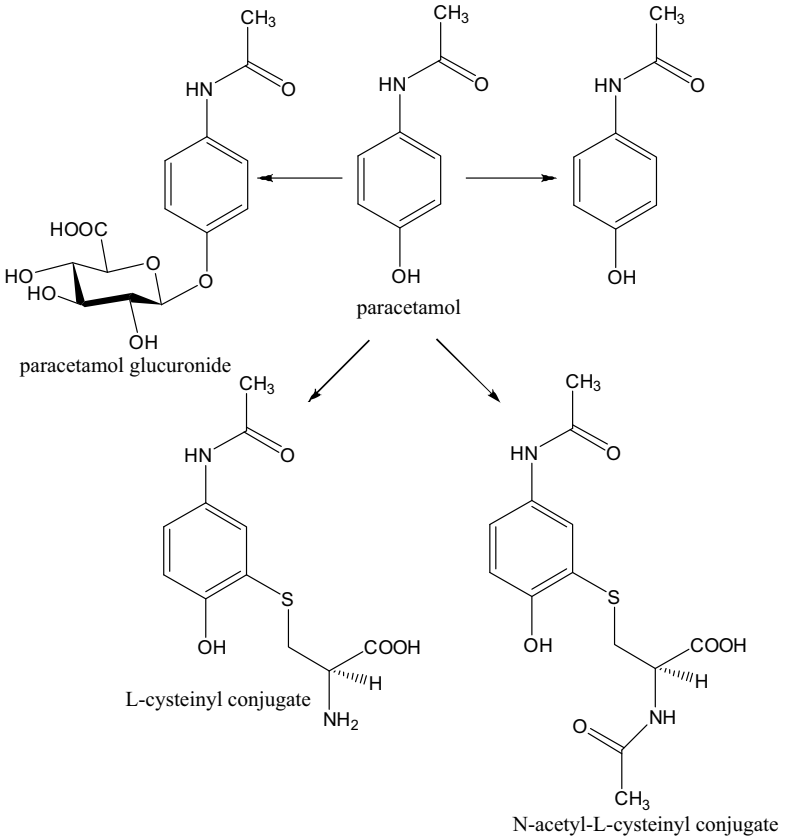

FIGURE 5-3. Structures of metabolites from the metabolic fate of paracetamol or acetaminophen [12].

for specific sample preparation, depending on the matrix or origin of the sample and the type of column used for the analysis. These variables may increase the complexity in the area of reproducibility of the analysis. Pham-Tuan et al. [29] developed an HPLC method using a short monolithic column with a rapid gradient and a high flow rate to perform rapid, detailed profiling of a large number of urine samples. This method was converted to a slow shallow gradient, high-resolution method to identify the chromatographic peaks of interest using LC-MS-NMR [29]. In metabolomics, LC-MS and NMR used separately and in parallel have become the common techniques for fingerprinting metabolic profiles to analyze the individual small molecule components of interest from organisms or biological systems. However, when both techniques are online as LC-MS-NMR, it becomes easier to correlate MS and NMR data with each chromatographic peak of the sample mixture [30]. The settings of LC-MS-NMR are not straightforward. As a consequence, hyphenated LC-MS-NMR is not commonly used in

laboratories, even though it is commercially available [30]. Overall, metabolic profiling for metabolomics or metabonomics analysis requires the measurement of biological systems to identify modifications of their physiological, pathophysiological, and developmental stimuli. These modifications come from responses outside their fingerprints on their expected endogenous metabolic profiles from biological samples such as urine, serum, or biological tissue extracts. Because of the complexity of injecting biological samples with complex matrices directly to the LC-MS-NMR, the common approach to gathering MS and NMR data separately is to use LC-MS and NMR separately [31,32]. In addition, metabolic profiling has a

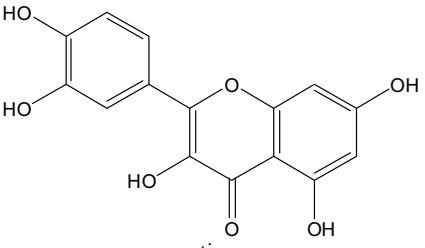

quercetin

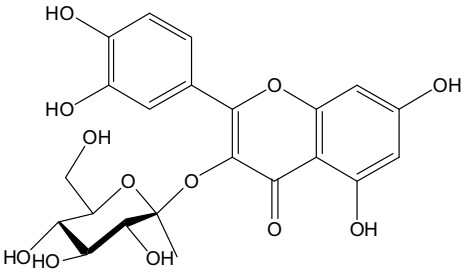

quercetin-3-β-D-glucopyranoside

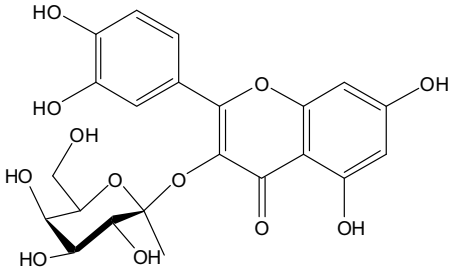

quercetin-3-β-D-galactopyranoside

FIGURE 5-4. Structures of quercetin, quercetin-3-β-D-glucopyranoside, and quercetin-3-β-D-galactopyranoside from apple extract [33].

potential to highlight biomarkers, toxicity, and pathology mechanisms for preclinical and drug development processes, which prompts for the need of better accuracy and synchronization of the data coming from MS and NMR. This approach may favor a combination of LC-MS and NMR (LC-MS-NMR), which is not used routinely for this type of analysis [31,32].

5.2.5. Others Areas

Based on the literature available, LC-MS-NMR has not been applied as extensively to other areas as has LC-NMR. A couple of research studies have been carried out in the food analysis area. Spraul et al. [33] used LC-MS-NMR to investigate the components of an apple peel extract using a 20 : 1 splitting ratio for flow into the NMR and MS, respectively, using an ion trap with electrospray as the ionization source. Quercetin, quercetin-3-β-D-glucopyranoside, and quercetin-3-β- D-galactopyranoside were clearly identified from the apple extract using MS and NMR (Figure 5-4) [33]. Gil et al. [34] used LC-MS-NMR to analyze the aromatic composition of beer from a commercial ale, grape juice from the pulp and seed of red grapes, and phenolic wine extract from red wine. The system used a 95 : 5 splitter to divide the flow going into the NMR and MS, respectively. The ionization source for the MS instrument was electrospray in the positive and negative modes. UV and MS triggered the loop collection of chromatographic peaks of interest for further analysis. Three modes were used to operate the LC-MS-NMR system: on-flow, time-sliced, and loop collection. MS data were acquired only in the on-flow mode and during analysis of the peaks coming from the loop collector. The time-sliced mode was not appropriate for obtaining MS data because of the stoppage of flow during NMR acquisition [34].

5.3. CONCLUSIONS AND FUTURE TRENDS

LC-MS-NMR has not been applied as extensively as LC-NMR for the structural elucidation analysis of components of complex mixtures. Natural products and drug metabolism are the principal areas of its application. Few applications have been extended to drug discovery, metabonomics/metabolomics, and food analysis. One of the possible reasons for fewer applications to other areas is the complexity of having two analytical techniques with different requirements connected to the HPLC. Some of those requirements are sensitivity, flow rate, solvent composition, the need of deuterated solvents for the NMR, and their complexity for the MS. Another indication is the cost of the instruments needed for an LC-MS-NMR system. When several techniques are required, the preferred method for the analysis of complex mixtures is isolation. Isolation facilitates the acquisition of two-dimensional

heteronuclear NMR data, such as the $^{1}H–^{13}C$ HMBC type, and MS data from different instruments and sources that are not compatible with NMR and its requirements. The coming years will provide more information on how LC-MS-NMR can be used for the structural elucidation of components from complex mixtures.

REFERENCES

[1] K. Albert, *On-Line LC-NMR and Related Techniques*, Wiley, Chichester, England, 2002.

[2] M.V. Silva Elipe, Advantages and Disadvantages of Nuclear Magnetic Resonance Spectroscopy as Hyphenated Technique, *Anal. Chim. Acta* **497** (2003) 1–25.

[3] J.C. Lindon, J.K. Nicholson, and I.D. Wilson, Directly Coupled HPLC-NMR and HPLC-NMR-MS in Pharmaceutical Research and Development, *J. Chromatogr. B* **780** (2000) 233–258.

[4] Z. Yang, Online Hyphenated Liquid Chromatography–Nuclear Magnetic Resonance Spectroscopy–Mass Spectrometry for Drug Metabolite and Nature Product Analysis, *J. Pharm. Biomed. Anal.* **40** (2006), 516–527.

[5] S. Urban and F. Separovic, Development in Hyphenated Spectroscopic Methods in Natural Product Profiling, *Fron. Drug Des. Discov.* **1** (2005), 113–166.

[6] M. Sandvoss, A. Weltring, A. Preiss, K. Levsen, and G. Wuensch, Combination of Matrix Solid-Phase Dispersion Extraction and Direct On-Line Liquid Chromatography–Nuclear Magnetic Resonance Spectroscopy–Tandem Mass Spectrometry as a New Efficient Approach for the Rapid Screening of Natural Products: Application to the Total Asterosaponin Fraction of the Starfish *Asterias rubens*, *J. Chromatogr. A* **917** (2001), 75–86.

[7] J. Fritsche, R. Angoelal, and M. Dachtler, On-Line Liquid Chromatography–Nuclear Magnetic Resonance–Mass Spectrometry Coupling for the Separation and Characterization of Secoisolariciresinol Diglucoside Isomers in Flaxseed, *J. Chromatogr. A* **972** (2002), 195–203.

[8] Y. Lin, S. Schiavo, J. Orjala, P. Vouros, and R. Kautz, Microscale LC-MS-NMR Platform Applied to the Identification of Active Cyanobacterial Metabolites, *Anal. Chem.* **80** (2008), 8045–8054.

[9] D. Dai, J. He, R. Sun, R. Zhang, H.A. Aisa, and Z. Abliz, Nuclear Magnetic Resonance and Liquid Chromatography–Mass Spectrometry Combined with an Incompleted Separation Strategy for Identifying the Natural Products in Crude Extract, *Anal. Chim. Acta* **632** (2009), 221–228.

[10] E.F. Queiroz, J.-L. Woldender, and K. Hostettmann, Modern Approaches in the Search for New Lead Antiparasitic Compounds from Higher Plants, *Curr. Drug Targets* **10** (2009), 202–211.

[11] G.B. Scarfe, I.D. Wilson, M. Spraul, M. Hofmann, U. Brauman, J.C. Lindon, and J.K. Nicholson, Application of Directly Coupled High-Performance Liquid Chromatography–Nuclear Resonance–Mass Spectrometry to the Detection and Characterisation of the Metabolites of 2-Bromo-4-trifluoromethylaniline in Rat Urine, *Anal. Commun.* **34** (1997), 37–39.

[12] K.I. Burton, J.R. Everett, M.J. Newman, F.S. Pullen, D.S. Richards, and A.G. Swanson, On-Line Chromatography Coupled with High Field NMR and Mass Spectrometry (LC-NMR-MS): A New Technique for Drug Metabolite Structure Elucidation, *J. Pharm. Biomed. Anal.* **15** (1997), 1903–1912.

[13] G.B. Scarfe, B. Wright, E. Clayton, S. Taylor, I.D. Wilson, J.C. Lindon, and J.K. Nicholson, ^{19}F-NMR and Directly Coupled HPLC-NMR-MS Investigations into the Metabolism of 2-Bromo-4-trifluoromethylaniline in Rat: A Urinary Excretion Balance Study Without the Use of Radiolabeling, *Xenobiotica* **28** (1998), 373–388.

[14] G.J. Dear, J. Ayrton, R. Plumb, B.C. Sweatman, I.M. Ismail, I.J. Fraser, and P.J. Mutch, A Rapid and Efficient Approach to Metabolite Identification Using Nuclear Magnetic Resonance Spectroscopy, Liquid Chromatography/Mass Spectrometry and Liquid Chromatography/Nuclear Magnetic Resonance Spectroscopy/Sequential Mass Spectrometry, *Rapid Commun. Mass Spectrom.* **12** (1998), 2023–2030.

[15] G.B. Scarfe, B. Wright, E. Clayton, S. Taylor, I.D. Wilson, J.C. Lindon, and J.K. Nicholson, Quantitative Studies on the Urinary Metabolic Fate of 2-Chloro-4-trifluoromethylaniline in the Rat Using ^{19}F-NMR Spectroscopy and Directly Coupled HPLC-NMR-MS, *Xenobiotica* **29** (1999), 77–91.

[16] J.P. Shockcor, S.E. Unger, P. Savina, J.K. Nicholson, and J.C. Lindon, Application of Directly Coupled LC-NMR-MS to the Structural Elucidation of Metabolites of the HIV-1 Reverse-Transcriptase Inhibitor BW935U83, *J. Chromatogr. B* **748** (2000), 269–279.

[17] G.J. Dear, R.S. Plumb, B.C. Sweatman, J. Ayrton, J.C. Lindon, J.K. Nicholson, and I.M. Ismail, Mass Directed Peak Selection, An Efficient Method of Drug Metabolite Identification Using Directly Coupled Liquid Chromatography–Mass Spectrometry–Nuclear Magnetic Resonance Spectroscopy, *J. Chromatogr. B* **748** (2000), 281–293.

[18] G.B. Scarfe, J.K. Nicholson, J.C. Lindon, I.D. Wilson, S. Taylor, E. Clayton, and B. Wright, Identification of the Urinary Metabolites of 4-Bromoaniline and 4-Bromo-[*carbonyl*-^{13}C]-acetanilide in Rat, *Xenobiotica* **32** (2002), 325–337.

[19] M. Spraul, A.S. Freud, R.E. Nast, R.S. Withers, W.E. Maas, and O. Corcoran, Advancing NMR Sensitivity for LC-NMR-MS Using a Cryoflow Probe: Application to the Analysis of Acetaminophen Metabolites in Urine, *Anal. Chem.* **75** (2003), 1546–1551.

[20] S. Bajad, M. Coumar, R. Khajuria, O.P. Suri, and K.L. Bedi, Characterization of a New Rat Urinary Metabolite of Piperine by LC/NMR/MS Studies, *Eur. J. Pharm. Sci.* **19** (2003), 413–421.

[21] L.F. Duarte, C. Legido-Quigley, D.A. Parker, J.R. Swann, M. Spraul, U. Braumann, A.M. Gil, E. Holmes, J.K. Nicholson, G.M. Murphy, H. Vilca-Melendez, N. Heaton, and J.C. Lindon, Identification of Metabolites in Human Hepatic Bile Using 800 MHz ^{1}H NMR Spectroscopy, HPLC-NMR/MS and UPLC-MS, *Mol. BioSyst.* **5** (2009), 180–190.

[22] D. Bao, V. Thanabal, and W.F. Pool, Determination of Tacrine Metabolites in Microsomal Incubate by High Performance Liquid Chromatography–Nuclear Magnetic Resonance/Mass Spectrometry with a Column Trapping System, *J. Pharm. Biomed. Anal.* **28** (2002), 23–30.

[23] M.-H. Wann, Application of LC-NMR in Pharmaceutical Analysis, *Sep. Sci. Technol.* **6** (2005), 569–579.

[24] R.M. Holt, M.J. Newman, F.S. Pullen, D.S. Richard, and A.G. Swanson, High-Performance Liquid Chromatography/NMR Spectrometry/Mass Spectrometry: Further Advances in Hyphenated Technology, *J. Mass Spectrom.* **32** (1997), 64–70.

[25] O. Corcoran and M. Spraul, LC-NMR-MS in Drug Discovery, *Drug Discov. Rev.* **8** (2003), 624–631.

[26] P.A. Keifer, Flow NMR Applications in Combinatorial Chemistry, *Curr. Opin. Chem. Biol.* **7** (2003), 388–394.

[27] K. Mohanraj, Impurity Profiling of Active Pharmaceutical Ingredients, *Chem. Ind. Dig.* (2009), 89–95.

[28] K. Pilaniya, H.K. Chandrawanshi, U. Pilaniya, P. Manchandani, P. Jain, and N. Singh, Recent Trends in the Impurity Profile of Pharmaceuticals, *J. Adv. Pharm. Tech. Res.* **1** (2010), 302–310.

[29] H. Pham-Tuan, L. Kaskavelis, C.A. Daykin, and H.-G. Janssen, Method Development in High-Performance Liquid Chromatography for High-Throughput Profiling and Metabolomic Studies of Biofluid Samples, *J. Chromatogr. B* **789** (2003), 283–301.

[30] S. Moco, R.J. Bino, R.C.H. De Vos, and J. Vervoort, Metabolomics Technologies and Metabolite Identification, *Trends Anal. Chem.* **26** (2007), 855–866.

[31] C.J. Clarke and J.N. Haselden, Metabolic Profiling as a Tool for Understanding Mechanism of Toxicity, *Toxicol. Pathol.* **36** (2008), 140–147.

[32] F. Dieterle, B. Riefke, G. Scholotterbeck, A. Ross, H. Senn, and A. Amberg, NMR and MS Methods for Metabonomics, in J.C. Gautier (ed.), *Drug Safety Evaluation: Methods and Protocols* (Methods in Molecular Biology), Springer-Verlag, New York, 2011, Vol. 691, pp. 385–415.

[33] M. Spraul, U. Braumann, M. Godejohann, and M. Hofmann, Hyphenated Method in NMR, *Magn. Reson. Food Sci.* **262** (2001), 54–66.

[34] A.M. Gil, I.F. Duarte, M. Godejohann, U. Braumann, M. Maraschin, and M. Spraul, Characterization of the Aromatic Composition of Some Liquid Foods by Nuclear Magnetic Resonance Spectrometry and Liquid Chromatography with Nuclear Magnetic Resonance and Mass Spectrometric Detection. *Anal. Chim. Acta* **488** (2003), 35–51.

6

Hyphenation of NMR with Other Analytical Separation Techniques

6.1. INTRODUCTION

HPLC is a very effective separation analytical technique used widely in hyphenated form—LC-MS, LC-NMR, and LC-MS-NMR—as seen in Chapters 3, 4 and 5. However, not all types of separation analysis can use HPLC. Other separation analytical techniques are commonly used. Examples of these techniques are gas chromatography (GC), gel permeation chromatography (GPC), size-exclusion chromatography (SEC), supercritical fluid chromatography (SFC), supercritical fluid extraction (SFE), capillary electrophoresis (CE), capillary electrochromatography (CEC), capillary zone electrophoresis (CZE), capillary isotachophoresis (cITP), capillary HPLC (capLC), and solid-phase extraction (SPE). These techniques have been hyphenated with NMR: GC-NMR, GPC-NMR, SEC-NMR, SFC-NMR, SFE-NMR, CE-NMR, CEC-NMR, CZE-NMR, cITP-NMR, capLC-NMR, and SPE-NMR. In addition, SPE has been hyphenated with MS and NMR: SPE-MS-NMR. In This chapter we give an overview of applications of these hyphenated analytical techniques with NMR in a variety of fields.

LC-NMR and Other Hyphenated NMR Techniques: Overview and Applications, First Edition. Maria Victoria Silva Elipe.

6.2. GC-NMR

Early in the 1960s, a combination of gas chromatography (GC) and NMR was established by collecting a sample coming from a GC instrument into an NMR glass microtube through a 17-gauge syringe with a large needle [1]. The top of the needle was connected to a Luer lock with a $\frac{1}{4}$-inch T-connector, which was attached to the GC instrument. After the fraction of interest was trapped in the tube, the nut to the T-connector was removed to disconnect the tube from the GC instrument, and the needle was disconnected from the Luer lock. Next, the solvent was added to fill the bubble at the end of the tube for NMR analysis [1]. In the 1970s there were similar attempts to combine GC and NMR, by trapping the fraction of interest from the GC instrument in more sophisticated NMR tubes considered as flow cells and placing them in the NMR instrument for analysis [2,3]. Neither of these procedures are what we consider today a hyphenated GC-NMR technique. The first hyphenated GC-NMR instrument came in 1981 from Buddrus and Hertzog [4]. It was demonstrated by converting the NMR tube into a flow cell with both sides opened, with the coil around the tube placed inside the magnet of the NMR instrument and one end of the open NMR tube connected to the GC instrument and the other end to waste [4]. A mixture of diethyl ether, 2,2-dimethyl butane, and cyclopentane was injected into the GC column for separation. The system worked only as on-flow mode by flowing at 5.2 mL/min and acquiring NMR data while the individual fractions were passing through the flow cell. Due to the settings, an external lock was needed. Because the NMR tube was not spinning, the data showed lower resolution than when regular settings were used while spinning the NMR tube in a field of 100 MHz for ^{1}H [4]. With the improvement in NMR technology, the hyphenation of GC and NMR has followed a development similar to that in regular LC-NMR. Currently, the NMR flow cell consists of a custom-made solenoildal microcoil around a fused-silica capillary tube inside an NMR magnet that is connected to a GC instrument through capillary tubing [5,6]. NMR experiments are performed as the on-flow and stop-flow modes of the gas phase of the sample [5,6]. GC-NMR is not available commercially; it is still in the development stage to be used in the analysis of complex mixtures in academia and industry. The coming years may show potential uses for this technique and more robust instrumentation if there is enough demand to solve structural problems of gases that require NMR structural determination.

6.3. GPC-NMR

Online or on-flow gel permeation chromatography (GPC) with NMR as GPC-NMR methodology has been applied extensively to the analysis of the molecular weight and structure of polymers in complex mixtures [7–17].

Hatada et al. [7–12,14] investigated poly(methyl methacrylate) (PMMA) and poly(butyl methacrylate) copolymers prepared with t-C_4H_9MgBr in toluene by on-flow GPC-NMR to determine their molecular weight and polymer size by calculating the average number of monomers based on the ratio of the areas of the end terminal monomer unit with a signal from the polymer by ^1H NMR. In addition to PMMA, other polymers, such as polystyrene, poly(butyl acrylate) (pBA), and polybutadiene mixtures have been analyzed successfully using GPC-NMR [13,15–17]. An important contribution of GPC-NMR analysis is the molecular weight dependence of tacticity, because it contributes to an understanding of the mechanism of steroregulation in polymerization. The major drawbacks for GPC-NMR are the low sensitivity of NMR compared to that of other analytical techniques, the relatively short T_1 for polymers, and the need to acquire sufficient scans to obtain a reasonable signal-to-noise ratio. However, a significant advantage is the short duration of the analysis, which takes around 60 min for 1 mg of sample. Van Gorkom and Hancewicz [13] have carried out multivariate curve resolution on GPC-NMR data to analyze the correlation of the molecular weight and the chemical information for severely overlapped chromatographic peaks during the elution, which also show overlapping in the spectroscopic data. Hiller et al. [17] developed an online setup for on-flow and stop-flow GPC-NMR experiments on olefin homopolymers and copolymers as well as polyolefin blends at temperatures up to 130°C to separate and determine their sizes and compositions. GPC-NMR is not available commercially at the time of this writing. Therefore, the coming years will determine if there is enough demand for this technique to become commercialized.

6.4. SEC-NMR

Online or on-flow size-exclusion chromatography (SEC) with NMR as SEC-NMR methodology has been employed widely in the analysis of molecular weight distribution and the structure of polymers in complex mixtures [18–24]. Knowledge of the molecular weight distribution and chemical composition of the polymers in the sample mixture provide information on the polarization mechanism and facilitate our understanding of the relationship of the polymer structure and its material properties. Online SEC-NMR is an efficient method to determine the tacticity of the molar mass dependence of comonomer composition in a polymer sample. Ute et al. [18] applied SEC-NMR to determine the molecular weight distribution of poly(methyl methacrylate) (PMMA) quantitatively. The authors measured the ratio of the intensity signals for the end terminal proton signal (α-CH_3) and other signal internal to the polymer (t-C_4H_9) by ^1H NMR in a 750-MHz SEC-NMR

system with a 9.2-fold gain in sensitivity (signal-to-noise ratio) compared to a 500-MHz SEC-NMR instrument [18]. In a similar fashion, Ute et al. [19] have performed the same study at 750 MHz on ethylene-propylene-(2-ethylidene-5-norbomene) terpolymers (EPDM) using the on-flow and stop-flow modes. Other polymers studied using SEC-NMR are poly[styrene-*co*-(ethyl acrylate)]s [20], the copolymer obtained from copolymerization of *t*-butyl acrylate and ethyl methacrylate with *t*-butyllithium/bis(2,6-di-*t*-butylphenoxy)methylaluminum [21], uniform isotactic and syndiotactic poly(methyl methacrylate)s (*it*- and *st*-PMMA, respectively) [22], the polymer microstructure of polysaccharides alginates [23], and the molar mass of PS-*b*-PMMA block copolymer [24]. Off-line SEC-NMR is still preferred to on-flow or online SEC-NMR for the analysis of copolymers, but more examples are published in peer-reviewed journals, demonstrating the capabilities of online SEC-NMR for these studies. SEC-NMR is not available commercially at the time of this writing. Therefore, the coming years will determine if there is enough demand for this technique to become commercialized.

6.5. SFC-NMR

The hyphenation of supercritical fluid chromatography (SFC) with NMR (SFC-NMR) has an inherent advantage compared to the common LC-NMR hyphenated analytical technique. The fact that it does not need solvent suppression is a major advantage because the common solvent of the SFC system is CO_2, a "proton-free" solvent that does not interfere with measurements in ^{1}H NMR. Special NMR flow cells are needed to handle the high pressure of the SFC system. In the late 1980s, Allen et al. [25] carried out hyphenated SFC-NMR by fabricating a home-built NMR flow cell that handled variable temperature up to 100°C and pressures of about 3500 psi to observe ^{1}H and ^{14}N to identify the components of a fuel model sample to explore the capabilities of SFC-NMR. In the 1990s, new NMR flow probes were developed, one with a double wall containing deuteroacetonitrile for external ^{2}H lock [26] and the other one without that wall because shimming may be compromised when it interferes with the internal deuterium signal of the sample [27]. Since then, a variety of applications have been developed [26–35]. Analysis of plastifiers by 1D ^{1}H NMR in the on-flow mode [26] and of the components of coffee extract and black pepper extract in the on-flow and stop-flow modes including two-dimensional COSY45 [27] was performed on those designed probes. SFC-NMR has also been applied to the separation and structural analysis of monomeric acrylates [28–30], hydrocarbons [30], and separation and identification of the *cis*/*trans* isomers

of vitamin A by on-flow methodology [30,31]. SFC-NMR has been applied to obtain on-flow data for the NMR analysis of ethylbenzene as a testing compound and of a mixture of dibutyl and diallyl phthalate for the use of immobilized free radicals as the packing material of the column of the SFC-NMR system [32,33]. In both cases the column was inside the probe and near the NMR flow cell [32,33]. In addition, SFC-NMR has been used in food analysis for the decomposition of lipids targeting triglycerides from 40 commercial margarine products [34]. SFC-NMR is still underutilized for broader applications because it is not yet a common hyphenated analytical technique. SFC-NMR is not available commercially at the time of this writing. The coming years will determine if there is enough demand for this technique to be commercialized.

6.6. SFE-NMR

The hyphenation of supercritical fluid extraction (SFE) with NMR (SFE-NMR) is ideal for monitoring ^{1}H NMR supercritical fluid extraction processes with CO_2 as the eluent of the extraction. Spectra can be recorded in the on-flow and stop-flow modes, as in SFC-NMR, and as in SFC-NMR, solvent suppression is not needed for SFE-NMR, which is a major advantage compared to conventional LC-NMR but with the main difference of using a flow cell that can handle the SFE high-pressure system as in SFC-NMR [27,29,30,33,36]. Few applications have been carried out using SFE-NMR. Examples of applications are the analysis of the components of coffee extract and black pepper extract in the on-flow and stop-flow modes with the acquisition of two-dimensional COSY45 [27,29,30,33,36], and plastifiers from poly(vinyl chloride) (PVC) [33]. SFE-NMR is not available commercially at the time of this book writing. Again, the coming years will determine if there is enough demand for this technique to be commercialized.

6.7. CE-NMR

The low sensitivity of NMR, even when hyphenated with HPLC (LC-NMR), has encouraged the development of other options to increase its limited sensitivity. Even with the improvements in electronics and computer technologies, NMR is still a low-sensitive analytical technique. One way to improve the sensitivity is by reducing the volume of the sample from the microliter to the nanoliter range for NMR flow cell volume. Wu et al. [37]

coupled capillary electrophoresis (CE) with NMR (CE-NMR) by building a fused-silica capillary NMR flow cell with an RF microcoil directly around the cell that generated a detection volume for the flow cell of 5 to 200 nL in approximately 1 mm of length. The detection limit was below 50 ng for amino acids, with an acquisition time of 1 min. These types of cells are appropriate for capillary electrophoresis separation coupled to NMR (CE-NMR) [37]. However, the residence time for the chromatographic peaks from CE in the NMR flow cell is around 5 to 10 s, constraining the length of the NMR acquisition time and limiting its sensitivity [37]. Stop-flow experiments on CE-NMR were achieved by applying the voltage for 15 s, stopping the chromatography for 60 s, and acquiring NMR data during that time [38]. The process was repeated for each chromatographic peak, to avoid degradation in the chromatography that would potentially affect the NMR data for late-eluting peaks if the peaks broaden [38]. Schweitz et al. [39] acquired two-dimensional TOCSY under stop-flow conditions for around 100 ng of adenosine dinucleotide. Sweedler's group [40,41] developed a new methodology to obtain NMR data from the stop-flow mode of several chromatographic peaks without degrading the chromatography through stopping the flow in each chromatographic peak of interest. The new methodology consists of splitting the capillary after separation into several outlets, each directed to a different NMR detection coil in stop-flow. The group demonstrated the methodology with a mixture of two amines [40,41]. To improve the distortion of the NMR lines in CE-NMR, Li et al. [42] applied deconvolution by estimating the broadening function from a reference signal and using a gradient descent method that shows substantial improvement in the quality of the spectra. Another improvement from Sweedler's group [43] is the development of a cyclic NMR with two coils in two close loops where each loop has a coil for NMR detection. In this system, one analyte is directed to one coil and stopped in the respective NMR coil. The rest of the chromatogram is deviated to the second loop and its separation detected in the second NMR coil [43]. The researchers demonstrated the methodology by separating a mixture of three amino acids (Ala, Val, and Thr) in two cycles. During the time Ala was parked in one loop, a COSY spectrum was acquired on the corresponding coil, while the other two amino acids were separated in the other loop and detected in the coil of the second loop [43]. The idea is to build a system with multiple closed loops with a coil per loop for NMR detection, providing a cyclic CE-NMR methodology. However, more optimization is needed to achieve that possibility [43]. CE-NMR is an emerging technique that offers a large number of possible applications to analyze the structure of compounds in the micro- and nanogram range, although an important limitation is the lack of commercially available CE-NMR instrumentation [35].

6.8. CEC-NMR

Capillary electrochromatography (CEC) is an analytical separation technique that combines the high speed and efficiency of capillary electrophoresis with HPLC to separate charged analytes in small volumes. An electric field is directed into the capillary column of the CEC. If the material packing in the column is for reversed-phase separation, charged analytes are retained by the hydrophobic interaction with the stationary phase and by the electrophoretic mobility in the mobile phase. Electroosmotic flow (EOF) and pressure (pressurized electrochromatography) are the two options that govern the mobile phase in CEC. EOF is independent of the particle size of the packing material of the column, which facilitates the use of long columns packed with small-particle-size materials for better separation. In addition, CEC provides high separation efficiency similar to capillary electrophoresis in increasing the number of theoretical plates by a factor of 2 or 3 compared to overpressure-driven capillary HPLC. Those improvements explain why EOF offers twofold advantages over conventional pump systems and has been tested by hyphenating it with NMR [42,44–49]. CEC-NMR has been tested in the drug metabolism arena by on-flow and stop-flow modes to obtain one-dimensional ^{1}H NMR and two-dimensional ^{1}H–^{1}H TOCSY data on paracetamol metabolites from human urine [44,45]. Gfrörer et al. [47] analyzed two solutions as sample mixtures, a solution of the analgesic Tromapyrin, which contains acetaminophen (or paracetamol), caffeine and acetylsalicylic acid, and a mixture of caffeine and aspartame using isocratic and gradient elution modes. The authors tested the system in the on-flow mode for both sample mixtures and in the stop-flow mode acquiring two-dimensional ^{1}H–^{1}H TOCSY on aspartame [47]. Gfrörer et al. [48] modified CEC-NMR by applying an electric field to the separation column and not to the entire system to shorten the chromatographic run at different pressures as pressured CEC-NMR (pCEC-NMR). The separation of four unsaturated fatty acid methyl esters—palmitoleic, oleic, eicosenoic, and erucic acid methyl esters—was tested and went from 110 min with capillary HPLC-NMR to 13 min with pCEC-NMR, reducing the chromatographic separation 8.5-fold [48,49]. In addition to on-flow experiments on a mixture of fatty acid esters, the authors performed in the stop-flow mode to acquire a two-dimensional ^{1}H–^{1}H COSY spectrum on palmitoleic acid methyl ester to test the system [48,49]. CEC-NMR or pCEC-NMR is a promising hyphenated analytical technique that offers potential applications in many fields for the analysis of small quantities of analytes in a complex mixture, but a commercial system is not currently available. The coming years may provide more insights on for what applications this technique is most suitable and if possible instruments may become commercially available.

6.9. CZE-NMR

Capillary zone electrophoresis (CZE) is another analytical separation technique that achieves fast and efficient separation of charged analytes. The hyphenation of CZE with NMR (CZE-NMR) requires that the microcoil be mounted directly to the capillary to improve the filling factor to increase the NMR sensitivity. The sample is loaded outside the system, and the capillary is inserted in the NMR probe head for NMR analysis. This methodology involves using a new column for each analysis, which makes CZE-NMR more cumbersome and less practical [44–47]. CEC-NMR seems to have a larger sample capacity and a better signal-to-noise ratio than those of CZE-NMR [44–47]. Overall, CZE-NMR is more technically challenging than CEC-NMR, which makes its development and application more difficult than those of CEC-NMR [44–47].

6.10. cITP-NMR

NMR is a successful analytical technique for the structural elucidation analysis of organic compounds. However, the analysis of small quantities of analytes becomes a challenge due to the inherent low sensitivity of NMR. For complex mixtures, NMR has been hyphenated with HPLC (LC-NMR) and capillary techniques to target the analysis of small quantities, as discussed earlier. Trace analysis is becoming crucial for complex mixtures in the field of natural products and overall in drug discovery and development, which includes combinatorial chemistry and drug metabolism. Another capillary technique that has been hyphenated with NMR is capillary isotachophoresis (cITP) (cITP-NMR), which increases the sensitivity of NMR because it concentrates analytes through cITP to the low-microliter-volume range and separates diluted charged species based on their electrophoretic mobility. In 2001 Sweedler's group [50] coupled cITP with NMR (cITP-NMR) and proved the concept by injecting 7 μL of a test sample mixture containing 200 μM of each component (dipeptide Ala-Lys, 87% dye methyl green, and tetraethylammonium bromide or TEAB) for on-flow mode. In doing so, sensitivity increased by two orders of magnitude for a concentration range of on-flow mode. In addition, the authors injected TEAB for stop-flow mode and acquired COSY spectrum [50]. Wolters et al. [51] improved the instrumental coupling of cITP with NMR to isolate a mixture of atenolol as a makeup trace impurity at 200 μM concentration (Figure 6-1) and sucrose at 200 mM concentration. In addition, the authors have proven the capability of measuring pD and temperature to follow the process by adding *tert*-butyl alcohol as an internal reference to all cITP electrolyte solution for online

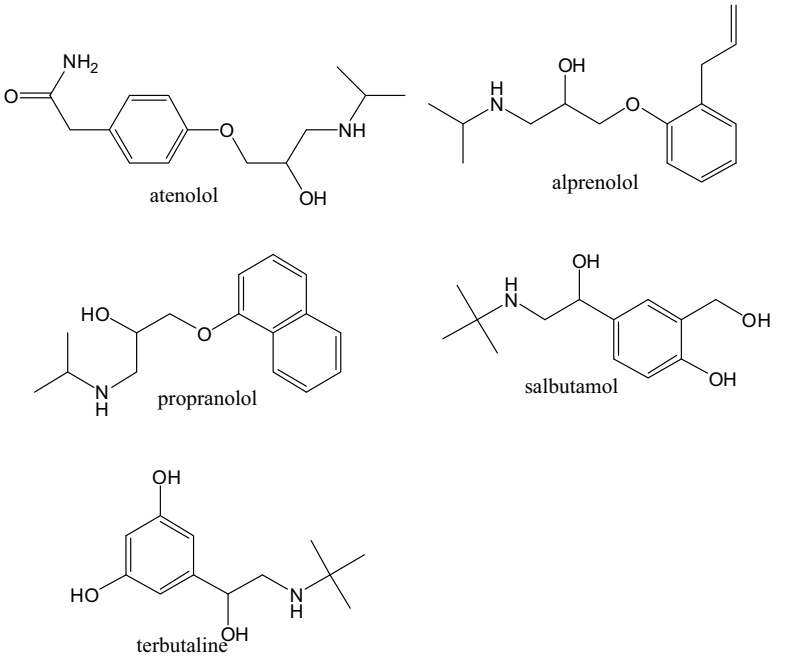

FIGURE 6-1. Structures of atenolol [51,52,54], alprenolol [53,54], propranolol [54], salbutamol [54], and terbutaline [54].

cITP-NMR [52]. Atenolol was used for these measurements [52]. There have been few applications of cITP-NMR during the last decade. Racemic alprenolol (Figure 6-1), a β-blocker used for cardiovascular disorders, was used to separate each individual enantiomer by on-flow cITP-NMR with cyclodextrines as a chiral selector in the nanomole range [53]. Other examples in this area are the studies carried out on the interaction of β-cyclodextrine with the pharmaceutical enantiomers *S*-alprenolol, *S*-atenolol, *R*-propranolol, *R*-salbutamol, and *S*-terbutaline (Figure 6-1) during cITP concentration [54]. On-flow cITP-NMR has been used as an analytical method to separate and analyze nanomole quantities of heparine oligosaccharides, used to prevent blood coagulation, and a heterogeneous mixture of trisulfated disaccharides [55,56]. In the field of natural products, cITP-NMR has been applied to separate and concentrate a cationic neurotoxin dimer of 6-bromo-2-mercaptotryptamine (Figure 6-2) from the marine snail *Calliostoma canaliculatum* [57]. The neurotoxin was concentrated almost 20-fold and isolated by cITP-NMR [57]. cITP-NMR has been tested to demonstrate its capability on the detection and separation of impurities present in drug formulations, with acetaminophen as an example of drug and 4-aminophenol as the impurity spiked 0.1% in acetaminophen [58]. In addition, cITP-NMR

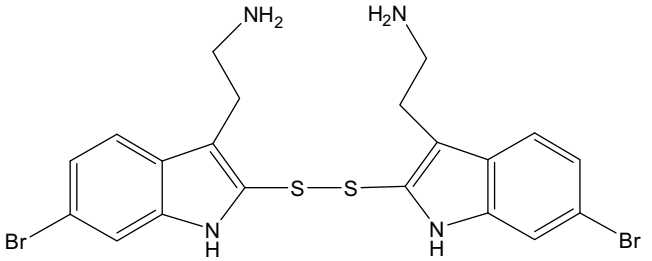

6-bromo-2-mercaptotryptamine

FIGURE 6-2. Structure of 6-bromo-2-mercaptoptryptamine dimer from the marine snail *Calliostoma canaliculatum* [57].

has been tested for use as a diagnostic tool in the mechanism of cITP stacking and electrophoretic migration [59]. cITP-NMR is also not available commercially.

6.11. CapLC-NMR

The first time that capillary separation was hyphenated with NMR for detection of a nanoliter sample volume in the NMR flow cell was by Sweedler's group in 1994 for the application of CE-NMR [37,60]. The hyphenation of capillary HPLC to NMR (capLC-NMR or CHPLC-NMR) came after CE-NMR with an RF microcoil wrapped directly to the fused-silica capillary as the NMR flow cell. The authors observed that having the copper wire attached directly to the fused-silica capillary provided an excellent filling factor for a 5-nL detection volume in the NMR flow cell [37,60]. In 1996, Albert et al. [61] tested the methodology on a 2-mm NMR capillary microprobe by injecting diethyl phthalate in deuterioacetone directly to the capillary cell to simulate stop-flow mode. Vitamin A acetate and a mixture of vitamin A acetate reaction products were also injected to the capillary HPLC attached to the NMR (capLC-NMR) for the on-flow and stop-flow modes to acquire a two-dimensional ^{1}H–^{1}H TOCSY spectrum of *trans*-vitamin A acetate (Figure 6-3) [61]. During the late 1990s and early 2000, the focus was on

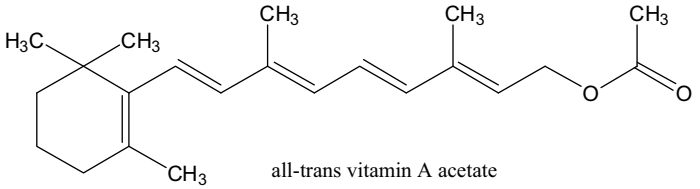

all-trans vitamin A acetate

FIGURE 6-3. Structure of *all-trans* vitamin A acetate [61].

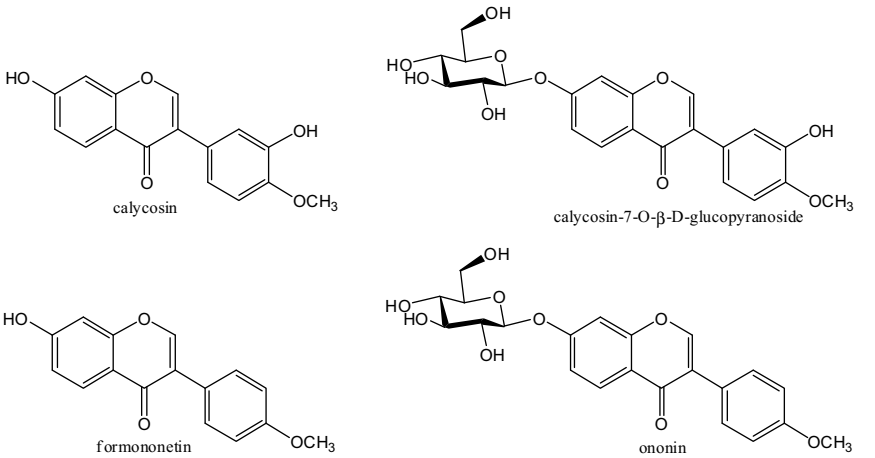

FIGURE 6-4. Structures of four isoflavonoids, calycosin, calycosin-7-*O*-β-glucopyranoside, formononetin, and ononin, analyzed by capLC-NMR [67].

the development of the hyphenated technique to improve the compatibility of the capillary HPLC with the low sensitivity of NMR, with the intention of increasing the signal-to-noise ratio by improving the design of the NMR flow cell and the conditions of the capLC. During that time, most of the peer-reviewed articles did not analyze real samples but, instead, used standard samples to prove the concept [41,46,48,62–65]. CapLC-NMR has been available commercially since early in 2000. Sweedler's group tested the first commercially available capLC-NMR with a mixture of known terpenoids for the on-flow and stop-flow modes [66].

CapLC-NMR has been applied primarily to the field of natural products discovery and drug metabolism. Albert's group [67] applied capLC-NMR to the structural elucidation of isoflavonoids from the plant extract *Radix astragali*. By LC-NMR and stop-flow capLC-NMR, the authors were able to demonstrate the capabilities and practical points of capLC-NMR for rapid determination of the structures of four isoflavonoids: calycosin, calycosin-7-*O*-β-D-glucopyranoside, formononetin, and ononin (Figure 6-4) [67]. In a similar fashion, Rehbein et al. [68] collaborated with Andrew Webb to construct a double-resonance solenoidal NMR microcoil 4 mm in length and 2 μL in active volume to apply for characterization of the main stereoisomers of bixin, 9′-*Z*-bixin, and all-*E*-bixin (Figure 6-5), light- and air-sensitive carotenoids from *Bixin orellana*. Sandvoss et al. [69] tested capLC-NMR for its application in drug metabolism, exploring the limits of detection (LOD) for a signal-to-noise ratio greater than 3, and the practical use of stop-flow experiments for direct analysis of plasma samples in a commercial capLC-NMR instrument. LOD was tested with a test compound with a molecular

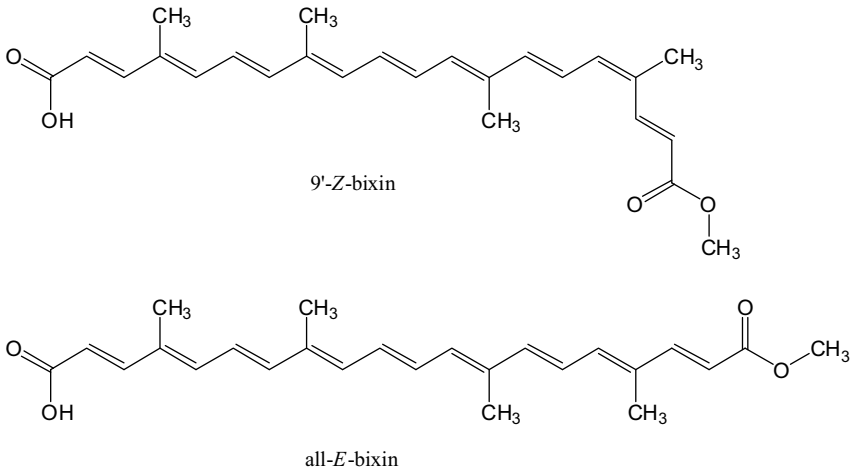

9'-*Z*-bixin

all-*E*-bixin

FIGURE 6-5. Structures of 9′-*Z*-bixin and all-*E*-bixin, carotenoids from *Bixin orellana* [68].

weight of 318 Da, and the authors determined the LOD at approximately 100 ng or 0.35 nmol when acquiring 1D ^{1}H NMR for 1 h in the stop-flow mode and around 25 ng or 85 pmol when acquiring overnight [69]. The authors also indicated that handling the sample in such small volumes requires special care to maintain reliable results and avoid potential precipitation, which may clog the capillary tubing [69]. In addition, the use of deuterated solvents provides better-quality spectra without or with little need of solvent suppression techniques [69]. The system was tested by injecting rat plasma after protein precipitation that came from dosing 50 mg/kg of diclofenac into rats to analyze its metabolites, two hydroxyl metabolites and a glucuronide (Figure 6-6) [69]. CapLC-NMR is beginning to be broadly used as a hyphenated technique, and the coming decade will reveal how much industrial and academic laboratories will use the technique.

6.12. SPE-NMR

Solid-phase extraction (SPE) has been used extensively before NMR analysis when LC and NMR are off-line and prior to LC-NMR. SPE provides two benefits: the elimination of undesirable protonated solvents and additives from the extraction or separation processes, and concentration of the analytes of interest prior to NMR analysis by NMR or LC-NMR. In the last decade, SPE has also been hyphenated to LC-NMR (SPE-NMR or LC-SPE-NMR). SPE is used in front of the LC to preclean samples, or at the end of the LC to preconcentrate the analyte(s) of interest before NMR analysis. The analytes of interest trapped in the SPE cartridges are eluted and sent to the NMR flow cell

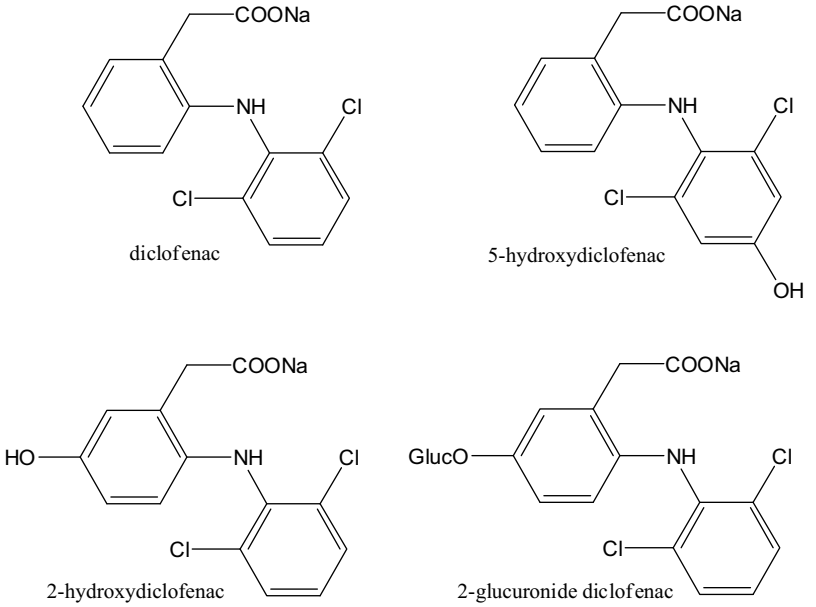

FIGURE 6-6. Structures of diclofenac, 5-hydroxydiclofenac, 2-hydroxydiclofenac, and 2-glucuronide diclofenac [69]. Glucuronic acid (Gluc) is bonded to diclofenac through the anomeric position of glucuronic acid.

in deuterated solvent(s), eliminating or minimizing the need for solvent suppression techniques. The main advantage of SPE is that deuterated solvents are not needed for chromatographic separation when SPE is used to preconcentrate the analytes of interest after chromatographic separation. In this case, NMR is not a limiting factor in HPLC separation regarding restrictions on the type of solvent, solvent composition for optimal separation, and flow rate. In addition, with SPE-NMR it is possible to acquire two-dimensional homonuclear and heteronuclear NMR experiments, such as ^{1}H–^{1}H COSY, ^{1}H–^{1}H TOCSY, ^{1}H–^{1}H NOESY, ^{1}H–^{1}H ROESY, ^{1}H–^{13}C HSQC, and ^{1}H–^{13}C HMBC. Many of them are not possible in conventional LC-NMR, especially for heteronuclear experiments. The slowest step for SPE-NMR is the drying process of the samples in the cartridges when individual analyte is trapped in a cartridge prior to NMR analysis. When several cartridges need to be dried, this process can take overnight. Overall, SPE-NMR facilitates the structural elucidation of a small amount of analytes in samples with complex mixtures. SPE-NMR has been used widely as a hyphenated technique in the fields of natural products [70–94], drug metabolism [95–98], drug development [99,100], trace analysis [101,102], drug degradation products [103–105], absolute configuration [106], and environmental concerns [107].

SPE-NMR has been used extensively for the structural analysis of major and minor components of natural products extracts [70–94]. Lambert

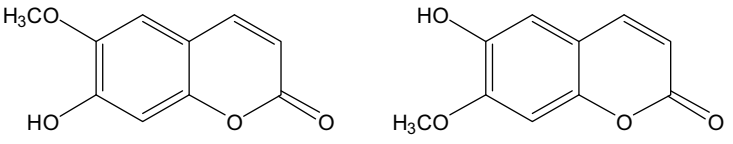

FIGURE 6-7. Structures of two positional isomers, scopoletin and isoscopoletin, from the root bark of *Croton membranaceus* [77].

et al. [77] performed good-quality two-dimensional NMR experiments (^{1}H–^{1}H NOESY, gradient ^{1}H–^{13}C HSQC, and gradient ^{1}H–^{13}C HMBC) to characterize the structures of two positional isomers, scopoletin and isoscopoletin (Figure 6-7), from the root bark of *Croton membranaceus*. The methodology included repeated peak trapping in the SPE section of the SPE-NMR of the two chromatographic peaks selected containing the compounds of interest, during the SPE cartridges, and flashing the trapped compounds separately in acetonitrile-*d*3 into a 30-µL NMR flow cell for NMR analysis [77]. The phenylpropanoids verbascoside and isoverbascoside (Figure 6-8) were the major components of *Blepharis aspera* [83]. Mmatli et al. [83] isolated and confirmed by SPE-NMR that their structures are subjected to metal

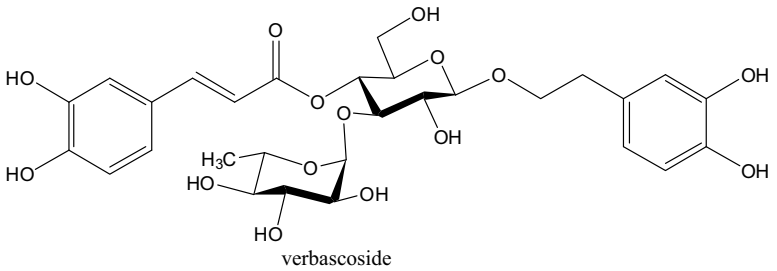

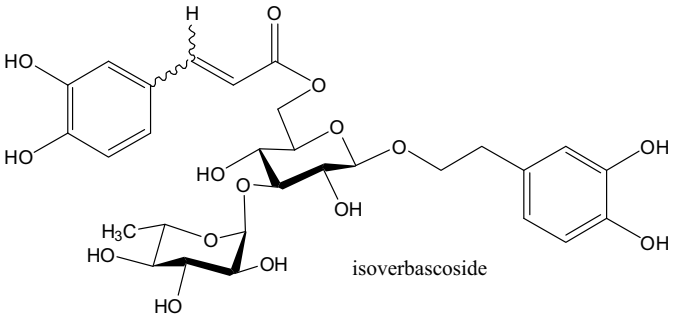

FIGURE 6-8. Structure of verbascoside and isoverbascoside, the major components of *Blepharis aspera* [83].

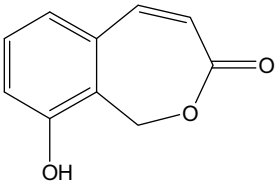

FIGURE 6-9. Structure of broth of 9-hydroxyenzo[*c*]oxepin-3[1*H*]-one from the cultured fungus *Pestalotiopsis virgatula* [93].

complexation with nickel, iron (only for verbascoside), and copper, which may explain why this plant survives in a metal-rich soil in Selkirk, Bostwana [83]. A novel natural product (Figure 6-9) was identified by SPE-NMR from analysis of the crude extract of fermentation from *Pestalotiopsis virgatula* fungus culture [93]. Two-dimensional gradient $^{1}H–^{13}C$ HSQC and gradient $^{1}H–^{13}C$ HMBC were essential in determining its structure [93].

SPE-NMR has been used less frequently in other areas related to pharmaceutical applications, such as drug metabolism [95–98], drug development [99,100], trace analysis [101,102], drug degradation products [103–105], and absolute configuration [106]. An example in drug metabolism is the study of the metabolic profiling of ibuprofen from human urine where SPE-NMR helped identify two metabolites, 2-hydroxyibuprofen and carboxy-ibuprofen (Figure 6-10) [96]. Larsen et al. [100] used SPE-NMR to study the impurity profile of an enema formulation of 5-aminosalicylic acid (5-ASA) with citric acid. The reaction of a high-dose formulation of 5-ASA with the excipient citric acid during storage gave rise to three impurities (Figure 6-11) that were identified by SPE-NMR, leading to a recommendation not to use citric acid in the formulation [100]. SPE-NMR was the key to characterizing the structure of the degradation product of a drug candidate (TCH346; see Figure 6-12) in the formulation form critical for its drug development process [103]. The degradation product identified, dibenzo[*b*,*f*]oxepine-10-carbaldehyde (Figure 6-12), affected the stability of the drug candidate, due to its increase in overtime [103]. Conventional electrospray and atmospheric pressure chemical ionizations for mass spectrometry with positive and negative modes failed to determine the molecular ion of the degradation product. GC–MS with chemical ionization (CI) was the only MS technique that provided molecular ion information. The MS fragmentation pattern was carried out by CI-MS/MS with an ion trap spectrometer. However, a definitive structure with SPE-NMR was possible only after over 300 injections were collected to obtain enough material for NMR analysis [103]. Based on the structure of the degradation product, the authors proposed a degradation pathway for its formation during storage over time, which is thought to be through the oxidation pathway depicted in Figure 6-12 [103]. Another

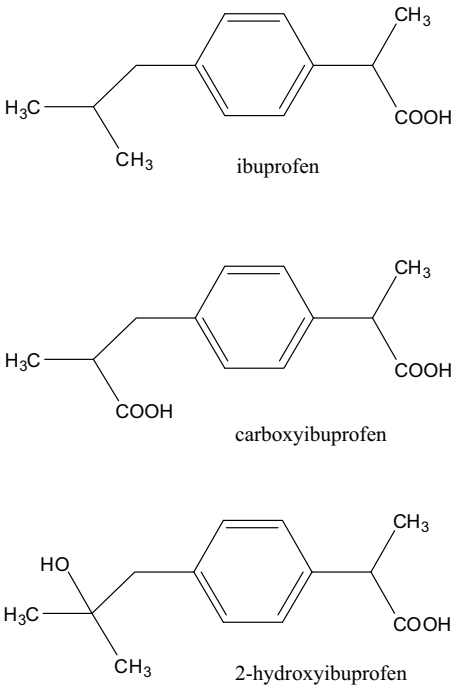

FIGURE 6-10. Structures of ibuprofen and its two metabolites, 2-hydroxyibuprofen and carboxyibuprofen [96].

interesting study is the application of SPE-NMR for the rapid determination of the three degradation products of the drug loxoprofen sodium hydrate for its adhesive tape formulation under heat stress at 80°C for up to 3 weeks in storage (Figure 6-13) [104]. The three degradation products were present at low levels, 3.3% for DP-1, 0.6% for DP-2, and 1.8% for DP-3, but high enough to pursue its structural elucidation. The shorter NMR analysis time resulted from the consecutive trapping of the chromatographic peaks containing the degradation products of interest in the SPE-NMR system [104].

An example of the application of SPE-NMR in the environmental area is the study of the components of nonliving natural organic matters from samples collected from freshwater environments and alkaline soil extract [107]. From this study, the authors were able to determine the structures of 1-ethyl-4-methoxybenzene and (2*E*)-3-(4-hydroxy-3-methoxyphenyl)acrylic acid (Figure 6-14) as part of the components of soil from the Harvard Forest at Petersham, Massachusetts [107].

SPE-NMR has been applied in a greater variety of cases than other analytical separation hyphenated NMR techniques for the structural elucidation of components from a mixture, due to its advantage of concentrating chromatographic peaks of interest on SPE cartridges, from subsequent

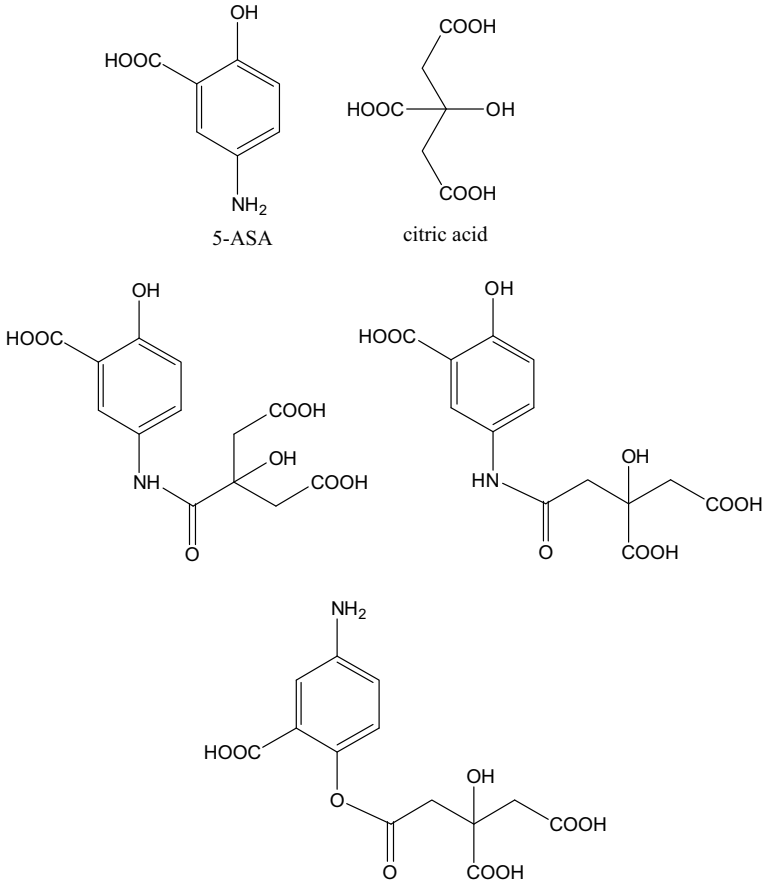

FIGURE 6-11. Structures of 5-aminosalicylic acid (5-ASA), citric acid, and its three impurities from a high-dose enema formulation of 5-ASA with citric acid [100].

injections prior to NMR analysis. Another advantage is the use of deuterated solvents only for NMR analysis and not for the separation part of the SPE-NMR system. SPE-NMR is an excellent technique for trace analysis, and it is becoming a standard method in many areas, especially in the pharmaceutical environment.

6.13. SPE-MS-NMR

A further hyphenation of SPE-NMR with MS is SPE-MS-NMR (also termed SPE-NMR-MS) to obtain a complete set of data for a comprehensive structural elucidation analysis of the analytes of interest from complex mixtures. As indicated in Section 6.12, SPE-NMR has been demonstrated to be an

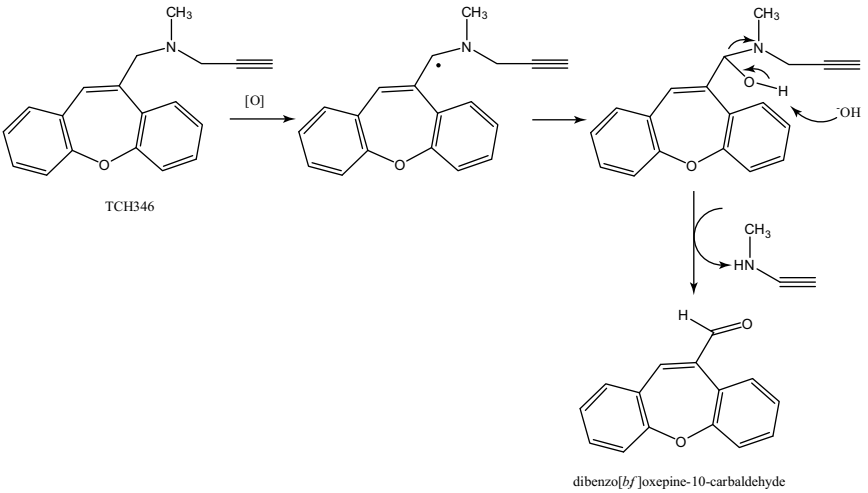

FIGURE 6-12. Proposed degradation pathway of the drug TCH346 into dibenzo[*b,f*]oxepine-10-carbaldehyde under storage over time [103].

important tool in many areas in academia and industry, and it is becoming a routine instrument in advanced laboratories. A general setting for SPE-MS-NMR is splitting the flow rate with a ratio of 95 : 5 going to the NMR and MS, respectively, but having the SPE unit before the NMR instrument and after splitting the flow to trap the chromatographic peaks of interest and concentrate them in SPE cartridges after several injections before NMR analysis. With this configuration, SPE-MS-NMR should be named more appropriately as LC-MS-SPE-NMR, based on the sequence of events, but to avoid complexity in naming, SPE-MS-NMR is the name adopted in this book. In some cases, an additional pump may be placed before splitting the flow to make up flow if necessary. Because the SPE unit concentrates and dries the chromatographic peaks of interest, the HPLC unit does not need to use deuterated solvents for its solvent system, which eliminate having deuterated molecular ions for the analytes of the mixture in the MS. As in SPE-NMR, after concentration and drying of the analytes of interest, the flow going into the NMR flow cell will be carried out with deuterated solvents to facilitate NMR studies by minimizing the need for solvent suppression. In many laboratories, SPE-MS-NMR is becoming a handy methodology for the analysis of complex mixtures. The technique has the potential to be converted into a standard tool in industry and academia to approach the structural determination of analytes of interest that are part of complex mixtures. SPE-MS-NMR can potentially minimize the timing of the traditional method of isolation before NMR and MS analysis and accelerate the structural analysis. Another potential application of SPE-MS-NMR is the analysis of minor compo-

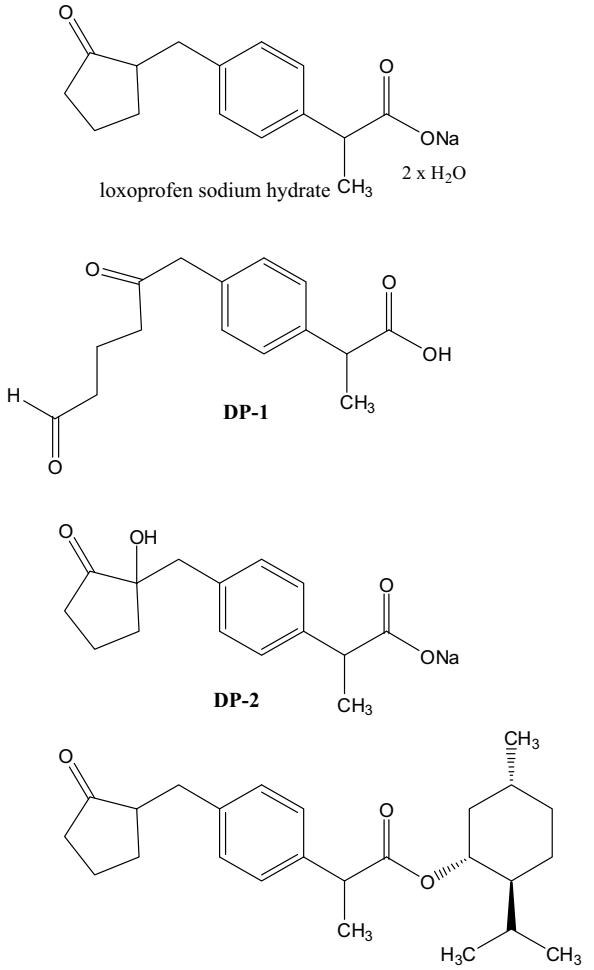

FIGURE 6-13. Structures of the drug loxoprofen sodium hydrate and its three degradation products, DP-1, DP-2, and DP-3, or loxoprofen L-menthol ester from its adhesive tape formulation under heat stress at 80°C for up to 3 weeks in storage [104].

nents of complex mixtures, due to the increase in their concentrations with several injections in the SPE unit. SPE-MS-NMR has been used widely as a hyphenated technique in the natural products [108–122], drug metabolism [123–127], drug discovery [128], and environmental [129,130] fields.

SPE-MS-NMR has been used extensively for the structural analysis of major and minor components of natural products extracts [108–122]. Seger et al. [109] used SPE-MS-NMR to elucidate the structures of four minor components from the root tuber extract of *Harpagophytum procumbens* DC

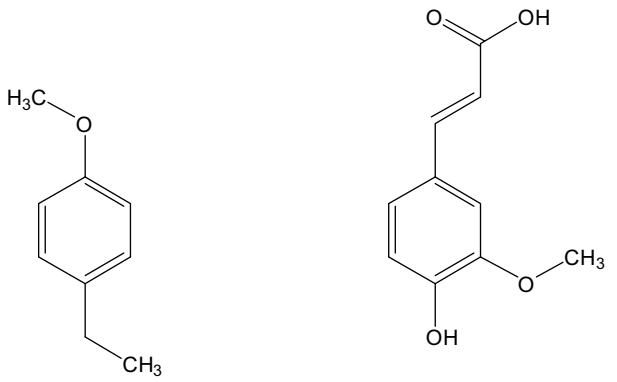

1-ethyl-4-methoxybenzene (2*E*)-3-(4-hydroxy-3-methoxyphenyl)acrylic acid

FIGURE 6-14. Structures of 1-ethyl-4-methoxybenzene and (2*E*)-3-(4-hydroxy-3-methoxyphenyl) acrylic acid as nonliving natural organic matter from samples collected from soil in the Harvard Forest at Petersham, Massachusetts [107].

(Pedaliaceae), a potential phytomedicine plant for the treatment of rheumatism, polyarthritis, and osteoarthritis. With SPE-MS-NMR, the authors were able to determine the structures of four isobaric iridoid glycoside regioisomers present in the plant as minor components. The compounds were identified as *E*/*Z* pairs of 6′-*O*-(*p*-coumaroyl)-harpagide (6′-PCHG) and 8-*O*-(*p*-coumaroyl)-harpagide (8-PCHG) (Figure 6-15). One of the four compounds was a new natural product, 8-(*Z*)-PCHG, and two were new constituents for *H. procumbens*, 6′-(*Z*)- and 6′-(*E*)-PCHG [109]. The authors also compared the analysis by collecting the chromatographic peaks into loops prior to NMR analysis. SPE-MS-NMR was a better approach than the loop collector, showing sensitivity enhancement for the SPE-MS-NMR compared to the loop collector LC-NMR approach [109]. In a similar manner, Christen's group [110] compared both methodologies, loop collector versus SPE-MS-NMR, for the structural analysis of four isomeric tropane alkaloids (Figure 6-16) from the stem bark of *Schizanthus grahamii* Gill (Solanaceae) from Chile using a cryogenic NMR probe. The authors observed an increase in NMR sensitivity that was 25% higher for SPE-MS-NMR than for LC-NMR with loop collectors. The main consideration recommended by the authors for SPE-MS-NMR is to use the correct material in the SPE cartridge for the chromatographic peak to be retained. SPE-MS-NMR provided MS and NMR data for individual peaks, making the results of the structural analysis unambiguous [110]. Another example is the application of SPE-MS-NMR for the identification of the three drugs—amlodipine (calcium channel blocker agent), indapamine (diuretic), and valsartan (angiotensin II receptor blocker) (Figure 6-17)—as adulterant components of the antihypertensive herbal-

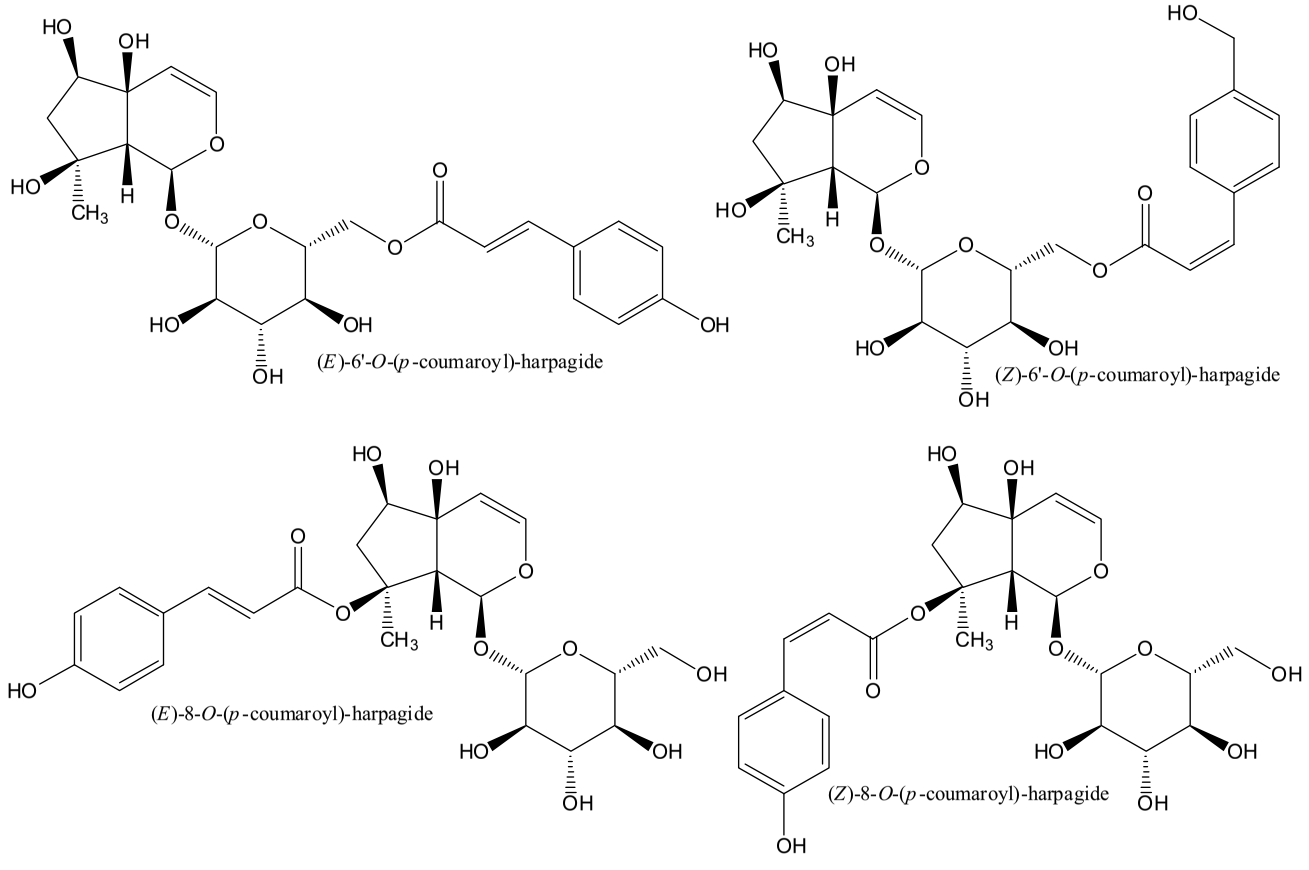

FIGURE 6-15. Structures of (*E*)-6′-*O*-(*p*-coumaroyl)-harpagide or 6′(*E*)-PCHG, (*Z*)-6′-*O*-(*p*-coumaroyl)-harpagide or (*Z*)-6′-PCHG, (*E*)-8-*O*-(*p*-coumaroyl)-harpagide or (*E*)-8-PCHG, and (*Z*)-8-*O*-(*p*-coumaroyl)-harpagide or (*Z*)-8-PCHG as minor components from the root tuber extract of *Harpagophytum procumbens* DC (Pedaliaceae) [109].

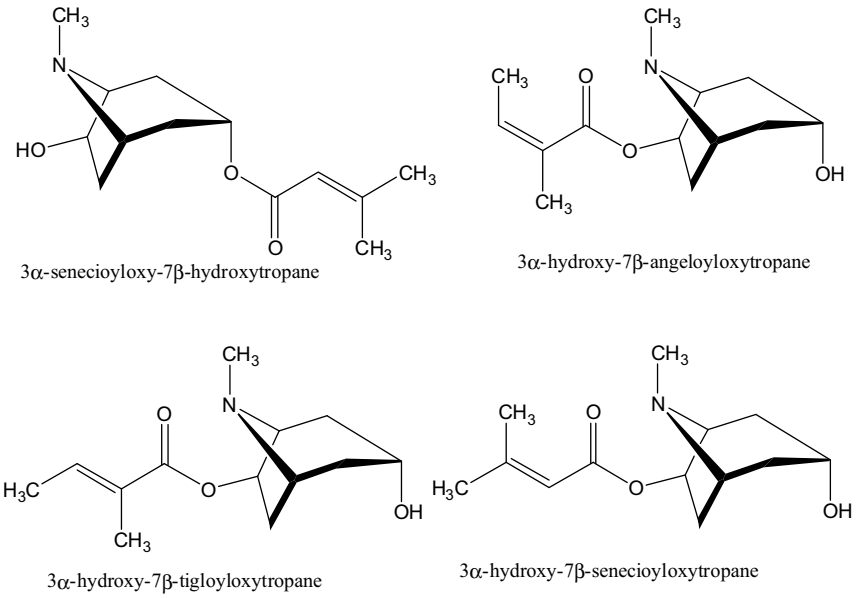

FIGURE 6-16. Structures of four isomeric tropane alkaloids—3α-senecioyloxy-7β-hydroxytropane, 3α-hydroxy-7β-angeloyloxytropane, 3α-hydroxy-7β-tigloyloxytropane and 3α-hydroxy-7β-senecioyloxytropane—from the stem bark of *Schizanthus grahamii* Gill (Solanaceae) from Chile [110].

based Chinese medicine Gold Nine Soft Capsules [121]. SPE-MS-NMR, together with in vivo activity in rats, was crucial for rapid quantitation of the contents of the three active ingredients, which were not listed on the herbal medicine's label [121].

SPE-NMR has been used primarily in pharmaceutical applications such as in the drug metabolism [123–127], drug discovery [128], and environmental [129–130] fields. Lewis et al. [124] compared capLC-NMR with SPE-MS-NMR with a cryogenic probe to determine the pros and cons of both alternatives. The authors recommended capLC-NMR for mass-limited samples, and SPE-MS-NMR with cryogenic probes where the loading of the column is limited but it is possible to concentrate material with SPE for NMR analysis. Test analysis of both techniques was carried out with a druglike molecule from urine to analyze its metabolites (B, C, and D) from a molecule with an adamantine type of molecule, compound A (Figure 6-18) [124]. Ceccarelli et al. [127] applied SPE-MS-NMR to the metabolic profile of the lead compound, 5-aminothiazole-4-carboxylic acid amide (Figure 6-19), in the metabotropic glutamate receptor type 5 (mGlu) allosteric inhibition program. The study provided information on the structure of the major metabolites from rat and on human liver microsomes tested on 14 recombinant human CYP450 enzymes. Five main metabolites were formed, and three

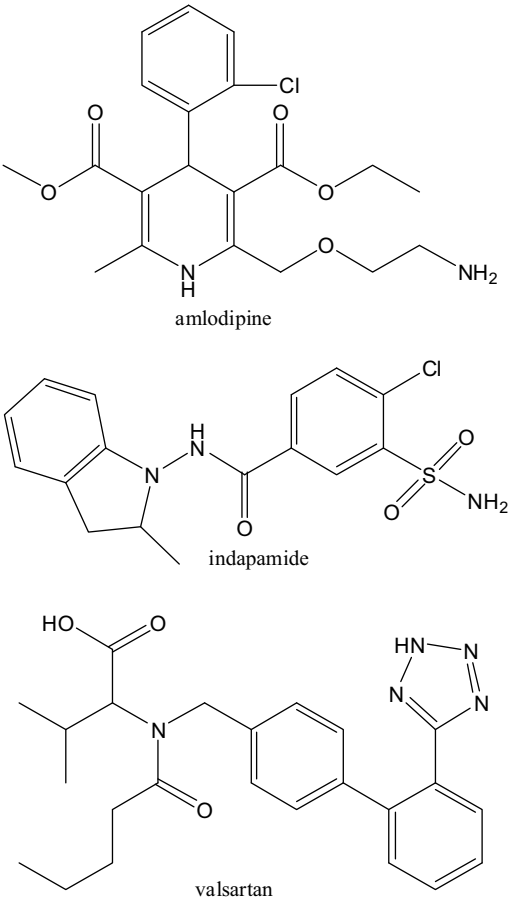

FIGURE 6-17. Structure of three drugs—amlodipine (calcium channel blocker agent), indapamine (diuretic), and valsartan (angiotensin II receptor blocker)—as adulterant components of the antihypertensive herbal-based Chinese medicine Gold Nine Soft Capsules [121].

CYP450 isoforms, CYP1A2, CYP2C18, and CYP2D6, were identified as being responsible for those transformations (Figur 6-19) [127].

In the environmental arena, SPE-MS-NMR has been used in contaminated groundwater from a former ammunition destruction site in the Susten-Stone Glacier in Switzerland for an analysis of the content of traditional explosives, such as 2,4,6-trinitrotoluene (TNT), hexogen (RDX), and octogen (HMX), TNT degradation products, and stabilizer's of powders and propellants [129]. SPE-MS-NMR was used to analyze one of the most important commercial anionic surfactants, alkylbenzenesulfonate (LAS), a mixture of homologs and isomers, used in cases of severe contamination by sewage [130]. It was possible using SPE-MS-NMR to obtain MS and NMR data on the 20 mayor LASs species successfully [130].

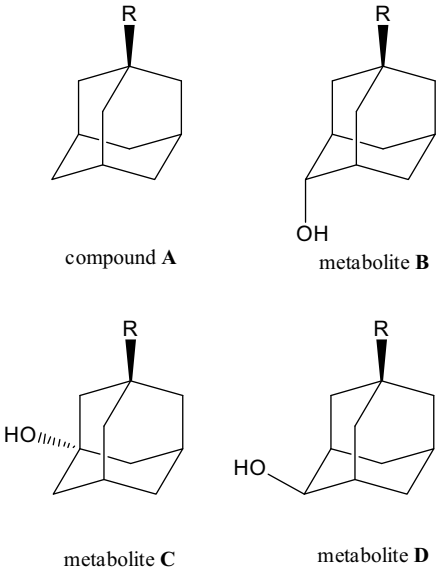

FIGURE 6-18. Structures of compound A and its metabolites, B, C, and D, from urine [124].

SPE-MS-NMR has been used in a variety of cases for the structural elucidation of components from mixtures. SPE provides an advantage in the concentration of chromatographic peaks of interest from subsequent injections prior to NMR analysis. MS is performed before the SPE-NMR section,

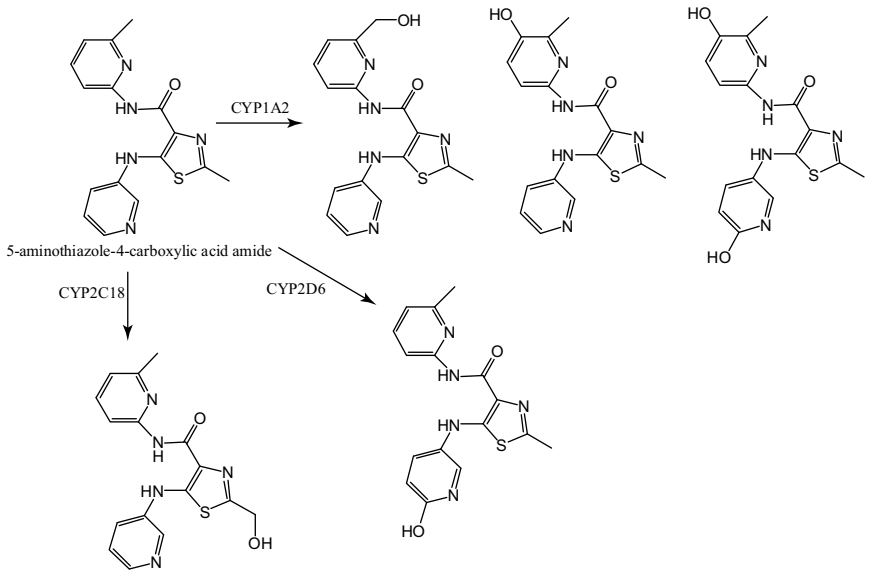

FIGURE 6-19. Structure of 5-aminothiazole-4-carboxylic acid amide and its five metabolites with the corresponding CYP isoforms responsible for their formation [127].

which has the benefit of not using deuterated solvents before SPE. Deuterated solvents are used only when the sample is transferred from the SPE cartridge to the NMR flow cell, as described in SPE-NMR. SPE-MS-NMR is an excellent combination of techniques that provides complete structural analysis of major and minor analytes from complex mixtures. Currently, the use of SPE-MS-NMR is not as extensive as the use of SPE-NMR. The coming years will determine the practicality of this multiple hyphenated technique.

6.14. CONCLUSIONS AND FUTURE TRENDS

Besides the traditional hyphenation of HPLC and NMR as LC-NMR, other separation analytical techniques have been hyphenated with NMR. Those techniques are GC, GPC, SEC, SFC, SFE, CE, CEC, CZE, cITP, capLC, and SPE. Capillary separation techniques such as CE, CEC, CZE, cITP, and capLC have provided options for the analysis of small components of complex mixtures and trace analysis. SPE has also been demonstrated to be valuable for those types of analysis because it makes possible concentration of the chromatographic peaks of interest in cartridges by subsequent injections. These analytical separation techniques hyphenated with NMR have made feasible the structural analysis of minor components of mixtures not possible by traditional LC-NMR but possible only by time-consuming separation and isolation procedures. Only capLC-NMR and SPE-NMR are commercially available, both used much more than the other techniques. SPE-NMR is the only technique hyphenated with MS (SPE-MS-NMR) at the time of this writing of which the author is aware. SPE-MS-NMR is also available commercially and accessible to laboratories in industry and academia, as demonstrated by peer-reviewed publications during last decade. The two main areas of application of these hyphenated techniques are natural products and drug metabolism. Few applications in the areas of drug discovery and development, trace analysis, drug degradation products, absolute configuration of organic compounds, and environmental analysis have been reported for some of these techniques. There are two major drawbacks to appling these techniques to complex analysis, not all of them available commercially. Those that are available are costly, due to the complexity of the instrumentation, and they require training and experience in multiple analytical techniques. CapLC-NMR and, especially, SPE-NMR have provided more applications, including the acquisition of two-dimensional heteronuclear NMR data, such as the ^{1}H–^{13}C HMBC type, with less demand for solvent suppression. The SPE-NMR and capLC-NMR techniques are becoming common in many laboratories. SPE-MS-NMR seems to follow its simple SPE-NMR version but at a lower rate of usage. The other hyphenated NMR techniques need to

be available commercially to increase their applications in industry and academia. The coming years will provide more information on which techniques are used most often for the structural elucidation of components from complex mixtures.

REFERENCES

[1] E.G. Brame, Jr., Combining Gas Chromatography with Nuclear Magnetic Resonance Spectroscopy, *Anal. Chem.* **37** (1965), 1183–1184.

[2] T. Tsuda, Y. Ojika, M. Izuda, I. Fujishima, and D. Ishii, The Combination of Gas Chromatography and Nuclear Magnetic Resonance, *J. Chromagr.* **69** (1972), 194–197.

[3] K.L. Gallaher and J.G. Grasselli, Analysis by Optimized Gas Chromatography/Infrared/Nuclear Magnetic Resonance Techniques, *Appl. Spectrosc.* **31** (1977), 456–463.

[4] J. Buddrus and H. Herzog, Coupling of Chromatography and NMR: Study of Flowing Gas Chromatography Fractions by Proton Magnetic Resonance, *Org. Mater. Reson.* **15** (1981), 211–213.

[5] M. Kühnle, D. Kreidler, K. Holtin, H. Czesla, P. Schuler, W. Schaal, V. Schuring, and K. Albert, Online Coupling of Gas Chromatography to Nuclear Magnetic Resonance Spectroscopy: Method for the Analysis of Volatile Stereoisomers, *Anal. Chem.* **80** (2008), 5481–5486.

[6] M. Kühnle, K. Holtin, and K. Albert, Capillary NMR Detection in Separation Science, *J. Sep. Sci.* **32** (2009), 719–726.

[7] K. Hatada, K. Ute, Y. Okamoto, M. Imanari, and N. Fujii, On-Line GPC/NMR Experiments Using the Isotactic Poly(methyl methacrylate) with Well-Defined Chemical Structure, *Polym. Bull.* **20** (1988), 317–321.

[8] K. Hatada, K. Ute, T. Kitayama, M. Yamamoto, T. Nishimura, and M. Kashiyama, On-Line GPC/NMR Analyses of Block and Random Copolymers of Methyl and Butyl Methacrylates Prepared with *t*-C_4H_9MgBr, *Polym. Bull.* **21** (1989), 489–495.

[9] K. Hatada, K. Ute, T. Kitayama, T. Nishimura, M. Kashiyama, and N. Fujimoto, Studies on the Molecular Weight Dependence of Tacticity of Anionically Prepared PMMAs by On-Line GPC/NMR, *Polym. Bull.* **23** (1990), 549–554.

[10] K. Hatada, K. Ute, M. Kashiyama, and M. Imanari, Direct Determination of Molecular Weight and Its Distribution by the Absolute Calibration Method Using the On-Line GPC/NMR, *Polym. J.* **22** (1990), 218–222.

[11] K. Hatada and K. Ute, On-Line GPC/NMR Analysis of Polymer and Oligomer, *Polym. Mater. Sci. Eng.* **62** (1990), 332.

[12] D. Berek, M. Jančo, T. Kitayama, and K. Hatada, Separation of Poly(methyl methacrylate)s According to Their Tacticity, *Polym. Bull.* **32** (1994), 629–635.

[13] L.C.M. Van Gorkom and T.M. Hancewicz, Analysis of DOSY and GPC-NMR Experiments on Polymers by Multivariate Curve Resolution, *J. Magn. Reson.* **130** (1998), 125–130.

[14] K. Hatada, Stereoregular Uniform Polymers, *J. Polym. Sci. A* **37** (1999), 245–260.

[15] H. Händel and K. Albert, GPC-NMR Coupling, in K. Albert (ed.), *On-Line LC-NMR and Related Techniques*, Wiley, Chichester, England, 2002, pp. 181–218.

[16] J. Wu and K. Beshah, Complex Polymer Mixture Analysis by On-Line LC (GPC)-NMR, in H.N. Cheng and A.D. English (eds.), *NMR Spectroscopy of Polymers in Solution and in the Solid State*, American Chemical Society, Washington, DC, 2003, pp. 345–357.

[17] W. Hiller, H. Pasch, T. Macko, M. Hofmann, J. Ganz, M. Spraul, U. Braumann, R. Streck, J. Mason, and F.V. Damme, On-Line Coupling of High Temperature GPC and ^{1}H NMR for the Analysis of Polymers, *J. Magn. Reson.* **183** (2006), 290–302.

[18] K. Ute, R. Niimi, S.-Y. Hongo, and K. Hatada, Determination of Molecular Weight Distribution by Size Exclusion Chromatography with 750 MHz ^{1}H NMR Detection (On-Line SEC-NMR), *Polym. J.* **30** (1998), 439–443.

[19] K. Ute, R. Niimi, K. Hatada, and A.C. Kolbertb, Ethylene–Propylene–Diene Terpolymers (EDPM) by 750 MHz On-Line SEC-NMR, *Int. J. Polym. Anal. Charact.* **5** (1999), 47–59.

[20] I. Krämer, H. Pasch, H. Händel, and K. Albert, Chemical Heterogeneity Analysis of High-Conversion Poly[styrene-*co*-(ethyl acrylate)]s by NMR and On-Line Coupled SEC-NMR, *Macromol. Chem. Phys.* **200** (1999), 1734–1744.

[21] T. Kitayama, M. Tabuchi, and K. Hatada, Monomer-Selective Living Copolymerization of *t*-Butyl Acrylate and Ethyl Methacrylate with *t*-Butyllithium/Bis(2,6-di-*t*-butylphenoxy)methylaluminium, *Polym. J.* **32** (2000), 796–802.

[22] K. Ute, R. Niimi, M. Matsunaga, K. Hatada, and T. Kitayama, On-Line SEC-NRM Analysis of the Sterocomplex of Uniform Isotactic and Uniform Syndiotactic Poly(methyl metacrylate)s, *Macromol. Chem. Phys.* **202** (2001), 3081–3086.

[23] T.G. Neiss and H.N. Cheng, Coupled SEC-NMR Analysis of Alginates, in H.N. Cheng and A.D. English (eds.), *NMR Spectroscopy of Polymers in Solution and in the Solid State*, American Chemical Society, Washington, DC, 2003, pp. 382–395.

[24] W. Hiller, M. Hehn, T. Hofe, and K. Oleschko, Online Size Exclusion Chromatography–NMR for the Determination of Molar Mass Distribution of Copolymers, *Anal. Chem.* **82** (2010), 8244–8250.

[25] L.A. Allen, T.E. Glass, and H.C. Dorn, Direct Monitoring of Supercritical Fluids and Supercritical Chromatographic Separations by Proton Nuclear Magnetic Resonance, *Anal. Chem.* **60** (1988), 390–394.

[26] K. Albert, U. Braumann, L.-H. Tseng, G. Nicholson, E. Bayer, M. Spraul, M. Hofmann, C. Dowle, and M. Chippendale, On-Line Coupling of Supercritical

Fluid Chromatography and Proton High-Field Nuclear Magnetic Resonance, *Anal. Chem.* **66** (1994), 3042–3046.

[27] U. Braumann, H. Händel, K. Albert, R. Ecker, and M. Spraul, On-Line Monitoring of the Supercritical Fluid Extraction Process with Proton Nuclear Magnetic Resonance Spectroscopy, *Anal. Chem.* **67** (1995), 930–935.

[28] K. Albert, U. Braumann, R. Streck, M. Spraul, and R. Ecker, Application of Direct On-Line Coupling of HPLC and SFC with ^{1}H NMR Spectroscopy for the Investigation of Monomeric Acrylates, *Fresenius J. Anal. Chem.* **352** (1995), 521–528.

[29] K. Albert, On-Line Use of NMR Detection in Separation Chemistry, *J. Chromatogr. A* **703** (1995), 123–147.

[30] K. Albert, Supercritical Fluid Chromatography–Proton Nuclear Magnetic Resonance Spectroscopy Coupling, *J. Chromatogr. A* **703** (1997), 65–83.

[31] U. Braumann, H. Händel, S. Strohschein, M. Spraul, G. Krack, R. Ecker, and K. Albert, Separation and Identification of Vitamin A Acetate Isomers by Supercritical Fluid Chromatography–^{1}H NMR Coupling, *J. Chromatogr. A* **761** (1997), 336–340.

[32] H. Fischer, L.-H. Tseng, M. Raitza, and K. Albert, Application of Immobilized Free Radicals in Supercritical Fluid Chromatography Hyphenated with Proton Nuclear Magnetic Resonance Spectroscopy, *Magn. Reson. Chem.* **38** (2000), 336–342.

[33] H. Fischer and K. Albert, SFC-NMR and SFE-NMR, in K. Albert (ed.), *On-Line LC-NMR and Related Techniques*, Wiley, Chichester, England, 2002, pp. 195–218.

[34] E. Trezza, A.M. Haiduc, G.J.W. Goudappel, and J.P.M. van Duynhoven, Rapid Phase-Compositional Assessment of Lipid-Based Food Products by Time Domain NMR, *Magn. Reson. Chem.* **44** (2006), 1023–1030.

[35] S.L. Eldridge, A.K. Korir, C.E. Merrylwell, and C.K. Larive, Hyphenated Chromatographic Techniques in Nuclear Magnetic Resonance Spectroscopy, *Adv. Chromatogr.* **46** (2008), 351–390.

[36] M. Spraul, U. Braumann, M. Godejohann, and M. Hofmann, Hyphenated Method in NMR, *Magn. Reson. Food Sci.* **262** (2001), 54–66.

[37] N. Wu, T.L. Peck, A.G. Webb, R.L. Magin, and J.V. Sweedler, ^{1}H-NMR Spectroscopy on the Nanoliter Scale for Static and On-Line Measurements, *Anal. Chem.* **66** (1994), 3849–3857.

[38] D.L. Olson, M.E. Lacey, A.G. Webb, and J.V. Sweedler, Nanoliter-Volume ^{1}H NMR Detection Using Periodic Stopped-Flow Capillary Electrophoresis, *Anal. Chem.* **71** (1999), 3070–3076.

[39] J. Schewitz, K. Pusecker, P. Gfrörer, U. Götz, L.-H. Tseng, K. Albert, and E. Bayer, Direct Coupling of Capillary Electrophoresis and Nuclear Magnetic Resonance Spectroscopy for the Identification of a Dinucleotide, *Chromatography* **50** (1999), 333–337.

[40] A.M. Wolters, D.A. Jayawickrama, A.G. Webb, and J.V. Sweedler, NMR Detection with Multiple Solenoidal Microcoils for Continuous-Flow Capillary Electrophoresis, *Anal. Chem.* **74** (2002), 5550–5555.

[41] D.A. Jayawickrama and J.V. Sweedler, Hyphenation of Capillary Separations with Nuclear Magnetic Resonance Spectroscopy, *J. Chromatogr. A* **1000** (2003), 819–840.

[42] Y. Li, M.E. Lacey, J.V. Sweedler, and A.G. Webb, Spectral Restoration from Low Signal-to-Noise, Distorted NMR Signals: Application to Hyphenated Capillary Electrophoresis–NMR, *J. Magn. Reson.* **162** (2003), 133–140.

[43] D.A. Jayawickrama and J.V. Sweedler, Dual Microcoil NMR Probe Coupled to Cyclic CE for Continuous Separation and Analyte Isolation, *Anal. Chem.* **76** (2004), 4894–4900.

[44] K. Pusecker, J. Schewitz, P. Gfrörer, L.-H. Tseng, K. Albert, E. Bayer, I.D. Wilson, N.J. Bailey, G.B. Scarfe, G.J. Schewitz, J.K. Nicholson, and J.C. Lindon, On-Flow Identification of Metabolites of Paracetamol from Human Urine Directly Coupled CZE-NMR and CEC-NMR Spectroscopy, *Anal. Commun.* **35** (1998), 213–215.

[45] J. Schewitz, P. Gfrörer, K. Pusecker, L.-H. Tseng, K. Albert, E. Bayer, I.D. Wilson, N.J. Bailey, G.B. Scarfe, J.K. Nicholson, and J.C. Lindon, Directly Coupled CZE-NMR and CEC-NMR Spectroscopy for Metabolite Analysis: Paracetamol Metabolites in Human Urine, *Analyst* **123** (1998), 2835–2837.

[46] K. Pusecker, J. Schewitz, P. Gfrörer, L.-H. Tseng, K. Albert, and E. Bayer, On-Line Coupling of Capillary Electrochromatography, Capillary Electrophoresis, and Capillary HPLC with Nuclear Magnetic Resonance Spectroscopy, *Anal. Chem.* **70** (1998), 3280–3285.

[47] P. Gfrörer, J. Schewitz, K. Pusecker, L.-H. Tseng, K. Albert, and E. Bayer, Gradient Elution Capillary Electrochromatography and Hyphenation with Nuclear Magnetic Resonance, *Electrochromatography* **20** (1999), 3–8.

[48] P. Gfrörer, L.-H. Tseng, E. Rapp, K. Albert, and E. Bayer, Influence of Pressurized Capillary Electrochromatography with Nuclear Magnetic Resonance Spectroscopy, *Anal. Chem.* **73** (2001), 3234–3239.

[49] E. Rapp, A. Jakob, A.B. Schefer, E. Bayer, and K. Albert, Splitless On-Line Coupling of Capillary High-Performance Liquid Chromatography, Capillary Electrochromatography and Pressurized Capillary Electrochromatography with Nuclear Magnetic Spectroscopy, *Anal. Bioanal. Chem.* **376** (2003), 1053–1016.

[50] R.A. Kautz, M.E. Lacey, A.M. Wolters, F. Foret, A.G. Webb, B.L. Karger, and J.V. Sweedler, Sample Concentration and Separation for Nanoliter-Volume NMR Spectroscopy Using Capillary Isotachophoresis, *J. Am. Chem. Soc.* **123** (2001), 3159–3160.

[51] A.M. Wolters, D.A. Jayawickrama, C.K. Larive, and J.V. Sweedler, Capillary Isotachophoresis/NMR: Extension to Trace Impurity Analysis and Improved Instrumental Coupling, *Anal. Chem.* **74** (2002), 2306–2313.

[52] A.M. Wolters, D.A. Jayawickrama, C.K. Larive, and J.V. Sweedler, Insights into the cITP Process Using On-Line NMR Spectroscopy, *Anal. Chem.* **74** (2002), 4191–4197.

[53] D.A. Jayawickrama and J.V. Sweedler, Chiral Separation of Nanomole Amounts of Alprenolol with cITP/NMR, *Anal. Bioanal. Chem.* **378** (2004), 1528–1535.

[54] V.K. Almeida and C.K. Larive, Insights into Cyclodextrin Interactions During Sample Stacking Using Capillary Isotachophoresis with On-Line Microcoil Detection, *Magn. Reson. Chem.* **43** (2005), 755–761.

[55] A.K. Korir, V.K. Almeida, D.S. Malkin, and C.K. Larive, Separation and Analysis of Nanomole Quantities of Heparine Oligosaccharides Using On-Line Capillary Isotachophoresis Coupled with NMR Detection, *Anal. Chem.* **77** (2005), 5998–6003.

[56] A.K. Korir and C.K. Larive, On-Line NMR Detection of Microgram Quantities of Heparin-Derived Oligosaccharides and Their Structure Elucidation by Microcoil NMR, *Anal. Bioanal. Chem.* **388** (2007), 1707–1716.

[57] A.M. Wolters, D.A. Jayawickrama, and J.V. Sweedler, Comparative Analysis of a Neurotoxin from *Calliostoma canaliculatum* by On-Line Capillary Isotachophoresis/^{1}H NMR and Diffusion ^{1}H NMR, *J. Nat. Prod.* **68** (2005), 162–167.

[58] S.L. Eldridge, V.K. Almeida, A.K. Korir, and C.K. Larive, Separation and Analysis of Trace Degradants in a Pharmaceutical Formulation Using On-Line Capillary Isotachophoresis–NMR, *Anal. Chem.* **79** (2007), 8446–8453.

[59] A.K. Korir, V.K. Almeida, and C.K. Larive, Visualizing Ion Electromigration During Isotachophoretic Separations with Capillary Isotachophoresis–NMR, *Anal. Chem.* **78** (2006), 7078–7087.

[60] N. Wu, T.L. Peck, A.G. Webb, R.L. Magin, and J.V. Sweedler, Nanoliter Volume Sample Cell for ^{1}H NMR Application to On-Line Detection in Capillary Electrophoresis, *J. Am. Chem. Soc.* **116** (1994), 7929–7930.

[61] K. Albert, G. Schlotterbeck, L.-H. Tseng, and U. Braumann, Application of On-Line Capillary Liquid Chromatography–Nuclear Magnetic Resonance Spectrometry Coupling for the Analysis of Vitamin A Derivatives, *J. Chromatogr. A* **750** (1996), 303–309.

[62] M.E. Lacey, R. Subramanian, D.L. Olson, A.G. Webb, and J.V. Sweedler, High-Resolution NMR Spectroscopy of Sample Volumes from 1 nL to 10 μL, *Chem. Rev.* **99** (1999), 3133–3152.

[63] R. Subramanian, W.P. Kelley, P.D. Floyd, Z.J. Tan, A.G. Webb, and J.V. Sweedler, A Microcoil NMR Probe for Coupling Microscale HPLC with On-Line NMR Spectroscopy, *Anal. Chem.* **71** (1999), 5335–5339.

[64] M.E. Lacey, A.G. Webb, and J.V. Sweedler, NMR Spectroscopy in Microdomains, in K. Albert (ed.), *On-Line LC-NMR and Related Techniques*, Wiley, Chichester, England, 2002, pp. 221–236.

[65] A.B. Schefer and K. Albert, Capillary Separation Techniques, in K. Albert (ed.), *On-Line LC-NMR and Related Techniques*, Wiley, Chichester, England, 2002, pp. 237–246.

[66] M.E. Lacey, Z.J. Tan, A.G. Webb, and J.V. Sweedler, Union of Capillary High-Performance Liquid Chromatography and Microcoil Nuclear Magnetic Resonance Spectroscopy Applied to the Separation and Identification of Terpenoids, *J. Chromatogr. A* **922** (2001), 139–149.

[67] H.B. Xiao, M. Krucker, K. Putzbatch, and K. Albert, Capillary Liquid Chromatography–Microcoil ^{1}H Nuclear Magnetic Resonance Spectroscopy and Liquid Chromatography–Ion Trap Mass Spectrometry for On-Line Structure Elucidation of Isoflavonoids in *Radix astragali*, *J. Chromatogr. A* **1067** (2005), 135–143.

[68] J. Rehbein, B. Dietrich, M.D. Grynbaum, P. Hentschel, K. Holtin, M. Kuehnle, P. Schuler, M. Bayer, and K. Albert, Characterization of Bixin by LC-NMR and LC-NMR, *J. Sep. Sci.* **30** (2007), 2382–2390.

[69] M. Sandvoss, A.D. Roberts, I.M. Ismail, and S.E. North, Direct On-Line Hyphenation of Capillary Liquid Chromatography to Nuclear Magnetic Resonance Spectroscopy: Practical Aspects and Application to Drug Metabolite Identification, *J. Chromatogr. A* **1028** (2004), 259–266.

[70] N.T. Nyberg, H. Baumann, and L. Kenne, Application of Solid-Phase Extraction Coupled to an NMR Flow-Probe in the Analysis of HPLC Fractions, *Magn. Reson. Chem.* **39** (2001), 236–240.

[71] N.T. Nyberg, H. Baumann, and L. Kenne, Solid-Phase Extraction NMR Studies of Chromatographic Fractions of Saponins from *Quillaja saponaria*, *Anal. Chem.* **75** (2003), 268–274.

[72] C. Clarkson, D. Stærk, S.H. Hansen, and J.W. Jaroszewski, Hyphenation of Solid-Phase Extraction with Liquid Chromatography and Nuclear Magnetic Resonance: Application of HPLC-DAD-SPE-NMR to Identification of Constituents of *Kanahia laniflora*, *Anal. Chem.* **77** (2005), 3547–3553.

[73] S. Christophoridou, P. Dais, L.-H. Tseng, and M. Spraul, Separation and Identification of Phenolic Compounds in Olive Oil by Coupling High-Performance Liquid Chromatography with Postcolumn Solid-Phase Extraction to Nuclear Magnetic Resonance Spectroscopy (LC-SPE-NMR), *J. Agric. Food Chem.* **53** (2005), 4667–4679.

[74] A. Pukalskas, T.A. van Beck, and P. de Waard, Development of a Triple Hyphenated HPLC–Radical Scavenging Detection–DAD-SPE-NMR System for the Rapid Identification of Antioxidants in Complex Plant Extracts, *J. Chromatogr. A* **1074** (2005), 81–88.

[75] G. Miliauskas, T.A. Van Beek, P. de Waard, R.P. Venskutonis, and E.J.R. Sudhölter, Identification of Radical Scavenging Compounds in *Rhaponticum carthamoides* by Means of LC-DAD-SPE-NMR, *J. Nat. Prod.* **68** (2005), 168–172.

[76] M. Lambert, D. Stærk, S.H. Hansen, M. Sairafianpour, and J.W. Jaroszewski, Rapid Extract Dereplication Using HPLC-SPE-NMR: Analysis of Isoflavonoids from *Smirnowia iranica*, *J. Nat. Prod.* **68** (2005), 1500–1509.

[77] M. Lambert, D. Stærk, S.H. Hansen, and J.W. Jaroszewski, HPLC-SPE-NMR Hyphenation in Natural Products Research: Optimization of Analysis of *Croton membranaceus* Extract, *Magn. Reson. Chem.* **43** (2005), 771–775.

[78] C.-Y. Wang and S.-S. Lee, Analysis and Identification of Lignans in *Phyllanthus urinaria* by HPLC-SPE-NMR, *Phytochem. Anal.* **16** (2005), 120–126.

[79] V. Exarchou, Y.C. Fiamegos, T.A. Van Beek, C. Nanos, and J. Vervoort, Hyphenated Chromatographic Techniques for the Rapid Screening and Identification of Antioxidants in Methanolic Extracts of Pharmaceutically Used Plants, *J. Chromatogr. A* **1112** (2006), 293–302.

[80] C. Clarkson, D. Stærk, S.H. Hansen, P.J. Smith, and J.W. Jaroszewski, Discovering New Natural Products Directly from Crude Extracts by HPLC-SPE-NMR: Chinane Diterpenoids in *Harpagophytum procumbens*, *J. Nat. Prod.* **69** (2006), 527–530.

[81] C. Clarkson, D. Stærk, S.H. Hansen, P.J. Smith, and J.W. Jaroszewski, Identification of Major and Minor Constituents of *Harpagophytum procumbens* (Devil's Claw) Using HPLC-SPE-NMR and HPLC-ESIMS/APICMS, *J. Nat. Prod.* **69** (2006), 1280–1288.

[82] M. Lambert, J.-L. Wolfender, D. Stærk, S.B. Christensen, K. Hostettmann, and J.W. Jaroszewski, Identification of Natural Products Using HPLC-SPE Combined with CapNMR, *Anal. Chem.* **79** (2007), 727–735.

[83] E.E. Mmatli, H. Malrod, S.R. Wilson, B. Abegaz, T. Greibrokk, E. Lundanes, K.E. Malterud, D. Petersen, and F. Rise, Identification of Major Metal Complexing Compounds in *Blepharis aspera*, *Anal. Chim. Acta* **597** (2007), 24–31.

[84] S. Sturn, C. Seger, M. Godejohann, M. Spraul, and H. Stuppner, Conventional Sample Enrichment Strategies Combined with High-Performance Liquid Chromatography–Solid Phase Extraction–Nuclear Magnetic Resonance Analysis Allows Analyte Identification from a Single Minuscule *Corydalis solida* Plant Tuber, *J. Chromatogr. A* **1163** (2007), 138–144.

[85] K. Sprogøe, D. Stærk, A.K. Jäger, A. Adsersen, S.H. Hansen, M. Witt, A.-K.R. Landbo, A.S. Meyer, and J.W. Jaroszewski, Targeted Natural Products Isolation Guided by HPCL-SPE-NMR; Constituents of *Hubertia* Species, *J. Nat. Prod.* **70** (2007), 1472–1477.

[86] S.-S. Lee, Y.-C. Lai, C.-K. Chen, L.-H. Tseng, and C.-Y. Wang, Characterization of Isoquinoline Alkaloids from *Neolitsea sericea* var. *aurata* by HPLC-SPE-NMR, *J. Nat. Prod.* **70** (2007), 637–642.

[87] E.C. Tatsis, S. Boeren, V. Exarchou, A.N. Troganis, J. Vervoort, and I.P. Gerothanasis, Identification of the Major Constituent of *Hypericum perforatum* by LC/SPE/NMR and/or LC/MS, *Phytochemistry* **68** (2007), 383–393.

[88] S.-H. Lam, C.-Y. Wang, C.-K. Chen, and S.-S. Lee, Chemical Investigation of *Phyllanthus reticulatus* by HPLC-SPE-NMR and Conventional Methods, *Phytochem. Anal.* **18** (2007), 251–255.

[89] C. Clarkson, E.V. Madikane, S.H. Hansen, P.J. Smith, and J.W. Jaroszewski, HPLC-SPE-NMR Characterization of Sesquiterpenes in Antimycobacterial Fraction from *Warburgia salutaris*, *Planta Med*. **73** (2007), 578–584.

[90] S.-S. Lee, H.-C. Lin, and C.-K. Chen, Acylated Flavonol Monoharmnosides, α-Glucosidase Inhibitors, from *Machilus philippinensis*, *Phytochemistry* **69** (2008), 2347–2353.

[91] Y.-L. Yang, W.-Y. Liao, W.-Y. Liu, C.-C. Liaw, C.-N. Shen, Z.-Y. Huang, and S.-H. Wu, Discovery of New Naural Products by Intact-Cell Mass Spectrometry and LC-SPE-NMR: Malbranpyrroles, Novel Polyketides from Thermophilic Fungus *Malbranchea sulfurea*, *Chem. Eur. J.* **15** (2009), 11573–11580.

[92] V. Goulas, V. Exarchou, A.N. Troganis, E. Psomiadou, T. Fotsis, E. Briasoulis, and I.P. Gerothanassis, Phytochemicals in Olive-Leaf Extract and Their Antiproliferative Activity Against Cancer and Endothelial Cells, *Mol. Nutr. Food Res.* **53** (2009), 600–608.

[93] J.R. Kesting, D. Stærk, M.V. Tejesvi, K.R. Kini, H.S. Prakash, and J.W. Jaroszewski, HPLC-SPE-NMR Identification of a Novel Metabolite Containing the Benzo[*c*]oxepin Skeleton from the Endophytic Fungus *Pestalotiopsis virgatula* Culture, *Planta Med*. **75** (2009), 1104–1106.

[94] H. Gao, M. Zehl, H. Kaehlig, P. Schneider, H. Stuppner, L. Moreno, Y. Banuls, R. Kiss, and B. Kopp, Rapid Structural Identification of Cytotoxic Bufadienolide Sulfates in Toad Venom from *Bufo melanosticus* by LC-DAD-MS^n and LC-SPE-NMR, *J. Nat. Prod.* **73** (2010), 603–608.

[95] N.P. Vasilev, M.K. Julsing, A. Koulman, C. Clarkson, H.J. Woerdenbag, I. Ionkova, R. Bos, J.W. Jaroszewki, O. Kayser, and W.J. Quax, Bioconversion of Deoxypodophyllotoxin into Epipodophyllotoxin in *E. coli* Using Human Cytochrome P450 3A4, *J. Biotechnol.* **126** (2006), 383–393.

[96] D. Djukovic, E. Appiah-Amponsah, N. Shanaiah, G.A. Nagana Gowda, I. Henry, M. Everly, B. Tobias, and D. Raftery, Ibuprofen Metabolite Profiling Using a Combination of SPE/Column-Trapping and HPLC–Micro-Coil NMR, *J. Pharm. Biomed. Anal.* **47** (2008), 328–334.

[97] F. Gillotin, P. Chiap, M. Frédérich, J.-C. Van Heugen, P. Francotte, P. Lebrun, B. Pirotte, and P. de Tullio, Coupling of Liquid Chromatography/Tandem Mass Spectrometry and Liquid Chromatography/Solid-Phase Extraction/NMR Techniques for the Structural Identification of Metabolites Following In Vitro Biotransformation of SUR1-Selective ATP-Sensitive Potassium Channel Openers, *Drug Metab. Dispos.* **38** (2010), 232–240.

[98] Y.-C. Lai, T.-F. Kuo, C.-K. Chen, H.-J. Tsai, and S.-S. Lee, Metabolism of Dicentrine: Identification of the Phase I and Phase II Metabolites in Miniature Pig Urine, *Drug Metab. Dispos.* **38** (2010), 1614–1722.

[99] M. Sandvoss, B. Bardsley, T.L. Beck, E. Lee-Smith, S.E. North, P.J. Moore, A. J. Edwards, and R.J. Smith, HPLC-SPE-NMR in Pharmaceutical Development: Capabilities and Applications, *Magn. Reson. Chem.* **43** (2005), 762–770.

[100] J. Larsen, D. Stærk, C. Cornett, S. Hansen, and J.W. Jaroszewski, Identification of Reaction Products Between Drug Substances and Excipients by HPCL-SPE-NMR: Ester and Amide Formation Between Citric Acid and 5-Aminosalicylic Acid, *J. Pharm. Biomed. Anal.* **49** (2009), 839–842.

[101] F. Xu and A.J. Alexander, The Design of an On-Line Semi-preparative LC-SPE-NMR System for Trace Analysis, *Magn. Reson. Chem.* **43** (2005), 776–782.

[102] A.J. Alexander, F. Xu, and C. Bernard, The Design of a Multi-dimensional LC-SPE-NMR System (LC^2-SPE-NMR) for Complex Mixture Analysis, *Magn. Reson. Chem.* **44** (2006), 1–6.

[103] C. Pa, F. Liu, Q. Ji, W. Wang, D. Drinkwater, and R. Vivilecchia, The Use of LC/MS, GC/MS, and LC/NMR Hyphenated Techniques to Identify a Drug Degradation Product in Pharmaceutical Development, *J. Pharm. Biomed. Anal.* **40** (2006), 581–590.

[104] T. Murakami, T. Kawasaki, A. Takemura, N. Fukutsu, N. Kishi, and F. Kusu, Identification of Degradation Products in Loxoprofen Sodium Adhesives Tapes by Extraction-Solid-Phase Extraction Coupled to Liquid Chromatography–Nuclear Magnetic Resonance Spectroscopy, *J. Chromatogr. A* **1208** (2008), 164–174.

[105] A. Mazumder, A. Kumar, A.K. Purohit, and D.K. Dubey, Application of High Performance Liquid Chromatography Coupled to On-Line Solid-Phase Extraction–Nuclear Magnetic Resonance Spectroscopy for the Analysis of Degradation Products of V-Class Nerve Agents and Nitrogen Mustard, *J. Chromatogr. A* **1217** (2010), 2887–2894.

[106] C. Seger, M. Godejohann, M. Spraul, H. Stuppner, and F. Hadacek, Reaction Product Analysis by High-Performance Liquid Chromatography–Solid-Phase Extraction–Nuclear Magnetic Resonance Applications to the Absolute Configuration Determination of Naturally Occurring Polyyne Alcohols, *J. Chromatogr. A* **1136** (2006), 82–88.

[107] A.J. Simpson, L.-H. Tseng, M.J. Simpson, M. Spraul, U. Braumann, W.L. Kingery, B.P. Kelleher, and M.H.B. Hayes, The Application of LC-NMR and LC-SPE-NMR to the Compositional Studies of Natural Organic Matter, *Analyst* **129** (2004), 1216–1222.

[108] V. Exarchou, M. Godejohann, T.A. Van Beek, I.P. Gerothanassis, and J. Vervoort, LC-UV–Solid-Phase Extraction–NMR-MS Combined with a Cryogenic Flow Probe and Its Application to the Identification of Compounds Present in Greek Oregano, *Anal. Chem.* **75** (2003), 6288–6294.

[109] C. Seger, M. Godejohann, L.-H. Tseng, M. Spraul, A. Girtler, S. Sturm, and H. Stuppner, LC-DAD-MS/SPE-NMR Hyphenation—A Tool for the Analysis of Pharmaceutical Used Plant Extracts: Identification of Isobaric Iridoid Glycoside Regioisomer from *Harpagophytum procumbens*, *Anal. Chem.* **77** (2005), 878–885.

[110] S. Bieri, E. Varesio, J.-L. Veuthey, O. Muňoz, L.-H. Tseng, U. Braumann, M. Spraul, and P. Christen, Identification of Isomeric Tropane Alkaloids from *Schizanthus grahamii* by HPLC-NMR with Loop Storage and HPLC-UC-MS/SPE-NMR Using a Cryogenic Flow Probe, *Phytochem. Anal.* **17** (2006), 78–86.

[111] D. Sørensen, A. Raditsis, L.A. Trimble, B.A. Blackwell, M.W. Sumarah, and J. D. Miller, Isolation and Structure Elucidation by LC-MS-SPE/NMR: PR Toxin- and Cuspidatol-Related Eremophilane Sesquiterpenes from *Penicillium roqueforti*, *J. Nat. Prod.* **70** (2007), 121–123.

[112] B. Schmidt, J.W. Jaroszewski, R. Bro, M. Witt, and D. Stærk, Combining PARAFAC Analysis of HPLC-PDA Profiles and Structural Characterization Using HPLC-PDA-SPE-NMR-MS Experiments: Commercial Preparations of St. John's Wort, *Anal. Chem.* **80** (2008), 1978–1987.

[113] K. Sprogøe, D. Stærk, H.L. Ziegler, T.H. Jensen, S.B. Holm-Møller, and J. W. Jaroszewski, Combining HPLC-PDA-MS-SPE-NMR with Circular Dichroism for Complete Natural Products Characterization in Crude Extracts: Levorotatory Gossypol in *Thespesia danis*, *J. Nat. Prod.* **71** (2008), 516–519.

[114] T. Grevenstuk, J.J.J. Van der Hooft, J. Vervoort, P. de Waard, and A. Romano, Iridoid and Caffeoyl Phenylethanoid Glycosides of the Endangered Carnivorous Plant *Pinguicula lusitanica* L. (Lentibulariaceae), *Biochem. Syst. Ecol.* **37** (2009), 285–289.

[115] C.A. Motti, M.L. Freckelton, D.M. Tapiolas, and R.H. Willis, FTICR-MS and LC-UV/MS-SPE-NMR Applications for the Rapid Dereplication of a Crude Extract from the Sponge *Ianthella flabelliformis*, *J. Nat. Prod.* **72** (2009), 290–294.

[116] J.R. Kesting, I.-L. Tolderlund, A.F. Pedersen, M. Witt, J.W. Jaroszewski, and D. Staerk, Piperidine and Tetrahydropyridine Alkaloids from *Lobelia siphilitica* and *Hippobroma longiflora*, *J. Nat. Prod.* **72** (2009), 312–315.

[117] M.M. Pedersen, J.C. Chukwujekwu, C.A. Lategan, J. Van Staden, P.J. Smith, and D. Staerk, Antimalarial Sesquiterpene Lactones from *Distephanus angulifolius*, *Phytochemistry* **70** (2009), 601–607.

[118] D. Staerk, J.R. Kesting, M. Sairafianpour, M. Witt, J. Asili, S.A. Emami, and J.W. Jaroszewski, Accelerated Dereplication of Crude Extracts Using HPLC-PDA-MS-SPE-NMR: Quinolinone Alkaloids of *Haplophyllum acutifolium*, *Phytochemistry* **70** (2009), 2055–1061.

[119] M. Pérez-Trujillo, A.M. Gómez-Caravaca, A. Segura-Carretero, A. Fernández-Gutiérrez, and T. Parella, Separation and Identification of Phenolic Componds of Extra Virgin Olive Oil from *Olea europaea* L. by HPLC-DAD-SPE-NMR/MS: Identification of a New Diastereoisomer of the Aldehydic Form of Oleuropein Aglycone, *J. Agric. Food Chem.* **58** (2010), 9129–9136.

[120] A. Castro, S. Mocco, J. Coll, and J. Vervoort, LC-MS-SPE-NMR for the Isolation and Characterization of *neo*-Clerodane Diterpenoids from *Teucrium luteum* subsp. *flavovirens*, *J. Nat. Prod.* **73** (2010), 962–965.

[121] J.R. Kesting, J.Q. Huang, and D. Sørensen, Identification of Adulterants in a Chinese Herbal Medicine by LC-MS-SPE/NMR and Comparative In Vivo Study Standards in a Hypertensive Rat Model, *J. Pharm. Biomed. Anal.* **51** (2010), 705–711.

[122] S. Agnolet, J.W. Jaroszewski, R. Verpoorte, and D. Staerk, ^{1}H NMR-Based Metabolomics Combined with HPLC-PDA-MS-SPE-NMR for Investigation of Standardized *Ginkgo biloba* Preparations, *Metabolomics* **6** (2010), 292–302.

[123] M. Godejohann, L.-H. Tseng, U. Braumann, J. Fuchser, and M. Spraul, Characterization of a Paracetamol Metabolite Using On-Line LC-SPE-NMR-MS and Cryogenic NMR Probe, *J. Chromatogr. A* **1058** (2004), 191–196.

[124] R.J. Lewis, M.A. Bernstein, S.J. Duncan, and C.J. Sleigh, A Comparison of Capillary-Scale LC-NMR with Alternative Techniques: Spectroscopic and Practical Considerations, *Magn. Reson. Chem.* **43** (2005), 783–789.

[125] A.W. Nicholls, I.D. Wilson, M. Godejohann, J.K. Nicholson, and J.P. Shockcor, Identification of Phenacetin Metabolites in Human Urine After Administration of Phenacetin-C^2H_3: Measurement of Futile Metabolic Deacetylation via HPLC/MS-SPE-NMR and HPLC-ToF MS, *Xenobiotica* **36** (2006), 615–629.

[126] B. Kammerer, H. Scheible, G. Zurek, M. Godejohann, K.-P. Zeller, C.H. Gleiter, W. Albrecht, and S. Laufer, In Vitro Metabolite Identification of ML3403, a 4-Pyridinylimidazole-Type p38 MAP Kinase Inhibitor by LC-Qq-TOF-MS and LC-SPE-Cryo-NMR/MS, *Xenobiotica* **37** (2007), 280–297.

[127] S.M. Ceccarelli, G. Schlotterbeck, P. Boissin, M. Binder, B. Buettelmann, S. Hanlon, G. Jaeschke, S. Kolczewski, E. Kunfer, J.-U. Peters, R.H.P. Porter, E.P. Prinssen, M. Rueher, I. Ruf, W. Spooren, A. Stämpfli, and E. Vierira, Metabolite Identification via LC-SPE-NMR-MS of the In Vitro Biooxidation Products of a Lead mGlu5 Allosteric Antagonist and Impact on the Improvement of Metabolic Stability in the Series, *ChemMedChem* **3** (2008), 136–144.

[128] C.A. Olsen, M. Lambert, M. Witt, H. Franzyk, and J.W. Jaroszewski, Solid-Phase Peptide Synthesis and Circular Dichroism Study of Chiral β-Peptoid Homooligomers, *Amino Acids* **34** (2008), 465–471.

[129] M. Godejohann, L. Heintz, C. Daolio, J.-D. Berset, and D. Muff, Comprehensive Non-target Analysis of Contaminated Groundwater of a Former Ammunition Destruction Site Using ^{1}H-NMR and HPLC-SPE-NMR/TOF-MS, *Environ. Sci. Technol.* **43** (2009), 7055–7061.

[130] S. Schmidt, C. Piechotta, M. Godejohann, T. Win, I. Nehls, and C. Mügge, Characterization of Commercially Available Linear Alkylbenzenesulfonates by LC-SPE-NMR/MS (Liquid Chromatography–Solid Phase Extraction–Nuclear Magnetic Resonance Spectroscoppy–Mass Spectroscopy), *Talanta* **82** (2010), 142–150.

7

Special Topics and Applications Related to LC-NMR

7.1. INTRODUCTION

Since the late 1970s, scientists have attempted the hyphenation of NMR with separation analytical techniques to target the structural elucidation of organic components from complex mixtures because NMR plays a major role in detecting how the atoms are bonded and spatially distributed in the molecule (see Sections 2.3 and 2.4 for more details on the historical development of hyphenated NMR). However, hyphenated NMR is not always the choice for that type of structural analysis. The classical methodology is to isolate the analytes of interest and perform structural analysis. This method is still used in many laboratories. There are cases of complex mixtures, chiral analysis, and reaction monitoring in which NMR has played a role in both modalities as an off-line and an online technique. Understanding when to carry out off-line or online analysis (depending on the type of sample and the question to be answered through the analysis) is crucial in providing accurate results in a timely fashion. In addition, approaches other than hyphenated NMR have been applied directly to complex mixtures for the structural analysis of their components. All those cases are discussed to evaluate the best options to use to solve analytical problems in those areas.

LC-NMR and Other Hyphenated NMR Techniques: Overview and Applications, First Edition. Maria Victoria Silva Elipe.

7.2. OFF-LINE VERSUS ONLINE NMR FOR STRUCTURAL ELUCIDATION

When to apply off-line or online NMR for structural analysis is the key to providing timely structural analysis results. If the hyphenated techniques are not available commercially, it is difficult to access them to solve problems. The selection of off-line or online analysis will depend on the type of sample and the difficulty of the analysis.

7.2.1. Cases Solved Off-Line

Separation analytical techniques commonly populate analytical laboratories for many types of analysis and profiling of complex mixtures. A vast number of analytical chemists are trained to use HPLC as a major technique for analyzing mixtures and separating their components. Only a small percentage of analysts are trained to perform NMR analysis. Therefore, the highly successful classical methodology is to separate the analytes of interest for off-line NMR analysis. In many of these cases, separation of the analytes is not problematic as long as the sample is stable during the isolation process. Many packing materials for column separation have been developed and are available commercially, providing an entire set of different conditions under which to separate components of complex mixtures with different properties, such as polarity, molecular size, ionic nature, and others. Sometimes there is no need to perform complete isolation of the components of mixtures to determine their structures. This was the case for the two dimer impurities (unknowns 1 and 2) of the drug substance AMG 517, where a partial purification with a fraction containing the two dimer impurities was analyzed by MS and NMR (Figure 7-1) [1]. During the kilogram scale-up production of the drug substance AMG 517, two new impurities (unknowns 1 and 2) were detected at greater levels than 0.1% in several batches and needed to be characterized, due to regulatory requirements for potential toxicological effects [1]. Preliminary LC-MS analysis indicated that potentially they matched the dimeric structure of the drug substance, and accurate mass determination suggested one unknown to be a simple dimer of AMG 517 and the other a dimer with an additional 32 mass units, potentially [dimer + 2O] or [dimer + S]. As indicated previously, an enriched fraction containing the two impurities was analyzed by conventional NMR in which the sample was dissolved in deuterated solvent (DMSO-*d*6) and transferred to a 2.5-mm NMR tube for NMR analysis. Comparing the NMR data of the fraction containing both dimers with AMG 517, it was concluded that both dimers were symmetric, with the monomers attached to the corresponding benzothiazole rings with a 2,4,7 substitution pattern for that ring compared to the drug substance AMG

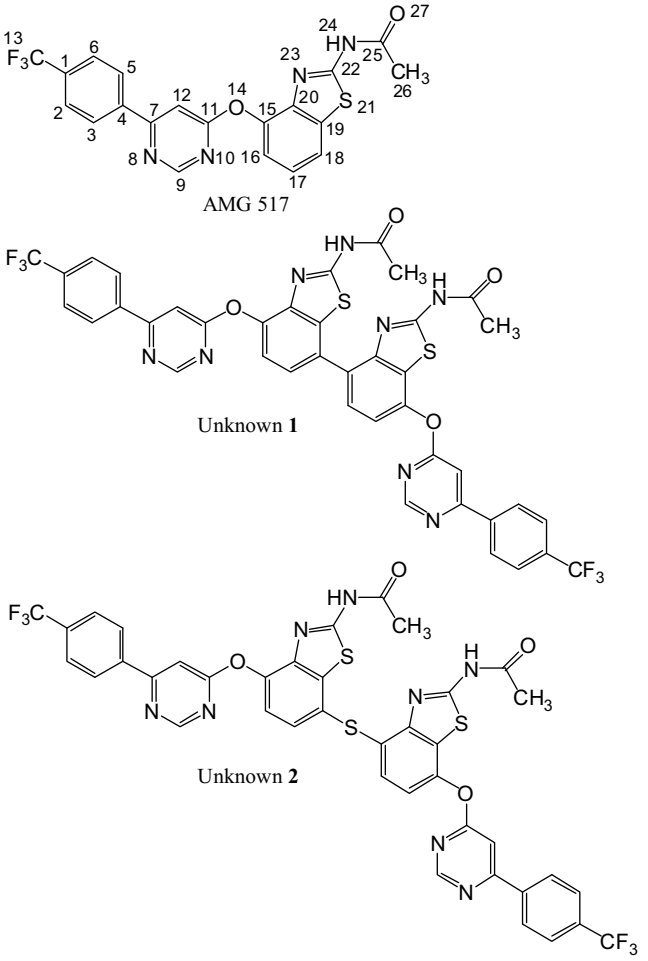

FIGURE 7-1. Structures of drug substance AMG 517 and its two dimer impurities (unknowns 1 and 2) [1]. The numbers on the structure of AMG 517 indicate the positions of the atoms used for NMR assignments.

517, which had a 2,7 substitution pattern for the benzothiazole ring. In addition, the proton and carbon chemical shifts of the benzothiazole rings were not significantly different. This points to the option of a simple dimer for one, with the other dimer having one sulfur between the two monomers instead of two oxygens somewhere in the dimer molecule (Figure 7-1) [1]. Figures 7-2 and 7-3 show the aromatic region of AMG 517 and an enriched fraction containing both impurity dimers for one-dimensional ^{1}H NMR spectra, a two-dimensional ^{1}H–^{13}C HSQC spectrum for the enriched fraction, and a two-dimensional ^{1}H–^{13}C HMQC spectrum for AMG 517—which point out the slight differences described above. Based on the NMR analysis and accurate

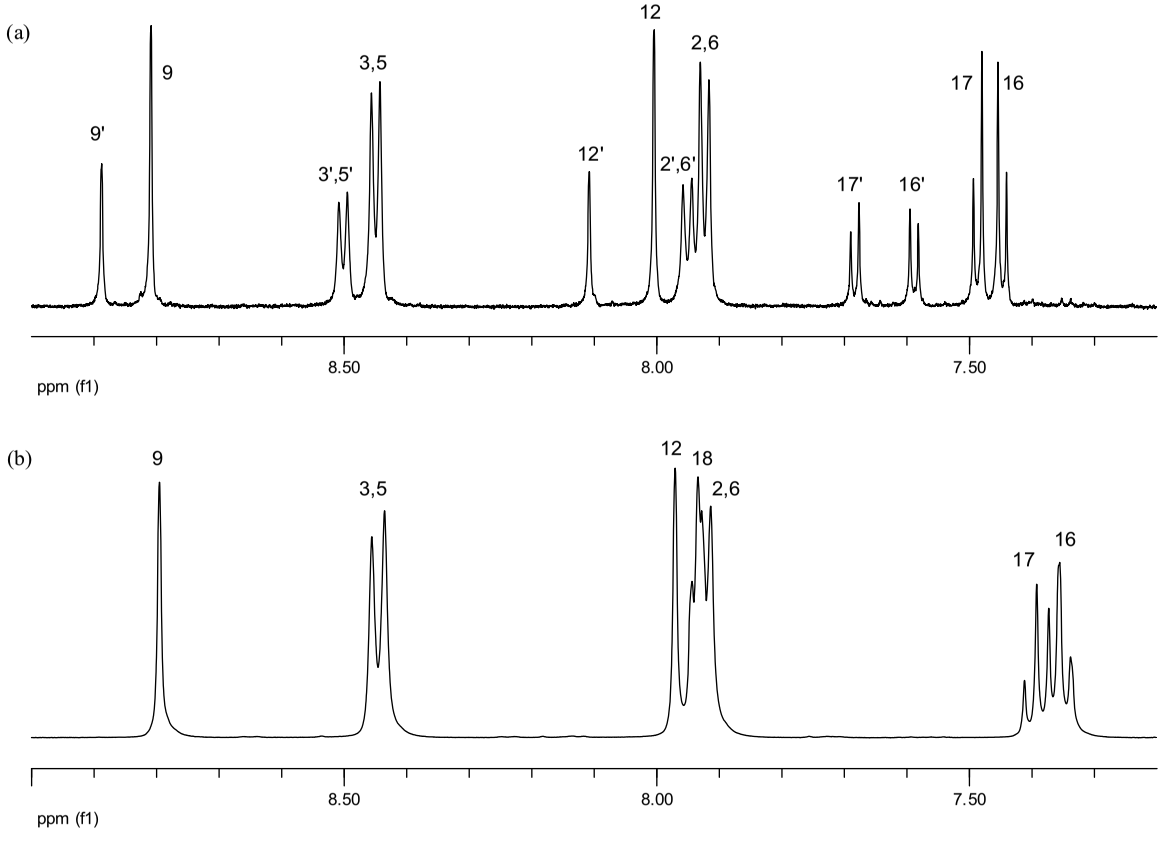

FIGURE 7-2. Aromatic region of the ^{1}H NMR spectra of the enriched impurity fraction (panel a, 600 MHz) and AMG 517 (panel b, 400 MHz) in DMSO-*d*6. Figure 7-1 shows the numerical atomic labeling for AMG 517 used for ^{1}H and ^{13}C NMR assignments. The numbers designated as prime (e.g., 2′) in panel a represent the signals of the impurity named unknown 1, and all others represent the signals of unknown 2 [1].

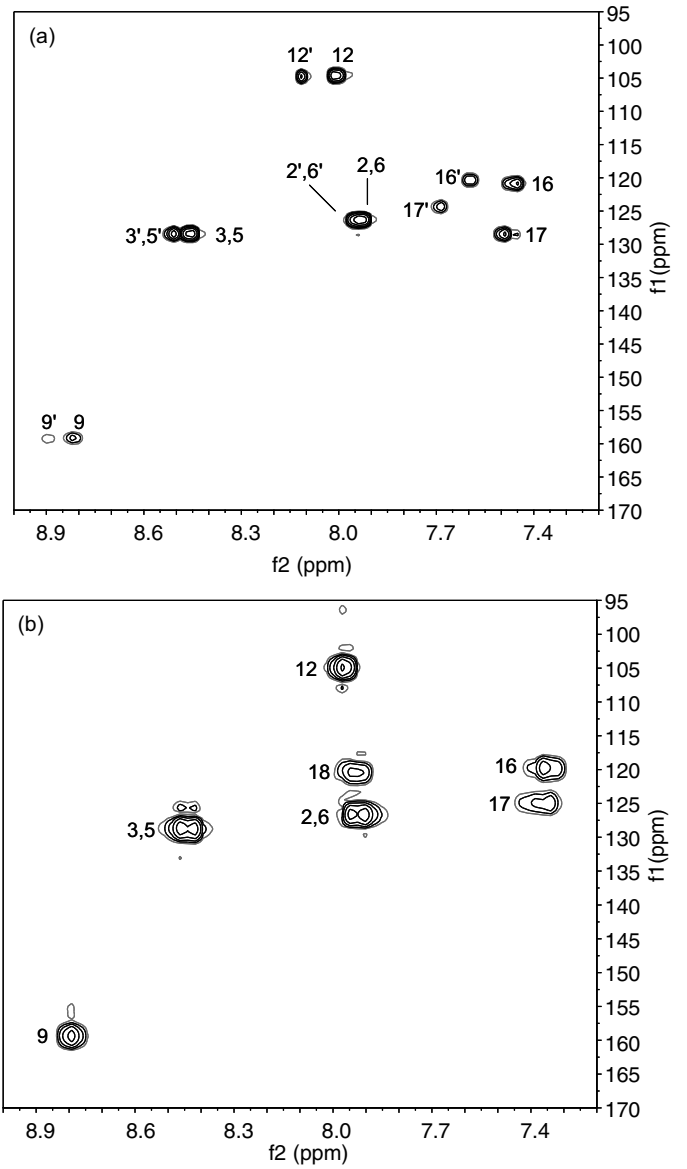

FIGURE 7-3. Aromatic region of the two-dimensional $^{1}H-^{13}C$ HSQC spectrum of the enriched impurity fraction (panel a, 600 MHz) and the two-dimensional $^{1}H-^{13}C$ HMQC spectrum of AMG 517 (panel b, 400 MHz) in DMSO-*d*6. Figure 7-1 shows the numerical atomic labeling for AMG 517 used for ^{1}H and ^{13}C NMR assignments. The numbers designated as prime (e.g., 2′) in panel a represent the signals of the impurity named unknown 1, and all others represent the signals of unknown 2 [1].

mass information, the structures proposed for the dimers were a simple dimer and [dimer + S] (Figure 7-1). Further investigation by the authors indicated that the source of dimer impurities present in the bezothiazole starting material was carried over through the synthetic process of AMG 517 (Figure 7-4) [1].

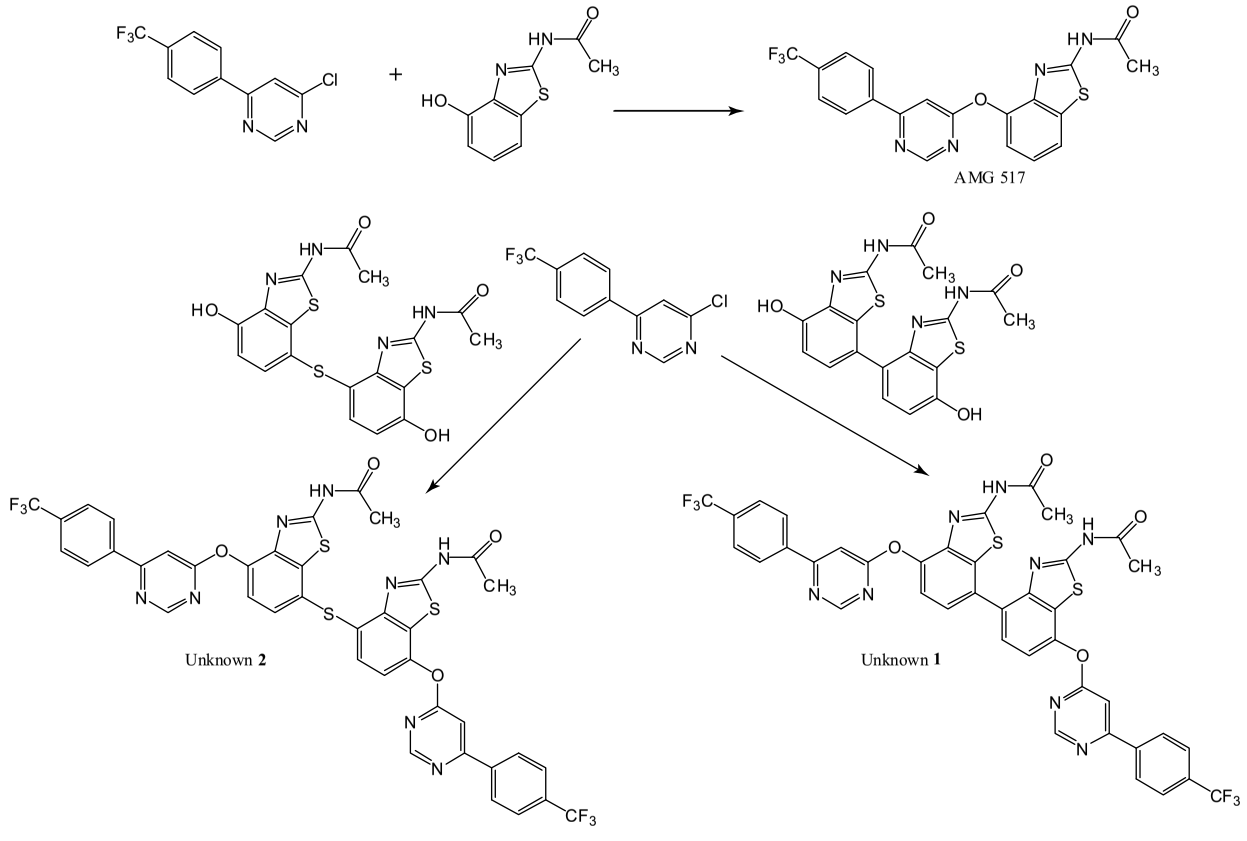

FIGURE 7-4. Synthetic formation of AMG 517 and proposed formation pathway for the two dimer impurities (unknowns 1 and 2) [1].

This case was solved without the use of hyphenated techniques except for LC-MS and without complete purification of the dimer impurities. The information gathered from HPLC, MS, and NMR was sufficient to propose the structures and the synthetic formation pathway of these impurities [1].

Sharman and Jones [2] indicated that LC-NMR is practical for major components but not as convenient for minor components of mixtures. The major drawbacks of LC-NMR for the analysis of minor components is the need to overload the column by injecting 1000 times the amount of sample to analyze 0.1% minor components, which is the threshold level for determining the structures of drug impurities based on regulatory requirements. This means that to analyze 1 μg of sample for a component that comprises 0.1% of the sample mixture, it is necessary to inject at least 1 mg of sample containing 0.1% of the impurity of interest. When the injection overloads the column, the chromatographic peaks are broad and occupy a larger volume than the typical volume of NMR flow cells. Therefore, only a portion of the chromatographic peak is "seen" by the receiver coil in the NMR flow cell [2]. Sharman and Jones [2] also indicated that when handling the sample in the NMR tube, there is no chance to lose it through complications from leakage through the plumbing of the LC-NMR system, and more NMR experiments can be conducted when the sample is in the NMR tube, as long as it is stable. LC-NMR provides some advantages for unstable and light-sensitive samples [3]. Sharman and Jones [2] claimed that the vast majority of samples are relatively stable, because unstable samples should not be detected or observed in the first place, especially considering that sample handling in an NMR tube is more robust than for LC-NMR [2]. In fact, isolation of the analytes of interest for their structural elucidation has not decreased in recent years, especially in the areas of impurities and degradation products [3–20]. Hiriyanna et al. [6] isolated the forced stress degradation products of olanzapine under acidic, basic, oxidative, and light conditions to determine their structures off-line by MS and NMR (Figure 7-5). Sharma's group [20] determined the structure of a new degradation product of sultamicillin during stability storage studies (Figure 7-6). For its characterization, the impurity was isolated and a complete set of one- and two-dimensional homo- and heteronuclear NMR experiments was performed. The stability data indicated that the degradation product was formed following temperature rises over time. During thermal stress conditions, sultamicillin degrades to ampicillin, releasing formaldehyde as a by-product that will react further with the amino group of sultamicillin, forming the degradation product after cyclization (Figure 7-6) [20].

Off-line NMR has the advantages of not being dependent on the width of the chromatographic peak of interest, HPLC conditions, and NMR solvent suppression techniques, because it is independent of HPLC conditions of

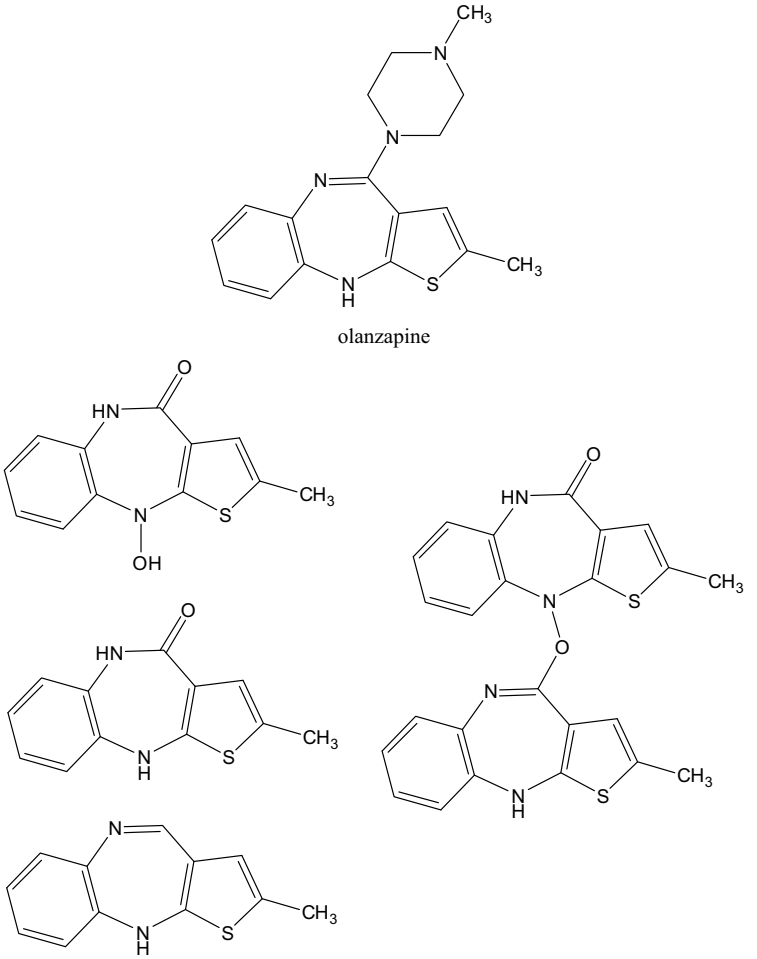

FIGURE 7-5. Structure of olanzapine and its isolated forced stress degradation products under acidic, basic, oxidative, and light conditions [6].

isolation. In addition to these factors, using deuterated solvents to dissolve the sample and transfer it to the NMR tube makes two-dimensional homo- and heteronuclear NMR experiments more convenient to perform than online or hyphenated LC-NMR because the amount of sample under the coil is well known in the NMR tube but not in the flow cell of the LC-NMR system.

7.2.2. Cases Solved Online

As shown in Chapters 4, 5 and 6, there are many cases of structural analysis of complex mixtures that have been solved by numerous separation analytical techniques hyphenated with NMR in the areas of natural products, drug

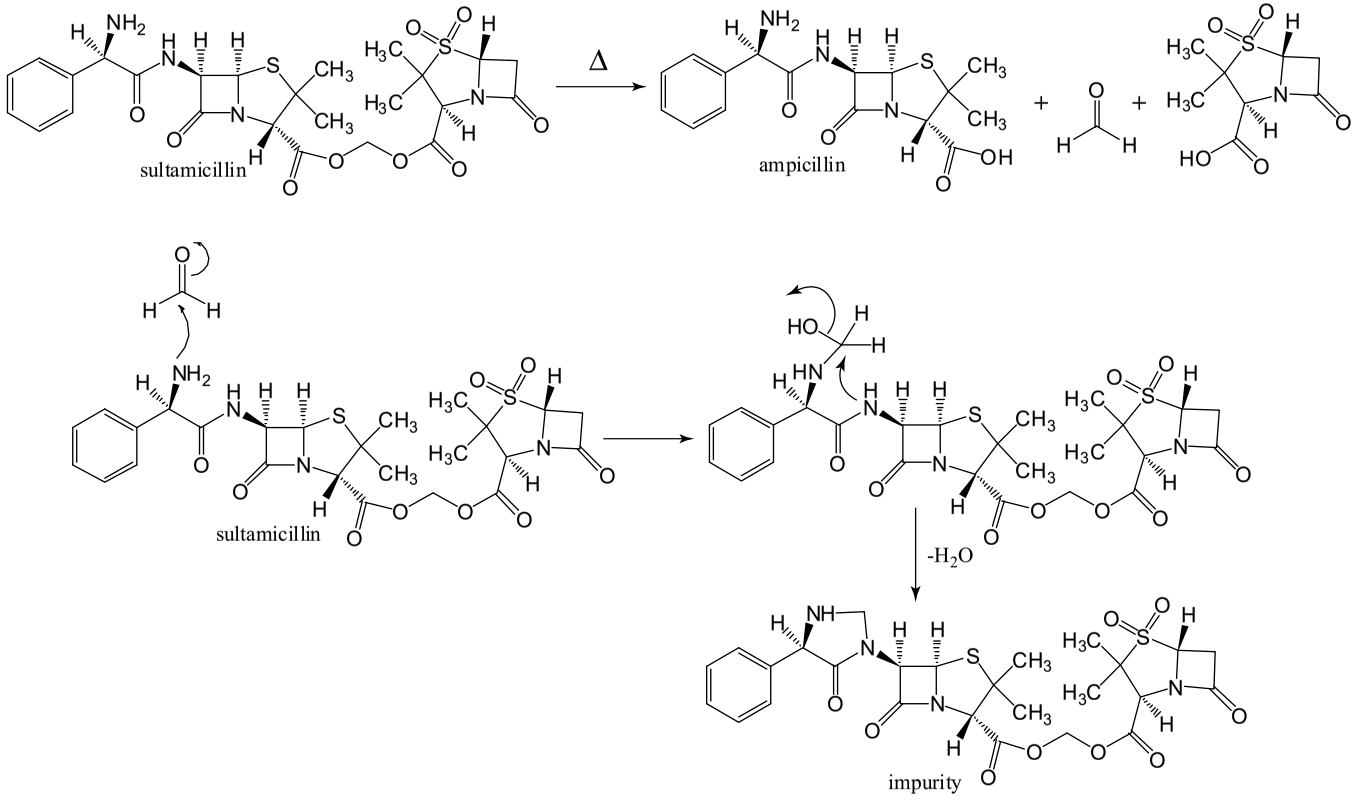

FIGURE 7-6. Thermal stress degradation of sultamicillin, which forms ampicillin by releasing formaldehyde that reacts with another molecule of sultamicillin to form the impurity structure determined by off-line NMR [20].

metabolism, drug discovery and development, drug degradation products and impurity characterization, food analysis, polymers, metabonomics and metabolomics, the environmental field, and others. Unstable or volatile analytes are ideal candidates for online structural determination by hyphenated NMR. As shown in Chapter 6, capillary analytical techniques are excellent options for trace analysis. However, most of those hyphenated techniques are not available commercially or are less accessible to analytical laboratories. SPE has bloomed as SPE-NMR and even SPE-MS-NMR for the structural analysis of minor components, including trace analysis. The advantage of SPE for structural analysis of the analyte of interest as part of a complex mixture is its concentration in an SPE cartridge by subsequent injections into the HPLC for separation. Once the analyte is concentrated and dried, it will be flushed toward the NMR flow cell with deuterated solvents for its structural analysis. With SPE-NMR, the NMR analysis is independent of the HPLC separation conditions, solvent system, and width of the chromatographic peak in the chromatogram during separation. The LC-MS-NMR technique is available commercially through NMR vendors, but it is not commonly available in many laboratories, due to its cost and the cumbersome combination of techniques with different sensitivities (see Chapters 3 and 5). Even though hyphenated NMR has been available since its development in the late 1970s as a noncommercial technology, it has not replaced the off-line approach of HPLC and NMR. As indicated earlier, the traditional methodology of isolating the analyte of interest is still in wide use. Online NMR has been used detached from HPLC for the purpose of rapid analysis but without separating the analyte of interest prior to NMR analysis. Those options have been covered somewhere else, as they are not the objective of this book [21].

7.3. ANALYSIS OF CHIRAL MOLECULES BY NMR

Determination of the absolute configuration of the chiral center of an organic molecule by NMR is challenging. The main issue is that NMR cannot distinguish enantiomers because they are mirror images, and magnetically active nuclei such as protons have the same chemical environment in both enantiomers. Diasteromers have some differences in the local chemical environment for some of the protons or other magnetically active nuclei in the molecule around the chiral center. Therefore, NMR will show some differences in the chemical shifts and even in some coupling constants around the chiral portion of the molecule. If the absolute configuration of one of the chiral centers in a molecule is known, it is possible to determine the relative stereochemistry of another chiral center in the molecule when it is in the surrounding area and no farther away than 5 Å, typically carried out by

one-dimensional NOE/ROE and two-dimensional NOESY/ROESY NMR experiments. The classical approach for these chemistry problems is by carrying out the analysis in an NMR tube. There have been some attempts to perform NMR experiments through hyphenated LC-NMR, as described below.

7.3.1. Classical Approach: Off-Line

The classical approach to conformational analysis by NMR is through one-dimensional NOE/ROE and two-dimensional NOESY/ROESY NMR experiments [22]. However, as indicated above, absolute configuration by NMR is not possible when measuring enantiomeric molecules directly and if no chiral information is known for diastereomeric molecules to determine the relative stereochemistry of chiral centers in spatial proximity. Knowing that NMR provides such detailed information on how the atoms are bonded in three-dimensional space, two indirect approaches have been developed to determine absolute stereochemistry in organic compounds. The first approach is through chemical derivatization with chiral agents, and the second is through exposing the molecule to an alignment medium.

The chiral derivatization approach, known as the *Mosher method*, was first described in 1973 [23]. The method uses the Mosher reagent, α-methoxy-α-trifluoromethylphenylacetate (MTPA) esters to distinguish the (*R*)- and (*S*)-absolute configuration of chiral compounds through differences in the chemical shifts of the derivatives due to anisotropic effects, depending on the orientation of the chiral ester toward the phenyl group of MTPA [23]. Since then, many other chiral agents have been developed [24,25]. The functional groups attached to the chiral center of interest that are derivatized are α-chiral secondary alcohols, β-chiral primary alcohols, α-chiral tertiary alcohols, α-chiral primary amines, secondary amines, α-chiral carboxylic acids, β-chiral carboxylic acids, chiral sulfoxides, and chiral polyhydroxylated compounds, studied by measuring the differences in the chemical shifts of ^{1}H, ^{19}F, and ^{13}C when applicable. A description of those methods may be found in the literature (e.g., references 24 and 25). Riguera's group [24,26] developed a faster method by mixing the auxiliary reagent bound to a solid matrix with the chiral substrate of interest directly in the NMR tube to acquire NMR data a few minutes after the mixing step and without the need for further chemical manipulation. The authors tested this methodology by derivatizing chiral alcohols and amines. In addition, they carried out the complexation of the resin bound to methoxyphenylacetic acid (MPA) esters or amides with Ba^{2+} ion coming from $BaClO_4$ added to the solution in the NMR tube for NMR analysis [24,26].

A new methodology applied to organic small molecules is the measurement of residual dipolar couplings (RDCs) when the analyte of interest is exposed to

an alignment medium [27–30]. The molecules of the analyte of interest are oriented in a particular manner based on the alignment media and the magnetic field. The absolute configuration of the chiral centers of the molecule can be determined through measuring RDCs under those conditions [27–30]. At the time of this writing, no alignment media were available commercially, making it difficult to convert this methodology in a routine analysis. For more information on this topic, see references 27 to 30.

7.3.2. Nonclassical Approach: Online

The online approach to determining the absolute configuration of molecules has been carried out only through chemical derivatization or by connecting a CD instrument to an LC-NMR system, as described in Section 4.2.9. Hyphenated NMR has not been used to determine RDCs, due to the need of pure materials. Its complexity in some of the NMR experiments required for RDCs, and other characteristics of LC-NMR, will not be a benefit when solvent suppression is required. In addition, the method will require the analyte to be under the alignment medium at all times, which would complicate adjusting the HPLC conditions to that case. For the case of chemical derivatization, LC-NMR has been employed to determine the absolute configuration of secondary alcohols coupled to (*R*)- and (*S*)-9-anthrylmethoxyacetic acid (9-AMA) as 9-AMA esters [31]. It has also been used for a new tetrahydrophenanthrene isolated from the aerial parts of the plant *Heliotropium ovalifolium* through its Mosher ester derivativatization in the stop-flow LC-NMR mode [32]. When applying CD to the stereochemistry study, LC-CD and LC-NMR has been combined (LC-CD-NMR) to determine in situ the absolute configuration of the individual enantiomeric chromatographic peaks of a pyridylananine derivative mixture in the stop-flow mode [33].

7.4. MONITORING CHEMICAL REACTIONS IN SITU

Reaction monitoring is an emerging area where analytical techniques are used to understand the kinetics of reactions, if the reactions go into completion, and the yield of the reactions. Reactions will contain a group of components comprised of the reactants, possible intermediates if they are stable, products, solvents, and additives that facilitate or catalyze the reactions. Reactions can be monitored in situ if a device can be placed in the reaction vessel and connected to an analytical instrument to monitor the reaction. Reactions can also be monitored on a small scale to study their kinetics through a variety of analytical techniques. NMR is a preferred technique that provides detailed

structural information on organic molecules. The traditional method of studying kinetics by NMR is based on the scale of the NMR tube. However, in recent years more attempts have been carried out using NMR to monitor reactions in situ in the reactors. Below is a description of both methods.

7.4.1. Classical Approach: Off-Line

The classical approach to monitoring reactions by NMR is through the NMR tube. However, this is limited to small-scale testing, and the kinetics may not be reproducible when the reaction is carried out in reactors on a large scale. In addition, solvent selection is another factor that affects kinetics. When deuterated solvents are used in the reaction, they make NMR operations easier with convenient lock, shimming, and referencing. However, deuterated solvents can affect the kinetics of reactions through their isotopic effect, as discussed in a study of the formation of formaldehyde polymer in water, D_2O, and methanol [34]. To minimize the isotopic effects, no-Deuterium NMR (no-D NMR) is an alternative method used to run the reaction in an NMR tube without deuterated solvents [35,36]. On a small scale, no-D NMR provides useful information on the kinetics and yield of the reaction without isotopic effects. The reagent concentrations must be in the molar range (0.1 to 1.0 M) for the protonated solvents, not to exceed a reagent/solvent ratio of 1 : 10 or 1 : 100 because organic solvents are normally at a concentration of 10 M. The effect of the dynamic range in concentrations between the solvents and the species in solution cannot exceed that range for NMR to be effective as a monitoring reaction tool [35,36]. A classical example is the Fisher esterification of acetic acid in ethanol catalyzed with sulfuric acid and followed in the NMR tube [35].

A proton is the common nucleus used to follow reactions by NMR, but other nuclei can sometimes be a better option when the one-dimensional ^1H NMR spectra are complex or when other magnetically sensitive nuclei are present in the molecule that can provide simple spectra and analysis. ^{19}F and ^{31}P which are 100% abundant in nature, with one-half nuclear spin ($I = 1/2$) and with 0.83 and 0.0663 relative sensitivity compared to ^1H, are part of many organic compounds. A recent case study by ^{31}P NMR is the hydrolysis reaction of phosphoryl trichloride, commonly known as phosphorus oxychloride ($POCl_3$) [37]. $POCl_3$ (1) is a common reagent used in many reactions in organic chemistry, such as the Vilsmeier–Haack and Bischler–Napieralski, Bechman rearrangement, and others. In addition, $POCl_3$ (1) is a very reactive compound, extremely irritative and exothermic, that requires extra care for its elimination from reactions during hydrolysis under acidic conditions. Therefore, $POCl_3$ (1) is more difficult to manage for large-scale reactions. The purpose of the study was to monitor the hydrolysis in high concentrations with

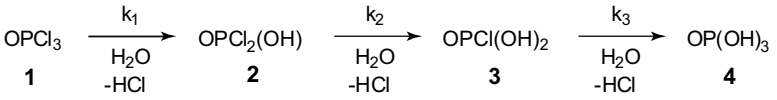

FIGURE 7-7. Mechanism of phosphorus oxychloride ($POCl_3$) hydrolysis [37].

no deuterated solvents (water/acetonitrile 1 : 3 v/v) in the NMR tube to understand the kinetics and the intermediate species formed during the hydrolysis at different pH and temperature values, and to provide safe quenching of energetic metastable intermediates [37]. The study confirmed that the hydrolysis goes through individual replacement of each chlorine atom by a hydroxyl until there is complete conversion to phosphoric acid (4) (Figure 7-7). In addition, the study proved what the literature proposed: that the rate constant k_3 was much greater than k_2, and that of $POCl_3$ (1) was rapidly converted to the first species, the dichlorophosphoric acid [$POCl_2(OH)$ (2)] intermediate, which was metastable with a long half-life, depending on temperature and pH conditions. Figure 7-8 depicts some snapshots by ^{31}P NMR of the hydrolysis reaction, with different temperatures and times showing that dichlorophosphoric acid [$POCl_2(OH)$ (2)] is a predominant

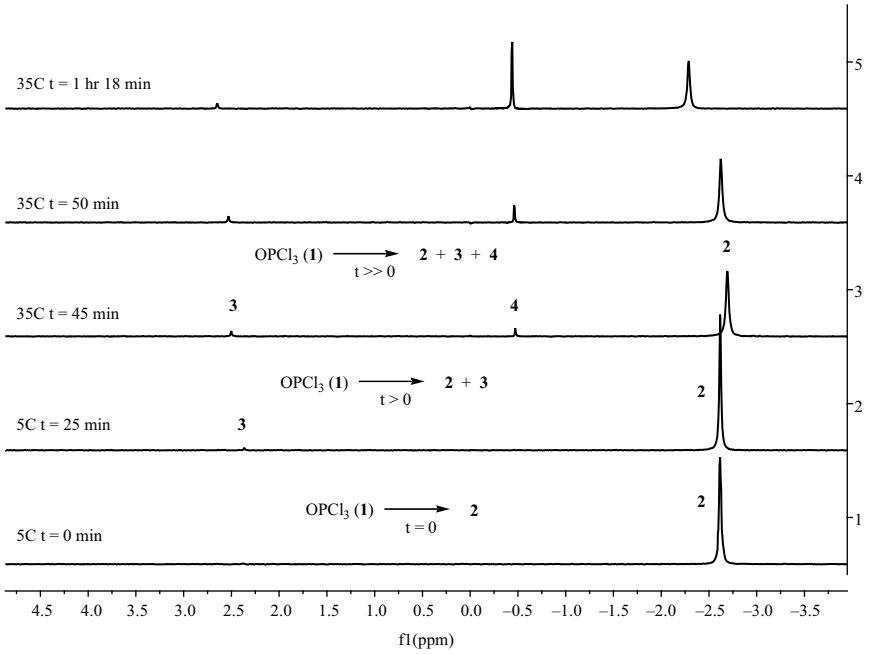

FIGURE 7-8. ^{31}P NMR reaction monitoring of the hydrolysis of $POCl_3$ at different temperatures and times [37]. The numbers corresponds to the species numbered in Figure 7-7.

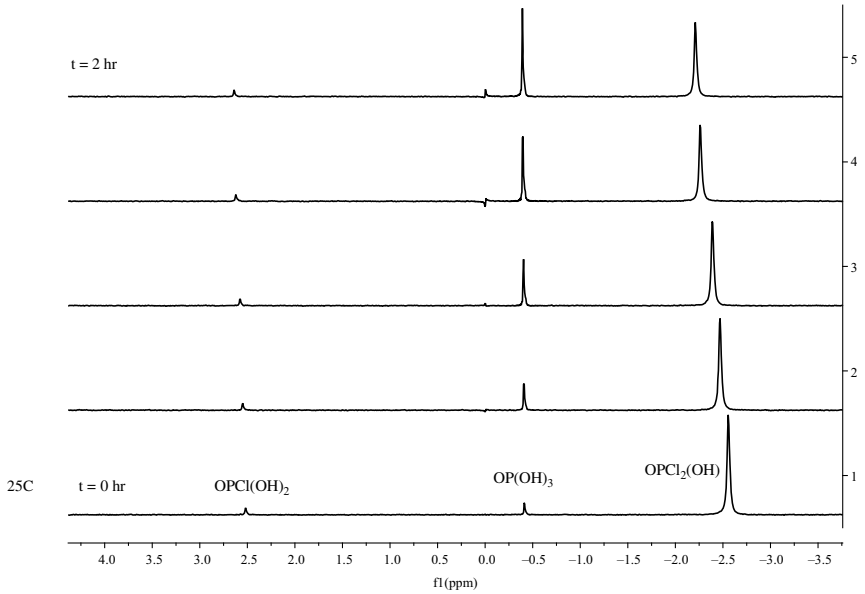

FIGURE 7-9. ^{31}P NMR of the decomposition kinetics of dichlorophosporic acid $POCl_2(OH)$ at 25°C [37].

species, and monochlorophosphoric acid [$POCl(OH)_2$ (3)] is a minor species that remains relatively constant during the reaction. Figure 7-9 depicts snapshots of the hydrolysis at 25°C when no base is added, and Figure 7-10, when 1 equivalent of base is added. Figure 7-10 shows that with base, the monochlorophosphoric acid [$POCl(OH)_2$ (2)] species is not detected because it converts rapidly to phosphoric acid (4) [37]. The signal of phosphoric acid (4) in the spectra in Figures 7-8 to 7-10 was not referenced to 0.00 ppm, to show the changes in chemical shifts due to changes in pH during the reaction under different conditions. The half-life of dichlorophosphoric acid [$POCl_2(OH)$ (2)] from the ^{31}P NMR studies was hours, depending on the pH and temperature in water/acetonitrile 1 : 3 v/v ($t_{1/2}$ = 26 h at 5°C, $t_{1/2}$ = 3.7 h at 25°C, $t_{1/2}$ = 1.1 h at 35°C, $t_{1/2}$ = 7.9 h at 5°C with 1 equivalent of NaOH) [37]. Based on these results, the researchers recommended quenching the excess $POCl_3$ (1) from the corresponding organic chemistry reaction at 20°C in the presence of base (1.5 equivalents of NaOH) to avoid the formation of metastable intermediate containing P−Cl bonds while considering of the solvent and product formation used in the corresponding organic chemistry reaction [37].

In academic settings, fast NMR methodologies such as the two-dimensional ultrafast (UF) TOCSY experiment are being used to monitor reactions in real time in the NMR tube + [38]. Herrera et al. [38] tested the methodology on one pot reaction with a simple ketone, 3-pentanone, and triflic anhydride in

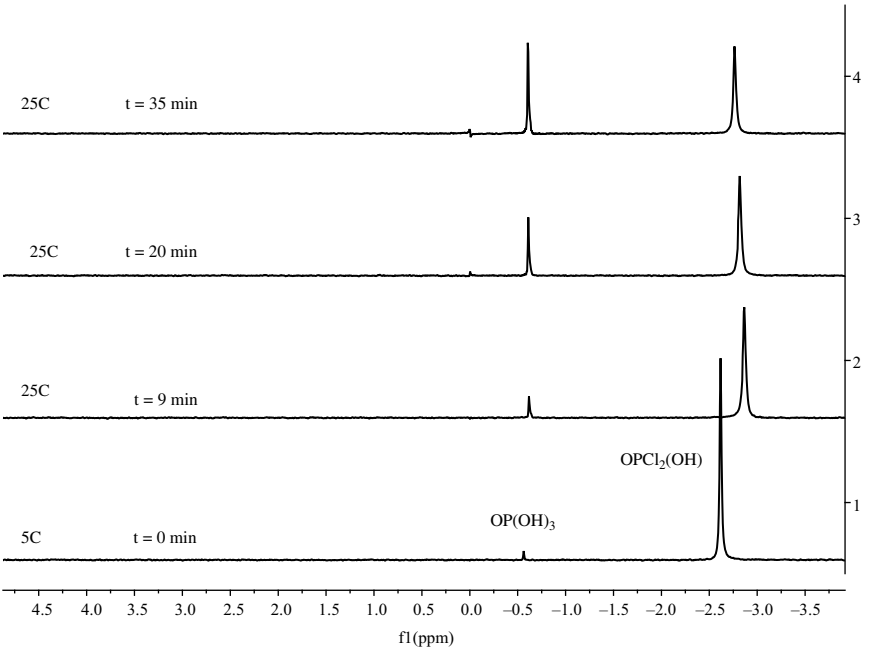

FIGURE 7-10. ^{31}P NMR of the decomposition kinetics of dichlorophosporic acid $POCl_2(OH)$ with 1 equivalent of base (per $POCl_3$) at 25°C [37].

deuterated acetonitrile in a 5-mm NMR tube. While aquiring UF TOCSY experiments during the reaction, the researchers were able to detect and determine the structures of intermediates of the reaction and its kinetics [38]. The only concern with these ultrafast NMR methodologies is that they are not available commercially or easy to use directly from any instrument. As they become available, more options may be applied to monitor reactions using two-dimensional NMR data from fast methodology such as UF TOCSY or even Hadamard spectroscopy.

7.4.2. Nonclassical Approach: Online

In recent years, researchers in the pharmaceutical industry and academia have been exploring the concept of monitoring reactions by NMR beyond the traditional methodology of the NMR tube [39–42]. As indicated above, the NMR tube methodology gives preliminary information on the kinetics and can be comparable when reactions are carried out at a small scale, especially without deuterated solvents, to avoid isotopic effects. However, when reactions are carried out at a scale larger than just a few milliliters, better methodologies are needed to understand in situ the kinetics and speciation, and how to control the reaction. NMR is the ideal technique to provide detailed

information on structural changes in the reagents toward formation of the product of the reaction through the intermediates of the reaction. To accomplish this measurement, the reactor and the NMR instrument have to be attached online. Bernstein's group [39,41,42] has applied online or on-flow NMR by connecting the reactor to the NMR through tubing, allowing the reaction mixture to go to the NMR flow cell to monitor the kinetics of the reaction in situ. In the settings they used, a filter was placed at the end of the tubing that was submerged in the reactor, to avoid solid material blocking the tubing in heterogeneous reactions. In addition, stainless steel tubing was used when solvents corrosive to PEEK tubing [e.g., tetrahydrofuran (THF)] were used. Conventional NMR flow cells provide limited uses for reactions, with minimum variations in pressure and temperature. When temperature and pressure are important variables and they are far from room-temperature conditions, an NMR flow cell for supercritical fluids chromatography (SFC) (SFC-NMR) is a better option [39,40]. Recently, Bernstein's group has developed an inexpensive and simple flow cell to monitor reactions that can handle low flow rates and pressures [42]. Another important consideration in reaction monitoring is to have the minimum distance between the reactor and the magnet of the NMR system, to maximize the residence times of the reaction in the NMR flow cell; to have a reasonable signal-to-noise ratio; and to minimize the distance between the reactor and the NMR to make the measurement of in situ reaction monitoring meaningful. Due to the changes in the species and their concentrations during the reaction, field homogeneity may become a problem, providing distorted NMR signals. To make the data acquisition useful to the study, shimming should only be performed before and after a reaction [41].

Researchers working on establishing the methodology for in situ monitoring reactions by NMR connected directly to chemical reactors are proving the concept by using small reactors attached by tubing to high-resolution NMR instruments, and testing the methodology with known reactions. Examples of reactions are simple imine–aminal formation [39], hydrogen bonding of methanol in near-critical and supercritical carbon dioxide conditions [40], Fisher esterifications [41], hydrolysis of urea [41], simple alkylation reactions [41], simple demesitylation [41], and hydrolysis of simple esters [42]. As more knowledge is gathered from those simple reactions in the coming years, more applications will become available for the pharmaceutical industry, with the potential to use this technique on process analytical technology platforms toward process control in manufacturing. Researchers are focusing on implementing high-resolution NMR in this application, but in a manufacturing setting there is also potential for low-resolution NMR. In addition, when the chemical process is at the manufacturing level, the kinetics and control of the reaction are well known, and the needs are in the process

control area. Therefore, simple NMRs, already being used in the petroleum industry, are a key to providing simple process control at low cost. The coming years will see a trend toward in situ reaction monitoring by online NMR in the research and manufacturing areas in the pharmaceutical industry and perhaps in other industries as well.

7.5. ANALYSIS OF MIXTURES OFF-LINE, ONLINE, AND BY OTHER NMR METHODOLOGIES

As is becoming obvious through the many examples and variations of the NMR methodology discussed in this book, mixture analysis is important in the pharmaceutical, chemical, and environmental industries, among others, and in academia. We have presented many examples of the application of hyphenated separation technologies, NMR and MS-NMR being the two main technologies in the structural elucidation arena. However, there are cases where separation is not used to analyze complex mixtures. In this final section of the chapter we deal with those cases to understand when and how to apply separation technology hyphenated with NMR and when to carry out direct analysis of mixtures without separation.

7.5.1. Traditional Analysis of Mixtures by Off-Line HPLC and NMR

As mentioned in Section 7.2.1, isolation of individual components of mixtures is the classical approach to analyzing the structure of compounds from complex mixtures. The two principal reasons for the use of off-line HPLC and NMR are (1) the need for two-dimensional heteronuclear NMR experiments that are less sensitive than the common proton homonuclear two-dimensional NMR experiments for complete structural elucidation of analytes of interest, to avoid ambiguity as to their structural assignment, and (2) when direct analysis of a complex mixture by LC-NMR does not provide data of sufficient quality for NMR analysis. When an analyte of interest is unstable and decomposes during analysis, neither LC-NMR nor off-line NMR is a good choice for structural analysis. Isolation of unstable analytes before NMR analysis will also become an issue, due to sample instability during the process. An example of instability is the structural analysis of unstable metabolites from caspofungi acetate (MK-0991), a semisynthetic pneumocandin developed for systematic fungal infections such as those caused by *Candida* and *Aspergillus* species [43]. Urine samples from healthy human beings exposed to MK-0991 collected over time indicated the presence of two metabolites, M1 and M2, as hydrolysis products of MK-0991, which were

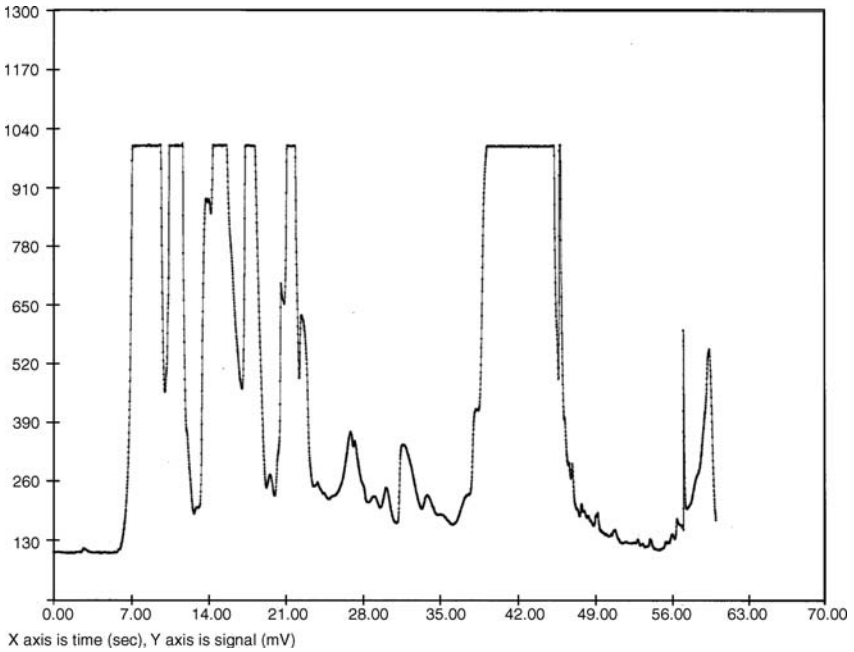

FIGURE 7-11. UV chromatogram of the on-flow experiment of human urine of caspofungin acetate [43].

polar and unstable. Direct injection of a urine sample into an LC-NMR system was not successful, due to the complex chromatography (Figure 7-11). M2 was highly polar and extremely unstable under acidic conditions. Therefore, the metabolite was transformed to a less polar product that it was possible to isolate for NMR analysis, identified as *N*-acetyl-4(*S*)-hydroxy-4-(4-hydroxyphenyl)-L-threonine γ-lactone (M2D). Consequently, the underivatized M2 was identified as γ-hydroxy acid, *N*-acetyl-4(*S*)-hydroxy-4-(4-hydroxyphenyl)-L-threonine (Figure 7-12). Chemical derivatization of M1 as des-acetyl-M2 provided the clues of its structure. M2 was also derivatized with ethyl chloroformate under basic conditions to avoid the lactonization by forming an ethoxycarbonyl M2 derivative (Figure 7-12). Figure 7-13 shows the ^{1}H NMR spectra of M2D in three deuterated solvent systems. In deuterated acetonitrile (ACN-*d*3) it was not possible to observe the phenolic proton, and the proton signal of the *N*-acetyl group overlaps with the residual protonated signal of the deuterated solvent (ACN-*d*3). In DMSO-*d*6, those two signals are shown clearly, as well as the exchangeable protons from the phenol, the hydroxyl, and the NH of the *N*-acetyl. The phenol and hydroxyl groups were exchanged when D_2O was added to the NMR solution (Figure 7-13). Figure 7-14 shows the ^{1}H NMR spectrum of the ethoxycarbonyl of M2 in DMSO-*d*6, where the exchangeable protons are visible with a small amount of lactone in the

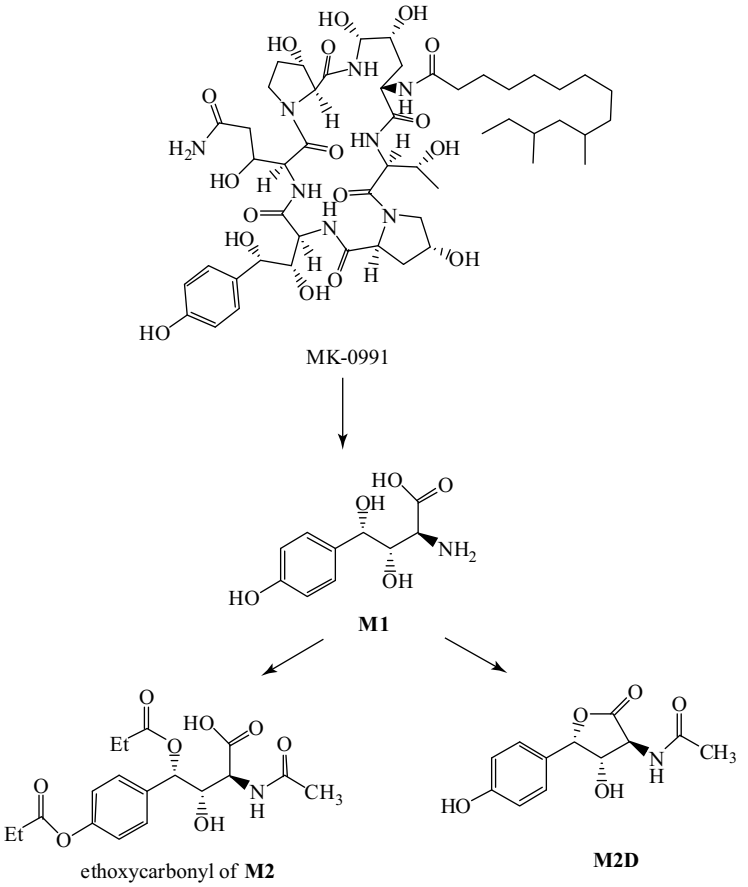

FIGURE 7-12. Metabolism pathway and structures of caspofungi acetate (MK0991) and its metabolites M1 and M2 as the ethoxycarbonyl of M2 and the lactone M2D [43].

spectrum [43]. Chemical derivatization was the key to determining the structures of the polar metabolites of caspofungi acetate (MK-0991) [43].

Separation of the analyte of interest is the best approach when its structure is not known or when changes in the structure are difficult to predict. An example in this category is the structural elucidation of one of the glutathione adducts of compound I (Figure 7-15), a potent thrombin inhibitor, which went through an unexpected biotransformation via rearrangement of a pyrazinone ring [44]. Incubations of compound I in human and rat liver microsomes fortified with glutathione (GSH) revealed the presence of two GSH adducts, GSH-1 and GSH-2, which required extensive structural analysis to determine the metabolic activation pathways and provide guidance on the design of a better drug candidate to minimize the metabolic activation of chemically reactive intermediates [44]. LC-MS/MS revealed a different fragmentation pattern, where

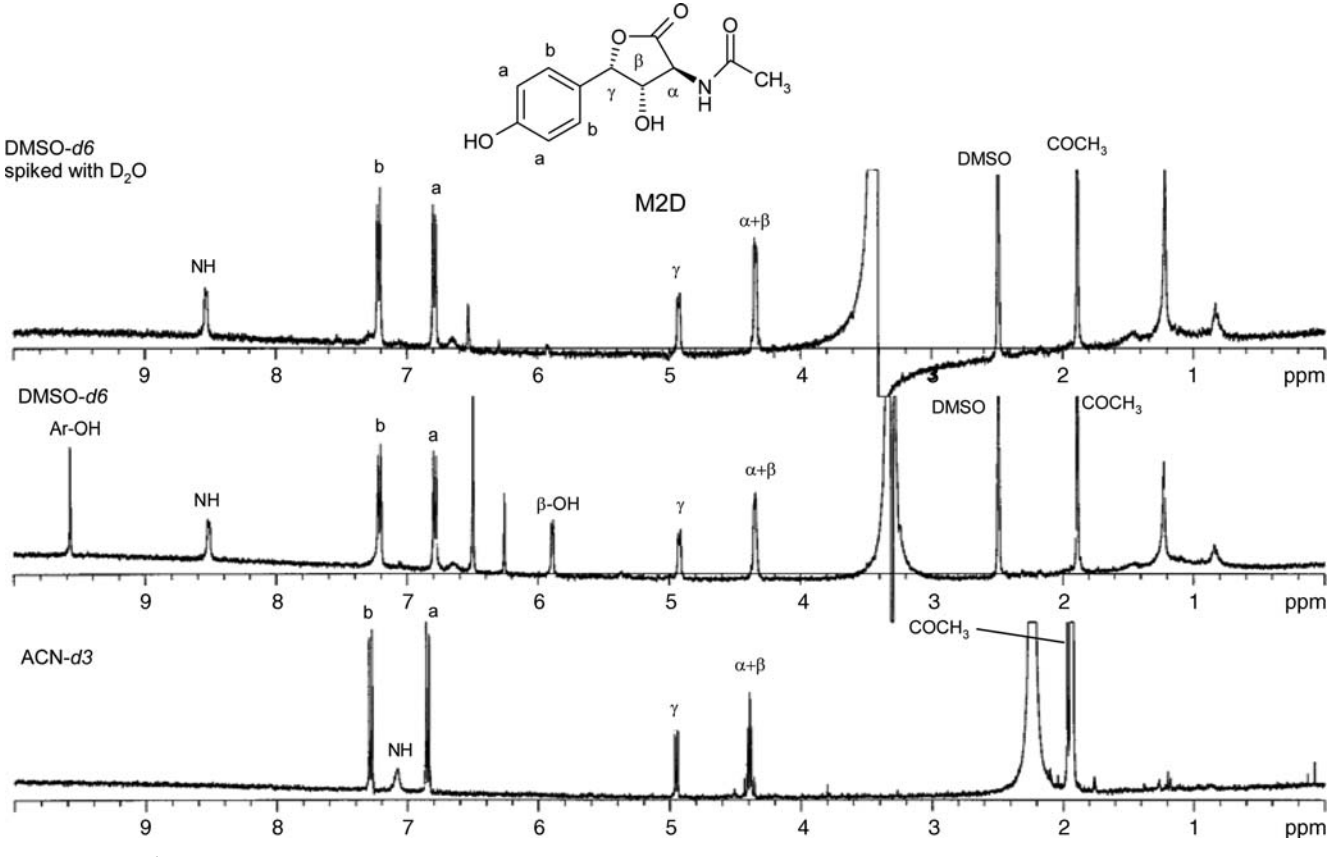

FIGURE 7-13. [1] NMR spectra of the lactone M2D derivative of M2 metabolite of caspofungi acetate (MK-0991) in ACN-*d*3 (bottom), DMSO-*d*6 (middle), and DMSO-*d*6 spiked with D_2O (top) [43].

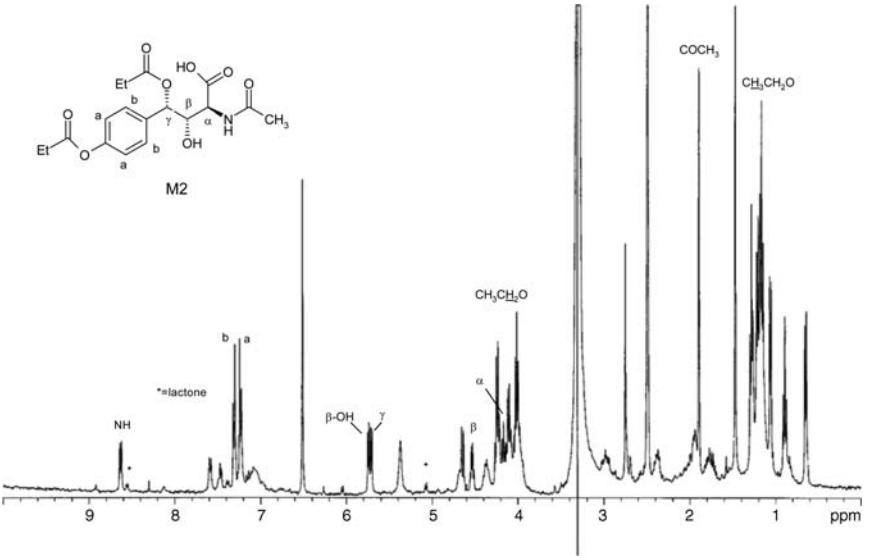

FIGURE 7-14. ^{1}H NMR spectrum of the ethoxycarbonyl derivative of M2 metabolite of caposfungi acetate (MK-0991) from human urine in DMSO-*d*6 [43].

GSH-1 lost GSH, as expected, in the two fragments with *m*/*z* 431 and *m*/*z* 609, and GSH-2 showed only fragment *m*/*z* 609, suggesting different bonding to compound I of the sulfur in glutathione (Figure 7-16). Figure 7-17 depicts the aliphatic region of the ^{1}H NMR spectra of compound I, GSH, and GSH-1

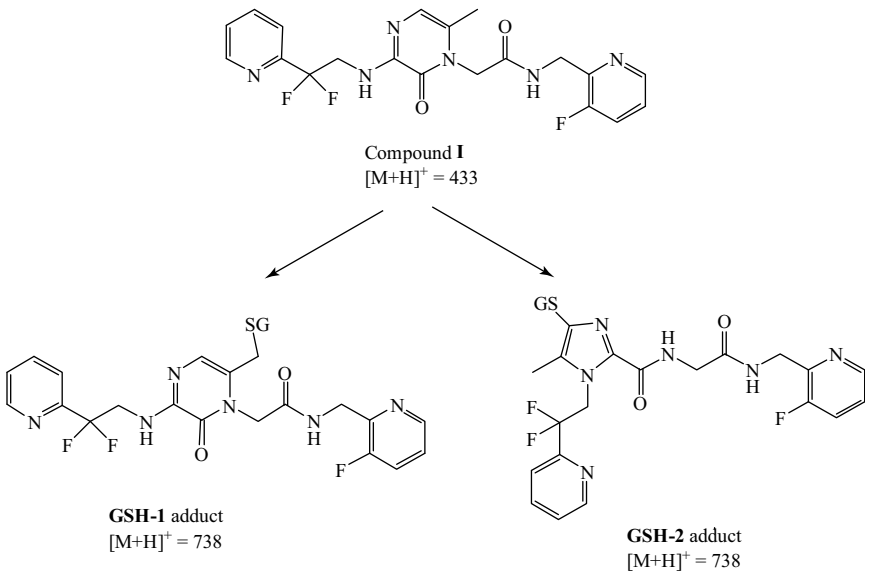

FIGURE 7-15. Structure of compound I and its two glutathione adducts, GSH-1 and GSH-2, isolated from human and rat liver microsomes [44].

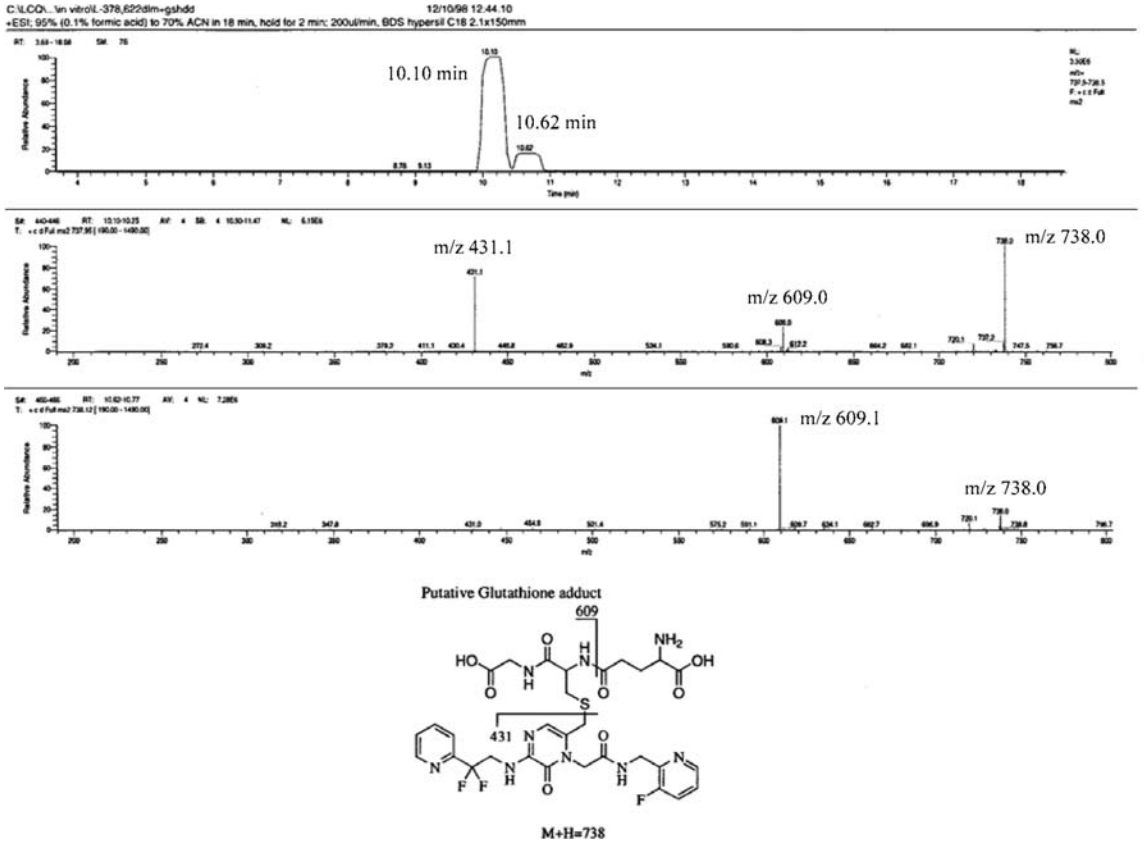

FIGURE 7-16. Total ion chromatogram (TIC) (top) and LC-MS/MS spectra of GSH-1 adduct (middle) and GSH-2 adduct (bottom) on *m/z* 738 [44].

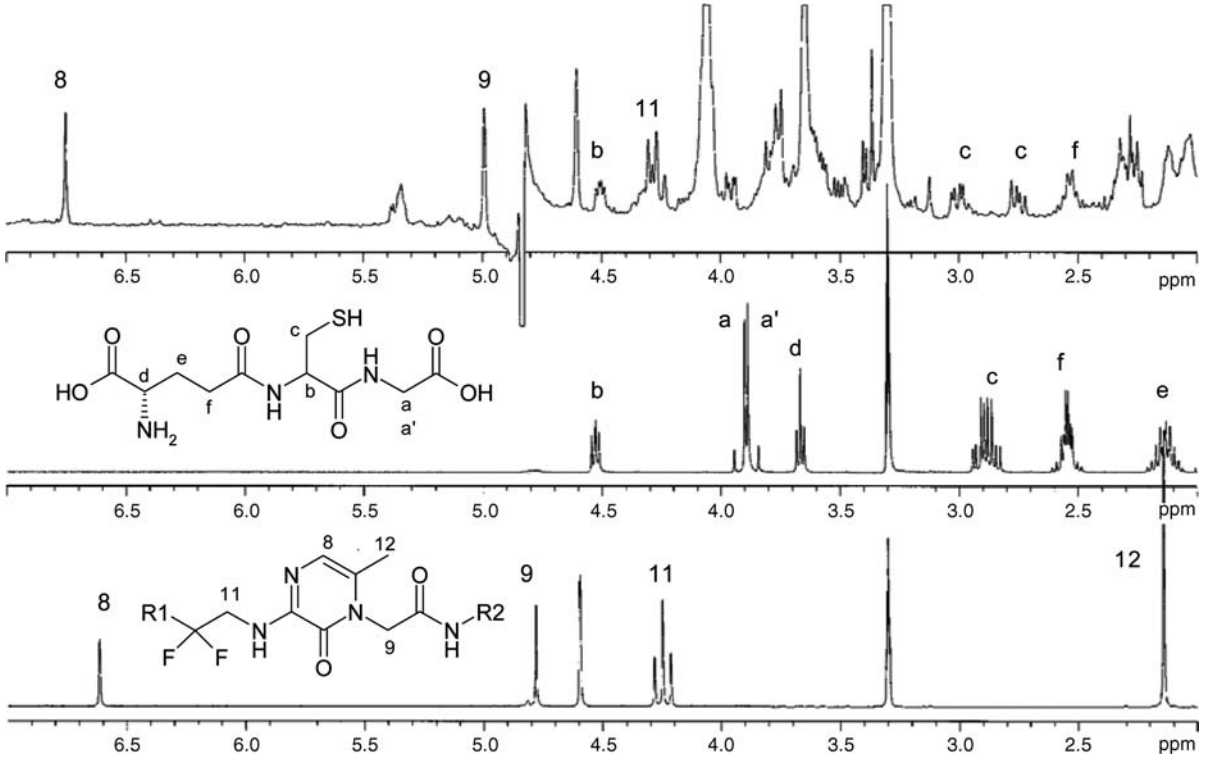

FIGURE 7-17. ^{1}H NMR spectra of the aliphatic region of compound I (bottom), GSH (middle), and isolated GSH-1 adduct (top) in CD_3OD [44].

adduct where the position of the aliphatic protons of GSH-1 are predictable following the same behavior as that of compound I and GSH. Figure 7-18 depicts the aliphatic region of the ^{1}H NMR spectra of compound I, GSH, and GSH-2 adduct, where major differences are noted for GSH-2 adduct with the absence of proton 8, proton 9 upfield-shifted, and proton 11 downfield-shifted compared to compound I. The initial proposal of a simple GSH adduct in position 8 for GSH-2 adduct was not plausible because of the difference in ^{1}H–^{13}C HMBC and NOE correlations compared to compound I. The GSH-2 adduct showed fewer C−H correlations in the ^{1}H–^{13}C HMBC spectrum than for compound I (Figure 7-19). The NMR experiments that revealed key information to suggest the structure of the GSH-2 adduct were one-dimensional NOE and two-dimensional NOESY (Figures 7-20 and 7-21). Both experiments showed the spatial correlation of the methyl protons (12) with the methylene protons (11), which are far apart in compound I (Figures 7-19 to 7-21). The structures proposed for both GSH adducts, GSH-1 and GSH-2, can accommodate the MS and NMR data without exceptions. Based on those structures, the researchers proposed a different mechanism of formation for both GSH adducts. Figure 7-22 depicts the mechanism proposed for the formation of GSH-1 adduct: via the typical two-electron oxidation of the 6-methyl-2-oxo-3-aminopyrazinone moiety through the expected electrophilic imine–methine intermediate. Figure 7-23 depicts the proposed mechanism of formation of the GSH-2 adduct through the addition of GSH to an epoxide formed by CYP450-mediated oxidation of the double bond in position 5–6 of the pyrazinone of compound I. After the opening of the epoxide from the GSH addition, the intermediate species is unstable as carbinolamine, which can easily open the ring to a more stable keto form, then rearrange it self by cyclizing with the external amino of the pyrazinone ring. After aromatization, it gives rise to the imidazole ring on the GSH-2 adduct (Figure 7-23) [44]. This work would be difficult to solve using hyphenated NMR experiments, due to the complexity of the GSH-2 structure, which required two-dimensional homo- and heteronuclear experiments that are better performed with isolated materials, to minimize such other factors as solvent suppression. Hyphenated NMR would not provide enough information to propose the structure of the GSH-2 adduct.

7.5.2. Online NMR Analysis of Mixtures

Hyphenated NMR came into being to determine the structures of analytes from complex mixtures. In Chapters 3, 4, 5, and 6 we have described many examples of cases where online NMR has solved this type of analysis problem successfully. In some cases, online NMR hyphenated with analytical separation techniques including MS has been applied to natural products, drug

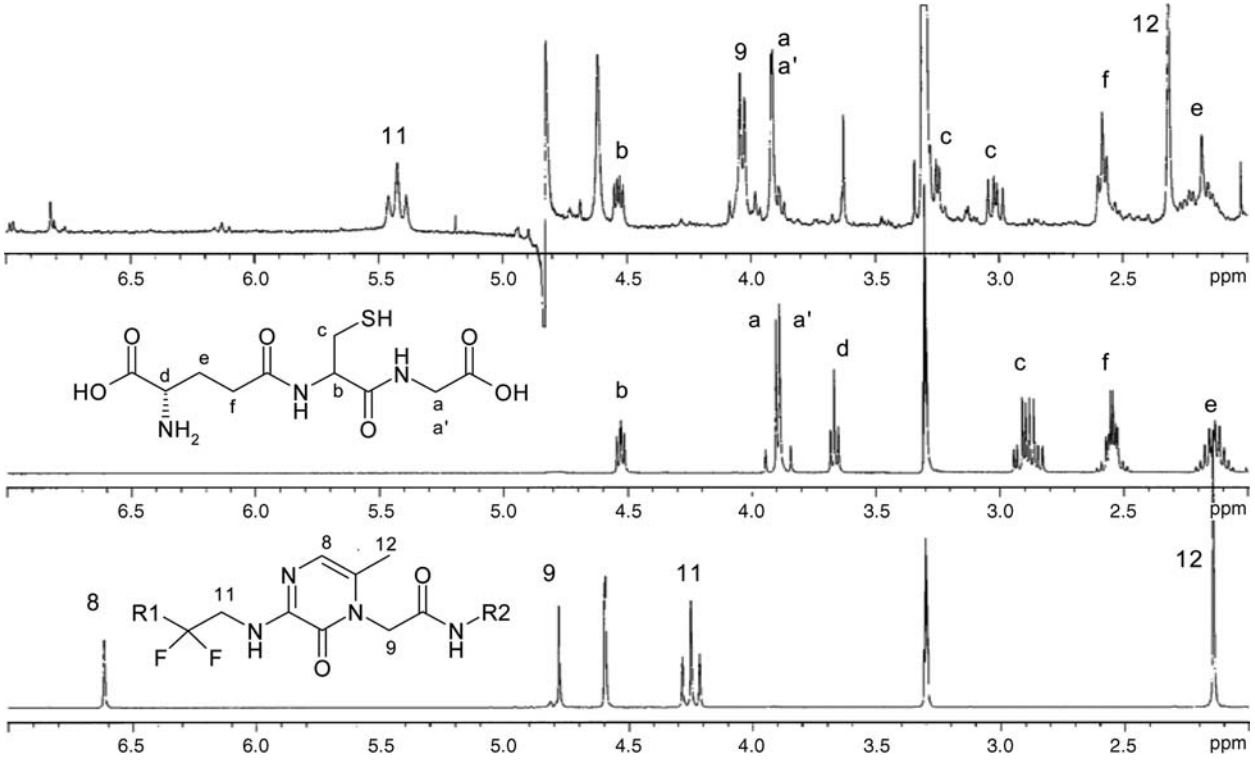

FIGURE 7-18. ^{1}H NMR spectra of the aliphatic region of compound I (bottom), GSH (middle), and isolated GSH-2 adduct (top) in CD_3OD [44].

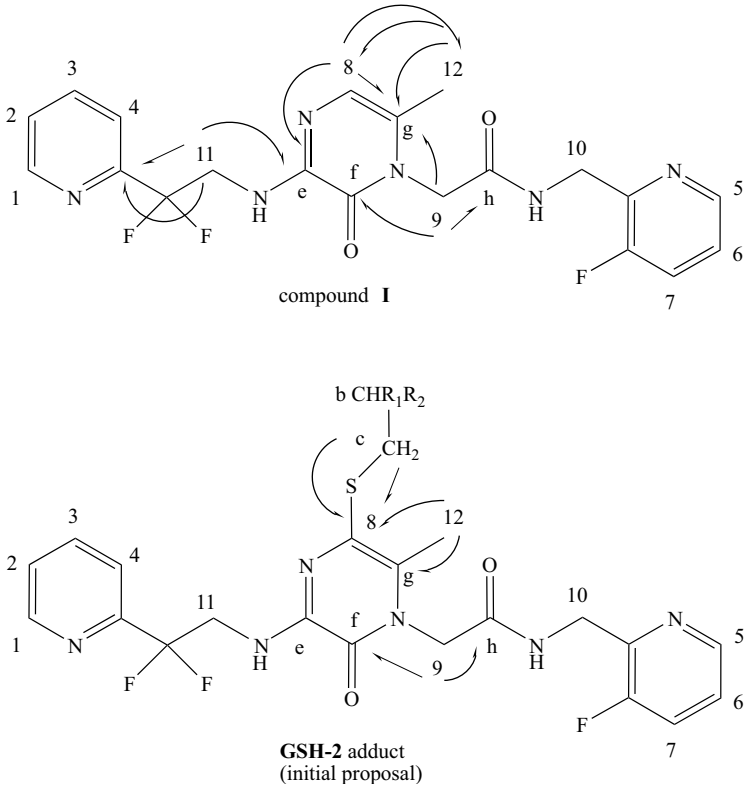

FIGURE 7-19. $^{1}H–^{13}C$ HMBC correlations around the pyrazinone ring for compound I (top) and the initial proposed structure for GSH-2 adduct (bottom) with R_1 and R_2 as part of glutathione [44].

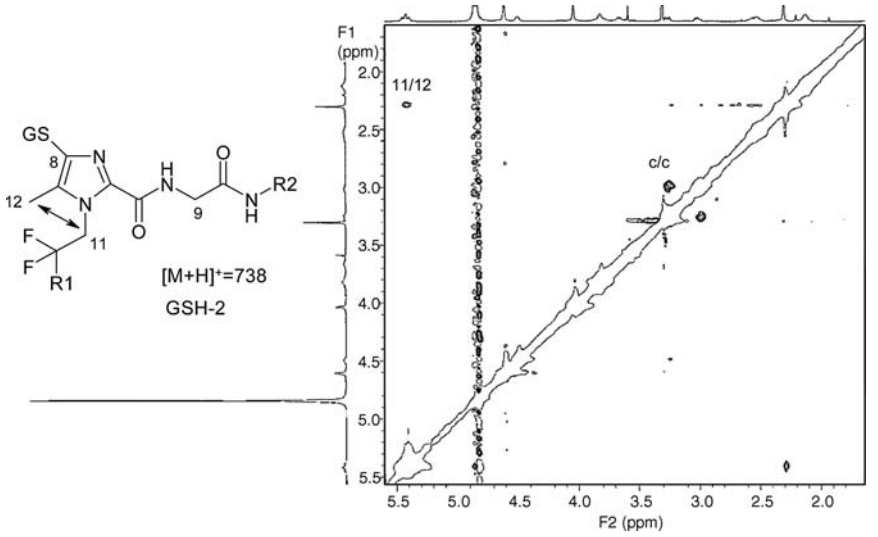

FIGURE 7-20. Apliphatic region of two-dimensional NOESY spectrum of GSH-2 adduct in CD_3OD [44].

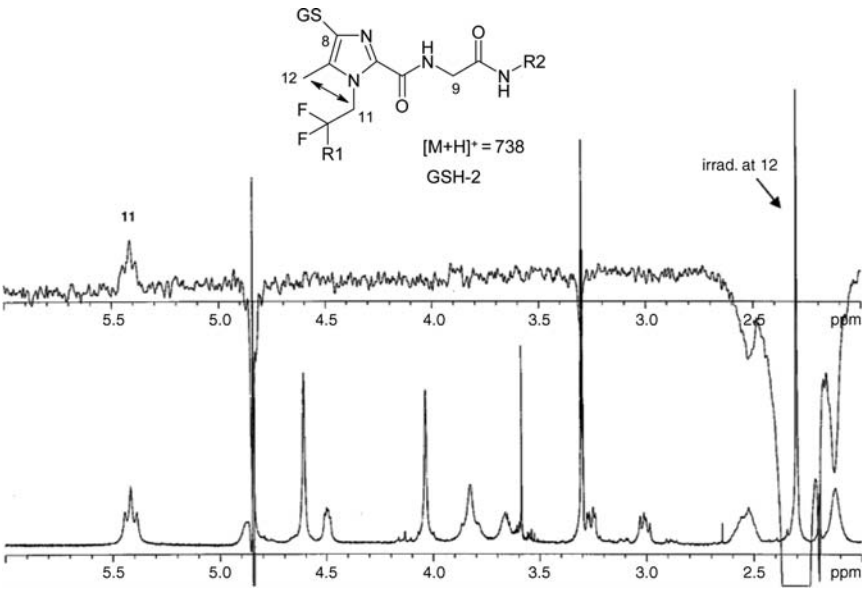

FIGURE 7-21. Aliphatic region of the ^{1}H NMR spectrum of GSH-2 adduct (bottom) and one-dimensional NOE experiment of GSH-2 irradiating the methyl protons at position 12 (top) [44].

metabolism, drug discovery and development, drug degradation products and impurity characterization, food analysis, polymers, metabonomics and metabolomics, the environmental field, and other areas. From volatile to nonvolatiles and from stable to nonstable components of mixtures, LC-NMR has

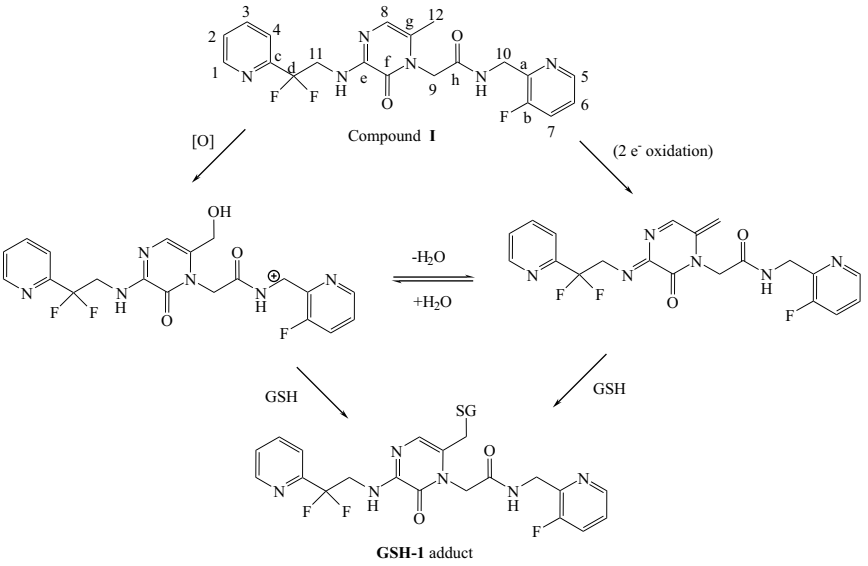

FIGURE 7-22. Proposed mechanisms for formation of the GSH-1 adduct [44].

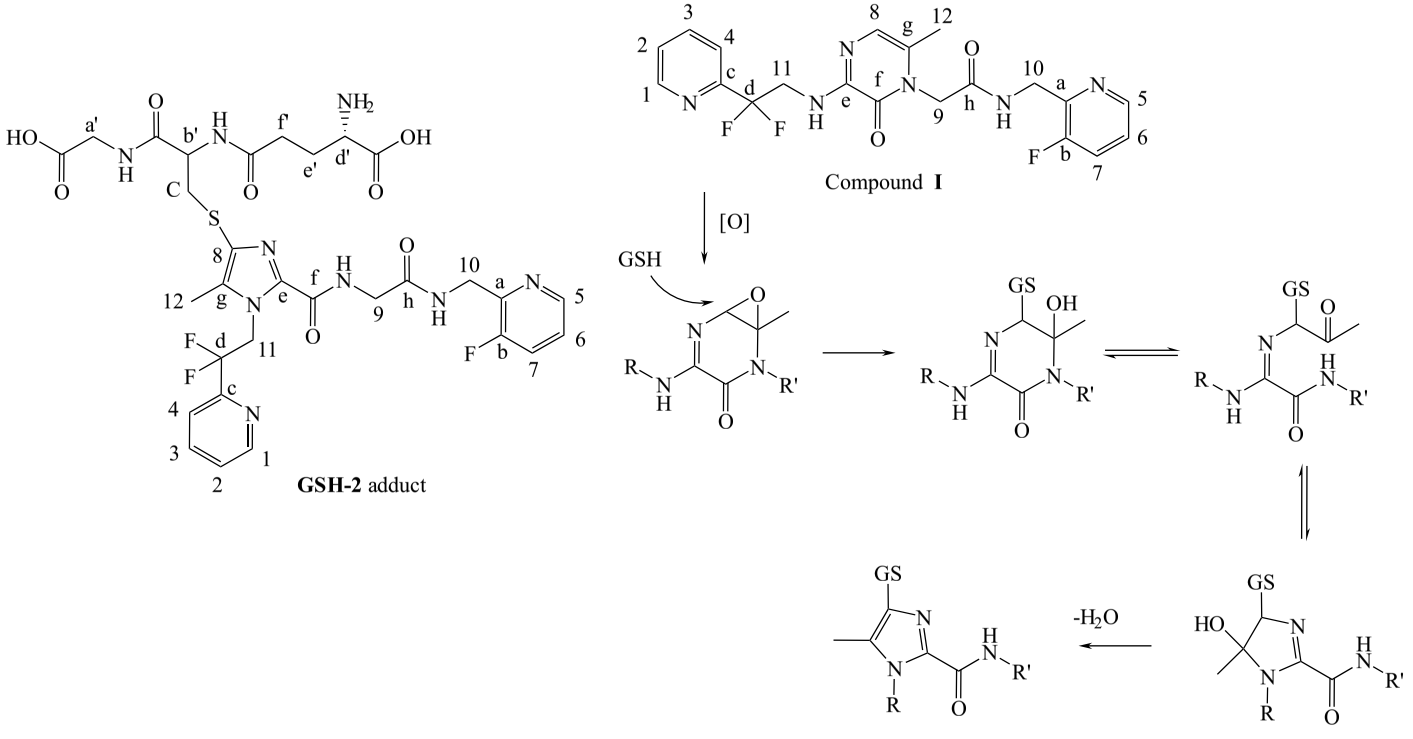

FIGURE 7-23. Structure of GSH-2 adduct (left) and proposed mechanism for formation of the GSH-2 adduct (right) [44].

provided another alternative to the conventional isolation and structural analysis carried out in an NMR tube. The target of LC-NMR and other hyphenated NMR techniques is to obtain structural data from the analytes of interest while avoiding or minimizing the overlapping of signals from other components of the mixture.

7.5.3. Other NMR Methodologies That Mimic LC-NMR Separation

Separation and isolation of a component of interest for the purpose of NMR analysis is time consuming. In addition, using hyphenated NMR techniques requires making some compromises as to the need for solvent suppression techniques, detection of only a percentage of the chromatographic peak around the coil in the NMR flow cell, and limitations on the solvent systems used, to be compatible with the LC and NMR sections of the system. In addition, concerns about not detecting exchangeable protons due to certain solvent selection for hyphenated NMR limit the structural analysis. Furthermore, even when using SPE cartridges in an SPE-NMR system to concentrate the analyte of interest, the technique may take overnight to dry the analyte in the cartridge for NMR analysis a day later. There are times where partial structural information is sufficient to solve certain analytical issues, and either isolation of the analyte before NMR analysis or using hyphenated NMR may not be the best choice for a rapid analysis of the components of mixtures. Analyzing complex mixtures directly by NMR can be complex using ^{1}H NMR, but it can be less cumbersome using ^{19}F NMR if the analyte of interest has fluorine in its structure. Partial structural information regarding analytes of mixtures can be obtained by selective excitation experiments such as one- or two-dimensional TOCSY, and by diffusion experiments such as one- or two-dimensional diffusion-ordered spectroscopy (DOSY). Those types of NMR experiments mimic separation by selectively seeing a portion of the molecule based on spin system information or by separating the molecules of the mixture based on their sizes by the different diffusion coefficients.

A one- or two-dimensional TOCSY experiment is the classical approach to looking into a mixture with no prior separation of its components. One-dimensional TOCSY has been used in forensic cases to identify heroin from street doses that contain mixtures of components [45]. In a few minutes it is possible to obtain the "fingerprint" information for heroin without the need for chemical or physical treatment prior to the analysis [45]. Sandusky and Raftery [46] applied the information from semiselective one-dimensional TOCSY on rat and human urine samples to principal components analysis (PCA) to distinguish rapidly the subtle differences in metabolite

concentrations in the fields of metabonomics and metabolomics. Similar to the previous study, one-dimensional TOCSY was applied to insect venom using a 1-mm cryogenic NMR probe to determine the major components of the mixture without the need for extensive purification prior to the NMR analysis [47]. Brüschweiler's group [48,49] has applied information obtained from one-dimensional TOCSY experiments to public Web servers to identify and determine the quantitative metabolite concentrations for biomarker identification in mixture analysis by covariance NMR.

Another option for analyzing a mixture without isolation of its components is by one- and two-dimensional DOSY NMR experiments. Molecules with different molecular weight or different three-dimensional shape (e.g., spheroidal versus ellipsoidal) will have different diffusion coefficients under the gradients in NMR diffusion experiments, and they can be distinguished and "separated" in the experiment. Two-dimensional DOSY experiments have been employed to analyze solutions of mixtures of polymers from industrial polypropylene and polystyrene samples to distinguish the components of the mixtures based on their different translational diffusion coefficients as a reflection of their molecular weight distributions [50]. Mistry et al. [51] measured diffusion coefficients to distinguish monomeric and dimeric components as impurities from a sample mixture of production batches of fluticasone propionate. Two-dimensional DOSY experiments have been used as a screening methodology to distinguish which small molecules bind to polymers commonly conducted for biological activity in drug discovery [52]. Another example of the application of two-dimensional DOSY based on the shape of molecules is distinguishing between two isomers in a mixture that have identical mass but different diffusion coefficients, because one is spherical and the other is ellipsoidal [53]. In the natural products arena focused on medical applications, two-dimensional DOSY is a useful tool for the analysis of complex mixtures in herbal dietary supplements marketed as natural substances to detect active and inactive ingredients and determine if any of the compounds are not listed as ingredients and should perhaps be considered as potential adulterants in the formulation [54]. To enhance the use of two-dimensional DOSY, Kavakka et al. [55] demonstrated that using a soluble polymer, poly(vinylpyrrolidine) (PVP), considered as a "stationary phase," can "separate" the components of the mixture in the DOSY experiment based on their interaction with PVP, giving rise to more distinct diffusion coefficients than if PVP were not present. As an application of one- and two-dimensional DOSY experiments in the drug metabolism area, Khera et al. [56] have analyzed the major metabolites of ethacrynic acid and mefenamic acid from rat bile to be their glucuronic conjugates (Figure 7-24) as a fast methodology to obtain information about the major metabolites present in the sample mixture.

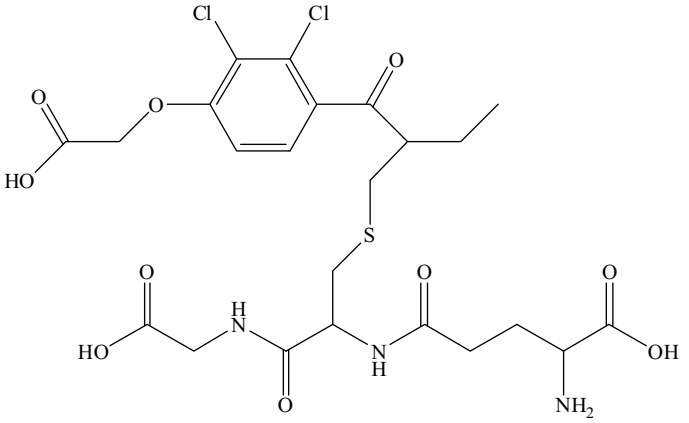

glutathione adduct of ethacrynic acid

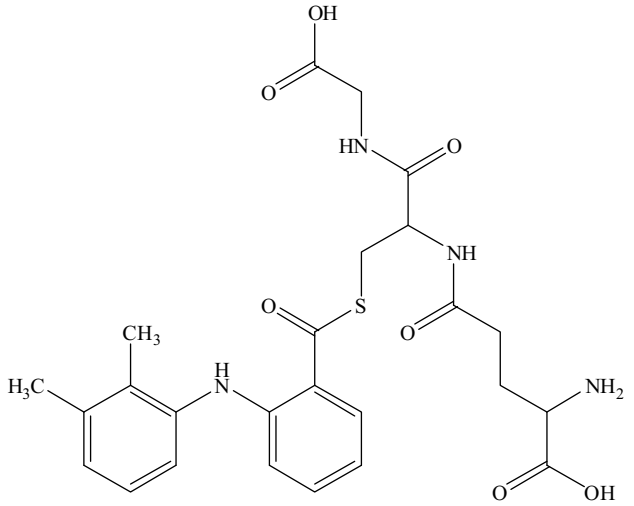

glutathione adduct of mefenamic acid

FIGURE 7-24. Structures of the glutathione adducts of ethacrynic acid (top) and mefenamic acid (bottom) [56].

7.6. CURRENT TRENDS

Complex sample mixtures can be analyzed using various methodologies with or without separation of the individual components. Structural analysis by NMR is possible in both cases, depending on the amount of information needed, the target of the study, and the complexity of the mixture. These parameters should facilitate the decision as to whether to use hyphenated or

nonhyphenated NMR for the structural analysis of mixture components. Some specific studies, such as chiral determination and reaction monitoring kinetics, can be performed off-line in an NMR tube or injected directly to the NMR flow cell as online methodology. On the other hand, some mixture analyses can be performed without isolation and by specific experiments such as by one- and two-dimensional TOCSY and DOSY. Depending on the information needed and the resources, analysts decide on the best approach for the studies. The current trend is decided case by case based on the expertise available, the information needed, and the methodologies available. The coming years will provide more information as to how the methodologies discussed in this chapter will find more common use in industrial and academic laboratories.

REFERENCES

[1] M.V. Silva Elipe, Z.J. Tan, M. Ronk, and T. Bostick, A Multidisciplinary Investigation to Determine the Structure and Source of Dimeric Impurities in AMG 517 Drug Substance, *Int. J. Anal. Chem.* 2009, article ID 768743, 12 pages, doi: (online article).

[2] G.J. Sharman and I.C. Jones, Critical Investigation of Coupled Liquid Chromatography–NMR Spectroscopy in Pharmaceutical Impurity Identification, *Magn. Reson. Chem.* **41** (2003), 448–454.

[3] R.A. Seburg, J.M. Ballard, T.-L. Hwang, and C.M. Sullivan, Photosensitized Degradation of Losartan Potassium in an Extemporaneous Suspension Formulation, *J. Pharm. Biomed. Anal.* **42** (2006), 411–422.

[4] A.L. Huidobro, F.J. Rupérez, and C. Barbas, Isolation, Identification and Determination of the Major Degradation Product in Alprazolam Tablets During Their Stability Assay, *J. Pharm. Biomed. Anal.* **44** (2007), 404–413.

[5] S.G. Hiriyanna, K. Basaviaih, H.N. Pati, and B.K. Misha, Separation, Isolation, and Characterization of Isoform Impurities of Gemcitabine Formed During the Anomerization of Protected α-Gemcitabine to Gemcitabine, *J. Liq. Chromatogr. Relat. Technol.* **30** (2007), 3093–3105.

[6] S.G. Hirayanna, K. Basavaiah, P.S.K. Goud, V. Dhayanithi, K. Raju, and H.N. Pati, Identification and Characterization of Olanzapine Degradation Products Under Oxidative Stress Conditions, *Acta Chromatogr.* **20** (2008), 81–93.

[7] M. lin, M. Li, A.V. Buevich, R. Osterman, and A.M. Rustum, Rapid Structure Elucidation of Drug Degradation Products Using Mechanism-Based Stress Studies in Conjunction with LC-MSn and NMR Spectroscopy: Identification of a Photodegradation Product of Betamethasone Dipropionate, *J. Pharm. Biomed. Anal.* **50** (2009), 275–280.

[8] M. Kračun, A. Kocijan, A. Bastarda, R. Grahek, J. Plavec, and D. Kocjan, Isolation and Structure Determination of Oxidative Degradation Products of Atorvastatin, *J. Pharm. Biomed. Anal.* **50** (2009), 729–736.

[9] Q. Chen, D. Zielinski, J. Chen, S. Nowak, and C.C. Zhou, Structural Identification and Characterization of Potential Degradants of Zotarolimus on Zotarolimus-Coated Drug-Eluting Stents, *J. Pharm. Biomed. Anal.* **50** (2009), 778–786.

[10] V.G. Dongre, P.D. Ghugare, P. Karmuse, D. Singh, A. Jadhav, and A. Kumar, Identification and Characterization of Process Related Impurities in Chloroquine and Hydroxychloroquine by LC/IT/MS, LC/TOF/MS and NMR, *J. Pharm. Biomed. Anal.* **49** (2009), 873–879.

[11] M. Xia, T.-J. Hang, F. Zhang, X.-M. Li, and X.-Y. Xu, The Stability of Biapenen and Structural Identification of Impurities in Aqueous Solution, *J. Pharm. Biomed. Anal.* **49** (2009), 937–944.

[12] V.J. Kumar, P.B. Gupta, K.S.R.P. Kumar, K.V.V.P. Rao, K.R. Rao, S.J. Prasana, J.H.K. Sharma, and K. Mukkanti, Identification and Characterization of New Degradation Products of Cefepime Dihydrochloride Monohydrate Drug Substance During Stress Stability Studies, *Anal. Sci.* **26** (2010), 1081–1086.

[13] Y. Sato, D. Breslin, H. Kitada, W. Minagawa, T. Nomoto, X.-Z. Qin, and S.B. Karki, Parenteral Formulation and Thermal Degradation Pathways of a Potent Rebeccamycin Based Indolocarbazole Topoisomerase I Inhibitor, *Int. J. Pharm.* **390** (2010) 128–133.

[14] P. Srinivasu, D.V. Subbarao, R.V.K. Vegesna, and K.S. Babu, A Validated Stability-Indicating LC Method for Acetazolamide in the Presence of Degradation Products and Its Process-Related Impurities, *J. Pharm. Biomed. Anal.* **52** (2010), 142–148.

[15] M.K. Mone and K.B. Chandrasekhar, Degradation Studies of Pentoxifylline: Isolation and Characterization of a Novel *gem*-Dihydroperoxide Derivative as Major Oxidative Degradation Product, *J. Pharm. Biomed. Anal.* **53** (2010), 335–342.

[16] Y. Li, D.Q. Liu, S. Yang, R. Sudini, M.A. McGuire, D.S. Bhanushali, and A.S. Kord, Analytical Control of Process Impurities in Pazapanib Hydrochloride by Impurity Fate Mapping, *J. Pharm. Biomed. Anal.* **52** (2010), 493–507.

[17] B. Raman, B.S. Sharma, P.D. Ghugare, S. Nandavadekar, D. Singh, P.K. Karmuse, and A. Kumar, Structural Elucidation of Process-Related Impurities in Escitalopram by LC/ESI-MS and NMR, *J. Pharm. Biomed. Anal.* **53** (2010), 895–901.

[18] H.S. Neto, F.A.P. Barros, F.M.S. Carvalho, and J.R. Matos, Thermal Analysis of Prednicarbamate and Characterization of Thermal Decomposition Product, *J. Therm. Anal. Calorim.* **102** (2010), 277–283.

[19] L. Turco, S. Provera, O. Curcuruto, E. Bernabe, A. Nicoletti, L. Martini, D. Castoldi, Z. Cimarosti, D. Papini, C. Marchioro, and R. Dams, Detection, Identification and Quantitation of a New De-fluorinated Impurity in Casopitant Mesylate Drug Substance During Late Phase Development: An Analytical Challenge Involving a Multidisciplinary Approach, *J. Pharm. Biomed. Anal.* **54** (2011), 67–73.

[20] V.J. Kumar, P.B. Gupta, K.S.R.P. Kumar, U.K. Ray, B. Sreenivasulu, G.C.S. Kumar, K.R. Rao, and H.K. Sharma, Identification, Isolation and Characterization of a New Degradation Product in Sultamicillin Drug Substance, *J. Pharm. Biomed. Anal.* **54** (2011), 582–587.

[21] P.A. Keifer, Flow Techniques in NMR Spectroscopy, *Annu. Rep. NMR Spectrosc.* **62** (2007), 1–47.

[22] D. Neuhaus and M.P. Williamson, *The Nuclear Overhauser Effect in Structural and Conformational Analysis*, 2nd ed., Wiley, New York, 2000.

[23] J.A. Dale and H.S. Mosher, Nuclear Magnetic Resonance Enantiomer Reagents: Configurational Correlations via Nuclear Magnetic Resonance Chemical Shifts of Diasereomeric Mandelate, *O*-Methylmandelate, and α-Methoxy-α-trifluoromethylphenylacetate (MTPA) Esters, *J. Am. Chem. Soc.* **95** (1973), 512–519.

[24] J.M. Seco, E. Quiñoá, and R. Riguera, The Assignment of Absolute Configuration by NMR, *Chem. Rev.* **104** (2004), 17–117.

[25] T.J. Wenzel, *Discrimination of Chiral Compounds Using NMR Spectroscopy*, Wiley, Hoboken, NJ, 2007.

[26] S. Porto, J. Durán, J.M. Seco, E. Quiñoá, and R. Riguera, "Mix and Shake" Method for Configurational Assignment by NMR: Application to Chiral Amines and Alcohols, *Org. Lett.* **5** (2003), 2979–2982.

[27] L. Verdier, P. Sakhaii, M. Zweckstetter, and C. Griesinger, Measurement of Long Range H,C Couplings in Natural Products in Orientating Media: A Tool for Structure Elucidation of Natural Products, *J. Magn. Reson.* **163** (2003), 353–359.

[28] C.M. Thiele, Use of RDCs in Rigid Organic Compounds and Some Practical Considerations Concerning Alignment Media, *Concepts Magn. Reson. A* **30A** (2007), 65–80.

[29] G. Kummerlöwe and B. Luy, Residual Dipolar Couplings as a Tool in Determining the Structure of Organic Molecules, *Trends Anal. Chem.* **28** (2009), 483–493.

[30] C. Gayathri, N.V. Tsarevsky, and R.R. Gil, Residual Dipolar Couplings (RDCs) Analysis of Small Molecules Made Easy: Fast and Tuneable Alignment by Reversible Compression/Relaxation of Reusable PMMA Gels, *Chem. Eur. J.* **16** (2010), 3622–3626.

[31] J.M. Seco, L.-H. Tseng, M. Godejohann, E. Quiñoa, and R. Riguera, Simultaneous Enantioresolution and Assignment of Absolute Configuration of Secondary Alcohols by Directly Coupled HPLC-NMR of 9-AMA Esters, *Tetrahedron Asymmetry* **13** (2002), 2149–2153.

[32] D. Guilet, A. Guntern, J.-R. Loset, E.F. Queiroz, K. Ndjoko, C.M. Foggin, and K. Hostettmann, Absolute Configuration of a Tetrahydrophenenthrene from *Heliotropium ovalifolium* by LC-NMR of Its Mosher Esters, *J. Nat. Prod.* **66** (2003), 17–20.

[33] T. Tokunaga, M. Okamoto, K. Tanaka, C. Tode, and M. Sugiura, Chiral Liquid Chromatography–Circular Dichroism–NMR for Estimating Separation Conditions of Chiral HPLC Without Authentic Samples, *Anal. Chem.* **82** (2010), 4293–4297.

[34] I. Hahnestein, M. Albert, H. Hasse, C.G. Kreiter, and G. Maurer, NMR Spectroscopic and Densimetric Study of Reaction Kinetics of Formaldehyde Polymer Formation in Water, Deuterium Oxide, and Methanol, *Ind. Eng. Chem. Res.* **34** (1995), 440–450.

[35] T.R. Hoye, B.M. Eklov, T.D. Ryba, M. Voloshin, and L.J. Yao, No-D NMR (No-Deuterium Proton NMR) Spectroscopy: A Simple Yet Powerful Method for Analyzing Reaction and Reagent Solutions, *Org. Lett.* **6** (2004), 953–956.

[36] T.R. Hoye, J.E. Kabrhel, and R.C. Hoye, No-D NMR Study of the Pathway for *n*-BuLi "Oxidation" of 1,5,-Cyclooctadiene to Dilithium Cyclooctatetraene Dianion [Li_2COT^{2-}], *Org. Lett.* **7** (2005), 275–277.

[37] M.M. Achmatovicz, J.T. Coyler, O.R. Thiel, J. Tomaskevitch, J. Hu, M.V. Silva Elipe, J.S. Tedrow, and R.D. Larsen, Hydrolysis of Phosphoryl Trichloride ($POCl_3$). Characterization, In Situ Detection and Safe Quenching of Energetic Metastable Intermediates, *Org. Process Res. Dev.* **14** (2010), 1490–1500.

[38] A. Herrera, E. Fernández-Valle, R. Martínez-Álvarez, D. Molero, Z.D. Pardo, E. Sáez, and M. Gal, Real-Time Monitoring of Organic Reactions with Two-Dimensional Ultrafast TOCSY NMR Spectroscopy, *Angew. Chem. Int. Ed.* **48** (2009), 6274–6277.

[39] M.A. Bernstein, M. Stefinovic, and C.J. Sleigh, Optimising Reaction Performance in the Pharmaceutical Industry by Monitoring with NMR, *Magn. Reson. Chem.* **45** (2007), 564–571.

[40] M. Maiwald, H. Li, T. Schnabel, K. Braun, and H. Hasse, On-Line ^{1}H NMR Spectroscopic Investigation of Hydrogen Bonding in Supercritical and Near Critical CO_2-Methanol up to 35 MPa and 403 K, *J. Supercritical Fluids* **43** (2007), 267–275.

[41] M. Maiwald, O. Steinhof, C. Sleigh, M. Bernstein, and H. Hasse, Quantitative High-Resolution Online NMR Spectroscopy in Pharmaceutical Reaction and Process Monitoring, in U. Holzgrabe, I. Wawer,and B. Diehl (eds.), *NMR Spectroscopy in Pharmaceutical Analysis*, Elsevier, Oxford, England, 2008, pp. 471–491.

[42] M. Khajeh, M.A. Bernstein, and G.A. Morris, A Simple Flowcell for Reaction Monitoring by NMR, *Magn. Reson. Chem.* **48** (2010), 516–522.

[43] S.K. Balani, X. Xu, B.H. Arison, M.V. Silva, A. Gries, F.A. DeLuna, D. Cui, P.H. Kari, T. Ly, C.E.C.A. Hop, R. Singh, M.A. Wallace, D.C. Dean, J.H. Lin, P.G. Pearson, and T.A. Baillie, Metabolites of Caspofungin Acetate, a Potent Antifungal Agent, in Human Plasma and Urine, *Drug Metab. Dispos.* **28** (2000), 1274–1278.

[44] R. Singh, M.V. Silva Elipe, P.G. Pearson, B.H. Arison, B.K. Wong, R. White, X. Yu, C.S. Burgey, J.H. Lin, and T.A. Baillie, Thrombin Inhibitor: Evidence for

Novel Biotransformation Involving Pyrazinone Ring Oxidation Rearrangement, and Covalent Binding to Proteins, *Chem. Res. Toxicol.* **16** (2003), 198–207.

[45] N. Suryaprakash, M. Azoury, Z. Goren, and R. Jelinek, Identification of Heroin in Street Doses Using 1D-TOCSY Nuclear Magnetic Resonance, *J. Forensic Sci.* **45** (2000), 963–969.

[46] P. Sandusky and D. Raftery, Use of Semiselective TOCSY and the Pearson Correlation for the Metabonomics Analysis of Biofluids Mixtures: Application to Urine, *Anal. Chem.* **77** (2005), 7717–7723.

[47] F. Zhang, A.T. Dossey, C. Zachariah, A.S. Edison, and R. Brüschweiler, Strategy for Automated Analysis of Dynamic Metabolic Mixtures by NMR: Application to an Insect Venom, *Anal. Chem.* **79** (2007), 7748–7752.

[48] S.L. Robinette, F. Zhang, L. Brüschweiler-Li, and R. Brüschweiler, Web Server Based Complex Mixture Analysis by NMR, *Anal. Chem.* **80** (2008), 3606–3611.

[49] F. Zhang, S.L. Robinette, Brüschweiler-Li, and R. Brüschweiler, Web Server Suite for Complex Mixture Analysis by Covariance NMR, *Magn. Reson. Chem.* **47** (2009), S118–S122.

[50] A. Jerschow and N. Müller, Diffusion-Separated Nuclear Magnetic Resonance Spectroscopy of Polymer Mixtures, *Macromolecules* **31** (1998), 6573–6578.

[51] N. Mistry, I.M. Ismail, R.D. Farrant, M. Liu, J.K. Nicholson, and J.C. Lindon, Impurity Profiling in Bulk Pharmaceutical Batches Using ^{19}F NMR Spectroscopy and Distinction Between Monomeric and Dimeric Impurities by NMR-Based Diffusion Measurements, *J. Pharm. Biomed. Anal.* **19** (1999), 511–517.

[52] P. Hodge, P. Monvisade, G.A. Morris, and I. Preece, A Novel NMR Method for Screening Soluble Compound Libraries, *Chem. Commun.* (2001), 239–240.

[53] P. Thureau, A. Thévand, B. Ancian, P. Escavabaja, G.S. Armstrong, and V.A. Mandelshtam, Identification of Two Isomers from an Organic Mixture by Double-Stimulated-Echo NMR and Construction of the DOSY Spectra by the Regularized Resolvent Transform Method, *ChemPhysChem* **6** (2005), 1510–1513.

[54] S. Balayssac, S. Trefi, V. Gilard, M. Mallet-Martino, R. Martino, and M.-A. Delsuc, 2D and 3D DOSY 1H NMR, a Useful Tool for Analysis of Complex Mixtures: Application to Herbal Drugs or Dietary Supplements for Erectile Dysfunction, *J. Pharm. Biomed. Anal.* **50** (2009), 602–612.

[55] J.S. Kavakka, I. Kilpeläinen, and S. Heikkinen, General Chromatographic NMR Method in Liquid State for Synthetic Chemistry: Polyvinylpyrrolidone Assisted DOSY Experiments, *Org. Lett.* **11** (2009), 1349–1352.

[56] S. Khera, M. Grillo, P. Schnier, and S. Hollis, Application of Diffusion-Edited NMR Spectroscopy for the Structural Characterization of Drug Metabolites in Mixtures, *J. Pharm. Biomed. Anal.* **51** (2010), 164–169.

Index

LC-NMR and Other Hyphenated NMR Techniques: Overview and Applications, First Edition. Maria Victoria Silva Elipe.